Mesh Distributed Coordination Function for Efficient Wireless Mesh Networks Supporting QoS

Von der Fakultät für Elektrotechnik und Informationstechnik
der Rheinisch-Westfälischen Technischen Hochschule Aachen
zur Erlangung des akademischen Grades eines Doktors der
Ingenieurwissenschaften genehmigte Dissertation

vorgelegt von

Master of Engineering
Rui Zhao

aus Sichuan, China

Berichter: Universitätsprofessor Dr.-Ing. Bernhard Walke
Universitätsprofessor Dr. Petri Mähönen

Tag der mündlichen Prüfung: 23. April 2007

To my wife Dongjing and our child Youzhen

To my parents

ABSTRACT

Wireless Mesh Networks (WMN) are receiving growing attention. They can widely find applications in Wireless Local Area Networks (WLAN), Wireless Metropolitan Area Networks (WMAN), Wireless Personal Area Networks (WPAN) and Wireless Sensor Networks (WSN), helping to substantially improve the network performance, cut down the operation cost and bring more convenience to both operators and end users. There are lots of open research issues in the field. Among them, the design of the Media Access Control (MAC) protocol is the most challenging one.

This thesis proposes Mesh Distributed Coordination Function (MDCF), a novel MAC protocol that can be used to construct efficient WMNs supporting Quality of Service (QoS). MDCF applies Time Division Multiple Access (TDMA) to share the radio medium in a fully distributed manner. It is able to run on a single frequency channel independent of physical schemes. Transmissions in MDCF networks take place in periodic time slots in a dynamic Time Division Duplex (TDD) mode of operation. A novel synchronization algorithm, operating under fully distributed control, is proposed for synchronizing mesh points (MP) for TDMA operation in the multi-hop environment. MDCF is well designed to properly handle highly loaded situations, hidden stations, exposed stations and capture effect which usually appear in a mesh environment and may dramatically deteriorate the network performance. For QoS support, besides a prioritized, collision eliminating and fair channel access mechanism, a distributed Radio Resource Control (RRC) protocol is used to evaluate and allocate a fair portion of bandwidth to a specific traffic flow. The assigned portion of the bandwidth for a flow is adaptable with the traffic load and overall channel utilization. As a result, MDCF is able to efficiently exploit channel capacity, fairly distribute bandwidth and support multi-hop relaying of a large number of concurrent various traffic services in a WMN.

The performance of MDCF is extensively evaluated by both analytical and simulation approaches. The results exhibit the outstanding performance of MDCF, significantly outperforming the IEEE 802.11 Distributed Coordination Function (DCF) and Enhanced Distributed Coordinated Access (EDCA), in both single-hop and mesh environments.

MDCF has been submitted as a MAC proposal for the IEEE 802.11 Task Group s (TGs), which is formed to develop mesh WLANs. It can also be tailored for WMAN, WPAN and WSN mesh applications.

KURZFASSUNG

Das Konzept der Wireless Mesh Networks (WMNs) erfährt momentan eine wachsende Beachtung. Es gibt für sie in großem Maße Einsatzbereiche in Wireless Local Area Networks (WLANs), Wireless Metropolitan Area Networks (WMANs), Wireless Personal Area Networks (WPANs) und Wireless Sensor Networks (WSNs). Das Konzept hilft dabei, die Leistunbgsfähigkeit dieser Netze grundlegend zu verbessern, die Kosten zu reduzieren und mehr Benutzerfreundlichkeit sowohl auf der Seite der Betreiber als auch auf der Anwenderseite zu bieten. Es gibt sehr viele offene Fragen in diesem Forschungsbereich. Unter diesen stellt der Entwurf eines Protokols für die Kanalzugriffssteuerung (MAC) die größte Herausforderung dar.

In dieser Arbeit wird ein neues Protokol für die Kanalzugriffssteuerung vorgeschlagen, das für den Aufbau drahtloser vermaschter Netze, die Dienstgüte untertzützen, genutzt werden kann. Dieses Protokol wird als Mesh Distributed Cordination Function (MDCF) bezeichnet. Das MCDF Verfahren nutzt die Time Division Multiple Access (TDMA) Technik um die Funkressourcen in einer verteilten Weise zu nutzen. Es ist damit unabhängig von der physikalischen Übertragungstechnik möglich, einen einzelnen Frequenzkanal zu nutzen. Für die Datenübertragung werden periodische Zeitschlitze in einem dynamischen Time Division Duplex (TDD) Verfahren genutzt. Für die vollkommen verteilte Synchronisation der einzelnen Stationen in einem Multi-Hop Netz wird ein neuer Algorithmus vorgeschlagen. Die MCDF Kanalzugriffssteuerung bietet Funktionalitäten, um die üblichen Probleme, welche die Leistungsfähigkeit von vermaschten Funknetzen stark beeinflussen können, zu handhaben. Dabei handelt es sich um Situationen mit hoher Last im Netz, um sogenannte Hidden und Exposed Stations und um den Capture Effect. Um Dienstgüte unterstützen zu können, wird neben Priorisierung, Kollisionsauflösung und gerechtem Kanalzugriff eine verteilte Funkressourcensteuerung (RRC) genutzt. Mit Hilfe dieser Steuerung wird die Aufteilung der Bandbreite auf die einzelnen Datenströme koordiniert. Der zugewiesene Ressourceanteil pro Datenstrom dabei kann in Abhängigkeit von Verkehrslast und Ressourcenauslastung dynamisch angepasst werden. Dies führt dazu, dass das MDCF Verfahren eine effiziente Auslastung der Kanalkapazität, eine gerechte Aufteilung der Funkressourcen und Multi-Hop Datenübertragung für eine große Anzahl von unterschiedlichen Diensten in einem vermaschten Funknetz ermöglicht.

Die Leistung der entwickelten Kanalzugriffssteuerung wurde sowohl mit analytischen als auch mit simulativen Verfahren detailiert untersucht. Die Ergebnisse belegen die hervorragenden Leistungsmerkmale des Verfahrens im Vergleich mit der IEEE 802.11 Distributed Coordination Function (DCF) und dem Enhanced Distributed Coordinated Access (ECDA). Die Untersuchungen wurden für sogenannte Single-Hop Szenarien

und für vermaschte Umgebungen durchgeführt.

Das im Rahmen dieser Arbeit entwickelte MCDF Verfahren wurde als Vorschlag für eine Kanalzugriffssteuerung (MAC) bei der Arbeitsgruppe IEEE 802.11s eingereicht, deren Ziel die Entwicklung von vermaschten WLANs ist. Daneben kann die MCDF Technik auch für vermaschte WMAN, WPAN und WSN Anwendungen eingesetzt werden.

TABLE OF CONTENT

CHAPTER 1

Introduction

Wireless networks have experienced tremendous success in the past few years. People are expecting more advanced wireless services but at low cost. The increased demand is driving the rapid evolution of the underlying technologies. Wireless Mesh Networks (WMN) are emerging as the key players in the next generation wireless networks. This thesis proposes Mesh Distributed Coordination Function (MDCF), a fully distributed MAC protocol for constructing efficient WMNs supporting Quality of Service (QoS).

1.1 An Emerging Key Technology

A WMN contains at least two elements: mesh points (MP) and mobile stations (MS). MPs, which are fixed or movable, form a multi-hop network with each other in an ad-hoc manner. Based on that, a WMN is created: An MS in a WMN communicates with a nearby MP at a time and may switch to another one when necessary, whilst MPs relay traffic by means of multi-hop operation. As a result, a self-formed WMN can be kept with high mesh connectivity and MSs only need greatly simplified communication functions. It is evident that WMNs are substantially different from cellular networks and traditional ad-hoc networks.

Multi-hop relaying helps to extend the radio coverage without using costly base stations, improve the traffic performance in given scenarios [22], reduce the transmitting power of MSs and promote the robustness of a network. An MP can be a user terminal, performing the required computing tasks, like a computer. However, it can also be a very small device and put into a place simply for increasing mesh connectivity or relaying traffic. In a WMN, only a few MPs operate as portal or gateway, providing access to other networks like the Internet. Obviously, the WMN enables the easy, fast and cost-efficient deployment of wireless networks. Creation of a WMN leads to cost reduction in operating and deploying wireless networks, and brings more convenience to both operators and end-users.

WMNs can be applied in Wireless Local Area Networks (WLAN), Wireless Metropolitan Area Networks (WMAN), Wireless Personal Area Networks (WPAN) and Wireless Sensor Networks (WSNs). Next generation WLANs, WMANs and high speed WPANs are intended to offer high quality multimedia communication services at low cost in different scenarios. Those applications require high data transmission rates, which are possible to be implemented only on high carrier frequencies. From the view of feasibility and availability, operation frequencies for those networks shall be above 3 GHz [21]. However, transmission on such bands suffers from serious propagation attenuation and from low obstacle penetration. Multi-hop capability therefore is a mandatory property of such wireless networks in order to achieve low terminal power consumption, wide service coverage, and low operation cost [104]. Moreover, transport of multimedia traffic requires that QoS requirements of data packets are met. QoS support can be guaranteed in an environment where high station connectivity can be ensured. With above introduced features, WMNs are expected to be a key element of those systems. Major industrial organizations, like 802.11 (WLAN), 802.16 (WMAN), 802.15 (WPAN) are actively working on introducing multi-hop mesh elements in their next generation standards. Unlike the aforementioned systems, extreme low power consumption and implementation cost are primary concerns of WSNs [23], where WMNs however can also be of help in reaching the goals.

1.2 Motivation and Areas of Interest

There are lots of challenging issues in wireless mesh networking, such as [24], [11] mesh routing, mesh security, mesh connectivity control, media access control (MAC), etc.. The thesis focuses on the MAC protocol, the most challenging one.

A WMN aims at easy configuration and deployment, high mesh connectivity and fault tolerance. It should be formed in an ad-hoc manner and hence capable of self-organizing and self-healing. Therefore, control of a WMN should be distributed. Besides, it is worth noting that the multi-hop capability of a system with central control is quite limited. The control overhead for multi-hop operation in a centrally controlled network increases dramatically with the number of relaying stations [98] and the number of hops. Accordingly the transmission efficiency decreases significantly with the number of relaying stations. The thesis concentrates on introducing a MAC protocol with distributed control for WMNs.

The wireless medium is a shared medium. Highly loaded situations, hidden stations, exposed stations and capture effect usually appear in a WMN and may dramatically deteriorate the network performance. Existing MAC protocols with distributed control such as the IEEE 802.11 Distributed Coordination Function (DCF) [1], IEEE 802.11 Enhanced Distributed Coordination Access (EDCA) [2], and Hiperlan/I [36] cannot efficiently handle those issues in the multi-hop environment, resulting in a serious underutilization of the bandwidth and unfairness to stations [28], [45].

Even if high mesh connectivity is guaranteed, the implementation of QoS in a WMN is extremely difficult to achieve under distributed control of the network and the harsh state of the multi-hop environment. The QoS metrics including delay, jitter, packet loss ratio and throughput impose a great challenge for ensuring QoS in mesh. Currently wireless solutions with perfect QoS support can only be found in one hop systems with central control on per connection basis, like one-hop PTP mode in WiMAX [13], GSM [72] and UMTS [72] etc..

In summary, two challengs lie in designing MAC protocols for WMNs 1): finding out effective means to enable efficient transmission in mesh networks under distributed control 2): Implementation of QoS support in mesh.

1.3 Contributions of the Thesis

This thesis proposes Mesh Distributed Coordination Function (MDCF), a fully distributed MAC protocol that can be used to construct efficient WMNs with QoS guarantee. It can be tailored to suit the needs of different application scenarios.

The MDCF evolved from the wireless channel oriented ad-hoc multi-hop broadband (W-CHAMB) protocol [93]-[98]. It is based on Time Division Multiplex Access (TDMA) technology, able to operate on a single frequency channel and run independent of physical transmission schemes. The major contributions of the thesis are:

- ✓ A distributed synchronization algorithm is proposed for synchronizing MPs for TDMA operation in the mesh environment.
- ✓ A two-stage prioritized access mechanism is proposed to implement a prioritized, highly collision eliminating and fair channel access.
- ✓ Algorithms are proposed for properly handling highly loaded situations, hidden stations, exposed stations and signal capture in the multi-hop environment.
- ✓ An on demand Time Division Duplex (TDD) turnaround scheme is proposed for duplex transmission link to significantly enhance the channel utilization.
- ✓ Fully distributed Radio Resource Control (RRC) algorithms are proposed to enhance the channel utilization and guarantee the QoS of real-time traffic flows.
- ✓ A Radio Link Control (RLC) protocol is developed for implementing error and flow controls suiting the multi-hop environment.
- ✓ Evaluation of the performance of MDCF both by analytical and simulation approaches. The accuracy of the analytical model is verified by simulations.

1.4 Outline

The thesis is organized as follows:

Chapter 2 introduces the necessary background including the wireless channel model and properties of WMNs. Then related work and the state of the art of wireless mesh networking are described.

Chapter 3 presents a detailed description of MDCF, including the channel access scheme, on demand TDD turnaround, a distributed synchronization algorithm enabling MPs to perform TDMA operation in the multi-hop mesh environment, the algorithms to handle hidden and exposed stations, and capture in mesh, multi-hop operation, the radio resource control, the radio link control and packet multiplexing in mesh, besides other.

Analytical performance analysis of MDCF is provided in Chapter 4. The extensive simulation investigation of the performance of MDCF is performed in Chapter 5. Conclusion and outlook are presented in Chapter 6.

CHAPTER 2

Wireless Mesh Networks

Evolved form traditional ad-hoc networks, WMNs are expected to serve for a wide range of applications in a near future. However the broadcast nature of the radio medium poses a great deal of challenges for creating an efficient WMN. The harsh state of the multi-hop environment and the distributed nature of WMNs make the implementation of QoS in WMNs extremely difficult. Considerable research efforts are underway to address the issues.

This chapter first introduces the wireless channel model. Several terms which will be used throughout the thesis are defined. Section 2.2 describes the properties of wireless multi-hop networks. Four phenomena, which should be well handled by a MAC protocol for efficient WMNs, are listed. Design considerations of MAC protocols for WMNs are outlined in Section 2.3. The metrics introduced there will be used in the remaining parts of the thesis. The interest of the thesis is on studying the MAC protocols for WMNs. A description of the related work and standardization activities is presented in Section 2.4.

2.1 Wireless Channel Model

The wireless medium is a shared medium. Multiple stations may access the channel at the same time. Concurrent transmissions on the same carrier frequency may result in mutual destruction of the carried messages. Signal strength attenuates with the transmission distance. The received signal strength P_R at a receiver is given by:

$$P_R = P_T g_T g_R \left(\frac{\lambda}{4\pi} \right)^2 \left(\frac{1}{d^{\gamma}} \right) \tag{2.1}$$

Where P_T is the transmission power, g_T is the transmission antenna gain, g_R is the receiving antenna gain, d is the distance between sender and receiver, λ is the wavelength, and γ is the attenuation coefficient between 2 (free space) to 5 (indoor) [72].

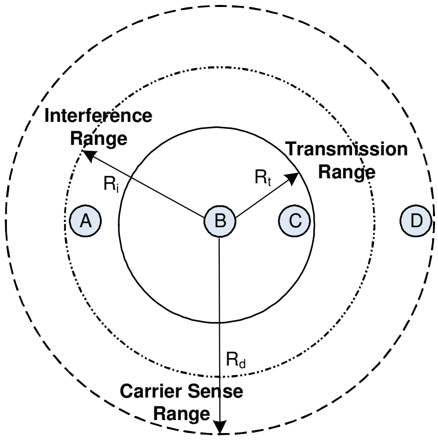

Figure 2-1. Transmission range, interference range and carrier sense range in a wireless multi-hop network. The figure shows the three ranges of station B.

The capability of a receiver to decode or sense a message depends on the Signal-to-Interference-and-Noise-Ratio (SINR). Two kinds of messages are used in MDCF networks: data packets and energy signals. Energy signals are in band busy tones [49], [26], carrying only binary information. Therefore, the received energy signals overlapping in time at a receiver will strengthen rather than weaken each other, like a logical OR operation. Let *N*, *S* and *I* be the powers of noise, signal and interference, respectively. The *SINR* for data packets and energy signals is given by:

$$SINR = \begin{cases} \dfrac{S}{\sum I + N} & \text{for Data packets} \\ \dfrac{S + \sum I}{N} & \text{for Energy signals} \end{cases} \tag{2.2}$$

We define three terms: *transmission range*, *carrier sense range* and *interference range* that are used in the thesis.

- ***Transmission range*** R_t–Without concurrent transmissions from other stations, a station in the transmission range of another station can decode data packets from it.
- ***Carrier sense range*** R_d–Without concurrent transmissions from other stations, a station in the carrier sense range of a station can sense its transmission, but may not be able to decode data packets.
- ***Interference range*** R_i– When a transmission is ongoing, any transmission from a station in the interference range of a receiving station shall corrupt data packets destined to the receiving station.

As is to be shown later, $R_i >> R_t$. However, interference can be avoided if potential interfering stations can sense the signal of the transmitting station and keep silent. This is to say, interference can be avoided if the physical carrier sense threshold is properly set so that $R_i = R_d$. This is however difficult to achieve in the radio environment. In practice (as shown later), $R_i \geq R_d > R_t$. Figure 2-1 shows an example. Station C, D and A is in the transmission range, carrier sense range and interference range of B, respectively. When B transmits, C can decode the messages from B, while D can sense the transmission but cannot decode the messages. Transmissions from station A shall corrupt another concurrent transmission destined to B.

Now we simply reveal the relations between R_i, R_d and R_t by analyzing a simple interference model. The results can help to understand the importance of properly setting the carrier sense and decoding thresholds in a radio environment. Let CS_{th} and D_{th} be signal strength thresholds of sensing the carrier and decoding messages, respectively; let K denote $g_T g_R (\lambda / 4\pi)^2$; and let $Max(R_i)$, $Max(R_d)$ and $Max(R_t)$ be the maximum value of R_i, R_d and R_t, respectively. It can be derived from Eq. (2.1): $Max(R_t) = (KP_t/D_{th})^{1/\gamma}$, $Max(R_d) = (KP_t/CS_{sh})^{1/\gamma}$. Their relation is:

$$Max(R_d) = Max(R_t) \times (\frac{D_{th}}{CS_{th}})^{1/\gamma} \tag{2.3}$$

Figure 2-2a reveals the relation of $Max(R_d)$ with $Max(R_t)$ under different D_{th} / CS_{th} values. It is shown that $Max(R_d)$ can be 1.33 to 30 times of $Max(R_t)$ under different attenuation factors γ and D_{th}/CS_{th} values. A higher D_{th}/CS_{th} under a given γ or a lower γ under a given D_{th}/CS_{th} leads to a higher $Max(R_d) / Max(R_t)$. It is worth noting that the ratios of D_{th}/CS_{th} may range from 5 dB from 30 dB in an environment when multiple modulation and coding schemes are available, like in IEEE 802.11a [3].

Suppose in the network shown in Figure 2-1, station C is transmitting to B with a transmission power of P_T^T when A is transmitting with a transmission power of P_T^I. Station C and A are d_t and d_i away from station B, respectively. Station A is an interference source to B at this scenario. Let P_r^T and P_r^I be the received signal strengths at B from C and A, respectively, $SINR_B$ be the $SINR$ at station B. Given that $P_r^I >> N$ (noise power), $SINR_B$ is:

$$SINR_B = \frac{P_r^T}{P_r^I} = \frac{P_T^T}{P_T^I} \times (\frac{d_i}{d_T})^{\gamma}$$

A message will fail to be decoded if $SINR_B < D_{th}/N$. This means that station A shall cause interference to the receiver B if:

$$(\frac{d_i}{d_T})^{\gamma} < \frac{D_{th}}{N} \times \frac{P_T^I}{P_T^T}$$

$$d_i < (\frac{D_{th}}{N} \times \frac{P_T^I}{P_T^T})^{1/\gamma} \times d_T \tag{2.4}$$

Eq. (2.4) suggests that R_i is highly dependent on the transmission distance of the ongoing transmission d_t. From the definitions, It is clear that when $d_i > Max(R_i)$, trans-

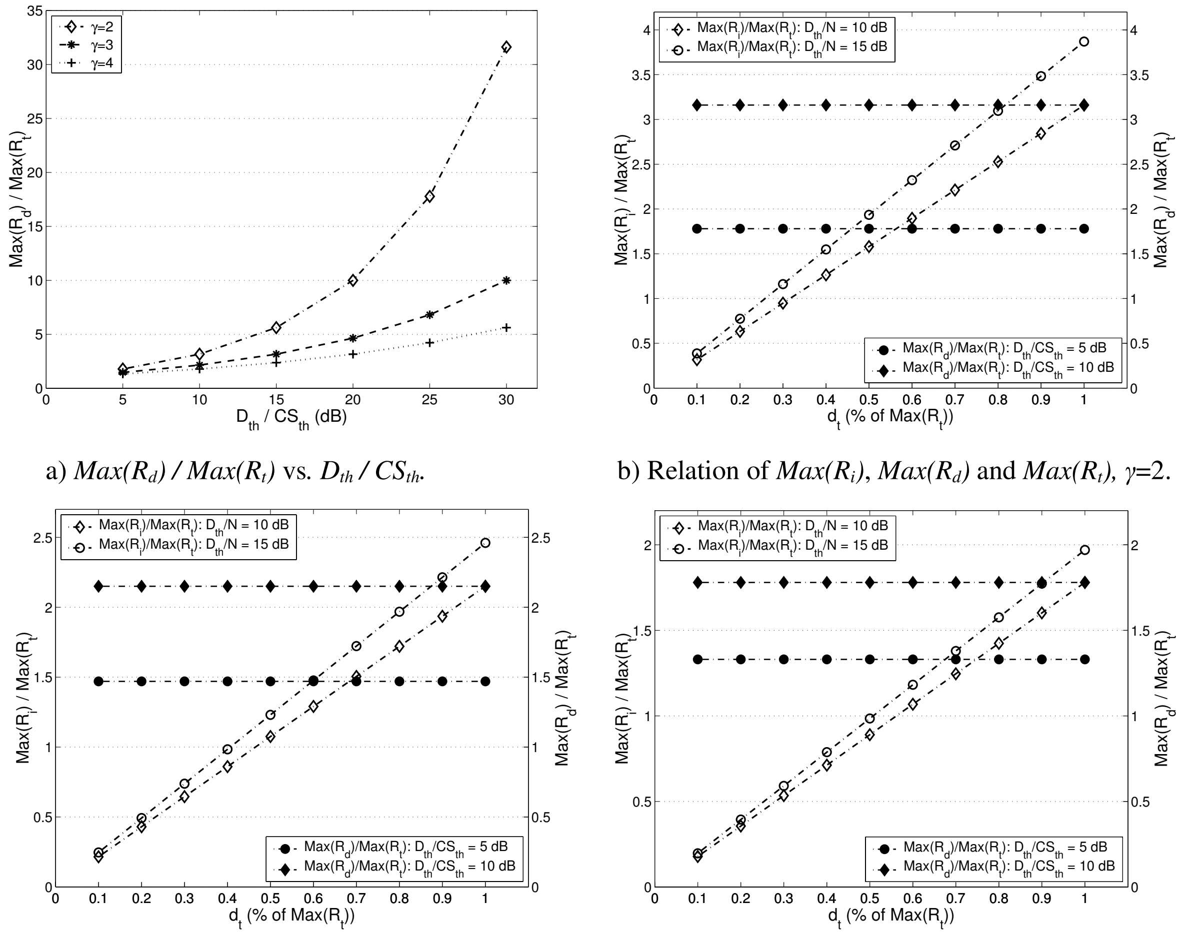

a) $Max(R_d) / Max(R_t)$ vs. D_{th} / CS_{th}.

b) Relation of $Max(R_i)$, $Max(R_d)$ and $Max(R_t)$, γ=2.

c) Relation of $Max(R_i)$, $Max(R_d)$ and $Max(R_t)$, γ=3.

d) Relation of $Max(R_i)$, $Max(R_d)$ and $Max(R_t)$, γ=4.

Figure 2-2. Relation between the maximum carrier sense range, the maximum transmission range and the maximum interference range. Figures b, c, d are achived assuming $P_r^I = P_r^T$.

missions from A will not cause interference to the reception at station B. Hence $Max(R_i)$ is given by:

$$Max\,(R_i) = d_t \times (\frac{D_{th}}{N} \times \frac{P_r^I}{P_r^T})^{1/\gamma} \tag{2.5}$$

Further, we have,

$$\frac{Max\,(R_i)}{Max\,(R_t)} = \frac{d_t}{Max\,(R_t)} \times (\frac{D_{th}}{N} \times \frac{P_r^I}{P_r^T})^{1/\gamma} \tag{2.6}$$

Based on Eq. (2.3), and Eq. (2.6), the relations of $Max(R_i)$, $Max(R_d)$ and $Max(R_t)$ under different γ values are plotted in Figure 2-2b, c and d assuming that $P_r^I = P_r^T$. It is clear to see that a longer distance d_t ($d_t \leq Max(R_t)$) results into a longer $Max(R_i)$ (note that

$Max(R_t)$ is a fixed value since D_{th} is fixed*)*. Varying CS_{th} helps to adapt the carrier sense range. The proper selection of CS_{th} to make the carrier sense range cover the interference range is important for a carrier sense multiple access (CSMA) system. The reason for this has been stated before. It is evident that $D_{th} > CS_{th} > N$. As indicated in Figure 2-2b, c and d, a smaller D_{th} (in dB: D_{th} / N) leads to a smaller $Max(R_i)$: given $\gamma = 2$ and $d_t = Max(R_t)$ when $D_{th} / N = 10$ dB, $Max(R_i) = 3.1\ Max(R_t)$, whilst when $D_{th} / N = 15$ dB, $Max(R_i) = 3.9\ Max(R_t)$. The selection of a smaller CS_{th} (then D_{th} / CS_{th} is bigger) results into a larger carrier sense range: given $\gamma = 2$ when $D_{th} / CS_{th} = 10$ dB, $Max(R_d) = 3.1\ Max(R_t)$, whilst when $D_{th} / CS_{th} = 5$ dB, $Max(R_d) = 1.7\ Max(R_t)$. As shown in Figure 2-2b, c and d, when let $D_{th} / CS_{th} = 10$ dB, a potential interfering station can sense most transmissions which it shall cause interference to, because $Max(R_d)$ covers the larger parts of R_i. In contrast to this, if let $D_{th} / CS_{th} = 5$ dB, $Max(R_d)$ only reaches a part of $Max(R_i)$. Under the setting, obviously, some stations cannot detect an on-going transmission which they shall cause interference to if they transmit. Comparing the results shown in Figure 2-2b, c and d, it can be found that when γ is increasing, both $Max(R_i)$ and $Max(R_d)$ are decreasing. However the relative relations of $Max(R_i)$, $Max(R_d)$ and $Max(R_t)$ to each other keep the same.

The preceding results reveal the relation of the transmission range, carrier sense range and interference range using the simple model shown in Figure 2-1. In a real mesh environment, the situation becomes more complicated, since 1) P_r^I is not necessary be same as P_r^T and 2) the number of interfering stations is uncertain. However, from the analysis, it is clear that the carrier sense threshold CS_{th} should be well selected in order to avoid interference while exploiting spatial reuse. Nevertheless, a small CS_{th} helps to avoid interference but reduces the capability of spatial reuse, whilst a big CS_{th} value shall result in unacceptable interference. Moreover the maximum interference range ($Max(R_i)$) highly depends on the distance between receiver and transmiter (d_t). Therefore, setting a fixed CS_{th} causes that a station either over- or under- evaluate the interference in a mesh environment.

For ease of analysis, in the following, we assume that

- When station A is in the carrier sense range of B, a simultaneous transmission from station A shall interfere with another transmission to station B.
- When station A is out of the carrier sense range of B, a simultaneous transmission from station A shall not interfere with another transmission to station B.
- $Max(R_d) = 2Max(R_t)$ (this is close to the pratical use, see [85]).

2.2 Properties of Multi-hop Networks

A MAC protocol for efficient multi-hop networks should be able to properly handle the following phenomena, which usually appear in wireless multi-hop networks. Figure 2-3 is used for illustration.

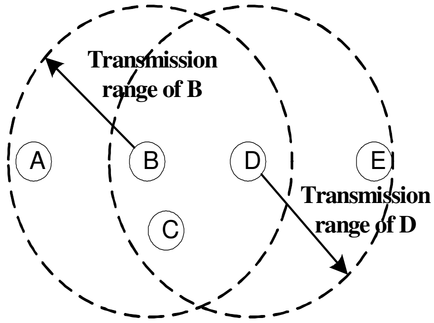

Figure 2-3. A wireless multi-hop network: each station is with the same transmission power. It is assumed that $Max(R_d) = 2Max(R_t)$.

- ***Highly loaded situations*** – Multi-hop forwarding brings multiple traffic. An n-hop transmission leads to n times increase of overall network traffic compared to a one-hop transmission. In Figure 2-3, the multi-hop transmission from station A to E needs 3 one-hop links (A -> B, B -> D, D -> E) established for relaying, bringing 3 times overall traffic compared to the one-hop case. As a result, a multi-hop network shall be quite often in a highly loaded situation, resulting in a significant amount of contention for channel access. The IEEE 802.11 Enhanced Distributed Coordination Access (EDCA) cannot effectively handle the situation as will be shown in the simulation analysis part (Chapter 5.4.1).
- ***Hidden stations*** – Supposing an ongoing transmission from station A to B, a hidden station E is one that is out of carrier sense range of A but its transmission shall cause collision to the reception at B. In 802.11 DCF/EDCA networks, hidden stations cause collisions and serious unfairness [28].
- ***Exposed stations*** –Supposing an ongoing transmission from station B to A, an exposed station E is one that is within the carrier sense range of B but its transmission shall not cause collision to the reception at A. Exposed stations result in the underutilization of bandwidth and unfairness in 802.11 DCF/EDCA networks [28].
- ***Capture*** – Station B is in the transmission range of A and C. When A and C transmit simultaneously to B and the signal strength received from C is much higher than that from A, then B can decode the message from C and the signal from A is considered to be interference power. In this case, station C shall capture the channel. Capture results in serious unfairness in 802.11 DCF/EDCA networks [31],[33].

2.3 Design Issues of MAC Protocols for WMNs

A MAC protocol for WMNs should provide solutions for highly loaded situations, the hidden station, exposed station and capture problems. The efficiency of a MAC protocol for multi-hop mesh networks can be evaluated by following metrics:

- ***Channel Utilization*** – The fraction of time used for transmitting user data packets in a given period. Both, high overhead MAC protocols and inefficient MAC pro-

Table 2-1. Traffic services, their traffic behavior and QoS requirements.

Traffic	Load (Mbps)	Packet size (bytes)	Max Delay (ms)	Max Packet loss ratio (PLR)
VoIP	0.0224	160	60	6%
Video conference	Mean:0.256 Max:1.28	512	100	0.1%
DVD	9.8 peak	1500	200	10^-7
HDTV	19.2-24	1500	200	10^-7
WWW	-	Mean:480 Max:66666	-	0
FTP (TCP)	-	1500	-	0

tocols result in low channel utilization. A protocol for WMNs is considered inefficient if its spatial reuse and/or collision avoidance capability is poor.

- ***Fairness*** – Traffic flows of the same QoS level should gain equally chances to use the wireless medium. However, highly loaded situations, hidden stations, exposed stations and capture may lead to unfairness. The fairness can be calculated by Jain's fairness index [25]:

$$F_J = \frac{(\sum_{i=1}^{m} \gamma_i)^2}{m \sum_{i=1}^{m} \gamma_i^2} \tag{2.7}$$

  Where m is the total number of flows and γ_i is the proportion of received packets of flow i during run time. F_J is equal to 1 when all flows equally share the bandwidth, and equal to $1/m$ when a flow monopolizes the network.

- ***End-to-end delay*** – Elapsed time between the generation of a packet at the source station and the correct reception of the packet at the final destination station. The delay performance depends on protocol capabilities of avoiding collision and exploiting spatial reuse. It also depends on the protocol efficiency of channel access and achieving fairness.
- ***Throughput*** – The volume of user data transferred between two stations in a given period. Throughput is the most frequently used MAC performance metric.
- ***QoS support*** – A MAC protocol should exhibit preferences to a high QoS level traffic flow in order to guarantee its specified throughput, packet loss ratio (PLR), packet delay and jitter requirements. The preferences include channel access preference and channel usage preference. Table 2-1 lists some of traffic services and their QoS requirements [9].

2.4 Related Work

The research and industry efforts on designing MAC protocols for efficient wireless multi-hop networks are outlined in the first part. The second part gives an overview of efforts on developing MAC protocols aiming at support QoS under fully distributed control. A description of the ongoing IEEE 802 standardization activities on the multi-hop mesh networking is presented in the third part.

2.4.1 MAC Protocols for Wireless Multi-hop Networks

The study of MAC protocols for multi-hop networks has been extensively performed over years. IEEE 802.15.1 (Bluetooth) [4] and IEEE 802.15.3 [5] are two standardized Wireless Personal Area Networks (WPAN) protocols. IEEE 802.15.3 is intended for high rate WPAN networks, supporting data rates of 20 Mbps or more, while Bluetooth is for wireless communications between portable devices supporting data rates up to 723.2 kbps. Both the high rate and Bluetooth WPAN networks operate under central control. Bluetooth systems implement multi-hop operation by relaying data between multiple frequency channels. However, channel searching and switching in Bluetooth needs quite a lot of time. On the contrary, an 802.15.3 network implements multi-hop on a single frequency channel. A relaying station in an 802.15.3 network must use the time slots allocated by the piconet coordinators (PNC) to transmit both data and control packets with the source and destination stations. The multi-hop capability of 802.15.3 networks is very limited. Its multi-hop solution targets at small scale scenarios.

In Dual Busy Tone Multiple Access (DBTMA) [26], busy tones are transmitted on a separate control channel to calm down hidden stations, while data is transmitted on the data channel. A Wireless Collision Detection (WCD) [27] scheme is proposed based on a transceiver architecture, which overlays the data and feedback channel into a single frequency channel. The feedback signals are used to assist in properly handling hidden and exposed stations.

The Ready to Send (RTS) and Clear to Send (CTS) dialogue is used in the IEEE 802.11 DCF [1] and EDCA [2] to avoid collisions caused by hidden stations. The scheme works well in a single-hop or two-hop network. But it solves neither the hidden nor exposed station problems in beyond two-hop networks. As an additional result, the back-off policy of the 802.11 DCF/EDCA in favor of the last transmitting station may cause serious unfairness [28]. Lots of effort has been put on improving the fairness performance of 802.11 DCF/EDCA networks, such as Distributed Fair Scheduling [29], Max-Min Fair Share [30] and Power Adaptation for Starvation Avoidance [31]. However no effective and efficient approach has been reported so far which can be applied to 802.11 DCF/EDCA multi-hop networks.

Extending the 802.11 DCF/EDCA to utilize the multiple channels offered by the IEEE 802.11a/b/g PHYs to improve the performance of 802.11 Basic Service Set (BSS) networks has been extensively studied. Slotted Seeded Channel Hopping (SSCH) [34] is a link layer protocol able to run over the unmodified DCF MAC and to increase the capacity of a DCF network by utilizing frequency diversity. Jungmin et al. [32] propose a MAC protocol, which requires only one transceiver per host to utilize multiple channels to improve the traffic performance. Dynamic Channel Assignment (DCA) [35] is a protocol that assigns channels in an on-demand style. There, one dedicated control channel is used to exchange RTS/CTS packets while other channels are used for transmitting data packets. It turns out that those multi-channel protocols also can improve the performance of multi-hop networks. The hidden station, exposed station and capture problems are mitigated since communicating station pairs may transmit in different frequency channels. However, there is no special mechanism in those protocols to handle capture, hidden and exposed stations in the multi-hop environment. Consequently, those problems are far from being resolved and may substantially deteriorate the traffic performance of a multi-hop network.

Some efforts have been put on adapting the 802.11 DCF to support the directional and smart antenna technology [39] or other technologies like Code Division Multiple Access (CDMA) [40] [43]. However, more efforts should be spent to make a wireless network operable in multi-hop environments by using those ideas.

Some work aims at enhancing the multi-hop performance of the 802.11 DCF/EDCA without using the multiple frequency channels or other new hardware equipments. In Distributed Reservation Request Protocol (DRRP) [44], communicating stations inform their neighbor stations about the planned transmissions when exchanging RTS/CTS packets. Potential hidden stations restrain their transmission according to received reservation requests. However, due to the existence of hidden stations and exposed stations, some stations cannot successfully send out RTS or CTS packets. Stations cannot establish a correct knowledge of their neighbor's intended transmissions. Moreover, how to efficiently allocate radio resources for highly bursty traffic is another big challenge that is unsolved.

2.4.2 Distributed Control MAC Protocols Supporting QoS

The 802.11 EDCA and Hiperlan/I [36] are two standardized MAC protocols for supporting QoS in fully distributed broadband networks. Both schemes provide prioritized channel access but without a mechanism to allocate a fixed portion of bandwidth for QoS transmission. In essential, those protocols implement QoS in distributed networks by letting each station try its best-effort in its location. In EDCA, the idle duration before starting a frame transmission is set in favor of higher level QoS traffic. Moreover the values of contention window (CW) limits CWmin and CWmax, from which the random backoff is computed, are also set in favor of higher QoS traffic. The higher the QoS requirement, the smaller CWmin and CWmax. However, smaller CWs lead to higher probability of collision in a highly loaded network by high QoS level traffic, increasing packet drop ratio.

Channel access in Hiperlan/I consists of three phases: the prioritization phase, contention phase and transmission phase. The first two phases comprise a number of contention slots used to transmit access bursts. The number of contention levels is equal to the number of contention slots. The aim of the prioritization phase is to allow stations with the highest priority frame to participate in the next phase. The contention phase is used to allow only one station to transmit its packet in the transmission phase. To achieve these goals, the number of contention slots in the first two stages amounts up to 31, introducing quite a lot overhead for each access cycle. The normalized maximum throughput is less than 0.4 when packet sizes are less than 512 bytes [45]. Furthermore, there is no mechanism to ensure fairness and resolve capture, hidden station and exposed station problems. Sobrinho et al. [38] present black-burst (BB) contention for distributed prioritized channel access. BBs are pulses of energy, the durations of which are a function of the delay incurred by the stations until the channel became idle. Like in Hiperlan/I, the number of contention levels is equal to the number of BBs. In highly loaded situations, the number of BBs shall be large, leading to quite a lot of overhead. Even though, BB contention cannot ensure that only one station wins a contention.

2.4.3 IEEE 802 Standardization Activities on the Multi-hop Mesh Networking

- **IEEE 802.11 TGs**

The IEEE 802.11 Task Group “s” is currently studying the MAC amendments for Extended Service Set (ESS) mesh networks [8].

The SEE-Mesh group proposes two MAC proposals [11]: One is based on EDCA with its proposed congestion control mechanism; another one is called Common Control Frame (CCF) running on multiple channels and operates like DCA [35] but with a single radio. The first proposal applies for small scale and lightly loaded scenarios. For the second solution, in addition to disadvantages known from DCA, the common control channel could be overwhelmed by contention in a multi-hop network which usually is highly loaded. Accordingly, the system performance is significantly degraded. So far CCF has no effective mechanism to handle this adequate.

The Wi-Mesh group has developed two MAC proposals [12]: Distributed Controlled Channel Access (DCCA) and Mesh Coordination Function (MCF). DCCA uses standard 802.11e elements and operates following a 3-steps procedure: Minimum common capability set identification, Mesh Transmission Opportunity (MTXOP) negotiation and MTXOP data transmission. MCF uses the EDCA for contention-based access or DCCA when a mesh station is in the regime of the HCCA. The issues of highly loaded situations, fairness, capture, hidden station and exposed station problems have not been addressed in the proposals.

- **IEEE 802.15 mesh networking**

As aforementioned, the IEEE 802.15.1 (Bluetooth) [4] and IEEE 802.15.3 [5] are two standardized WPAN protocols capable to support multi-hop operation. Standard IEEE 802.15.3a [6] is based on Multi-band OFDM Alliance (MBOA) [41] physical layer using ultra wide band (UWB) technology and supporting data rates up to 480 Mbps. A new MAC protocol proposed by MBOA for the standard is capable of supporting WMNs [42]. IEEE 802.15.4 [7] is intended for low data rate applications with low battery consumption and low device cost. Its MAC protocol supports network topologies including star, cluster and mesh. In a mesh topology, a PNC like in 802.15.3 networks starts the network and maintains key network parameters. A relaying station must use the time slots allocated by the PNC to transmit both data and control packets with the source and destination stations.

- **IEEE 802.16 mesh networking**

The IEEE 802.16 is a solution with central control, able to provide wireless broadband service with QoS guarantee in metropolitan areas. The 802.16 standard [13] specifies systems to operate in the 10-66 GHz and considers only line-of-sight scenarios. The 802.16a amendment [14] covers operation in 2-11 GHz, with non-line-of-sight connections. It supports point-to-multipoint (PMP) and mesh topologies. A mesh network can be created either by using distributed scheduling or centralized scheduling. With the distributed scheduling, all the stations including the mesh Base Station (BS) shall coordinate their transmissions in their two-hop neighborhood and shall broadcast their schedules (available resources, requests and grants) to all their neighbors. Stations shall ensure that the resulting transmissions do not cause collisions with the data and control traffic scheduled by any other station in the two-hop neighborhood. With the centralized scheduling, resources are granted by the BS under central control. The mesh BS shall gather resource requests from all the mesh stations within a certain hop range. It shall determine the amount of granted resources for each link in the network both in downlink and uplink, and communicates these grants to all the mesh stations within the hop range.

A mesh network with central scheduling control has limited multi-hop capability. It can support only a very small number of stations in a mesh. The distributed scheduling mode operates in a connectionless fashion, and is not compatible with the PMP mode. There is no way to guarantee QoS. Moreover, a formed network suffers from both the hidden station and exposed station problems.

The IEEE 802.16's Relay Task Group is developing a draft under P802.16j PAR [15], aiming at mesh protocols compatible with the 802.16 PMP mode and supporting TGe compliant mobile stations.

CHAPTER 3

Mesh Distributed Coordination Function

Mesh Distributed Coordination Function (MDCF) has been developed in this thesis. It aims at being a MAC solution for efficient WMNs supporting QoS delivery of high quality multi-media traffic in multi-hop operation. This chapter presents a detailed description of MDCF. As a MAC protocol, MDCF is designed to fit into the IEEE 802 reference model. It contains three parts: Media Access Control Protocol (MACP), Radio Link Control Protocol (RLCP) and Mesh Routing & Security. A general description of MDCF is presented in Section 3.1. Section 3.2 introduces the mechanisms of MACP. Section 3.3 describes RLCP. The routing and security issues are presented in Section 3.4. *Note that since MDCF is proposed for WMNs, later on, unless otherwise stated, the term Mesh Point (MP) is used instead of station when MDCF is refered to.*

3.1 General Description

MDCF is a protocol with fully distributed control running on a single frequency channel. It is based on Time Division Multiple Access/Time Division Duplex (TDMA/TDD) technology. Transmissions take place in periodic time slots. The operation of a network requires that the involved MPs are synchronized. MDCF runs independent of physical (PHY) schemes. The possible PHY layers include: the IEEE802.11a [3]/b [1]/g [18]/n [19] PHYs, Ultra Wideband (UWB) [6], Orthogonal Frequency Division Multiple Access (OFDMA) [47], Multi Carrier Code Division Multiple Access (MC-CDMA) [46], and other forthcoming high or low data rate transmission schemes.

Unlike in 802.11 DCF/EDCA and Hiperlan/I networks, where an MP contends for channel access to send one or several data frames (TXOP in EDCA), an MP in an MDCF network contends for channel access to reserve one or more periodic traffic time slots for transmission. If successful, the reserved times slots are thereafter allocated as a

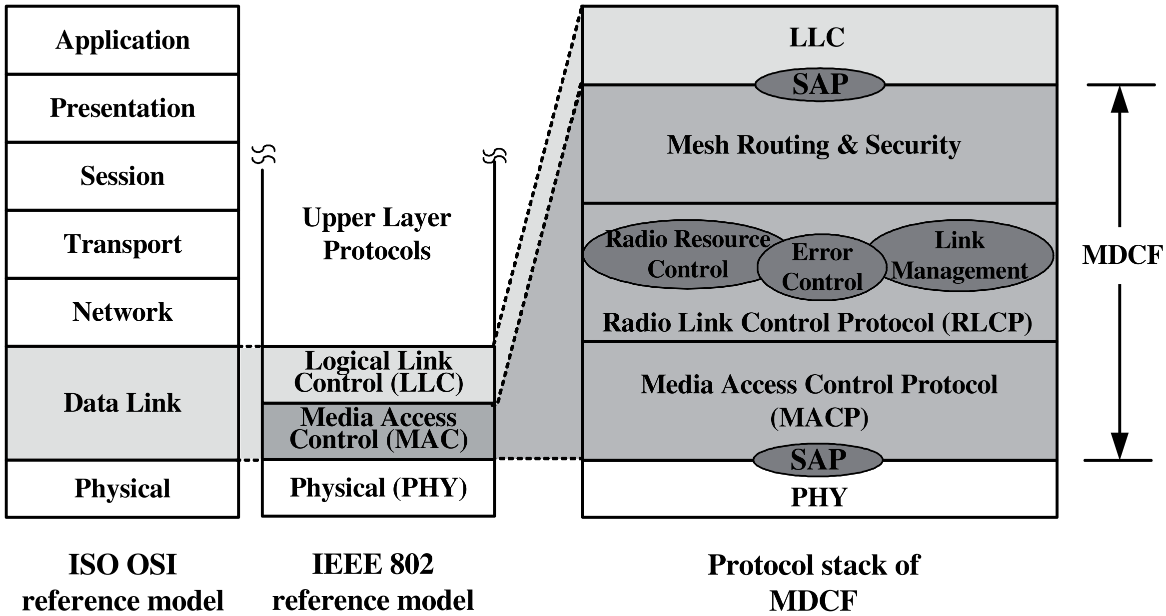

Figure 3-1. The protocol stack of MDCF.

TDMA duplex channel to the MP and its transmission partner. As a consequence, QoS can be guaranteed even when a network is highly loaded. Furthermore, the transmission efficiency of MDCF is independent on the packet size, different from 802.11 DCF/EDCA and Hiperlan/I. A Radio Resource Control (RRC) protocol operating fully under distributed control is used to evaluate and allocate a portion of bandwidth to a specific flow dependent on its QoS requirement. The number of traffic slots allocated for a flow is adaptable with the traffic load and overall usage of traffic slots in an MDCF mesh network.

An MP needs to perform the carrier sense function for channel access and also for determining free traffic slots. Energy signals, in-band busy tones [26], [49], play important roles in MDCF. They serve for 3 purposes: implementing a prioritized channel access with fairness guarantee, informing the use of specific traffic slots by a receiving MP, and implementing an on demand TDD turnaround scheme. Well designed by making use of energy signals, MDCF is able to properly handle high network load, hidden MPs, exposed MPs and signal capture which usually appear in a WMN and may dramatically deteriorate the network performance.

Reserved traffic slots forming a TDMA channel between two MPs are used to multiplex any packets transmitted on the link. Packet multiplexing on TDMA channel significantly enhances the channel utilization and reduces overall contention for channel access.

3.1.1 Architecture of MDCF Protocol Stack

All the functionalities of MDCF are mapped into the MAC layer, following the IEEE

802 reference model [17]. Figure 3-1 depicts the protocol stack of MDCF in the IEEE 802 reference model and its relation to the OSI 7-layer reference model [16]. MDCF provides the delivery service to the Logical Link Control (LLC) layer and utilizes the bit-stream transport service provided by the PHY layer. Two Service Access Points (SAP) form interfaces between MDCF and its adjacent layers.

MDCF comprises three sub-layers: Media Access Control Protocol (MACP), Radio Link Control Protocol (RLCP) and Mesh Routing & Security. MACP performs the prioritized channel access and transports its formatted packets following the TDMA/TDD mode of operation under fully distributed control. RLCP manages establishment of a radio link between RLCP entities, exchange of information via the radio link and adaptation of the radio resource (number of traffic slots) used for an established radio link. It mainly consists of three parts: Radio Resource Control (RRC), Error Control (EC) and Link management (LM). The Mesh Routing is responsible for discovering and maintaining the mesh topology. Based on the established knowledge of the mesh topology, an MP determines the optimal route for packet delivery. The security part serves for the purpose of securing information exchange in a WMN over the shared medium.

3.1.2 Brief Description of MACP

MACP is used by an MP to acquire the right to use the wireless medium in a fully distributed manner. It is based on TDMA/TDD technology. A MAC frame consists of a number of time slots. Traffic slots are used to transmit data packets. An MP is allowed to perform the media access procedure after it has achieved the TDMA frame synchronization with its network neighbors in its initiation stage.

When an MP has data to transmit, it first senses the carrier to check free traffic slots and then contends for channel access to transmit a request packet containing a number of traffic slots proposed for transmission. Channel access does favor high QoS level traffic. On reception of a request, the requested MP shall check whether to accept the request. In case of accepting, the MP transmits energy signals in energy channel slots paired to traffic channel slots to notify the requesting MP of the accepted traffic slots for transmission. Afterwards, transmissions take place like the following: the sending MP transmits packets in the traffic slots, and the receiving MP transmits energy signals to notify its neighbors that the specific traffic slots are in use. Energy signals may be used by the receiving MP to request the reverse channel transmission opportunity on some or all of the reserved traffic slots if it wants to transmit packets to the sending MP. Hence traffic slots are used in an on-demand-TDD mode.

Multi-hop operation is performed on a hop-by-hop basis, with each one-hop link operating independently from other links of a multi-hop route. The traffic slots reserved as a link by two MPs shall be used to multiplex any data packet routed via the link. The transmission sequence of competing packets is prioritized in each MP in favor of high

QoS level packets.

3.1.3 Brief Description of RLCP

A RLCP entity runs on the top of MACP and interacts with the LLC layer. A sending entity fragments a LLC protocol data unit (PDU) before passing it to MACP. A receiving entity reassembles the received packets into LLC PDUs and delivers it to the LLC layer.

Two types of delivery service are provided by RLCP via a one-hop link: the acknowledged mode (AM) for the error-free delivery service, and unacknowledged mode (UM) for connectionless services. A Selective Repeat Automatic Request (SR-ARQ) protocol is used to provide the error control and flow control service in the AM. A RLCP entity allocates service entities according to the traffic type. It may allocate a service entity solely for a flow. And it may also allow several traffic flows to share a service entity if their destinations and packet delay requirements are same. In a mesh network, a RLCP entity needs to maintain several service entities in parallel. It manages control of the overall buffer consumption.

RLCP also performs the Radio Resource Control (RRC). On reception of a link setup request indication from MACP, a RLCP entity shall consider in a fully distributed manner whether to accept the request or not. A RLCP entity may send a request to its MACP entity, asking it to contend for more traffic slots, or to perform the on-demand-TDD request, or to release some traffic slots. A decision made at RRC shall account for the transmission volume, traffic type and overall usage of traffic slots.

3.1.4 Frame Mapping in MDCF

MDCF consists of three distinct sub-layers. Each sub-layer provides services for its upper sub-layer. The PDU used in MACP, RLCP and Mesh Routing & Security are called MACP PDUs (MPDU), RLCP PDUs (RPDU) and Routing Security PDUs (RS_PDU), respectively. Figure 3-2 shows their mapping relations.

RS_PDUs are used by the Mesh Routing & Security sub-layer to implement the mesh topology discovery, topology maintenance, routes determination and security. They are mapped on the payload field of RPDUs. The RLCP fragments a LLC PDU into smaller RPDUs suitable for transmission over the lossy wireless medium. The length of a RPDU is dependent on the PHY data rate and the duration of a traffic slot. An MPDU is assembled in MACP by adding an MACP header in front of a RPDU. A PHY preamble is added to an MPDU before the MPDU is transmitted over the radio interface at a specified time slot. The preamble enables an MPDU to be decoded at the receiver side. The amount of PHY overhead includes Tx power on ramp, the preamble used for Automatic Gain Control (AGC), synchronization and channel estimation, Tx power off ramp and a guard time. Those overheads are PHY scheme and application dependent. For instance,

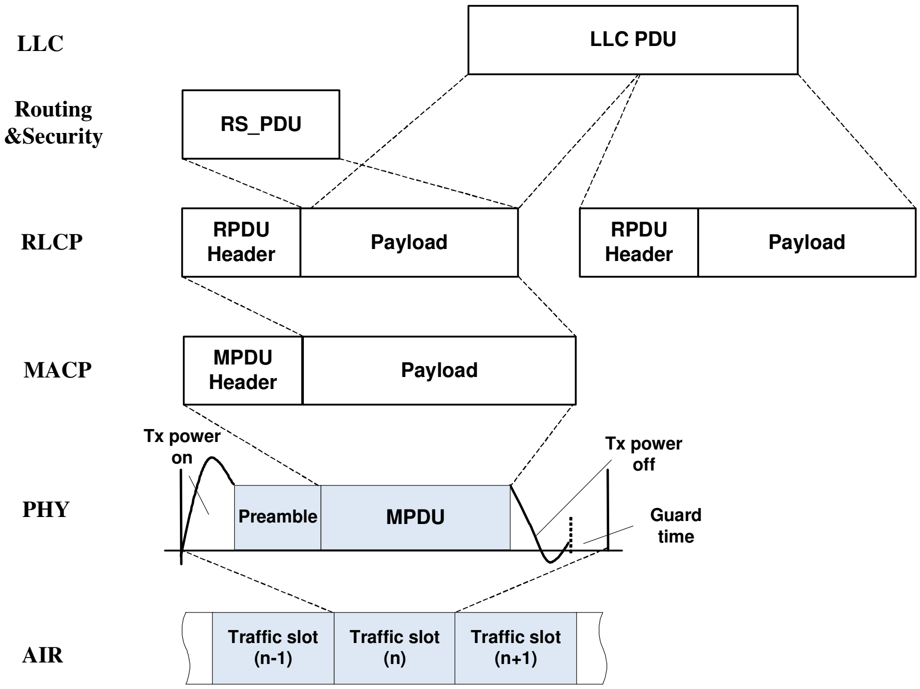

Figure 3-2. Frame mapping between adjacent sub-layers.

assuming the IEEE 802.11a PHY and WLAN application, the amount of the PHY overheads in a traffic slot is 9 µs in length.

The mapping of MPDU to PHY service data unit need not be 1:1 as shown in Figure 3-2, but would be n:1 or 1:n, dependent on the PHY cabpabilities.

3.2 Media Access Control Protocol (MACP)

Unless otherwise stated, all the following time parameters are example values assuming the IEEE 802.11a PHY [3] running on 5.2 GHz.

3.2.1 TDMA Frame and Energy Signals

An Energy signal is a non-modulated single on-off pulse, occupying a short time slice, e.g. 6 µs. A receiver only needs to sense it to derive the meaning. Hence, the influence range of an energy signal transmitter is up to the carrier sense range of it.

As shown in Figure 3-3, a TDMA frame contains a number of time slots that are logically grouped into 3 types:

- *Access Channel (ACH)*, where energy signals and access control data are transmitted to implement a prioritized and fair channel access.
- *Traffic Channel (TCH)*, where a slot can carry one MAC protocol data unit (MPDU) per TDMA frame.
- *Echo Channel (ECH)*, that each is paired to a TCH slot, resulting in the same

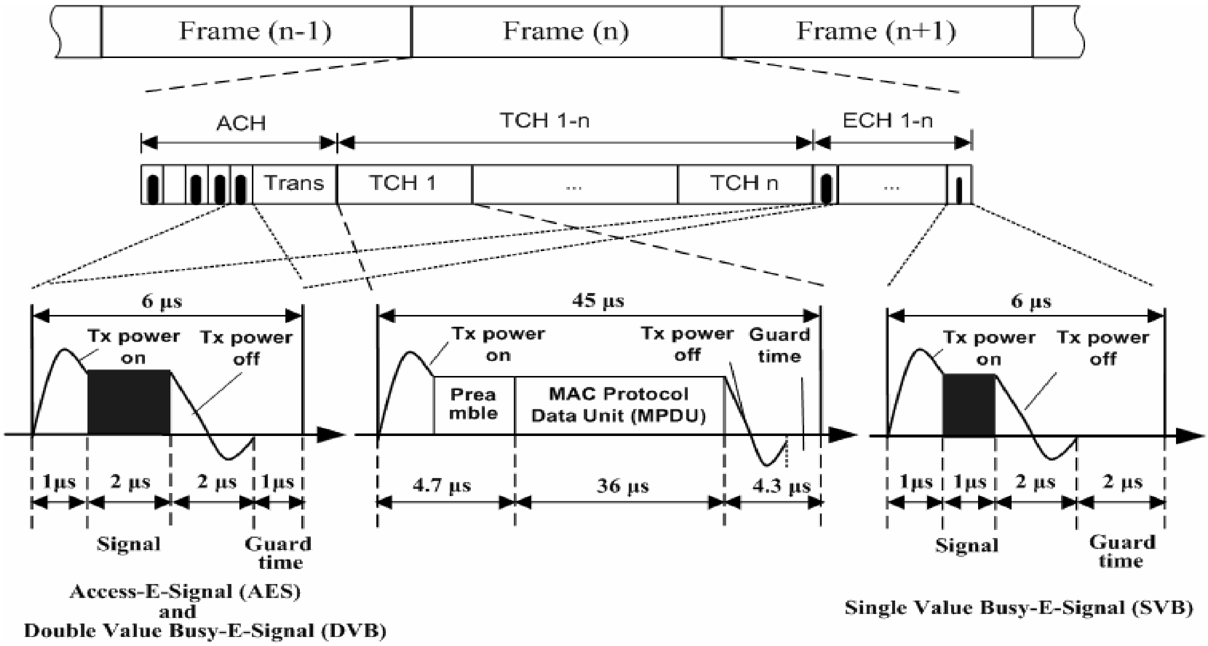

Figure 3-3. TDMA frame and energy signals.

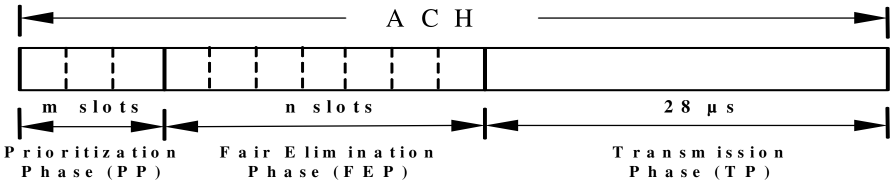

Figure 3-4. ACH structure.

number of ECH slots in a TDMA frame as that of TCH slots. An ECH is used to transmit an energy signal per frame by an MP receiving in the corresponding TCH to notify its nearby MPs that the corresponding TCH is in use.

Energy signals transmitted in the ACH (Access-E-Signals, AES) have a single burst nature, whilst those transmitted in ECHs are periodic and called Busy-E-Signals (BES). BES might be Single Value BES (SVB) or Double Value BES (DVB) according to the signal duration, see Figure 3-3.

An AES has the same waveform as a DVB. A SVB is transmitted on the ECH by a receiving MP for inhibiting hidden MPs. If the MP wants to turn-around the transmit direction in TDD mode, a DVB is sent in the ECH instead of a SVB.

An MPDU fits into a TCH slot, as shown Figure 3-3. It is preceded by a PHY preamble to enable decoding at the receiver. The MPDU length depends on the PHY mode. Table 5-1 shows an example assuming the IEEE 802.11a PHY. Each MPDU is allowed to carry up to 9 OFDM symbols. For different modulation schemes, the maximum lengths of MPDU vary from 27 bytes (BPSK, 6Mbps) to 243 bytes (64QAM, 54Mbps). Energy signals and MPDUs can be transmitted on the IEEE 802.11 a/b/g PHYs, requiring only minor driver modifications.

An ACH slot has three phases: Prioritization Phase (PP), Fair Elimination Phase (FEP) and Transmission Phase (TP), as shown in Figure 3-4. The PP and FEP consist of *m* and *n* contention slots, respectively, each slot one AES long. The PP is used to differentiate high QoS level traffic flows from others by prioritization. The FEP serves to guarantee with a high probability only one winner in each ACH contention and to ensure a fair channel access chance for each flow being maintained. A number of AESs are transmitted in the contention slots of the first two phases. Parameters like the number of TCHs in a TDMA frame, waveforms of energy signals, and number of contention slots in the ACH may be different for different PHY layers and applications, but are never changed during operation

Let TH^{O}_{TMT} be the normalized one-hop theoretical maximum throughput of MDCF assuming no packet loss during transmission, N_{TCH} the number of TCHs in a TDMA frame, N_{ECH} the number of ECHs in a MAC frame, P_{TDMA} the time period of a TDMA frame (unit: μs), P_{Con} the duration of a contention slot in the ACH, P_{TP} the duration of the TP, P_{ECH} the duration of an ECH slot, P_{TCH} the duration of a TCH slot, and O_{TCH} the amount of overheads in a TCH slot including durations of Tx power on, Tx power off, preamble and guard time. Form the definitions, we have:

$$P_{TDMA}=P_{Con}\times(m+n)+P_{TP}+P_{TCH}\times N_{TCH}+P_{ECH}\times N_{ECH} \tag{3.1}$$

Applying $N_{ECH} = N_{TCH}$ and $P_{ECH} = P_{Con}$ into Eq. (3.1) yields:

$$P_{TDMA}=P_{Con}\times(m+n)+P_{TP}+(P_{TCH}+P_{Con})\times N_{TCH} \tag{3.2}$$

TH^{O}_{TMT} is therefore given by:

$$\begin{aligned} TH^{O}_{TMT} &= \frac{(T_{TCH} - O_{TCH}) \times N_{TCH}}{P_{TDMA}} \\ &= \frac{P_{TCH} - O_{TCH}}{P_{TCH} + P_{Con} + [P_{Con} \times (m+n) + P_{TP}] / N_{TCH}} \end{aligned} \tag{3.3}$$

It is clear from Eq. (3.3) that the increase of N_{TCH} improves the efficiency of MDCF. When N_{TCH} -> ∞, TH^{O}_{TMT} reaches its maximum value: $(P_{TCH} - O_{TCH})/(P_{TCH} + P_{Con})$. However, a larger N_{TCH} results in a longer P_{TDMA}, as suggested in Eq. (3.2), causing a longer one-hop delay.

As will be described later, the more TCHs there are in a TDMA frame, the higher is the probability that one-hop transmissions of a multi-hop connection take place in parallel in a TDMA frame. When this happens, the transmitted packets shall experience low end-to-end delays. However, putting more TCHs into a TDMA frame results in a long TDMA frame, which adversely leads to long access delays and further long end-to-end packet delays. The detailed impact relation of the number of TCHs in a TDMA frame and duration of a TCH on the traffic throughput is shown in Eqs (4.16) and (4.20).

3.2.2 Prioritized Channel Access

MDCF is intended for WMNs with QoS guarantee. The channel access mechanism plays an important role for this. To support QoS, channel access should be prioritized and set in favor of high QoS level traffic. Furthermore, it should be highly eliminative, meaning that each access under contention with other access to the ACH generates only one winner. As a result, collisions can be avoided in the TP of the ACH. As introduced in Section 2.2, multi-hop networks tend to be highly loaded networks, with a large number of contentions for channel access. A highly eliminating access mechanism is critical to prevent collisions and avoid wasting scarce bandwidth. Moreover, channel access should be fair for competing end-to-end flows. The multi-hop environment is pretty complicated. Hidden MPs, exposed MPs and capture may result in serious unfairness of channel allocation [28], [31], [33]. Even those phenomena are well handled by MDCF. Highly load may cause unfairness. Without using effective mechanism to ensure fairness, neither QoS can be guaranteed, nor a network can operate stably: Unintentionally initiating a new connection might cause a network crash.

3.2.2.1 Contention Process

In Hiperlan/I [36] and the BB contention [38], a contention level is implemented by transmitting a number of continuous bursts or pulses of energy in contention slots. The number of contention levels is equal to the number of contention slots. In MDCF, a contention level is implemented by transmitting a number of AESs as a binary number in contention slots. The larger a binary number, the higher is a contention number. The amount of contention levels is equal to $2^{(\text{the number of contention slots})}$. This is a significant enlargement of contention levels. For instance, Hiperlan/I uses 31 contention slots to obtain 31 different levels whilst MDCF uses 12 slots to obtain 2^{12}= 4096 different levels. Only with so many contention levels, MDCF is able to implement a prioritized, highly eliminating and fair channel access. The contention levels in the PP and FEP are called PP contention levels (PPCL) and FEP contention levels (FEPCL), respectively. The amounts of PPCLs and FEPCLs are 2^m and 2^n, respectively.

When an MP wants to reserve TCHs for transmission, or broadcast a single packet in the TP, it needs to contend in the ACH for a chance to transmit in the TP.

The contention is performed as follows:

1) An MP selects a PPCL, $0 \leq \text{PPCL} \leq 2^m$-1, according to the type of traffic and the longest delay that the cached MPDUs have experienced. Section 3.2.2.2 gives a detailed description for the selection principle. The higher the number, the higher is the access priority.

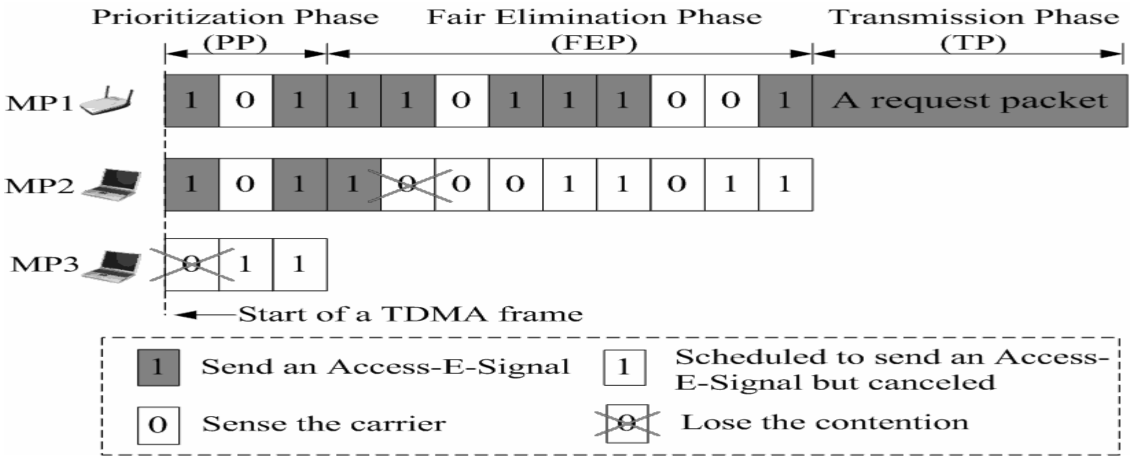

Figure 3-5. An example of channel access. MP1, MP2 and MP3 are in the mutual transmission range.

2) The MP checks the number bit by bit, when the bit is 1 it sends an AES, for 0 it listens. The most significant digit is transmitted first.

3) As long as the MP detects an energy signal during a listen period, it must cancel its pending energy signals and quit the contention.

4) If surviving the PP, the MP shall contend again in the FEP with a FEPCL, $0 \leq$ FEPCL $\leq 2^n$-1. A FEPCL is determined by the fair elimination principle described in Section 3.2.2.3.

5) If the MP wins in the above phases, it is allowed to transmit in the TP.

6) In case of losing, the MP shall contend again in the next TDMA frame.

Figure 3-5 illustrates a contention process. MP1, MP2 and MP3 contend for channel access at the same time. MP1 and 2 want to reserve TCH(s) for delivering Voice over IP (VoIP) packets to their partners, while MP3 wants to transmit video streams. Assume that the QoS priorities of the VoIP and video stream are 5 (101) and 3 (011) respectively. Both MP1 and 2 win in the PP by means of listening and sending AESs. After that, each of them generates a number and uses the number to compete again in the FEP. As shown in Figure 3-5, the generated numbers of MP1 and 2 for the FEP are 441 (110111001) and 283 (100011011) respectively. MP2 quits the FEP contention when it hears the second AES from MP1 in the FEP. Finally, MP1 sends out a request packet in the TP.

3.2.2.2 PP Contention levels (PPCLs)

Table 3-1 defines the PPCLs used in the PP. Beacons for synchronization are given the highest priority. Four traffic services are under consideration: voice, video, background and best-effort. Table 2-1 describes traffic services, their traffic behavior and their QoS requirements [9], [55]. According to the different packet delay requirements and their traffic behaviors, traffic flows are assigned with different access priorities. The Access

Table 3-1. PP Contention levels (PPCL) in MDCF.

Access Category	Traffic Type	Delay	PPCL
AC_Beacon	Control	-	7
AC_VO_HIGH	Voice	> 30 ms	6
AC_VO	Voice	<= 30 ms	5
AC_VI_SUP	Video	> 75 ms	5
AC_VI_HIGH	Video	(50 ms, 75 ms)	4
AC_VI	Video	<= 50 ms	3
AC_BK_HIGH	Background	> 200 ms	2
AC_BK	Background	<= 200 ms	1
AC_BE	Best Effort	-	0

Categories (AC) are ordered as: AC_VO (Voice, PPCL = 5), AC_VI (Video, PPCL = 3), AC_BK (background, PPCL = 1) and AC_BE (best effort, PPCL = 0). If pending traffic flows have been highly delayed, such as the delays (counted from the time that a packet was generated) for voice, video and background flows are over 30 ms, 50 ms and 200 ms, respectively, the corresponding PPCLs of those flows will be upgraded to AC_VO_HIGH, AC_VI_HIGH and AC_BK_HIGH, respectively. In case the delays of video MPDUs are over 75 ms (3/4 of the dropping threshold), their PPCLs are upgraded to AC_VI_SUP (PPCL = 5), which is equal to AC_VO. A voice flow generates traffic with a mean loaded of 0.0224 Mbps. In contrast, a video source is a highly loaded traffic with a mean load of 0.256 Mbps. This implies that in a period the service time of a voice flow on a TCH is much shorter than that of a video stream. Therefore, even when the MPDUs of a voice flow have the same residual life time as those of a video flow, they should be served first for achieving shorter overall delays and jitter [56]. The maximum allowed packet delay of video traffic is 200 ms. In a highly congested situation, video MPDUs of different flows shall experience long delays. Finely differentiating those MPDUs into different groups and letting the most stringent ones to be transmitted is an effective way to reduce the packet drop ratio. Based on this observation, video flows are classified into 3 groups (AV_VI, AV_VI_HIGH and VI_SUP) according to their experienced delay.

Amount of the PPCL levels is 8 (corresponding to m = 3), which is enough to serve 4 types of traffic flows in the multi-hop environment.

An MP may have many types of traffic flows destined to a same one-hop destination at a time. It shall determine its PPCL from the MPDU with the highest PPCL. The delay value used for determining the PPCL in a traffic flow is from the MPDU experienced the longest delay among all the pending MPDUs. Normally the MPDU is at the head of a transmission buffer, when the queueing discipline is First In First Out (FIFO).

It should be noted that a real-time MPDU is dropped (removed from the transmission buffer) as long as its delay is over 60 ms (Voice) or 100 ms (Video) [9].

3.2.2.3 Fair Elimination Channel Access

The number of contention levels in MDCF can be set very high without introducing too much overhead. Assume that the number of contention slots in the FEP is n, each with a duration of 6 μs. With an overhead of $6n$ μs, the amount of FEPCLs is up to 2^n. A fair elimination channel access is implemented in the FEP by making use of a wide range of contention levels. With this mechanism, even when a large number of MPs with the same level PPCL contend at the same time, after the FEP, only one survives and transmits in the TP, with a probability close to 1. Other MPs are eliminated for transmitting in the TP at the current TDMA frame. However, a fairness mechanism helps losing MPs to win a contention in future. The more often an MP loses the contention, the higher its chance will be to win in the next TDMA frame.

2^n contention levels (FEPCLs) are grouped into K equal sized non-overlapping Contention Number Groups (CNG): $[0, (2^n/K)-1]$, $[2^n/K, (2\times 2^n/K)-1]$, ..., $[(K-1)\times 2^n/K, 2^n-1]$. Each CNG contains $2^n/K$ contention levels.

At a time, there may be several MPs contending for channel access with same PPCL. Each contending MP maintains variables t^i counting the number of lost contentions for a given flow, where i is the flow ID. When an MP loses a contention in the FEP for competing for the flow i, it shall increment t^i by 1. If it wins, it reset t^i to 0.

When several flows in an MP request TCH reservation at the same time, the MP shall contend for the flow with the highest PPCL. If more than two flows contend with the same PPCL, the MP contends for the flow with the largest t^i. If there are more than two flows with the same largest t^i, the MP shall randomly select one flow and competes for it. The t^i values of other flows will be incremented by 1.

After winning the contention in the PP, an MP determines a CNG for generating a FEPCL. Each CNG is associated with a group selection threshold T^k, $k \in [0, K-1]$. If $T^k \le t^i < T^{k+1}$ when $k < K-1$, or $T^k \le t^i$ when $k = K-1$, then the k^{th} CNG is selected, from which a FEPCL randomly is generated. Note that a FEPCL from a higher CNG is bigger than that from a lower one. The amount of contention levels in a CNG is $2^n/K$, which should be big enough to ensure only one winner even under heavy contention.

3.2.2.4 Access Performance

To deepen the understanding of the channel access mechanism and highlight its advantages, this sub-Section shortly exhibits the access performance. A more detailed evaluation of the access mechanism is reported in the next chapter.

- ***Contention success probability***

Suppose that N MPs contend at the same time with the same PPCL and the FEPCLs are obtained from [0, 2^n -1]. Let $p(N)$ be the probability of only one winner in the contention. It can be derived:

$$p(N) = N\sum_{l=1}^{2^n} \frac{1}{2^n} \times (\frac{l-1}{2^n})^{N-1} \tag{3.4}$$

If N' of N MPs generate the FEPCL numbers from a same CNG, then:

$$p(N') = N'\sum_{l=1}^{2^n/K} \frac{K}{2^n} \times \left[\frac{K(l-1)}{2^n}\right]^{N'-1} \tag{3.5}$$

Assume that $N = 40$, $N' = 20$, the amount of contention slots in the FEP $n = 9$ and $K = 4$, then $p(N) = 0.961$ and $p(N') = 0.923$.

- ***Access delay***

Suppose that N MPs contend for TCH reservation at the same time when all the TCHs are free and each MP wants to reserve one TCH for use. Let P_{TDMA}, N_{TCH}, $E(D_{acc})$ the time period of a TDMA frame, the number of TCHs in a TDMA frame and the mean access delay, respectively. Assume the service time of a TCH is infinite and $N_{TCH} >= N$. $E(D_{acc})$ can be easily derived:

$$E(D^{O}_{acc}) = \frac{N-1}{2} \times P_{TDMA} \tag{3.6}$$

As an example, assume that $N = N_{TCH} = 16$, $P_{TDMA} = 1$ ms. It can be computed that $E(D^{O}_{acc})$ = 7.5 ms.

- ***Captureless channel access***

As introduced in Section 2.1 when being transmitted at the same time, instead of interfering with each other, energy signals strengthen each other to be sensed (binary OR). The *SINR* for energy signals can be computed by Eq. (2.2).

Take the contention process shown in Figure 3-5 as an example. No matter how MP1, 2, 3 are relatively located, as long as MP3 can sense an AES either from MP1 or 2, when MP1 and 2 transmit their own AES at the same time, MP3 can sense the transmission since energy signals strengthen each other. As analyzed before, the FEP ensures a high probability of only one winner in each ACH contention. Therefore in a potential interference area, there is only one MP that is allowed to transmit in the TP. No MP shall capture the channel access. Capture elimination on TCHs will be discussed later.

3.2.3 Link Setup and TCH Reservation

A *Link* in this thesis is defined as a physical path over the radio that is used to transfer MPDUs between two adjacent MPs. An MP wishing to transmit data MPDUs needs to setup a one-hop link and reserve TCHs agreed by the receiving MP. It first checks the local TCH status by performing carrier sensing. A TCH is considered free if:

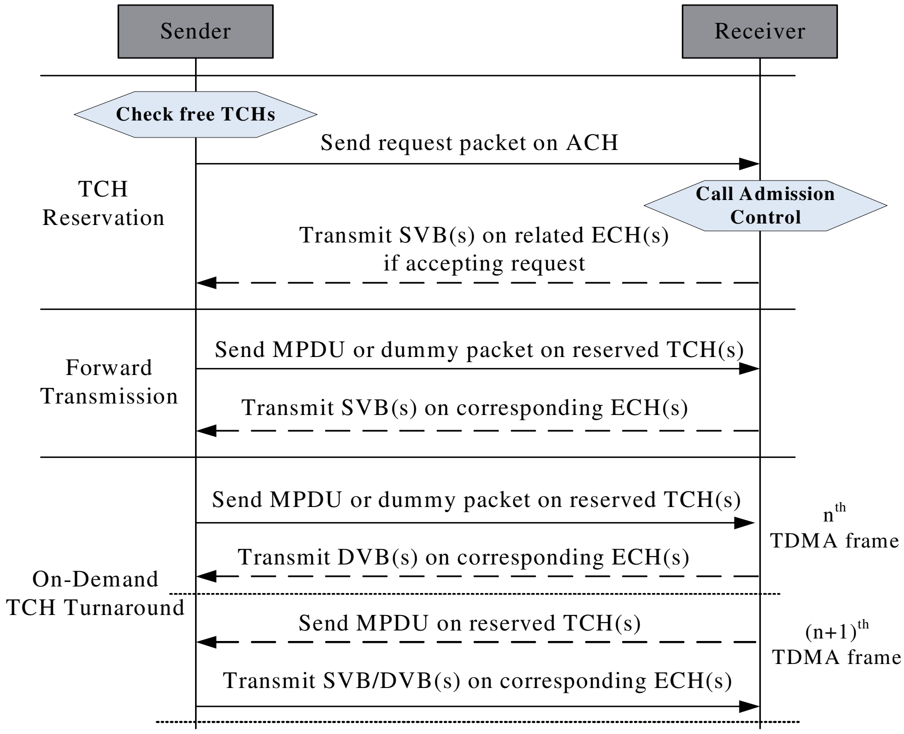

Figure 3-6. One-hop TCH reservation, transmission and on-demand TCH turnaround.

1) No carrier is sensed in the TCH, and
2) No BES is sensed in the ECH corresponding to the TCH.

Several TCHs can be used together for a traffic flow in order to meet its specific throughput and delay requirement. The requested number of TCHs in a TDMA frame is calculated at RLCP by considering the PHY modulation scheme and traffic behavior. Section 3.3.4.1 provides a detailed description. In case the amount of free TCH(s) meets the traffic needs, the MP would contend to transmit a request packet containing the receiver address, QoS-related traffic specification (QTS) and a list of proposed TCH slots in the TP of the ACH. On reception of the request packet, the requested MP determines whether to accept the request by evaluating the received QTS and the free TCH slots available at its location. The Call Admission Control (CAC) algorithm in RLCP performs this work. The request is accepted if:

1) the common free TCHs at both sides are adequate for the QoS delivery, and
2) establishment of the link will not corrupt the QoS of existing flows.

In case of accepting a request, the requested MP transmits SVB(s) in the ECH(s) associated to the accepted TCH(s). From the SVB(s), the requesting MP knows that the TCH(s) have been reserved, whereas nearby MPs derive that the TCH(s) are in use. Figure 3-6 shows the related message chart. Later on, transmission takes place in the reserved TCH(s). Please note that an end-to-end window based or TCP based flow

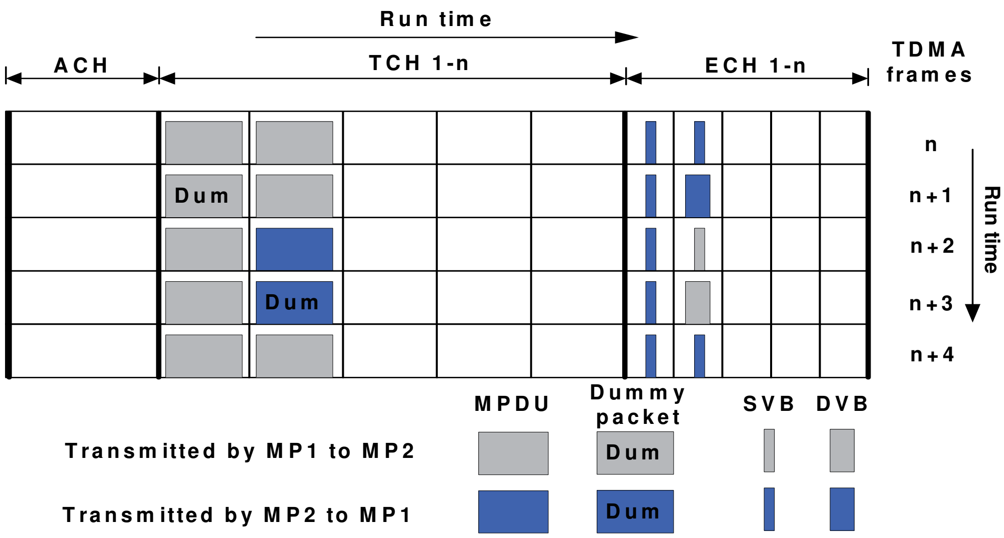

Figure 3-7. An example of packet transmission and on-demand TCH turnaround.

control located in the routing or transport layer should be applied to avoid sending two much packet by a source via a multi-hop connection that does want to be a bottleneck link on the route. This is however out of the scope of the thesis.

3.2.4 Transmission and On-demand TCH Turnaround

Hidden MPs are in the carrier sense range of a receiving MP but out of the carrier sense range of the transmitting MP as illustrated in Section 2.2. In MDCF, the receiving MP transmits SVBs or DVBs in ECHs paired to the TCHs where it receives data to inform hidden MPs that the specific TCHs are in use. As introduced, a TCH is considered free only when no carriers are sensed in the TCH and its paired ECH.

Reservation of fixed time slots to form a link for a transmission pair helps much to support QoS. But when traffic is bidirectional and especially asymmetric, how to efficiently utilize time slots is a challenging issue. An on-demand TCH turnaround scheme is proposed to address this issue. The transmission process is as follows:

Assume that two MPs reserve several TCHs, on each of which MP1 transmits either its MPDUs or dummy packets when it has no MPDU to transmit. As long as MP2 receives MPDUs or dummy packets in a reserved TCH (or a corrupted packet), it transmits a SVB in the ECH paired to the TCH, to signal the use of the TCH. If MP2 has MPDUs to send back, it transmits a DVB instead of a SVB in the ECH paired to a reserved TCH. If MP1 senses the DVB, from the next MAC frame on, it stops transmission in the TCH and starts to transmit energy signals in the related ECH, and MP2 starts to send its MPDUs in the TCH. This mechanism is called On-Demand TCH turnaround, see lower part of Figure 3-6.

Figure 3-7 gives an example. Assume that two TCHs are reserved by a transmission pair

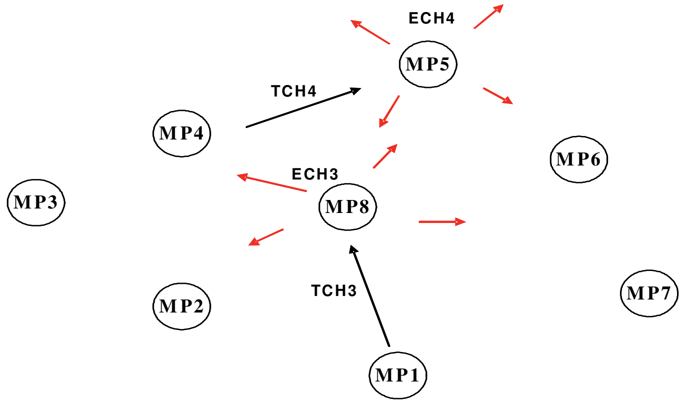

Figure 3-8. An example of calming down hidden MPs by transmitting BESes.

on which MP1 transmits MPDUs while MP2 transmits SVBs on the related ECHs. At the n+1th TDMA frame, MP2 has an MPDU to be sent to MP1. It transmits a DVB instead of a SVB on the related ECH of an intended TCH. Immediately after that frame, MP1 stops transmitting MPDU on the requested TCH but transmit a SVB on its related ECH, whilst MP2 transmits MPDUs on the requested TCH. At the n+3th TDMA frame, MP1 uses the same approach to acquire the transmission right back on the same TCH. Please note that with the example only, one of two TCHs used between MP1 and MP2 is being altered in its transmit direction, whilst the other one keeps its direction from MP1 to MP2.

On-demand TCH turnaround substantially increases the channel utilization efficiency. A receiving MP checks the number of pending MPDUs at both sides before turning around the channel. If necessary, one side shall initiate TCH reservation to request more TCHs. The related algorithm is presented in Section 3.3.4.3.

An example of calming down hidden MPs is shown in Figure 3-8. In the following context, the notation TCH n/ECH n means nth TCH slot/nth ECH slot in a TDMA frame. A transmission is ongoing between MP1 and MP8, where MP1 uses TCH 3 to transmit and MP8 replies with BESs on ECH 3 to inform its nearby MPs that the TCH 3 is in use. MP4 and MP5 are potential hidden MPs to MP1. If they have data to exchange, they shall select TCH(s) other than TCH 3 for transmission, since both of them can hear the BES on ECH 3 and hence deduce that TCH 3 is currently in use. In this example, TCH 4 is chosen by them.

Transmitting BESes on ECHs may help to calm down hidden MPs in the vicinity of a transmission pair. However this is not enough in a mesh environment. Additional mechanisms to calm down hidden MPs and the in-depth analysis are presented in the next section.

It is worth noting that each data MPDU does not need to contain the four addresses specified for the 802.11 DCF/EDCA MPDU. The address information has been exchanged earlier between a transmission MP pair during link setup. On reception of an

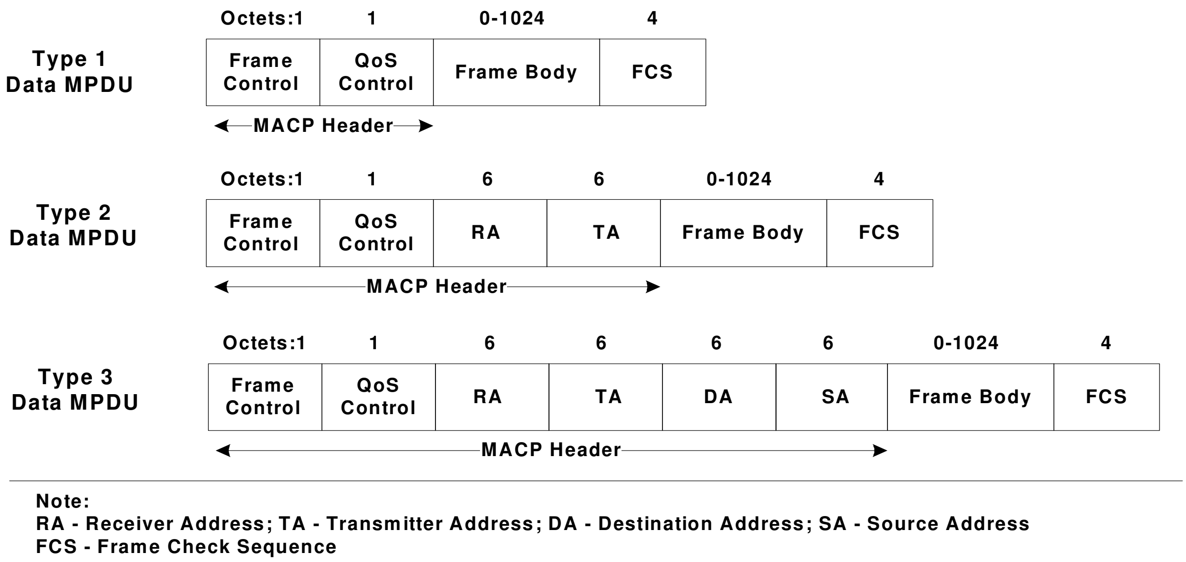

Figure 3-9. Frame formats of Data MPDUs.

MPDU in a TCH, an MP knows which MP has sent the MPDU and where it is destined for. Overhead is greatly reduced by this compared to DCF/EDCA. Three types of data MPDUs are defined. Figure 3-9 shows the formats. The header of Type 1 data MPDUs is 2 bytes long, containing no address information. In contrast, the header of 802.11 DCF MPDUs is 34 bytes in length. The header of Type 2 data MPDUs includes the MAC-addresses of the transmitting and receiving MPs, each MAC-address 6 bytes in length. Type 3 data MPDUs contain four MAC-addresses as with 802.11 DCF/EDCA. Type 1 data MPDUs are for unicast transmission while Type 2 and Type 3 are used for broadcast transmission. The field Frame Control indentifies frame type. The QoS Control field describes the type of traffic carried in a Data MPDU, and the number of pending Data MPDUs in the transmitter queue. Please refer to [109] for more details.

3.2.5 Calming down Hidden MPs in Mesh

Transmitting BESs helps to calm down some but not all hidden MPs of a transmission pair of two MPs in a multi-hop network. Additional mechanisms are proposed to assist in calming down hidden MPs while assuring good spatial reuse in mesh:

1) AESs are transmitted at twice the power level of MPDUs that are transmitted in TCHs and of request packets transmitted in the TP. It can be derived from Eq.(2.1) that twice the transmission power enlarges the carrier sense range by 1.15 to 1.4 assuming $\gamma \in [2, 5]$.

2) MPDUs in TCHs and BESs in ECHs are transmitted with the same transmission power. This assures a reasonable spatial reuse distance.

Suppose MP E in Figure 3-10 wants to reserve a TCH with F. E first checks the TCH occupancy status. Transmissions from B, C, D, F, G and H can be sensed by it, whilst

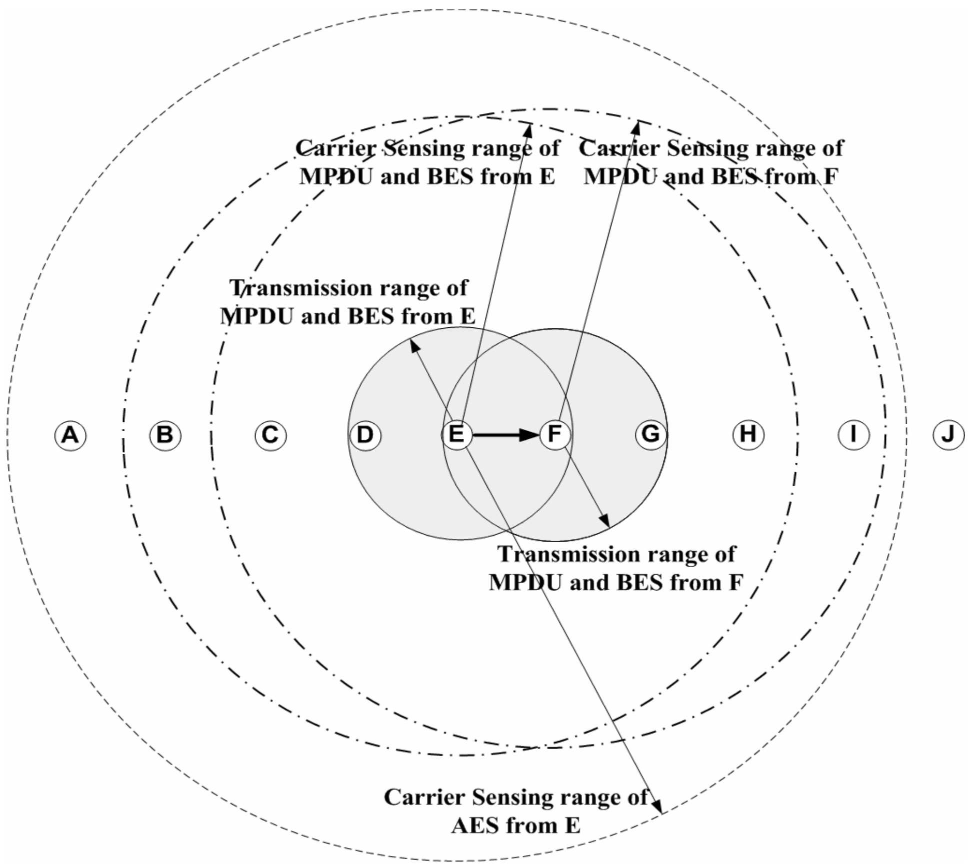

Figure 3-10. Calming hidden MPs in a MDCF multi-hop network.

transmissions from C, D, E, G, H and I can be sensed by F. E contends to send a request packet to F if it finds at least one free TCH. Using 2 times larger transmission power to send AESs, E extends its carrier sense range to cover a range until A and I when contending for channel access. As a consequence, there shall be only one winner (with a high probability) in the area covering A, B, C, D, E, F, G, H and I. In that area, it is not possible for a hidden MP pair to win contention in the same MAC frame. This prevents a hidden MP pair from reserving the same TCH. On receiving the request packet from E, F would select one or more TCHs that are not in use by B, C, D, G, H and I. Furthermore, since transmissions in the ACH and transmissions in TCHs take place in different time slots, contention for channel access and transmission of MPDUs will not interfere each other. When A and J want to transmit to some MPs, which are not in the carrier sense range of MPDUs and BESs transmitted by E and F, they may reuse the TCH being used by E and F. The spatial reuse distance is the sum of the transmission range and carrier sense range of MPDUs in this scenario.

In the 802.11 DCF/EDCA, the time information contained in RTS, CTS, DATA, and ACK packets is used to notify hidden MPs of reserved transmission time intervals. However this mechanism requires that hidden MPs are located in the transmission range of either *the sending MP or receiving MP. But the fact is that hidden MPs are often outside the transmission range of the sending and receiving MPs as explained in Section 2.1 and 2.2. A hidden MP most probably is able to sense those packets but not able to decode them. Therefore it only can roughly estimate the remaining time of an ongoing transmission and refrain itself for the duration of extended interframe space (EIFS). This mechanism cannot avoid interference even at the cost of setting a long EIFS. In contrast, MDCF establishes the knowledge of available TCHs purely by sensing the carrier. Consequently the knowledge is valid covering potential interfering MPs - hidden MPs.*

3.2.6 Handling of Exposed MPs and Capture

In Figure 3-10, assume a transmission is on-going between MPs E and F. When E transmits in a TCH, MPs B and C are potential exposed MPs of the transmission pair E-F. While, when F transmits in the same TCH (TCH turnaround), MPs H and I are potential exposed MPs of the transmission pair E-F. However as long as there are free TCHs in the vicinity of those MPs, they can reserve some for transmission. Therefore, exposed MP pairs may transmit concurrently in a TDMA frame if they are able to find disjunct TCHs that are free to be used. An exposed MP pair can fairly share the bandwidth.

In contrast, if it is a DCF/EDCA network, since B cannot sense transmissions from F, it may send a Ready to Send (RTS) to C. But C will reject the request since it can sense the transmission between E and F. Without receiving Clear to Send (CTS) from C, B derives that the network is busy and hence enlarges its back-off window, whereas E and F reset their back-off window after successful transmissions. If E and F have a large number of pending MPDUs, B will suffer from starvation. Similarly, C, D, G, H and I will be starved as well. The unfairness caused by exposed stations in DCF/EDCA multi-hop networks can hardly be resolved. Under MDCF control, this problem is eliminated.

As described in Section 3.2.2.4, channel access in MDCF is without signal capture. Since hidden MPs are calmed down during transmission of MPDUs in given TCHs, no parallel transmissions in the TCHs will interfere each other. Accordingly, no MP may capture a TCH in MDCF multi-hop networks.

Capture causes unfairness in a wireless network [33], [31]. To our best knowledge, we are not aware of any solutions able to resolve the capture impact in 802.11 DCF/EDCA multi-hop networks, although this topic has been extensively studied.

3.2.7 Packet Multiplexing

The reserved TCHs between two MPs are used to multiplex any MPDUs transmitted on the link. In a transmitting MP, MPDUs destined to the same MP are classified and put into 7 different priority queues according to their Access Categories shown in Table 3-1. The 7 priority queues are ordered as: VO_HIGH, VO, VI_SUP, VI_HIGH, VI,

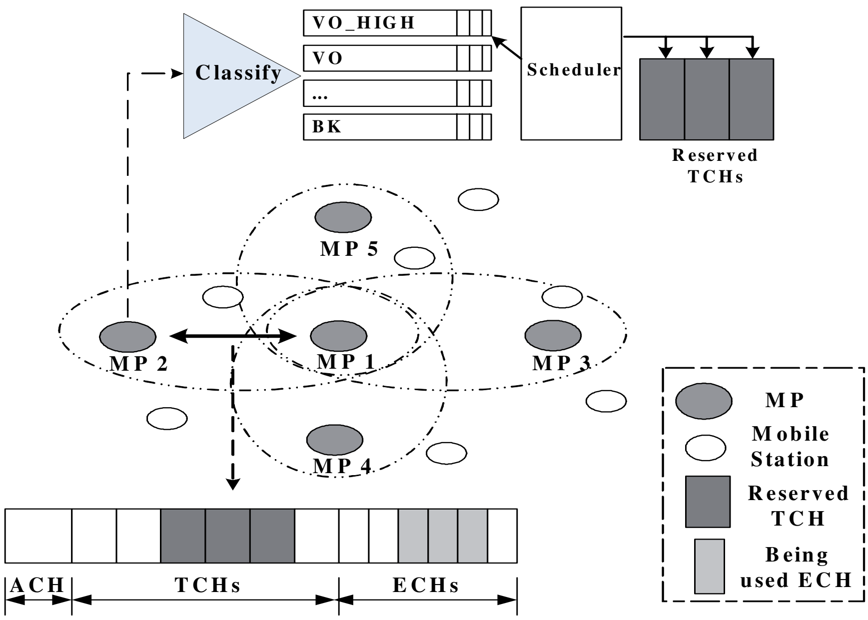

Figure 3-11. An example of packet multiplexing on reserved TCHs.

BK_HIGH, BK and BE. The VO_HIGH queue is given the highest priority.

Priority Queueing Weighted Round Robin (PQWRR) [57] is used as the queueing scheduling discipline. The overall queueing scheduling operates as Priority Queueing (PQ). The VO_HIGH queue is serviced first until the queue is empty. Then queues VO, VI_SUP, VI_HIGH are serviced one-by-one following the PQ fashion. The PQ scheduling assures that the most stringent real-time MPDUs are transmitted first. Consequently incurred packet delays and jitter of real-time traffic in this MP are relatively low. However in the PQ scheduling, if the volume of high priority traffic becomes excessive, the low priority traffic shall experience very long delay or even be dropped due to buffer overflow. In order to mitigate these problems, after all higher priority queues are empty, MPDUs in the queues VI, BK_HIGH, BK and BE may be scheduled in a Weighted Round Robin (WRR) [58] manner. The scheduler there allocates the chance to transmit for queues according to their weight set in favor of high priorities. Owing to the same length of MPDUs in all the queues, WRR fully exploits it advantages [52], [58], and in addition it is simple to implement. MPDUs per queue are scheduled in FIFO order.

Figure 3-11 illustrates the scheduler by example of an 802.11 ESS mesh network [8]. Four MPs form a multi-hop MDCF network on a single frequency channel while each of the MPs and its associated mobile stations communicate in a BSS network on another frequency channel. Assume that three TCHs are reserved for the link between MP 2 and 1. In MP 2, MPDUs from different peer-to-peer flows, directly destined to MP 1 are placed into different priority queues. The scheduler issues the grants separately for each queue. All the queued MPDUs are multiplexed into the reserved TCHs.

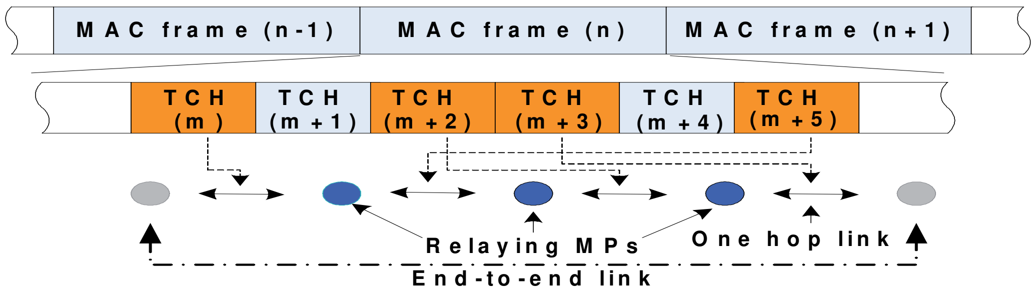

Figure 3-12. Multi-hop relaying and allocation of TCHs to a link.

Multiplexing of different streams to the same TCH(s) increases channel utilization. The bottleneck MPs will tend to have no more channel access overhead since it is then operating permanently on TCHs to its neighbor MPs unless some reserved TCHs may be forced released under high mesh traffic load (see Section 3.2.9.2). As a result, the network throughput and delay performance is optimized. In a more general WMN, the bottleneck MP may try to get access to more TCHs, and if successful, will starve the MPs keeping it with data packet. To prevent this, under high load, a timer is set for a TCH at a bottleneck MP since it is used to transmit non-real-time traffic. When the timer is expired, the related TCH is forced released. Hence, a stable balance in TCH allocation to the bottleneck MP and the other MPs is achieved and result then where some non-bottleneck MPs may compete and timewise will succeed to get TCHs allocated whilst other may then have to wait until a TCH becomes free.

3.2.8 Multi-hop Operation

A multi-hop transmission consists of multiple one-hop links in tandem that each independently operates on one or more TCHs in parallel. A relaying MP first receives MPDUs on a one-hop link and then transmits it to its next hop MP on another one-hop link. Figure 3-12 shows an example. The one-hop links may not have TCHs allocated in the same TDMA frame. A relaying MP may need to contend for establishing a one-hop link to transmit it forward. Error control and flow control offered by RLCP are performed on one-hop link basis. The end-to-end packet delay of a multi-hop connection is mainly attributed to retransmission delays at sequential one-hop links and access delay resulting from MPs contending for establishing one-hop links for transmitting. Under high load, end-to-end delay mainly comprises a sum total of access delays.

As shown in Figure 3-12, in MDCF networks the hop-to-hop relaying of a multi-hop connection might take place quasi-simultaneously, in different TCHs of a TDMA frame, resulting in low end-to-end delay. It appears that the more TCHs in a TDMA frame, the better is the delay performance. However this setting shall lead to a long TDMA frame and cause long access and retransmission delay. A trade-off between frame length and delay should be made. An analysis concerning this is performed in the next chapter.

The multi-hop routes of an end-to-end connection are determined by the Mesh Routing

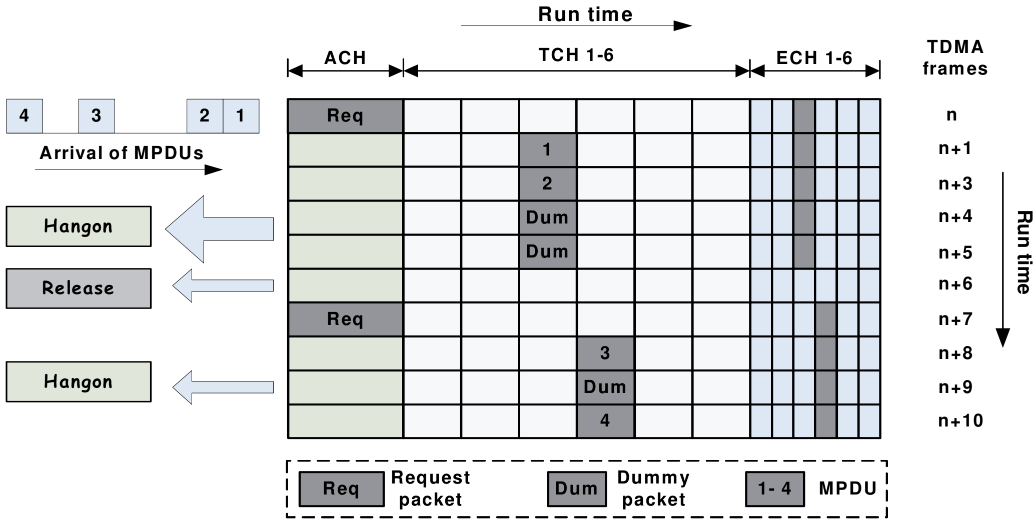

Figure 3-13. Release of a TCH on the expiration of the system wide specified hang-on time, which is 2 TDMA frames in this example.

& Security sub-layer. The MACP entity in an MP only cares for transport within one-hop with its peer entities located in adjacent MPs. However, the MACP entity needs to provide information like status and quality of the link to the Mesh Routing & Security sub-layer for enabling a radio-aware mesh routing protocol [9].

3.2.9 TCH Release

A TCH is released when one of the following conditions is met:

1) No MPDU is in the TCH transmitting buffers at both sides of an MP pair operating a link and a system wide specified hang-on time of the TCH is expired. The *hang-on time* is a time period that neighbor MPs should wait before releasing a reserved TCH when they have no MPDUs to transmit on the TCH. During hang-on, dummy packets are being transmitted.

2) Forced release of a TCH (may cause interruption of a link) that is used for transmitting dummy, background or best-effort MPDUs. This might happen when used TCHs are observed to fully utilize the TDMA frame.

3.2.9.1 Hang-On Release

When no MPDU is available for transmission on a reserved TCH at a time, the involved MPs will not release the TCH immediately. Instead, they hold the TCH for a certain period (hang-on time), to wait for the arrival of new MPDUs from the higher layer or from nearby MPs to be relayed on the TCH. If new MPDUs for that link will arrive during the hang-on time, the overhead to establish the TCH anew is saved. During hang-on, the sending and receiving MPs must transmit dummy packets and SVB on the TCH and its paired ECH, respectively, so that other MPs can sense it occupied. On expiration of the hang-on time, no more dummy and SVB are sent and the TCH is free.

Figure 3-13 exemplifies the process. Suppose at the n^{th} TDMA frame, two MPDUs in MP1 are waiting for transmission. Since MP1 has no reserved TCHs with the intended receiver MP2, it contends to transmit a request packet for reserving a TCH in the n^{th} TDMA frame. MP2 accepts the request by transmitting a BES on the ECH related to the agreed TCH. In the following two TDMA frames, MP1 transmits the 1^{st} and 2^{nd} MPDUs on the reserved TCHs. After that, the transmit buffer of MP1 is empty. However the transmission MP pair does not release the TCH immediately, but starts to count the hang-on time individually. MP1 transmits dummy packets and MP2 transmits SVBs during the hang-on period ($n+4^{th}$ and $n+5^{th}$ TDMA frames). The TCH is released at the $n+6^{th}$ TDMA frame on the expiration of the hang-on time (2 TDMA frames). No reserved TCH is available for transmission when the 3^{rd} MPDU arrives at the $n+7^{th}$ TDMA frame at MP1. MP1 must repeat the contention and transmission procedure exactly the same as before. At the $n+9^{th}$ TDMA frame, the TCH enters the hang-on state again when the 4^{th} MPDU arrives at MP1. Since the TCH is still reserved, the 4^{th} MPDU is transmitted at the $n+10^{th}$ TDMA frame. The new transmission triggers the reset of the hang-on timer at both sides.

TCH hang-on is aimed to reduce packet delay since the access delay at an MP may be avoided. For a specific flow, the longer the hang-on value is, the better will be the delay performance. On the other hand, a long hang-on time may lead to low channel utilization: If no MPDU arrives during the hang-on time, for the reserved TCH, it is completely wasted.

Finding an optimal hang-on value in a mesh network is of interest. It needs to account for the traffic behavior, mainly the interarrival time duration. Various traffic services can be roughly categorized as stream traffic such as voice and video, and TCP traffic like World Wide Web (WWW) and File Transmission Protocol (FTP) flows. A stream is generated at a specific pattern without considering the feedbacks from the receiver. However, it requires to be delivered under the QoS requirement. In contrast to this, a TCP source performs the error and congestion control during transmission. It sends a block of data packets at a time until the upper bound of the current congestion window is reached. Without receiving acknowledgements from the TCP sink, the source cannot continue to send higher sequence data packets. The interarrival time of packet blocks highly depends on the error control scheme in the MAC layer, the number of hops and the congestion situation of a network. Since TCP traffic is delay-tolerant, it is not of interest here.

The interarrival time of packets in a stream can be computed by:

$$I_T^A = \frac{Len_{APDU}}{SR_{APDU}} \tag{3.7}$$

Where I_T^A denotes the interarrval time of application packet data units (APDU),

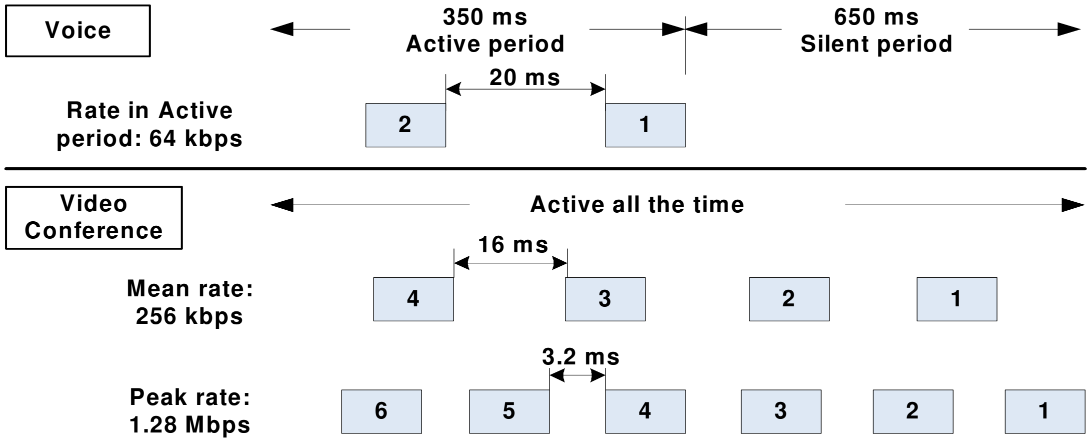

Figure 3-14. Interarrival times of real-time APDUs

Len_{APDU} the packet length of APDUs in bits, SR_{APDU} the stream generation rate at the application layer. An active period and silent period alternatively appear in a voice flow. The ratio of the active to silent period is 350: 650 [59]. Assuming the G.711 Codec [60], Len_{APDU} = 1280 bits and SR_{APDU} = 64 kbps. I_T^A of a voice stream is 20 ms. Considering the bidirectional nature of a voice communication, the average interarrival times of a voice traffic can be either 10 ms when the active periods of two sources overlap or otherwise 20 ms. In contrast to this, video traffic is highly bursty in nature. By using the information specified in Table 2-1, it can be calculated that the values of I_T^A for video conference traffic are 16 ms (mean rate) and 3.2 ms (peak rate), see Figure 3-14.

Let P_{TDMA} be the MAC frame length in ms, P_H be the hang-on time in units of MAC frames, I_T^M be the expected interarrival time of MPDUs on a TCH. As introduced before, MPDUs of different traffic types that are destined to different final destinations are multiplexed to a TCH. Therefore I_T^M may be much smaller than I_T^A. Assume $I_T^M = I_T^A/n$, where $n \geq 1$ is an estimated multiplex factor. P_H can be selected by the following equation:

$$P_H = Int\left[\frac{I_T^M}{P_{TDMA}}\right] = Int\left[\frac{I_T^A}{n \times P_{TDMA}}\right] \tag{3.8}$$

Where the function Int[•] returns the integer of a value.

In Eq. (3.8), I_T^A can be 20 ms, 10 ms, 16 ms and 3.2 ms, while n ∈ [1, 5]. Different combinations reflect different control policies. Selecting I_T^A = 20 ms and n = 1, P_H reaches its maximum value. Then a single voice stream can be guaranteed with the best quality (lowest delay), but the channel utilization is low. Using I_T^A = 2 ms and n = 5, P_H → 0 i.e. no hang-on period is used on average. This setting shall lead to a worse delay performance and high contention for TCHs.

3.2.9.2 Forced Release

Forced release may be applied to a TCH used to transmit traffic types “dummy”, “background” or “best-effort” by the MPs using it. This may happen in favor of real-time MPDUs waiting at other MPs, if the number of free TCHs in a TDMA frame is found to approach zero. Forced release of a TCH is performed by the sending MP through stopping transmission of MPDUs, or by the receiving MP by stopping transmitting BESs in the ECH. The short-term mesh network traffic volume can be estimated by an MP from observing utilization of all TCHs. An MP can adapt its own packet traffic volume so that under light utilization even low QoS-level MPDUs are transmitted, but only high QoS-level MPDUs are transmitted during high load.

When the MACP entity of an MP having reserved a TCH observes that all TCHs in a TDMA frame are reserved, it shall indicate the congestion situation to its RLCP entity. And the RLCP entity shall check whether with a reduced number of TCHs the MP would still be able to serve its real-time RPDUs in its buffer meeting the QoS requirement. Note that at a time, an MP may operate several reserved TCHs with different MPs. Under WMN congestion the RLCP entity needs to find one TCH sutiable for release on reception of an indication from its MACP entity. Section 3.3.4.4 provides a detailed description of the related RRC algorithm. Once the RLCP entity finds a TCH for release, it shall inform the MACP entity to perform the release action. Upon receiving the message from the RLCP entity, the MACP entity generates a control MPDU and sends it via reserved TCHs to its peer entity in a receiving MP selected by the RLCP entity, to ask for agreement to release a TCH. From the next TDMA frame on, the sending MP stops transmission on the TCH, while the receiving MP stops transmitting BESs on the ECH paired with the TCH if it correctly received the control MPDU. In case the sending MP detects that the receiving MP still transmits on the ECH, it knows that the control MPDU was lost and it shall repeat the control MPDU. After having released a TCH and a certain period is expired, if the MACP entity of an MP still observes the congestion situation, it shall indicate this again to its RLCP entity if the network is still congested. Please note that the above procedure is not suitable for a bottleneck MP, since the WMN capacity would then be reduced. To prevent the starvation caused by the bottleneck MP, under high load, a timer is set for a TCH at a bottleneck MP since it is used to transmit non-real-time traffic. When the timer is expired, the related TCH is forced released, see Section 3.2.7.

3.2.10 Adaptation of the Number of TCHs used for a One-hop Link

Reservation of part of the radio resource in a TDMA system for a link enables that QoS can be better guaranteed than in packet-based systems with reservation per packet such as 802.11 EDCA and Hiperlan/I. However, it is known that high-quality video streams are highly bursty in nature. Hence the allocation of a fixed share of the radio resource for transmitting video streams shall result in either a substantial waste of the bandwidth or a high queuing delay during a burst period. When adapting the number of TCHs reserved

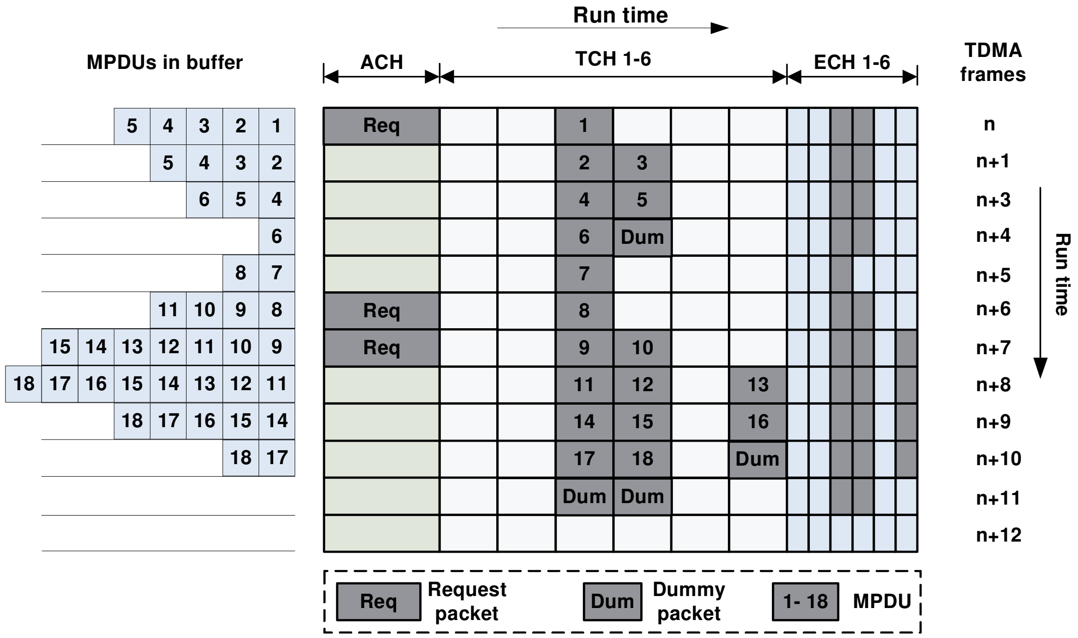

Figure 3-15. An example of adaptation of TCH number for a one-hop link. The hang-on time is 1 TDMA frame and the maximum allowed number of TCHs in a TDMA frame for the link is 3.

for a link to the current needs of a video stream, loosing capacity or introducing large packet delay peak can be avoided. MDCF has this capability.

1) An MP contends to reserve additional TCHs for a one-hop link if the reserved TCHs cannot satisfy the current traffic needs. The allowed maximum number of TCHs in a TDMA frame for a link at a time is related to the traffic type, traffic volume and channel utilization. The RRC algorithm in RLCP evaluates this.

2) A TCH not currently needed to satisfy QoS requirement of a stream shall be released as stated in Section 3.2.9.

Figure 3-15 illustrates how MDCF handles highly bursty video streams in an efficient way, satisfying the transmission needs while not wasting the radio resource. At the nth TDMA frame, MP1 has 5 MPDUs in its transmit buffer destined to MP2, with one TCH reserved. In order to deliver those MPDUs more quickly, it contends for transmitting a request in the ACH to MP2 for reserving one more TCH at the nth TDMA frame. On evaluating the request, MP2 agrees on reserving TCH 4 with MP1 and transmits a SVB on ECH 4 at the same TDMA frame. Note that the notation of "TCH/ECH n" is defined at Section 3.2.4. Afterwards, MP1 transmits MPDUs in TCH 3 and TCH 4, while MP2 transmits SVBs on ECH 3 and ECH 4. At the n+4th TDMA frames, MP1 only has one MPDU left and TCH 4 is not used. MP1 holds the TCH but starts the hang on procedure. The hang-on time in this example is 1 TDMA frame. At the n+5th TDMA frames, TCH 4 is still not used and the hang-on time is expired. Accordingly TCH 4 is released: MP1 stops transmitting dummy packets and MP2 stops transmitting BES. From n+6th to n+8th

TDMA frame, a relative high volume of MPDUs arrive at MP1 in a short time. Again, MP1 starts requesting TCHs to MP2. Correspondingly, TCH 4 and TCH 6 are reserved at the n+6th and n+7th TDMA frames, respectively. With 2 to 3 TCHs, MP1 delivers 10 MPDUs (from packet 9 to packet 18) in 4 TDMA frames (from n+7th to n+10th). From frame n+10th until n+12th, the reserved TCHs are released subsequently after expiration of their hang-on times. During all the transmitting, TCH 3 is kept. One TCH can satisfy and guarantee the delivery of a limited volume of traffic. Other TCHs should be requested when more traffic has to be served than can be carried by one TCH. MACP is able to adapt the share of the radio resource for a link according to the traffic needs. Consequently, highly bursty video streams can be delivered in time while a high channel utilization is achieved. The simulation results presented in Chapter 6 do prove this.

3.2.11 Broadcast and Multicast

Broadcast and multicast MPDUs can be Type 2 or Type 3 Data MPDUs, containing 2 or 4 addresses as introduced in Section 3.2.4. There are three means to broadcast or multicast MPDUs in MDCF multi-hop networks:

1) In case an MP has reserved TCHs for use with another MP, it will use one or some of the reserved TCHs to transmit broadcast/multicast MPDUs.

2) In case an MP does not have any reserved TCHs for use, it will select one MP from its one-hop neighbor list maintained in its cache, and send a TCH reservation request by contending in the ACH and then proceed according to 1.

3) An MP may transmit single broadcast/multicast MPDU in the TP of the ACH after winning an ACH contention if the size of the MPDU fits into the TP.

Broadcast/multicast transmissions in MDCF networks will not interfere with, or be interfered by other unicast transmissions in the multi-hop environment since interence free transmission via TCHs and via ACH-TP is guaranteed.

In contrast, 802.11 DCF/EDCA networks suffer from the serious hidden MP problem when performing broadcast/multicast. In 802.11 DCF/EDCA networks, no RTS/CTS exchange shall be used when broadcast/multicast packets are transmitted. In addition, no ACK shall be transmitted by any recipient of the broadcast/multicast. Since a receiving MP is not allowed to transmit any packets on reception of broadcast/multicast packets, the hidden MPs of a broadcast/multicast source MP have no way to know about the ongoing transmission. Their transmissions will cause interference to reception of the broadcast/multicast packets.

Delivery of broadcast/multicast MPDUs in an entire mesh network needs support by the specific higher layer protocol. A summary of various algorithms used to implement an efficient broadcast/multicast delivery in multi-hop networks is presented in [53].

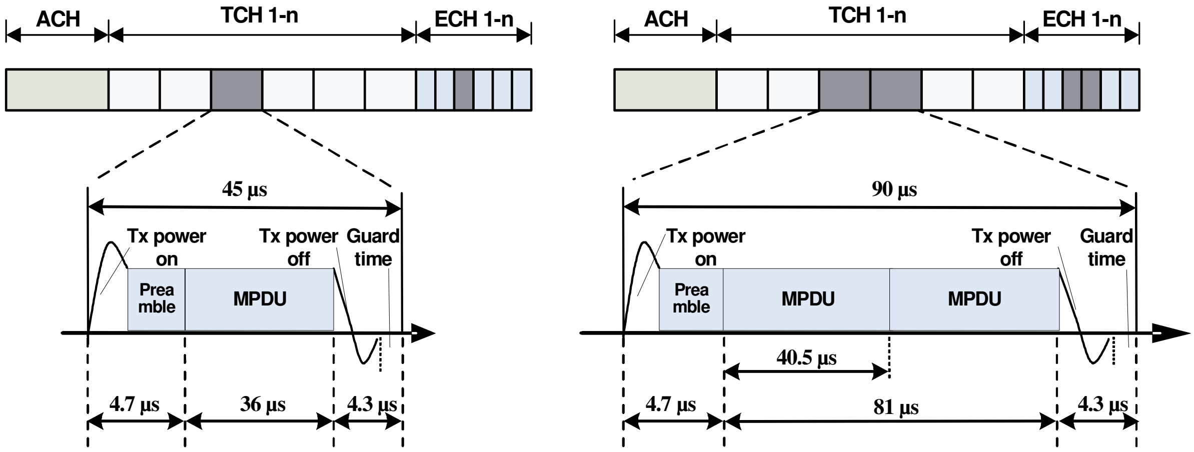

a) One TCH in use. b) Two adjacent TCHs used together.

Figure 3-16. An example of transmitting as MPDU trains.

3.2.12 MACP Protocol Data Unit (MPDU) Trains

Several TCHs may be used in parallel for transmission on a one-hop link (operating TCHs in parallel in MDCF is not limited to one frequency carrier). When two or more adjacent TCHs are used for a link, some control periods can be removed as shown in Figure 3-16b. As a result, a higher transmission efficiency can be achieved. When one TCH is used as shown in Figure 3-16a, the payload period is 36 µs while the amount of control periods is 4.7 + 4.3 = 9µs. The PHY transmission efficiency is 36/45 = 0.8. In contrast, when two adjacent TCHs are used combined for a one-hop link, if the intermediate control periods are removed, the PHY transmission efficiency is increased to 81/90 = 0.9.

However transmitting a longer MPDU on the lossy radio channel may cause a higher packet error ratio. Therefore, a long payload period must be fitted with several short MPDUs, each containing its own Cyclic Redundancy Check (CRC) information. The respective MPDUs form a so-called MPDU train. All MPDUs in a train have the same length and format. The number of MPDUs and length of MPDUs fitted into a multiple TCH payload period may depend on the radio channel quality and PHY mode used. An agreement for this should be reached between the communicating MPs.

3.2.13 Synchronization

3.2.13.1 Introduction

MDCF has lots of advantages over packet-oriented protocols like the 802.11 DCF/EDCA and Hiperlan/I in mesh environments. The advantages include: 1) Allocation of a scalable portion of the radio resource to one-hop links for guaranteeing QoS even in highly loaded situations. 2) Separation of contention for channel access and data transmission in different time domains to avoid its mutual interference. 3) Use of the TCH utilization in an interference-prone area for efficiently handling hidden and exposed MPs. 4) Knowledge of the short-term network traffic volume by monitoring the TCH utilization. The knowledge is important for the RRC protocol to take actions.

These advantages apply if a global synchronization is acquired among MPs for TDMA operation in the multi-hop environment. In order to communicate in the TDMA mode, MPs in a network must agree on a common frame structure and a frame start time for operation. Caused by different drift rates of oscillators in MPs, MPs may lose synchronization as time passes by. Therefore, the achieved synchronization is valid only for a while and needs to be maintained and refreshed from time to time.

In a centrally control single-hop wireless network, the synchronization function can be easily implemented. Mobile stations only need to synchronize to the central controller, which periodically broadcasts synchronization messages. However, implementing synchronization for TDMA operation under distributed control is not trivial. An 802.11 DCF/EDCA network requires that all stations in a network are synchronized for a number of reasons like power saving. But even if synchronization is not achieved, packet-oriented systems may function well for transmitting and receiving packets (except the 802.11b FHSS version). Contrary, in a distributed TDMA system, a non-synchronized MP may crash the network when transmitting.

This Section introduces a synchronization algorithm for MDCF, called MDCF timing synchronization function (MTSF). It operates in a fully distributed manner and can be used to synchronize MPs in an MDCF multi-hop network for TDMA operation.

3.2.13.2 Related Work

Numerous synchronization protocols have been proposed for distributed wired and wireless networks. Most of the protocols share a common idea: time information is periodically exchanged either by using packets or other formats of messages among stations. Recipients adjust their timer based on the received information.

The network time protocol (NTP) [61] is widely used in the internet for achieving clock synchronization. It is based on the assumption that the network is static. In the network, a hierarchy structure is built among stations in a predefined manner. Multiple root stations are synchronized to an external clock. The other stations are synchronized with their parent stations by analyzing packets carrying timestamps from the parent stations.

The IEEE 802.11 standard defines Time Synchronization Function (TSF) [1] for implementing synchronization in a distributed manner within a BSS network. Each station maintains a local time. Beacon packets containing time information of sending stations are broadcast periodically. A station adopts a time when the time specified in a beacon is later than its own, which means that a station only synchronize to a faster station. All stations in a network are given an equal chance to generate and transmit beacons. L.

Huang etc. points out [63] that TSF does not scale well. When the number of stations in a BSS is not small, there is a non-negligible probability that the stations may get out of synchronization. It cannot support a large-scale ad-hoc network. The scalability problem of TSF stems from the fact that faster stations cannot send out beacons timely in a highly dense network. A modification named Adaptive Timing Synchronization Procedure (ATSP) is proposed in [63], where stations adjust their frequencies to transmit beacons in each beacon interval anew. A faster station increases its beacon transmit frequency while a slower station decreases its frequency. J. So etc. [64] propose Multi-hop Timing Synchronization Function (MTSF) for synchronizing stations in a DCF/EDCA multi-hop network. MTSF is based on TSF. The basic idea is to have each station maintain a path to the station with the fastest running clock in a network, and propagate the time of the fastest station through the path. Sooner or later, every station can synchronize with the fastest station. Simulation results in [64] show that MTSF achieves stable clock accuracy at a low cost. However the design and evaluation of MTSF does not take the hidden station problem into consideration. In an environment where the collision cannot be avoided, timely propagation of beacons throughout a network cannot be guaranteed especially when the network is highly loaded. As introduced in Section 2.2, a multi-hop network tends to be highly loaded and the 802.11 DCF/EDCA cannot inhibit hidden stations to prevent collision in a multi-hop environment. Accordingly synchronization accuracy and stability can hardly be assured by using MTSF.

Several uncertain delays like the access delay and computation delay may considerably impact synchronization accuracy [67]. The Reference Broadcast Synchronization (RBS) [62] protocol considers those uncertain delays. In RBS, stations periodically send beacons using physical-layer broadcast. Receivers use the arrival time of beacons as point of reference for adjusting their clock. The uncertain delays are therefore largely eliminated. A high accuracy is achieved at the cost of high overhead and memory consumption. RBS does not scale for large networks.

Above protocols are designed for packet-oriented networks. Synchronization to an external clock is another category. Each station then does need an additional device for receiving the synchronization message. The Global Position System (GPS) [68] provides a generally available time synchronization source. The reception of the GPS signal requires a clear sky view, which is not available in lots of scenarios. W. Zhu [66] proposes a synchronization scheme for distributed TDMA operation by using the external radio clock signal DCF77. Synchronization based on an external clock is applicable to every kind of systems and is also perfectly suitable for multi-hop scenarios as long as the external signal is available. The need for an additional device and high power consumption makes external synchronization too costly for most applications.

3.2.13.3 General Description of MTSF and Definitions

Operation of an MDCF mesh requires that the frame level synchronization is achieved

Octets:1	1	6	6	6	4
Frame Control	QoS Control	TA	BSSID	Frame Body	FCS

MACP Header

Order	Field	Length in octet	Description
1	Transmitted time slot	1	Specifying the time slot used to transmit the beacon
2	Utilization of TCHs	4	Description of free and busy TCHs observed by the beacon transmitting MP
3	Reserved	1	For future use

Note:
TA - Transmitter Address; BSSID - Basic Service Set Identification
FCS - Frame Check Sequence

Figure 3-17. Beacon frame format.

between all MPs in the network. This function is provided by MTSF. MTSF is performed by all MPs in a fully distributed manner. *Synchronization* in an MDCF network is said to be achieved if the TDMA frames of any two MPs match sufficiently well for TDMA operation. Beacons are used to exchange information for synchronization among MPs. Figure 3-17 shows shows the beacon frame format. The field of Transmitter Address (TA) specifies the MAC address of the beacon transmitting MP. The Basic Service Set Identification (BSSID) field indentifies the ID of the BSS network where the beacon transmitting MP belongs. A *beacon* in MDCF is either transmitted in a TCH or ACH slot. The beacon frame body contains the information of the time slot where it was transmitted. From this information, a beacon receiving MP can derive the time instant that the beacon transmitting MP started its current TDMA frame. An MP does not need to maintain a local time. Instead, it only needs to record the start time instant of the last TDMA frame. Please note that the beacon frame body also contains the information of the utilization of TCHs observed by the beacon transmitting MP. The information serves for performing RRC, see Section 3.3.4.

Beasons are generated and transmitted periodically. According to the different roles in initiating synchronization, MPs are classed into 2 types. The *Type 1 MP* is the one that has right to send out the first beacon in a network, specifying the frame structure and the start time of a TDMA frame. Others are *Type 2 MPs*, which are not allowed to send out beacons before receiving a beacon. On receiving the first beacon, a Type 2 MP starts to schedule it own TDMA frame synchronizing to the beacon sender, marks its state as synchronized and thereafter participates into beacon generation. *In a single-hop MDCF network, every MP can be a Type 1 MP, whilst in a multi-hop MDCF network, only one MP can be Type 1 MP and others are Type 2 MPs*. The TDMA frame information, mainly the start time of the TDMA frame, is propagated from the Type 1 MP hop-by-hop throughout the entire network. After sending out the first beacon, the Type 1 MP acts same as the Type 2 MPs. The maintenance of synchronization is performed by all MPs in a fully distributed manner.

When an MP is synchronized, it attempts to transmit beacons if it does not receive a valid beacon in a predetermined time interval. The definition of the valid beacon is given in 3.2.13.4.2. A beacon should be transmitted using the most robust PHY mode, a high transmission power, or both, to assure a high *SINR* at receiving MPs. On reception of a valid beacon, an MP adjusts the start of the next TDMA frame, trying to synchronize to the beacon sender. In the period of no beacons received, an MP shall schedule periodical TDMA frames locally.

Oscillators at different MPs tick at different rates, leading to *clock drift* in a given period. The time difference between two MPs at an instant is called *time skew* which is mainly due to clock drift in a beacon interval. A compensation algorithm is used to alleviate the effect of clock drift. Based on that, a high precision synchronization is achieved at low overhead.

A mechanism is used to help an MP to determine whether it is located in an overlapped area in a multi-hop network. If so, it increases or otherwise reduces the frequency to transmit beacons. With this, synchronization for TDMA operation in a multi-hop network can be achieved.

The following definitions are used in this Section:

BT_S: The minimal integer used for calculating a beacon generation period.

BT_W: The window size used for calculating a beacon generation period.

d_i : A variable used to compensate the physical drift rate of MP i; d_i in units of ppm (parts per million).

D_{pro}: The amount of processing delay on the way from sending a beacon to the completion of analyzing a beacon, including the computation times at the sending and receiving MPs, and initialization times of antenna and transceivers.

max(x): The symbol denoting the maximum value of an uncertain value x.

P_{ACH}: The duration of an ACH including Prioritization Phase (PP), Fair Elimination Phase (FEP) and Transmission Phase (TP).

P_{FEP}: The duration of the FEP in an ACH.

PHY_B: The PHY data rate used to transmit beacons.

P_{PP}: The duration of the PP in an ACH.

P_{TCH}: The duration of a TCH.

$\boldsymbol{P_{TDMA}}$: The period of a TDMA frame.

$\boldsymbol{S_B}$: The length of the beacon frame in bits.

$\boldsymbol{ST_{Li}^n}$: The start time instant of the n^th TDMA frame at MP *i*.

$\boldsymbol{ST_{Ri}^n}$: The derived start time instant of the n^th TDMA frame of the beacon sending MP, which is derived at the receiving MP *i* without considering the propagation delay and the time skew between the beacon sending and receiving MPs.

$\boldsymbol{\Delta ST_{RLi}^n}$: The time difference between ST_{Ri}^n and ST_{Li}^n (i.e. $\Delta ST_{RLi}^n = ST_{Ri}^n - ST_{Li}^n$) calculated at MP *i*.

$\boldsymbol{T_{adj}}$: The time instant until an MP is allowed to adjust d_i since it is synchronized.

$\boldsymbol{TCH_i}$: An integer representing the i^{th} TCH slot where an MP receives a beacon. The one next to the ACH is the 1^st TCH, corresponding to TCH_1.

$\boldsymbol{T_{guard}}$: The guard time in an energy signal and also in a TCH.

$\boldsymbol{t_{ij}}$: The propagation delay between MP *i* and *j*.

$\boldsymbol{T_i^n}$: The local time when receiving the last bit of a beacon frame at the n^th TDMA frame at MP *i*.

$\boldsymbol{T_{slow}}$: The time instant from when an MP is only allowed to slowly adjust d_i.

$\boldsymbol{T_{SYN}}$: The time instant until an MP is synchronized.

$\boldsymbol{\Delta X_{ij}}$: The time skew between the sending MP *i* and the receiving MP *j* in a beacon interval. The time skew here is owing to the clock drift.

3.2.13.4 Use of Beacons

3.2.13.4.1 Beacon generation

Each MP in the synchronized state maintains an MTSF timer for beacon generation. An MP expects to receive beacons at a nominal duration. Otherwise, it shall generate and send a beacon. The beacon generation interval is defined by the parameter *MeshBeaconPeriod* within each MP. The *MeshBeaconPeriod* shall be a multiple of P_{TDMA}. It is randomly selected from $[BT_S \times P_{TDMA}, (BT_S+BT_W) \times P_{TDMA}]$. On the expiration of a beacon generation timer, an MP shall:

1) Select a TDMA slot to transmit a beacon. If at least one TCH is reserved by the MP for transmission, a TCH shall be selected for beacon transmission. Otherwise the beacon shall be sent on the ACH by contending with the highest priority.
2) Wait for the start of the selected slot, either ACH or TCH.
3) Stop preparing for beacon transmission, if a beacon arrives before the selected slot

starts.

4) Generate and send a beacon if contending in the ACH is successful, or if the selected TCH starts. Beacon carries the description of the time slot on which it is transmitted.

If an MP receives a beacon before the expiration of its beacon generation timer, it shall reset the timer with a newly selected *MeshBeaconPeriod*.

3.2.13.4.2 Beacon reception

An MP in the synchronized state shall utilize information contained in received beacons for calibrating. Two types of received beacons are distinguished:

1) *A valid beacon* is the one to contain the TDMA frame structure information that agrees with the local TDMA frame structure. Eq. (3.14) gives the principle to judge whether a received beacon is valid or not. An MP that receives a valid beacon is considered synchronized with the beacon sending MP. But it needs to calibrate the start of the next TDMA frame aiming at reducing $\Delta ST_{RLi}{}^{n}$ in future.

2) The second type of received beacons is the *invalid beacon*. In an invalid beacon the contained transmission channel description does not coincide with the local TDMA frame structure. An MP receiving an invalid beacon considers that it is in an interfered area and shall take the action described in Section 3.2.13.5.

3.2.13.5 The MTSF Finite State Machine

3.2.13.5.1 Description

The behavior of an MP for synchronization is described in the finite state machine shown in Figure 3-18. The MTSF finite state machine comprises four sates shown in Table 3-2. A description of the MTSF timers is presented in Section 3.2.13.5.2.

1) After switched on or waked up, an MP shifts its state from CLOSED to SCAN, and initiates a T1 timer if it is a Type 1 MP. In SCAN state, an MP scans for beacons. The duration of a T1 timer is determined by the parameter *MeshBeaconPeriodSCAN*. The *MeshBeaconPeriodSCAN* is multiple times larger than *MeshBeaconPeriodSYNCs*, considering the possible loss of beacons during transmission.

2) In case an MP receives a beacon in SCAN state, it shall schedule its first TDMA frame that is synchronized with the sending MP. At the same time, it cancels T1 if it is a Type 1 MP, switches its state to SYNC, and initiates a T2 timer with *MeshBeaconPeriodSYNC* which is randomly selected from a range. In case a Type 1 MP senses a signal which it cannot decode or the decoded packet is not a beacon frame, it resets its T1 timer. On the expiration of the T1 timer, a Type 1 MP sends a beacon, switchs its state to SYNC state and initiates a T2 timer.

3) Only in SYNC state, an MP is allowed to send and receive MPDUs on TDMA slots.

Table 3-2. The states used in the MTSF state machine.

State	Description	TDMA operation
CLOSED	Close state: the MP is inactive	Not allowed
SCAN	Scan state: the MP scanns for beacons	Not allowed
SYNC	Synchronized state: the MP is synchronized with adjacent MPs	Allowed
INT	Interfered state: the MP receives beaons with frame start times that are quite different.	Not allowed

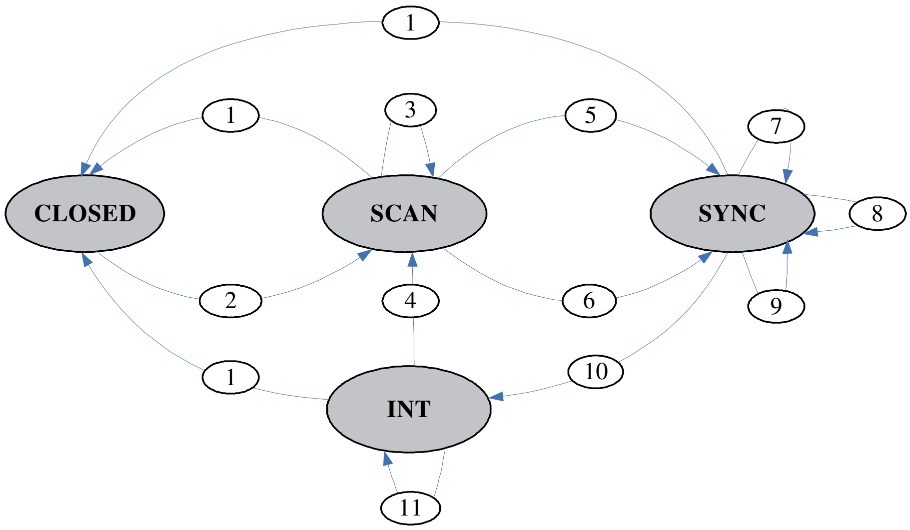

Input/Output

Note: 3 & 5 are only applicable for Type 1 mesh AP

1. Close or Sleep/
2. Switch On or Wake Up/Set T_1 Timer
3. Sense Signal/Reset T_1 Timer
4. Timer T_3 Expiration/
5. Timer T_1 Expiration/Send Beacon
6. Receive Beacon/Adopt Time Step, Cancel T_1 Timer & Set T_2 Timer
7. Timer T_2 Expiration/Send Beacon
8. Receive Valid Beacon /Renew Time Step & Reset T_2 Timer
9. Receive Beacons more than 2 in a T_2 Timer Interval /Send Beacon & Increase Beacon Generating Level
10. Receive Beacons or Other MPDUs at Wrong Time Slots over Specified Time/Cancel T_2 Timer & Set T_3 Timer
11. Receive Beacons with Different Time Steps /Reset T_3 Timer

Figure 3-18. Finite state machine of MTSF.

On the expiration of the T2 timer, an MP generates and sends a beacon as described in Section 3.2.13.4.1. After that, the MP initiates a new T2 timer for future use. When an MP receives a valid beacon, it adjusts the start of the next TDMA frame which it has scheduled locally. The adjustment algorithm is described in Section 3.2.13.6

4) In SYNC state, an MP receiving more than 2 beacons in a T2 timer interval shall

Table 3-3. Timers in the MTSF.

MTSF timer	Used state	Interval
T1	SCAN	MeshBeaconPeriodSCAN, $10 \times (BT_S+BT_W) \times P_{TDMA}$
T2	SYNC	MeshBeaconPeriodSYNC, Randomly from $[BT_S, BT_S+BT_W] \times P_{TDMA}$
T3	INT	MeshIntPeriod, $5 \times (BT_S+BT_W) \times P_{TDMA}$

increase the frequency to transmit beacons. The reason and approaches to change the frequency are presented at 3.2.13.7.

5) In SYNC state, in case an MP receives invalid beacons over a specified time, it shall switch its state to INT state, cancel T2 timer and initiate a T3 timer. The duration of a T3 is determined by *MeshIntPeriod*, a multiple times of the mean *MeshBeaconPeriodPeriodSYNC*.

6) In INT state, an MP is not allowed to send beacons and other MPDUs. Instead, it scans for beacons. If an MP receives a beacon with different TMDA frame structure or frame start times, it shall reset T3 timer and stay in the state. Otherwise, on the expiration of the T3 timer, it switches to SCAN state. The above policies apply when an MDCF MP thinks that it is working with homogeneous MPs on one or more frequency channels. However, when an MP detects foreign MPDUs like 802.11 DCF MPDUs or senses unknown signals on those frequency channels, it shall iniate the coexistence procedure, see [101] for details.

3.2.13.5.2 MTSF timers

MTSF relies on three timers: T1, T2 and T3. They are used in SCAN, SYNC and INT states, respectively. Table 3-3 presents a description.

The beacon generation is performed in a distributed manner. In SYNC state, each MP attempts to send beacons, see Section 3.2.13.4.1. After the completion of sending or receiving a beacon, an MP sets a new T2 timer for future beacon generation. The period used for setting a T2 timer is a multiple of P_{TDMA}. A period is the multiple of P_{TDMA} and a number randomly generated from $[BT_S, BT_S + BT_W]$. The mean beacon interval is $(BT_S + BT_W/2) \times P_{TDMA}$.

The T_1 timer is used in SCAN state, during which period an MP waits for the arrival of a beacon. The period of the T_1 timer is $10 \times (BT_S + BT_W) \times P_{TDMA}$.

The T_3 timer is used in INT state, during which period an MP checks whether it is still interfered by other MPs. The period of the T_3 timer is $5 \times (BT_S+BT_W) \times P_{TDMA}$.

3.2.13.6 On Reception of a Valid Beacon

On receiving a valid beacon, an MP shall adjust the start time of its next TDMA frame, trying to synchronize with the beacon sending MP.

3.2.13.6.1 The time skew when receiving a beacon

Assume that two MPs are exactly synchronized at a time. After a certain period, one sends a beacon, and another one successfully receives the beacon. There are a number of reasons leading to a time skew between two MPs at the instant when the receiving MP completes the analysis of the beacon frame:

1) The clock drift owing to the different drift rates of oscillators at two MPs since the previous synchronization time instant.
2) The propagation delay from sender to receiver.
3) The access delay starting from the instant that a beacon is generated until the instant it is transmitted over the radio.
4) Various processing delays including the computer times consumed at the sending and receiving MPs, and initialization times spent on antenna and transceiver etc.

In summary, the time skews caused by the first two reasons are non-deterministic. The skew values may be quite different from time to time and also from MP to MP. The time skews caused by the last two reasons are deterministic. In the MDCF TDMA system, a beacon is generated after an MP has gained the right to transmit on a slot. Therefore the access delay is deterministic. In a given environment, the amount of processing delays is almost a constant value independent of time. In MTSF, it is assumed that the sum of the access day and various processing delays is a fixed value. The remaining work is to estimate the propagation delay and clock drift.

3.2.13.6.2 Calibrating the TDMA frames

The drift rates of crystal oscillators found in most consumer electronics range from 1 ppm (parts per million) to 100 ppm. The variable d_i is used in each MP to compensate the oscillator drift effect when calculating the start of the next TDMA frame. The initial value of the variable is 0 and it is adjusted whenever receiving a valid beacon within a specified period from T_{SYN} to T_{adj}.

Assume at the nth TDMA frame MP i receives a beacon from j. The $ST_{Ri}{}^{n}$ and $ST_{Li}{}^{n}$ can be calculated directly from the definitions, which relations are depicted in Figure 3-19.

When no beacon arrives ($n > 1$), an MP schedules a new TDMA frame by:

$$ST_{Lj}^{n} = ST_{Lj}^{n-1} + P_{TDMA} + P_{TDMA} \times d_i \tag{3.9}$$

If a beacon is received in the TP of an ACH, $ST_{Ri}{}^{n}$ is calculated by:

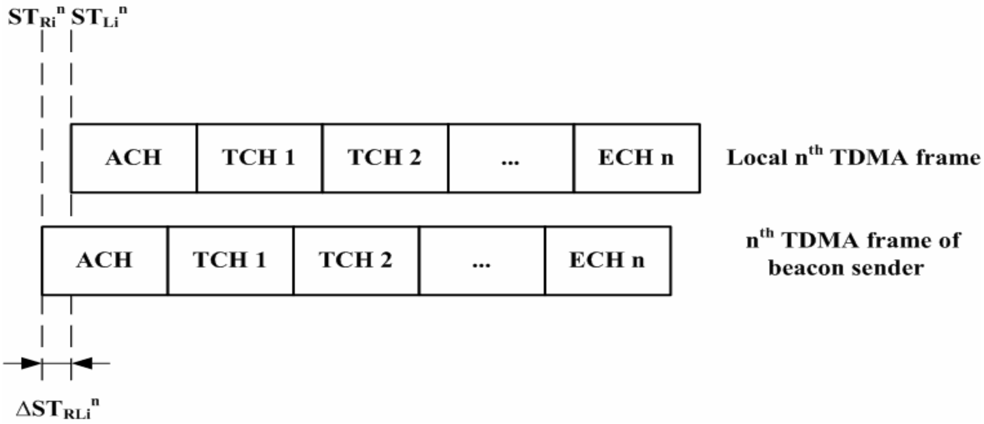

Figure 3-19. Time skew in TDMA operation.

$$ST_{Ri}^{n} = T_i^n - P_{PP} - P_{FEP} - D_{\mathrm{Pr}o} - S_B / PHY_B \qquad (3.10)$$

Otherwise if a beacon is received in a TCH_i, the equation for calculating $ST_{Ri}^{\ n}$ is

$$ST_{Ri}^{n} = T_i^n - P_{ACH} - (TCH_i) \times P_{TCH} - D_{\mathrm{Pr}o} - S_B / PHY_B \qquad (3.11)$$

On reception of the first beacon, MP i shall schedule the start time of the next TDMA frame is calculated by:

$$ST_{Li}^{1} = ST_{Ri}^{0} + P_{TDMA} \qquad (3.12)$$

Note that $ST_{Ri}^{\ n}$ is a derived value without considering the propagation delay and the clock drift. The value $\Delta ST_{RLi}^{\ n}$ ($\Delta ST_{RLi}^{\ n} = ST_{Ri}^{\ n} - ST_{Li}^{\ n}$) is equal to the propagation delay plus the clock drift between the sending and the receiving MPs in a beacon interval. Obviously, there exists:

$$t_{ij} - \left|\Delta X_{ij}\right| < \Delta ST_{RLi}^{n} < t_{ij} + \left|\Delta X_{ij}\right| \qquad (3.13)$$

The value $\Delta ST_{RLi}^{\ n}$ is very important for TDMA operation. If $\Delta ST_{RLi}^{\ n}$ is larger than the guard time in a time slot as illustrated in Figure 3-3, the TDMA operation cannot be correctly processed. It is clear that a received beacon is valid (see Section 3.2.13.4.2) only if $\Delta ST_{RLi}^{\ n}$ calculated at a receiving MP meets:

$$-\left|\max(\Delta X_{ij})\right| < \Delta ST_{RLi}^{n} < \max(t_{ij}) + \left|\max(\Delta X_{ij})\right| \qquad (3.14)$$

Based on the relation revealed by Eq. (3.13), the lowest boundary to select the guard time in a specified environment can be determined:

$$T_{guard} > \max(t_{ij}) + \left|\max(\Delta X_{ij})\right| \qquad (3.15)$$

Note that the $max(\Delta X_{ij})$ is determined by *MeshBeaconPeriodSYNC* and relative drift rate

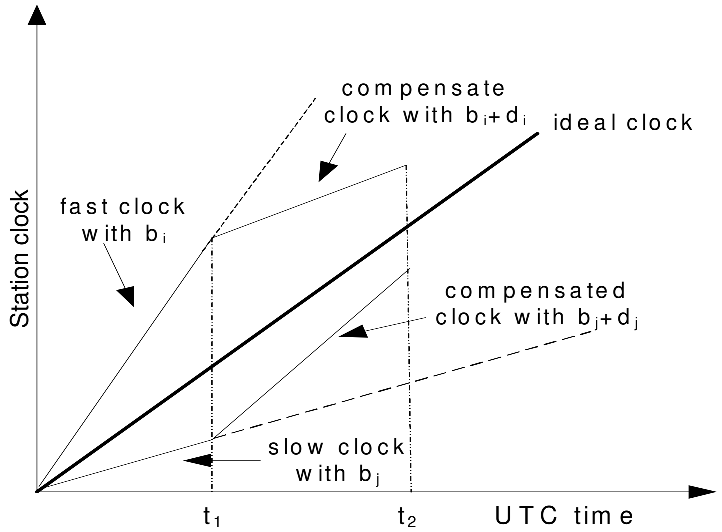

Figure 3-20. Compensation for clock drift.

between two MPs. The beacon intervals should be set as long as possible for the sake of reducing overhead and energy consumption. Upon receiving a beacon, an MP shall compute the start time of the next TDMA frame by:

$$ST_{Li}^{n+1} = ST_{Li}^{n} + \frac{\Delta ST_{RLi}}{\delta} + P_{TDMA} + P_{TDMA} \times d_i \tag{3.16}$$

Where δ is an integer, either 1 or 2. Let $\xi \in (0, 0.5]$ be an implementation dependent value. If $| max\ (\Delta X_{ij}) | < \xi T_{guard}$, $\delta = 1$, otherwise $\delta = 2$. When $| max\ (\Delta X_{ij}) | < \xi T_{guard}$, $\Delta ST_{RLi}{}^{n}$ is regarded mainly due to t_{ij}. Eq. (3.16) is therefore reduced to $ST_{Li}{}^{n+1} = ST_{Ri}{}^{n} + P_{TDMA} + d_i P_{TDMA}$. On the contrary, when $| max\ (\Delta X_{ij}) | \geq \xi T_{guard}$, the clock drift may contribute a lot to $\Delta ST_{RLi}{}^{n}$. Since ΔX_{ij} can be either a negative or a positive value, in order to mitigate the effect caused by the clock drift, δ is selected as 2.

The relation shown in Eq. (3.13) can be used to design a compensation mechanism for combating the clock drift. As shown in Eq. (3.9) and Eq.(3.16), when computing the start time instant of the next TDMA frame, an MP would use d_i to compensate the oscillator drift rate. After a certain period, the sum of the physical oscillator drift rate plus d_i in each MP in a network tends to get close. Consequently, higher synchronization accuracy would be achieved as indicated in Eq. (3.13) ($\Delta X_{ij} \rightarrow 0$).

3.2.13.6.3 Compensating for clock drift

A general applicable model [69] describing the clock error of oscillators with time is:

$$x(t) = a + bt + \frac{1}{2} D t^2 + \varepsilon(t) \tag{3.17}$$

Where $x(t)$ represents the time error of the oscillator relative to some standard; a is the initial time offset; b is the frequency offset; D is the frequency drift and $\varepsilon(t)$ represents the effect of random error. a, b and D are constants for a particular clock. $x(t)$ is a random variable by virtue of its dependence on $\varepsilon(t)$. $\varepsilon(t)$ is a white noise (i.e. random, uncorrelated, normally distributed, zero mean and finite variance).

Let a_i, b_i and D_i denote the initial time offset, frequency offset and frequency drift at MP i, respectively. Assume that MP i and j are synchronized after receiving a common beacon. Then the time skew in the next beacon interval between them is $\Delta X_{ij} = x_i(t) - x_j(t) - a_i - a_j$, where t is a beacon interval and $x_i(t)$ and $x_j(t)$ are clock error of oscillators at MP i and j, respectively. Obviously,

$$\Delta X_{ij} = (b_i - b_j) \times t + \frac{1}{2}(D_i - D_j)t^2 + \Delta\varepsilon(t) \tag{3.18}$$

From the measurement reported in [70], as long as the beacon interval t is within a range (eg. $t < 100$ s), the second term is negligible. Under this condition, the equation becomes:

$$\Delta X_{ij} = (b_i - b_j) \times t + \Delta\varepsilon(t) \tag{3.19}$$

b_i and b_j are physical frequency offsets and can not be changed. However, when scheduling a new TDMA frame, a variable d_i can be used by an MP to compensate for the clock drift. Figure 3-20 illustrates the scheme. X-axis is a standard time – Coordinated Universal Time (UTC) time, while y-axis shows the MP clock reading. The ideal clock exhibits a slope of one. MP i is a fast clock MP with $b_i > 0$, while MP j is a slow clock MP with $b_j < 0$. At the time instant t_1, the time skew is $\Delta X_{ij} = (b_i - b_j) \times t_1$. Given that the compensation factor d_i and d_j are used to schedule the new TDMA frame since at t_2, the time skew is $\Delta X_{ij} = (b_i + d_i - b_j - d_j) \times (t_2 - t_1)$, which value is much smaller than that at t_1.

The adjustment of d_i is divided into two phases: the fast compensation and slow compensation phases. After the second phase, d_i will not be changed anymore. In consumer applications, the drift rates b_i are between 1 ppm and 100 ppm [62]. The adjusting principles are based on the relation shown in Eq. (3.13). After the compensation, the $b_i + d_i$ is close to $b_j + d_j$.

The following pseudo code specifies how to calculate d_i for the fast and slow compensation phases:

When $T_{SYN} < T_i^n < T_{slow}$ (Fast compensation phase):

If $\Delta ST_{RLi}^{\ n} > max(t_{ij})$, *then* $d_i = d_i + 5$ *ppm*

Else if $\Delta ST_{RLi}^{\ n} > 2 \times max(t_{ij})/3$, *then* $d_i = d_i + 2$ *ppm*

Else if $\Delta ST_{RLi}^{\ n} < -2 \times max(t_{ij})/3$, *then* $d_i = d_i - 2$ *ppm*

Else if $\Delta ST_{RLi}^{n} < -\max(t_{ij})$, *then* $d_i = d_i - 5$ *ppm*

When $T_{slow} < T_i^n < T_{adj}$ (Slow compensation phase):

If $\Delta ST_{RLi}^{n} > \max(t_{ij})$, *then* $d_i = d_i + 2$ *ppm*

Else if $\Delta ST_{RLi}^{n} > 2 \times \max(t_{ij})/3$, *then* $d_i = d_i + 1$ *ppm*

Else if $\Delta ST_{RLi}^{n} < -2 \times \max(t_{ij})/3$, *then* $d_i = d_i - 1$ *ppm*

Else if $\Delta ST_{RLi}^{n} < -\max(t_{ij})$, *then* $d_i = d_i - 2$ *ppm*

3.2.13.7 Synchronization in Multi-hop Networks

In SYNC state, MPs that receive a valid beacon shall reset their T_2 timer. When a beacon is sent out in the ACH, the highly eliminating prioritized access mechanism guarantees that one beacon can be sent out only per beacon interval even under heavy load. As introduced in 3.2.13.4.1, an MP shall cancel its pending beacon transmission as long as it receives a valid one. Therefore in an area where MPs are in mutual transmit range, there is only one beacon in a T_2 timer interval. If an MP receives more than 2 beacons in a T_2 timer interval, the MP shall realize that it is in an overlap area of more than two transmission neighborhoods. Figure 3-21 shows two examples. MP 2, 3 and 4 in graph a), and MP 2, 3, 5 and 6 in graph b) are in overlap areas. In graph a) when MP 1 and 3 transmit their beacons in a beacon interval, MP 2 can receive beacons twice. In graph b), MP 3 receives beacons three times in a beacon interval if MP 2, 5 and 6 happen to transmit a beacon during a beacon interval. When an MP in an overlap area transmits beacons, the MPs, nearby but not that in the mutual transmission range, can receive the beacons: For instance in graph a), when MP 2 transmits a beacon, both MP 1 and 3 can hear. If MPs in overlap area transmit beacons more frequently than others, MPs in different transmission neighborhoods can be kept synchronized. In graph a), MP 1 and 5

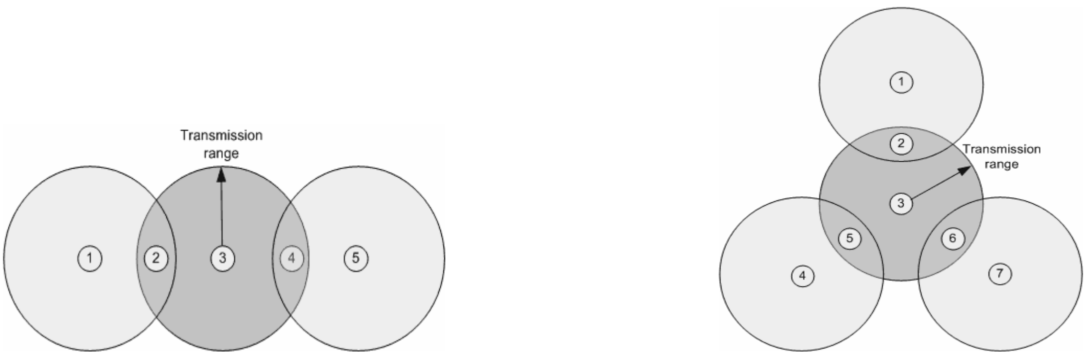

a) b)

Figure 3-21. Synchronization in multi-hop networks.

are 4 hops away. If the start times of their TDMA frames are not aligned over a period, saying 10 beacon intervals, they may get out of synchronization with each other as suggested by Eq. (3.19). If so, the channel utilization knowledge established in MPs 1 to 5 is no longer valid. However, if beacons are mostly transmitted by MP 2, 3 and 4, MP 1 and 5 can be kept synchronized since they follow the beacon frame information from MP 2 and 4, leading to a relatively shorter beacon period in a multi-hop network. The similar situation happens in graph b), which network covers a wider area.

There are two means for an MP to change its frequency to transmit beacon:

The first one is to divide BT_W into n smaller windows, i.e. n levels for setting beacon generation timers: [BT_S, $BT_S + BT_W \times (1/n)-1$], [$BT_S + BT_W \times (1/n)$, $BT_S + BT_W \times (2/n) -1$], … [$BT_S + BT_W \times (n-1)/n$, $BT_S + BT_W$-1]. All MPs start from the lowest level, i.e. the last one. In case an MP receives multiple beacons in a period of $(BT_S + BT_W) \times P_{TDMA}$ for more than a specified frame duration, it shall upgrade the window level by 1 for increasing the beacon transmit frequency. On the contrary, when an MP continuously transmits beacons exceeding a predefined number, it shall degrade the window level by 1 for reducing the beacon transmit frequency. This allows that other MPs also have chance to transmit beacons. Otherwise, the clock drift compensation algorithm (see Section 3.2.13.6.3), which requires mutual beacon exchange between adjacent MPs, may not take effect.

The second rule is to take advantage of the channel access scheme: 2^n FEPCLs used for contending in the FEP of the ACH are grouped into K equal sized non-overlapping CNGs. An MP adapts its beacon frequency sending level by adjusting the CNG used for contention: when it needs to increase the frequency to send out beacons, it chooses a higher level CNG, or chooses a lower level CNG in case it wants to decrease the frequency.

The combined use of the two approaches offers a high flexibility.

The synchronization algorithm described above has been evaluated and the concept is proven valid, see Section 5.2.

3.3 Radio Link Control Protocol (RLCP)

3.3.1 Service Modes

RLCP offers one-hop transmission services on the top of MACP. The services are implemented between peer-to-peer entities. There are two service modes: Unacknowledged Mode (UM) for connectionless point-to-point, multicast and broadcast applications, and Acknowledged Mode (AM) for reliable point-to-point applications. A selective repeat automatic request (SR-ARQ) protocol is a key component of AM, offering the error and flow control.

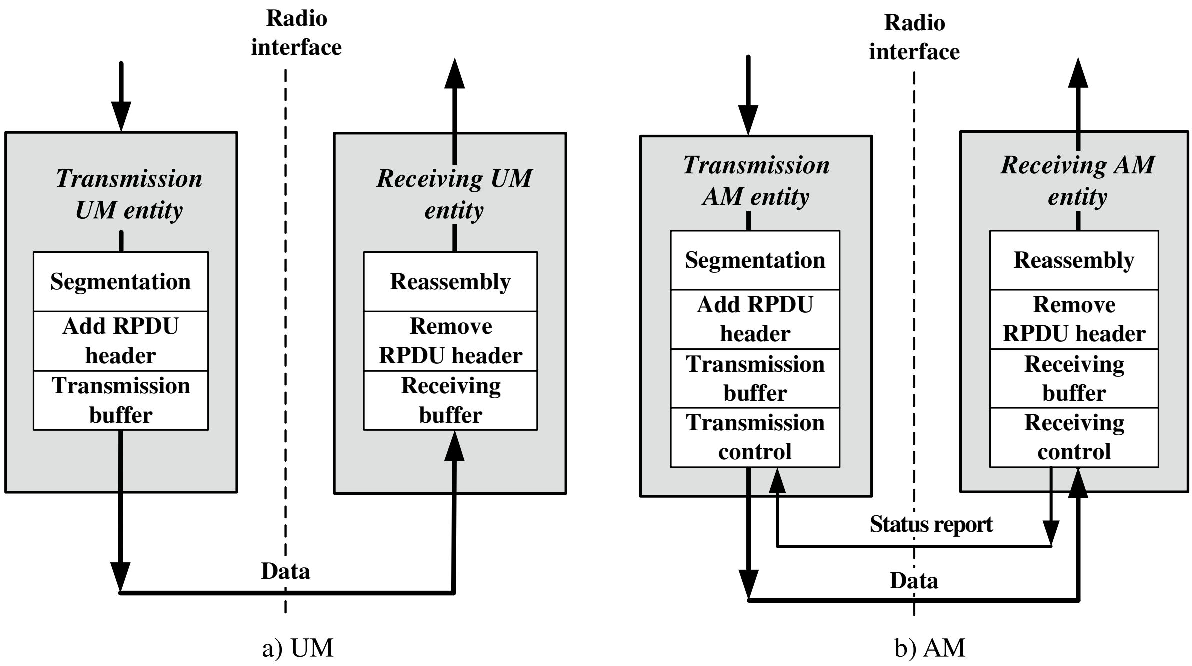

Figure 3-22. UM and AM services mode.

3.3.1.1 UM

Figure 3-22a illustrates the data delivery process between two UM entities over the radio. The transmission entity segments a received LLC PDUs into smaller RPDUs, and puts each of them into the transmission buffer after adding a RPDU header. On receiving RPDUs, the receiving UM entity removes RPDU headers, reassembles them into LLC RPUs and passes the LLC PDUs to the LLC layer.

3.3.1.2 AM

Figure 3-22b shows the data delivery process between two AM entities over the radio. The transmitting AM entity segments an upcoming LLC PDUs into smaller RPDUs, and puts each of them into the transmission buffer after adding a RPDU header. On receiving RPDUs, the receiving AM entity removes the RPDU headers, reassembles them into LLC RPUs and passes the LLC PDUs to the LLC layer. The transmission control module at the transmitting entity transmits data packets to the receiving control module at the receiving entity on the forward link, and the receiving control module sends receiving status reports to the transmission control modules on the backwards link. Owing to the on-demand-TDD turnaround feature offered by MACP, transmissions on the forward link and backwards link can be in a single TCH. The error and flow control is implemented by negotiation between two control modules.

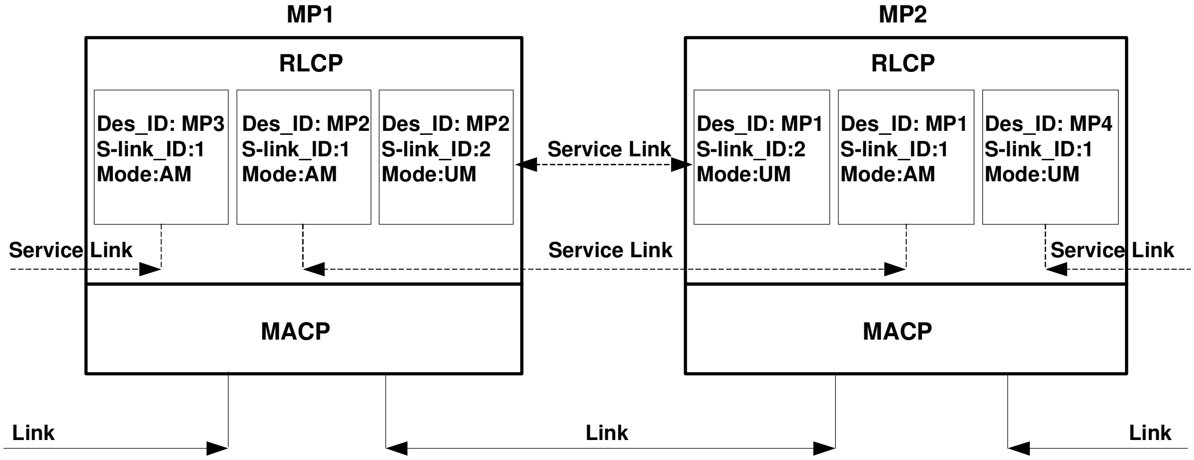

Figure 3-23. Allocation of service entities.

3.3.1.3 Allocation of Service Entities

RLCP manages the allocation of service entities for performing the UM or AM services. The peer-to-peer service entities need to establish service links before transmissions. A *service link* is defined as a logical path within one-hop which is used to transmit RPDUs between a pair of peer-to-peer service entities. It runs on the top of a link established between two peer-to-peer MACP entities. The definition of the link is given in Section 3.2.3. Service links between two RLCP entities share a link by multiplexing RPDUs as introduced in Section 3.2.7. Figure 3-23 shows their relation. It should be noted that each MP maintains one RLCP entity and one MACP entity, whilst a RLCP entity may maintain a number of service entities at a time.

A service entity is allocated according to the destination, service mode and QoS requirement. A service link identifier (S-link_ID), which is unique between a transmission pair, is assigned to each service entity. It is used to identify a service entity together with the destination identifier (Des_ID) in a RLCP entity. Data RPDUs with the same traffic type and Des_ID can share a service entity. However a traffic flow with a strict packet delay requirement, like a multi-hop real-time flow, may be allocated with an individual service entity. The parameters set for the service entity are suited for a quick delivery while guaranteeing a low PLR.

As suggested in Table 2-1, in comparison with the video traffic, the voice traffic requires low packet delay but it tolerates a relatively high PLR: The tolerable PLR of voice traffic is 6%. Therefore, the service entity for the single-hop voice traffic can be the UM entity if the channel condition is good enough. Let *PER* be the one-hop packet error ratio (PER), N_{hop} be the number of hops. The end-to-end PLR of a N_{hop} flow under the UM is:

$$PLR = 1 - (1 - PER)^{N_{hop}} \tag{3.20}$$

Given that the one-hop *PER* of voice flows is 2.5%, the end-to-end *PLR*s after 2 and 3 hop relaying are 4.94%, 7.31%, respectively. Hence, to ensure a low end-to-end PLR, a voice flow that needs to be relayed should be transmitted under the AM in each one-hop link. Unlike the voice traffic, the video traffic has extremely high PLR requirements but relatively low delay requirements, see Table 2-1. Therefore, a video flow should be transmitted under the AM no matter whether its final destination is single-hop or multi-hop away. TCP traffic is non-real-time traffic, but it requires zero PLR. Accordingly, a TCP flow should be transmitted under the AM even if it is a single-hop flow.

Figure 3-23 shows an example. Two service links are established between MP1 and MP2. Each is used by a pair of peer-to-peer service entities at the RLCP sub-layer: one under the UM and another under the AM. The two service links run on top of the underlying link established at the MACP sub-layer. Each service entity is uniquely identified by the combination of the S-link_ID and Des_ID. MP1 and 2 are in a mesh environment aiming at being able to perform multi-hop operation. They also maintain other RLCP service entities whose peer entities are in MP3 and 4, respectively.

3.3.2 Error Control and Flow Control

3.3.2.1 General

Error control schemes include Automatic Request (ARQ) and Forward Error Correction (FEC). In FEC, each packet is transmitted with appended redundant bits in the forward channel. The redundant bits help to recover the erroneous bits. The packet delay achieved by using FEC is smaller than using ARQ. However, the FEC overhead is fixed and not adaptable to the channel conditions. It can be implemented in the PHY layer or application layer but is not considered in the link layer.

Unlike FEC schemes, the transmission efficiencies of ARQ schemes adapt to the channel conditions. A better channel condition shall lead to a higher efficiency. There are three basic types of ARQ schemes. The Selective Repeat Automatic Request (SR-ARQ) protocol is known by its high transmission efficiency in comparison with the Stop-and-Wait (SW) and Go-Back-N (GBN). However, the high efficiency is achieved at the costs of high complexity, high buffer consumption and high delay and jitter that packets experience. The SW is the simplest and least efficient ARQ. But its delay and jitter performance is the best. The GBN-ARQ is in the middle of the SW-ARQ and SR-ARQ in all above mentioned fields. In lots of applications, the GBN is a good compromise.

In a SR-ARQ system, the transmitter maintains a retransmission buffer while the receiver maintains a receiving buffer. Each transmitted packet at the transmitter is put into the retransmission buffer waiting for the acknowledgement after transmission. Driven by the ARQ protocol, the receiver sends status report packets back to the transmitter from time to time. On reception of a status report packet, the transmitter removes the acknowledged packets from the retransmission buffer while it retransmits the others. Different with SW and GBN schemes, the retransmitted packets are not continuous in sequence number and the receiver must reassemble packets to deliver in sequence to its upper layer.

The acknowledgement mechanism plays a crucial role in a SR-ARQ protocol for achieving high transmission efficiency. The major acknowledgement approaches are:

1) ***Periodical polling*** – set a timer at the transmitter side. On the expiration of the timer, the transmitter sends a poll either by a dedicated packet or piggyback with a data packet to the receiver. The receiver sends a status report back to the transmitter on receiving the poll.
2) ***Periodical status report*** – set a timer at the receiver side. On the expiration of the timer, the receiver sends a status report back to the transmitter.
3) ***Window based polling*** – when the transmitting window is approaching its upper bound, the transmitter sends a poll.
4) ***Polling on every sending a predefined number of packets*** – once the number of sent packets are over the predefined threshold, the transmitter sends a poll. The number might depend on the size of a TCP packet fragmented into LLC packets, known at the transmitter.
5) ***Status report on every receiving a predefined number of packets*** – once the number of received packets is over the predefined threshold, the receiver sends a status report.
6) ***Polling with last packet in buffer*** – the transmitter sends a poll piggyback with the last data packet in the transmission buffer.
7) ***Polling with last packet in retransmission buffer*** –the transmitter sends a poll piggyback with the last data packet in the retransmission buffer.

3.3.2.2 A SR-ARQ Protocol Utilizing On-demand-TDD TCH Turnaround

A window based SR-ARQ is designed to perform the error and flow control for one-hop transmissions under the AM. It is built up by taking advantage of the on-demand-TDD turnaround feature offered by MACP. The key parameters of an ARQ entity can be set in favor of achieving high throughput, or low delay or low buffer consumption. With a right setting, the SR-ARQ protocol can be reduced to a SW or GNB like protocol aiming at low packet delay, low buffer consumption and low complexity while ensuring an adequate throughput.

The acknowledgement mechanisms listed above have their pro and con. Mechanism 1) and 2) are generally applicable: The correct completion of a status report in 1) requires that a poll packet and its triggered status report packet are correctly delivered over the lossy medium, whilst mechanism 2) only requires that a status report packet is correctly delivered. Therefore, if the backwards channel is always available, 2) is better than 1) in terms of efficiency. The transmission efficiency in mechanism 4) and 5) becomes low if the thresholds there are set small. But if the thresholds are too big, in case traffic comes intermittently, the jitter and delay shall be quite large, unacceptable for a QoS delivery. The approaches 3, 6 and 7 are auxiliary mechanisms.

Timely report of the receipt situation is important in an ARQ protocol. Without status reports, a transmitter has no way to determine whether to transmit new packets or to retransmit cached packets, and the transmission efficiency shall be low. In MDCF, TCHs used to transmit MPDUs by adjacent MPs may be in hang-on state or forced released as introduced in Section 3.2.9. When two peer-to-peer transmission entities generate a poll or a status report RPDU, they may have no reserved TCHs to transmit the control packet, and first need to contend with adjacent MPs to reserve a TCH before transmitting the control packet on the TCH. The access time clearly increases with the number of contending MPs. As a consequence, status reports may be substantially delayed, causing low transmission efficiency. This, apparently, must be avoided under MDCF.

MACP implements the on-demand-TDD TCH turnaround. When an MP transmission pair has reserved a TCH for use, status reports can be quickly delivered back to the transmitter in TDD mode of operation. An efficient acknowledgement mechanism is proposed for the SR-ARQ in MDCF by combining mechanism 4) and 5):

1) The ARQ transmitting entity sends a poll piggybacked to a data RPDU when the number of sent data RPDU exceeds a predefined threshold. The threshold is set according to the type of traffic. The transmit counter is reset after polling. On reception of a poll, the receiving entity sends back a status report RPDU back without delay.

2) The ARQ transmitting entity sets a timer when the retransmit and transmit buffers are being occupied. The timer is reset whenever a status report is received and the retransmit buffer is emptied. On the expiration of the timer, the transmitting entity sends a poll either by a dedicated RPDU or piggybacked to a data RPDU if available. The value of timer should be a bit longer than the equivalent frame period of sending a poll using the first method. A receive MP needs to contend to reserve a TCH to transmit a RPDU with the poll bit set in case the previously reserved TCH has been released.

The polling threshold used to compare with the counted number of sent packets should be a small value. Because a smaller value guarantees with high probability that a poll request can piggybacked to a data RPDU and be transmitted before a TCHs is released. This setting leads to relative low transmission efficiency since the overhead is substantial. However, the level of the degraded efficiency caused by this is controllable and much smaller than that caused by contending for channel access to reserve a TCH for transmitting control RPDUs.

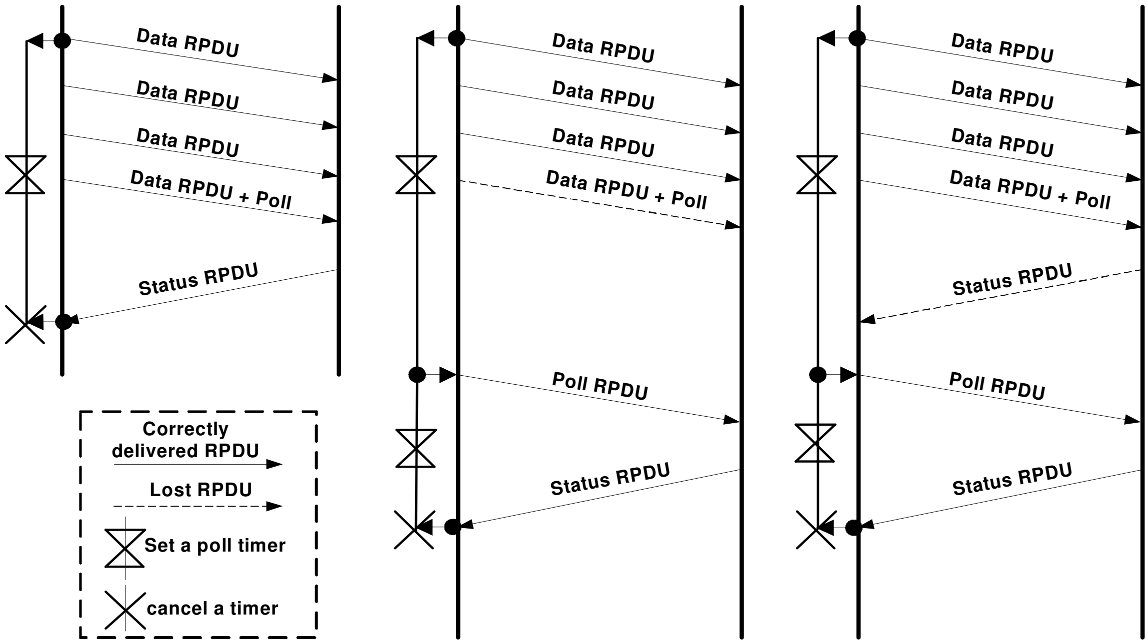

Figure 3-24. Status report mechanism of the SR-ARQ by takes advantage of the on-demand-TDD turnaround provided by MACP. A Poll RPDU (or Data RPDU + Poll) and its Status RPDU can be transmitted in the same TCH subsequently without a need to contend for channel access.

Figure 3-24 illustrates the scheme. In this example, the transmitting entity polls on every sending 4 RPDUs. In the left hand graph, the transmitter entity sends a poll piggyback with the fourth RPDU. And the ARQ receiving entity sends a status RPDU back immediately. As a result, the status RPDU arrives at the transmitting entity in the next TDMA frame. The arrival of the status RPDU causes the reset of the scheduled poll timer. In the middle graph, the fourth data RPDU carrying the poll request is assumed lost. The scheduled polling timer at the transmitting entity expires since it receives no status report in the next TDMA frame. On expiration of the timer, a Poll RPDU is sent. The transmitting MACP entity may need to contend for channel access to reserve a TCH if it has not TCH for use at the time. On receiving the poll, the receiving entity sends a status report back immediately on the reserved TCH. In the right hand graph, the status RPDU is lost during transmission. On expiration of the polling timer, a Poll RPDU is sent as in the middle graph.

3.3.2.3 Determination of Key ARQ Parameters for Specific Scenarios

MDCF is intended to support a wide range of applications in different scenarios having different requirements on using the ARQ protocol. In lots of scenarios, obtaining high throughput is the main target, while the major concern of some applications, like when delivering real-time services, is to achieve low packet delay and low jitter. Besides those, low buffer consumption and low implementation complexity is of concern for some applications. The designed SR-ARQ protocol can be tuned suitable for specific scenarios by changing the following parameters: the number of TCHs for use, poll threshold of sent RPDUs, poll timer period and window sizes.

Let *PER* be the packet error ratio; P_{TDMA} the time period of a TDMA frame (unit: µs), L_{RPDU} be the length of RPDUs in bytes; TH^{o}_{AM} be the one-hop SR-ARQ throughput; P_T be the threshold of the number of sent RPDUs that triggers to send a poll; T_P be the value of the polling timer; WIN_t and WIN_r be the transmit and receive window size, respectively.

Assume that the transmitting entity always has RPDUs to transmit and n_{TCH} TCHs are used for transmission. Figure 3-7 shows an example of the on-demand-TDD turnaround where a receiving MP completes to request the TDD turnaround on a TCH and returns the right to transmit on the TCH to the partner MP after two TDMA frames. This is an optimal case. Let N_{TDD} denote the number of TDMA frames needed to complete a process of sending a status RPDU on a TCH and returning the right to transmit on the TCH to the partner MP when using on-demand-TDD turnaround. N_{TDD} is configurable and its minimal value is 2 TDMA frame like in Figure 3-7.

From the definitions, it is clear that after every sending of P_T data RPDUs on n_{TCH} TCH slots (equal to P_T/ n_{TCH} TDMA frames), N_{TDD} TDMA frames on a TCH slot shall be used for completing a status report. Obviously, in $P_T/n_{TCH} + N_{TDD}$ TDMA frames, there are altogether $(P_T/n_{TCH} + N_{TDD}) \times n_{TCH}$ TCH slots, N_{TDD} of which are control overhead used for sending a status report. Given no packet is lost during transmission, then the highest transmission efficiency is $[P_T + (n_{TCH} - 1) \times N_{TDD}] / (P_T + n_{TCH} \times N_{TDD})$. The on-demand-TDD feature makes the SR-ARQ protocol operate in a slotted system since both data and acknowledgement packets are transmitted on reserved TCHs without a need to contend for channel access to gain a transmission chance. Therefore TH^{o}_{AM} can be computed by the formula suggested in [71]:

$$TH^{o}_{AM} = \frac{n_{TCH} \times L_{RPDU} \times 8}{P_{TDMA}} \times (1 - PER) \times \frac{P_T + (n_{TCH} - 1) \times N_{TDD}}{P_T + n_{TCH} \times N_{TDD}} \tag{3.21}$$

Note in practice, P_T is about 3 ~ 6 times of N_{TDD}, accordingly $[P_T + (n_{TCH} - 1) \times N_{TDD}] / (P_T + n_{TCH} \times N_{TDD})$ is close to 0.85 (more or less). Hence Eq. (3.21) can be reduced to:

$$TH^{o}_{AM} \approx \frac{n_{TCH} \times L_{RPDU} \times 6.8}{P_{TDMA}} \times (1 - PER) \tag{3.22}$$

As analyzed before, the buffer consumption at each side is highly dependent on the window size at it. Obviously, we have:

$$\begin{aligned} WIN_T &\geq P_T \\ WIN_r &\geq P_T \end{aligned} \tag{3.23}$$

Let T_{Ack} be the acknowledgement period (unit: TDMA frames), *p(n)* be the probability that a data RPDU is successfully transmitted at the n^{th} retransmission, R_{Max} the maximal retransmission time, and D^{O}_{AM} be the mean one-hop packet delay (unit: ms) under

AM. The one-hop mean delay then can be derived:

$$D_{AM}^{O} = E[(n-1)\times T_{Ack} \times P_{TDMA}] = P(1)\times 1\times P_{TDMA} + \sum_{n=2}^{R_{Max}} P(n)\times(n-1)\times T_{Ack} \times P_{TDMA}$$

From the definition, we have $T_{Ack} = P_T/n_{TCH}$. Thus:

$$D_{AM}^{O} = \left[p(1) + \sum_{n=2}^{R_{Max}} P(n)\times(n-1)\times\frac{P_T}{n_{TCH}} \right]\times P_{TDMA} \tag{3.24}$$

where

$$P(n) = (1 - PER)\times PER^{\,n-1}$$

The polling timer is used in the transmitter to resend a poll timely in case that the last data RPDU with the poll request or status RPDU was lost. The period T_P should meet:

$$2\times\frac{P_T}{n_{th}}\times P_{TDMA} > T_P \geq (\frac{P_T}{n_{th}} + N_{TDD})\times P_{TDMA} \tag{3.25}$$

Eqs. (3.21) – (3.25) quantify the behaviors of the designed SR-ARQ protocol. From the equations, it can be seen that a higher value of the polling timer P_T requires a larger buffer size (Eq. (3.23)), leading to a higher throughput (Eq. (3.21)) and also to a longer packet delay (Eq. (3.24)). Using multiple n_{TCH} in parallel for a link helps to improve both the throughput and delay performances. The key ARQ parameters suited for a specific application can be determined from these equations.

3.3.3 RLCP Transmission Processes

This section describes the transmission processes between peer service entities in RLCP. A RLCP transmission takes place only after a service link is established between two peer service entities. Establishment of a service link requires that an agreement is reached between two peer RLCP entities responsible for allocating service entities in their buffers used for the RLCP transmission. The way to allocate service entities is introduced in Section 0. Afterwards, the peer service entities exchange RPDUs via the service link as shown in Figure 3-23.

A service link is a logical link running on top of a link established between two MACP entities. A service link exist is irrespective of whether there are reserved TCHs for its underlying link. For instance, owing to the bursty nature of some traffic source, a pair of service entities does not have RPDUs to exchange for some interval time. Consequently, the reserved TCHs for the underlying link shall be released on the expiration of the hang-on time. However, the service link and related service entities still exist. They perform the transmission service as long as new RPDUs arrive.

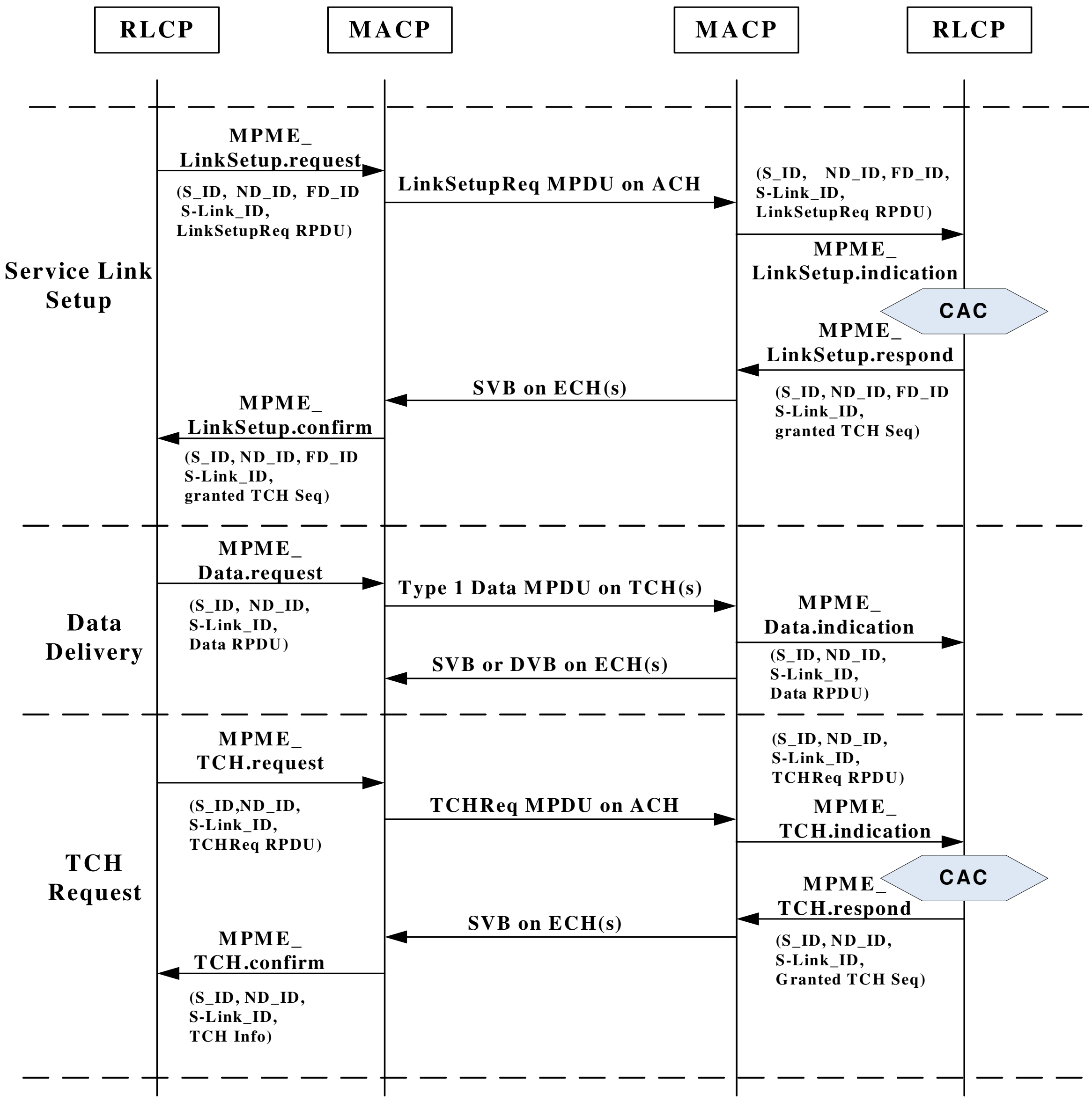

Figure 3-25. RLCP transmission processes.

Figure 3-25 describes the RLCP transmission processes. The MACP management entities (MPME) primitives are used to exchange information between a RLCP entity and it MACP entity in an MP. The symbol MPME_xx is used to denote a specific primitive. The specification describes what has been investigated in the simulation study in Chapter 5.

3.3.3.1 Service Link Setup

3.3.3.1.1 Single hop transmissions

On reception of a request packet from the LLC layer or Routing & Security sub-layer, a

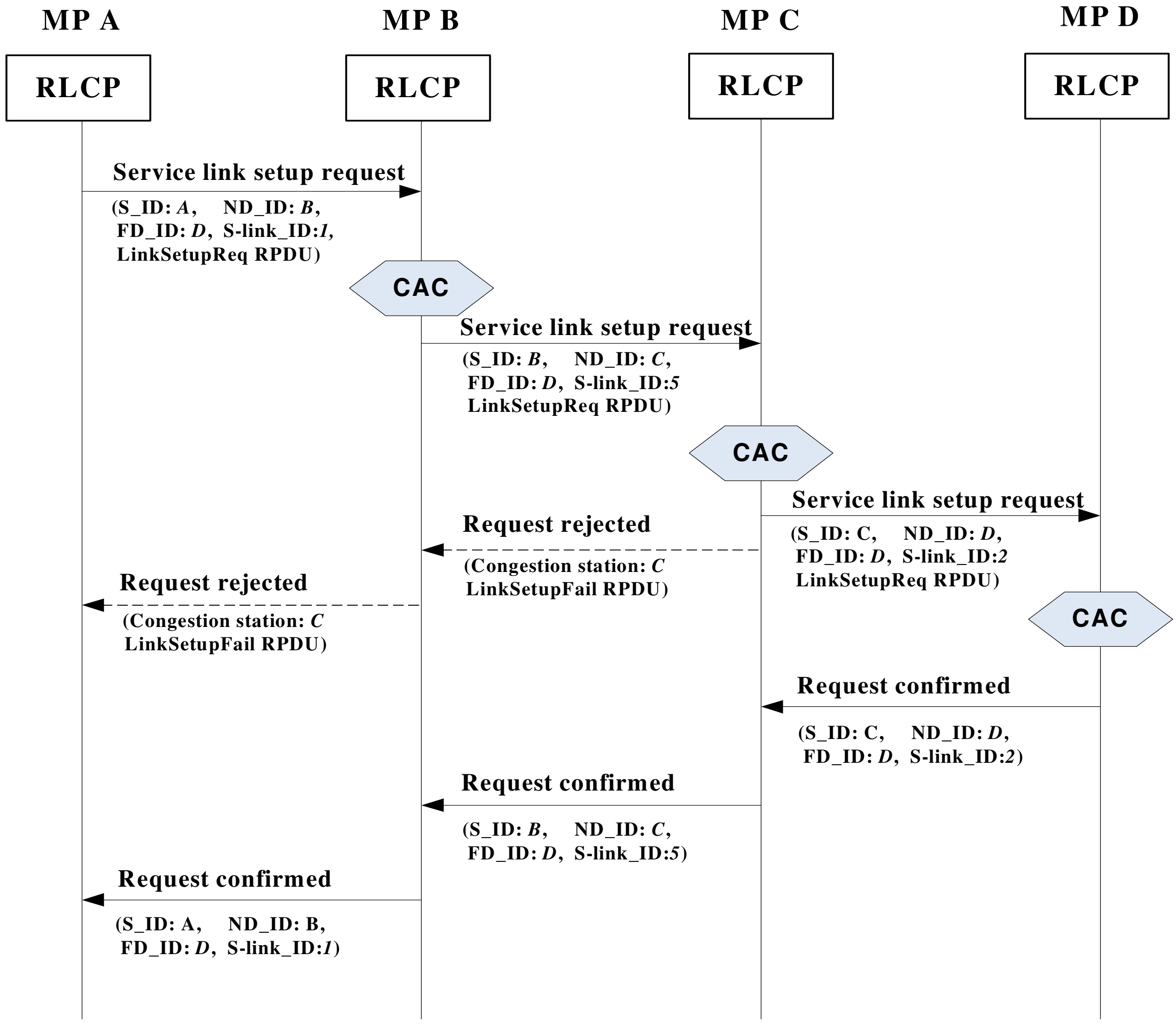

Figure 3-26. Setup of service links for a multi-hop transmission.

RLCP entity shall check whether a corresponding service entity has been allocated. If no proper service entity is found, the RLCP entity shall initiate the service link setup process with the intended peer RLCP entity. Note the allocation of a service entity needs to consider the traffic type and destination as explained in Section 0.

The requesting RLCP entity sends the primitive MPME_LinkSetup.request (S_ID, ND_ID, FD_ID, S-Link_ID, LinkSetupReq RPDU) to its MACP entity. The S-link_ID is a proposed service link identifier (ID) which is an integer and should be unique between a pair of peer RLCP entities. The fields of S_ID, ND_ID, FD_ID and LinkSetupReq RPDU denote the source MP ID, next hop destination MP ID, final destination MP ID and the control RPDU for the service link setup, respectively. The LinkSetupReq RPDU contains QoS related parameters of the requested traffic and a list of proposed TCHs for use. On the reception of the primitive, the MACP entity generates a LinkSetupReq MPDU carrying the LinkSetupReq RPDU, and contends for channel access to transmit the MPDU in the TP of the ACH. On reception of the MPDU, the receiving MACP entity notifies its RLCP entity via the primitive MPME_LinkSetup.indication (S_ID, ND_ID, FD_ID, S-Link_ID, LinkSetupReq RPDU). The CAC module in the requested RLCP entity shall evaluate whether to accept the link setup request by considering:

1) Whether the available resources can satisfy the requested QoS delivery.
2) Whether the establishment of the service link will corrupt the QoS of existing service links.

The CAC is performed in a fully distributed manner. Section 3.3.4.2 gives a detailed description. In case that the request is admitted and the ND_ID and FD_ID are same, the RLCP entity shall allocate a service entity in its buffer with the parameters suggested by the requesting entity. At the same time it informs its MACP entity via the primitive MPME_LinkSetup.respond (S_ID, ND_ID, FD_ID, S-Link_ID, granted TCH seq.). The field of the granted TCH seq. describes the sequence numbers of the accepted TCHs for use. Then the MACP entity shall transmit SVBs on the ECHs related to the TCHs informed in the primitive.

Upon receiving SVBs, the transmitting MACP entity generates a primitive MPME_LinkSetup.confirm (S_ID, ND_ID, FD_ID, S-Link_ID, granted TCH Seq.) and passes it to the requested RLCP entity. The information of granted TCHs is obtained at the transmitter side by observing the SVBs. On reception of the confirmation primitive, the RLCP entity allocates a service entity and is ready for transmission.

3.3.3.1.2 Multi-hop transmissions

The establishment of a sequence of service links for a multi-hop transmission needs consents of all the MPs along a multi-hop route. Figure 3-26 illustrates the process. MP A wants to initiate a real-time transmission to MP D. MP B and C are selected as relaying MPs. MP A sends a service link request packet to B. Note the combination of the ND_ID and S-Link_ID should be unique between two peer RLCP entities. On reception of the request, B performs the CAC check. If the request is admitted by B, it generates a service link setup request packet with the modified addresses on the received one from A, and sends it to C. C performs the CAC at its location upon receiving the request. If the request is not permitted, C sends a LinkSetupFail RPDU back to B to report its congestion situation. On the contrary, if the request is granted, C generates a service link setup request packet and sends it to D. MP D is the final destination where the packet fields ND_ID and FD_ID are same. Like in previous MPs, D performs the CAC check. If the request is admitted, it allocates a service entity following the information specified in the requested packet. Then it notifies C of the request confirmation using the way introduced in the last part. On reception of the request confirmation, C allocates a service entity in its buffer and notifies B of the request confirmation. B performs the same actions as in C. Upon receiving the request confirmation, A allocates a service entity in its RLCP entity. Until now, the establishment of the four service links for the multi-hop transmission is completed.

On reception of a LinkSetupFail RPDU, a RLCP indicates the congestion situation to its Routing & Security sub-layer. The routing algorithm shall perform the congestion control, refresh the state of its routing table, and search for an alternate route.

3.3.3.2 Data Delivery

After a service link for a specific traffic flow is established, the data delivery can be performed between two peer service entities. Assume that at least one TCH has been reserved for use at the underlying link. As illustrated in Figure 3-25, whenever the transmitting service has a data RPDU destined to its partner, it sends the primitive MPME_Data.request (S_ID, ND_ID, S-Link_ID, data RPDU) to its MACP entity. The data RPDU is contained in the primitive. In response to the request, the MACP entity generates a Type 1 Date MPDU by adding an MPDU header in front of the data RPDU, and then transmits it on the reserved TCHs. On reception of the Data MPDU, the receiving MACP entity takes out the contained data RPDU and uses it to generate the primitive MPME_Data.indication (S_ID, ND_ID, S-Link_ID, Data RPDU). Then it indicates the primitive to its RLCP entity. Upon receiving the primitive, the RLCP entity shall locate the intended service entity by checking the S_ID and S-Link_ID. As stated before, the combination of the S-Link_ID and destination ID uniquely identifies a service entity. After locating the service entity, the receiving RLCP entity passes the data RPDU to it. And the service entity shall process the packet in its buffer.

3.3.3.3 TCH Reservation Request

As stated before, the reserved TCHs might be released even though service entities in a RLCP entity still exist and new Data RPDU may arrive. When new data RPDUs come, in case that a RLCP entity finds no reserved TCHs for transmission or the number of the reserved TCHs cannot satisfy the QoS delivery, it shall initiate the TCH request process. The process is described in Figure 3-25. It is quite similar with the service link setup process. Those two processes differ in the CAC check in RLCP to handle a request. On reception of a TCH reservation request, a receiving RLCP entity shall grant the request as long as it finds free TCHs agreed with the requesting entity. Section 3.3.4.2 presents the details.

3.3.3.4 Adaptation of ARQ Parameters during Operation

As described in Section 0, the key ARQ parameters, like the poll threshold of sent RPDUs, poll timer period, transmission window size and receiving window size, have a great impact on the traffic performance. A pair of AM service entities can adjust those parameters during transmission adapted to the network load situation, for achieving a desired performance. The AM service entity, wishing to initiate the process of adjusting ARQ parameters, transmits an ARQParReq RPDU to its partner. On reception of the RPDU, the peer service entity shall change the parameters following the description specified in the RPDU, and then reply with an ARQParRes RPDU to the peer entity. On receiving the ARQParRes RPDU, the requesting service entity changes its own parameters.

3.3.4 Radio Resource Control (RRC)

RRC is very important for exploiting the channel capacity in an MDCF mesh network. It serves to efficiently utilize TCH slots, including the resource request, call admission control (CAC), resource control during transmission and TCH release. Following definitions are used in this section.

B(RL): The burstiness of a traffic flow (ratio of RL_P to RL_M).

min(a, b): Return the minimal value of *a* and *b*.

L_{RPDU}: The length of RPDUs in bytes.

$Num(RL_P)$, $Num(RL_M)$: The number of TCHs in a TDMA frame needed to transmit a traffic flow without causing much queue delay when the flow operates at {peak, mean} rate.

$Num(RQ_{TCH})$: The number of TCHs in a TDMA frame requested by an MP.

Num(G): The number of TCHs in a TDMA frame granted to an MP.

$Num(Need_{TCH})$: The number of TCHs in a TDMA frame needed by the requesting MP for transmission with its intended MP. It is calculated from the number of pending RPDUs in the transmit buffer and the number of TCHs in use with the partner MP.

$Num(Sum(AL_M))$, $Num(Sum(ML_M))$: The sum of number of TCHs needed to transmit all real-time traffic flows which are generated or relayed at (all the one-hop adjacent MPs of the requesting MP, the requesting MP), when each of the flows operates at its mean rate.

NUM(TCH): The number of TCHs in a TDMA frame.

$Num(TCH_A)$, $Num(TCH_S)$: The number of (TCH_A, TCH_S).

RL_P, RL_M: The (peak, mean) traffic load of a traffic flow.

TCH_A: Common free TCHs in a TDMA frame at both the requesting and requested MPs.

TCH_R, TCH_S: Free TCHs in a TDMA frame observed by the (requested, requesting) MP.

3.3.4.1 Resource Request

The one-hop Throughput under the AM is described in Eqs. (3.21) - (3.22). Let TH^{o}_{UM} be the one-hop UM throughput. Similarly, assuming that an UM transmitting entity always has RPDUs for transmission and n_{TCH} TCHs are used for transmission, we have:

$$TH^{o}_{UM} = \frac{n_{TCH} \times L_{RPDU} \times 8}{P_{TDMA}} \times (1 - PER) \tag{3.26}$$

Eq. (3.22) and Eq. (3.26) are derived based on the assumption that the transmitting entity always has RPDUs ready for transmission. But this is not true in reality. Because the mean interarrival time of RPDUs from a traffic flow may be longer than the period of a TDMA frame as described in Section 3.2.9.1. Therefore given n_{TCH} TCHs used for transmission, the actual throughput for a specific traffic flow is smaller than that indicated by Eq. (3.22) or Eq. (3.26). Let $U_T \in [0, 1]$ be the TCH utilization factor. It is evident that the factor is dependent on the prespecified hang-on time, interarrival time of RPDUs from the flow relative to the period of a TDMA frame and the estimated packet multiplexing factor (see Section 3.2.9.1).

Given that the mean rate and peak rate of a bursty traffic flow are RL_m and RL_P, respectively, the TCHs in a TDMA frame needed for transmission can be derived from Eq. (3.22) and Eq. (3.26):

$$\begin{aligned} Num(RL_m) &= RL_m \times F \times \frac{1}{U_T} \\ Num(RL_p) &= RL_p \times F \times \frac{1}{U_T} \end{aligned} \tag{3.27}$$

Where, when AM is used

$$F = \frac{P_{TDMA}}{L_{RPDU} \times 6.8 \times (1 - PER)}$$

or when UM is used

$$F = \frac{P_{TDMA}}{L_{RPDU} \times 8 \times (1 - PER)}$$

The PER in the above equation is an estimated packet loss ratio. The definitions of P_T, N_{DD} and L_{RPDU} are given in Section 0. L_{RPDU} is related to the PHY rate. Note that $Num(RL_m)$ and $Num(RL_P)$ are not integers but fractions.

Resource requests are divided into two types: The first type of request is for establishing a service link between two peer service entities. The second type is for reserving one or more TCHs for an established service link. An MP shall carefully check whether the

```
1  /* For background and best effort traffic:
2     (Applicable for both the service link setup request
3     and TCH reservation request) */
4
5  If      Num (TCH_S) > 0.2 × NUM (TCH)
6          Then  request the setup of a service link
7                or reservation of TCHs
8                and  Num (RQ_TCH) = min (Num (Need_TCH),
9                                        Num (TCH_A)-0.1× NUM (TCH))
10 Else    quit the request process
11
12 /* For real-time traffic:
13    (Applicable for the service link setup request) */
14
15 If      Num (RL_M)+ Num (Sum (ML_M))+Num (Sum (AL_M)) > NUM (TCH)
16         Then  quit the request process
17 Else if Num (RL_P) + Num (Sum (ML_M))+Num (Sum (AL_M)) > NUM (TCH)
18         and   B (RL) > 2
19         Then  quit the request process
20 Else if Num (TCHs) > 0
21         Then  request the setup of a service link
22               and Num (RQ_TCH)= min(Num (Need_TCH), Num (TCH_S))
23
24 /*For real-time traffic:
25    (Applicable for the TCH reservation request) */
26
27 If      Num (TCH_S) > 0
28         Then  request the reservation of TCHs
29               and Num (RQ_TCH)= min (Num (Need_TCH), Num (TCH_S))
31 Else    quit the request process
```

Figure 3-27. Resource request control algorithms.

available resource is sufficient to meet the QoS delivery before sending a request of first type, while when it intends to send a request of second type, it only checks whether free TCHs in a TDMA frame are available at the moment. Requests for different types of traffic are treated differently.

The pseudo code in Figure 3-27 shows the resource request control algorithms. Lines 1 – 10 describe the control algorithm when a request is needed for transmitting background or best effort MPDUs. It is applicable for controlling both the service link setup and TCH reservation requests. Only if the number of free TCHs in a TDMA frame observed by the requesting MP is over 20% of the amount of TCHs in a TDMA frame, the MP considers initiating a request (note that 20% is implementation dependent). This is to prevent non-real-time traffic flows from using the TCHs when the TDMA frame capacity is approximately saturated. For the same reason, $Num(RQ_{TCH})$ is not bigger than $0.1\times$ *NUM(TCH)*.

Lines 12 – 22 describes the algorithm for real-time traffic when an MP wishes to set up a service link with its partner. The MP checks whether the available resource, which is unused by the real-time flows in the one-hop neighborhood of the MP, are enough to satisfy the QoS delivery of requested traffic (lines 15-19). The checks also guarantee that the establishment of the service link shall not corrupt the QoS of the established real-time service links in the same neighborhood. If those checks are passed, as long as $Num(TCH_S) > 0$, the request shall be initiated. The information of $Num(Sum\ (L_P))$ and $Num(Sum\ (L_M))$ are collected at an MP by monitoring MPDUs sent by others within a certain period. When an MP transmits an MPDU, it put information of its own sum of the real-time loads in the MPDU. Since the load is expressed as the number of needed TCHs in a TDMA frame, the bits used to carry the information are very limited. On reception of the request confirmation, the MP shall adjust $Num(Sum(ML_M))$ += $Num(RL_M)$.

Lines 24 – 31 show the algorithm when an MP wants to reserve TCHs for existing service links delivering real-time traffic. As long as $Num(TCH_S) > 0$, the MP shall initiate a request.

3.3.4.2 Call Admission Control (CAC)

As introduced before, on reception of a service link setup or TCH Reservation request, the requested MP shall execute the CAC locally to evaluate whether to accept the request or not. An MP initiates the service link setup procedure when it has not established a service link with its intended partner. An MP transmission pair may release a reserved TCH for a number of reasons even when the service link still exists. On arrival of more RPDUs in a service entity at an MP when it has no or insufficient TCH capacity for use, it shall initiate the TCH Reservation request. Figure 3-28 shows the pseudo code describing the CAC alogrothm.

A requested MP shall calculate TCH_A on reception of a service link setup or TCH reservation request (Line 1) in Figure 3-28. It will grant the request for background or best effort traffic as long as $TCH_A > 0$ (lines 3 -10). A TCH used for background/best effort traffic may be forced released in high load. In case the request is for setting up a service link for real-time traffic, the CAC shall evaluate whether the QoS of requested traffic flow can be satisfied and the establishment of the link will corrupt the QoS of granted flows. Lines 12-28 describe the corresponding algorithm. Note that the $Num(RL_M)$ and $Num(RL_P)$ are calculated by Eq. (3.27) when an MP considers sending a request. When a requested MP receives a request for a multi-hop transmission, it shall double the received $Num(RL_M)$ and $Num(RL_P)$ before applying the values into the calculations shown at lines 18-20. On reception of a request of TCH Reservation for real-time traffic, the

```
1  TCH_A = TCH_S ∩ TCH_R   // Symbol ∩ denotes AND operator
2
3  /* For backgroup and best effort traffic:
4     (Applicable for both the service link setup request
5     and TCH reservation request) */
6
7  If       Num (TCH_A) > 0
8           Then    accept the request
9                   and Num (G)= min (Num (TCH_A), Num (RQ_TCH))
10 Else     reject the request
11
12 /* For real-time traffic:
13    (Applicable for the service link setup request) */
14
15 //Note: when a request is for a multi-hop transmission
16 // Num (RL_M) and Num (RL_P) should be double
17
18  If       Num (RL_M)+ Num (Sum (ML_M))+Num (Sum (L_M)) > NUM (TCH)
19           Then    reject the request
20 Else if Num (RL_P) + Num (Sum (ML_M))+Num (Sum (L_M)) > NUM (TCH)
21           and  B (RL) > 2
22           Then    reject the request
23 Else if  Num (TCH_A) < Num (RQ_TCH)
24           Then    reject the request
25 Else      accept the request
26           and Num (G)= Num (RQ_TCH)
27           and Num (Sum (ML_M))+=Num (RL_M)
28
29 /*For real-time traffic:
30    (Applicable for the TCH reservation request) */
31
32 If        Num (TCH_A) > 0
33           Then   accept the request
34                  and Num (G)= min (Num (TCH_A), Num (RQ_TCH))
35 Else      reject the request
```

Figure 3-28. Call admission control.

CAC grants the request as long as $TCH_A > 0$ (lines 29-35). Let $Num(RL_M^{n\text{-}hop})$ be the average number of TCHs in a TDMA frame needed for a n-hop real-time transmission. Given the spatial reuse distance is m hops, it can be derived that:

$$Num\ (RL_m^{n-hop}) = Min\ (n, m) \times RL_m \times F \times \frac{1}{U_T} \tag{3.28}$$

Eq. (3.28) suggests that a multi-hop transmission consumes multiple radio resource compared to a single hop transmission.

1 **If** $N_{RPDU}^{T} = 0$ ***or*** $(N_{TCH}^{M} > 0$ ***and*** $N_{RPDU}^{T}/N_{TCH}^{M} < Thr\_1)$
2 **Then** exit
3 **Else If** $N_{TCH}^{M} = 0$ **and** $N_{TCH}^{P} > 0$ **and** $N_{RPDU}^{T} < Thr\_2$
4 **Then** request On-demand TCH Turnaround
5 **Else if** $N_{TCH}^{P} > 1$ **and** $N_{RPDU}^{P}/(N_{TCH}^{P} - 1) < Thr\_3$
6 **Then** request On-demand TCH Turnaround
7 **Else if** $N_{TCH}^{F} > 0$ **and** $N_{RPDU}^{r} > 0$ **and**
8 $(N_{TCH}^{M} = 0$ ***or*** $N_{RPDU}^{r}/N_{TCH}^{M} > Thr\_4)$
9 **Then** initiate TCH Reservation
10 **Else if** $N_{TCH}^{F} > Thr\_5$ **and**
11 $(N_{TCH}^{M} = 0$ ***or*** $N_{RPDU}^{T}/N_{TCH}^{M} > Thr\_6)$
12 **Then** initiate TCH Reservation

Figure 3-29. Requesting on-demand-TDD or TCH reservation during transmission.

3.3.4.3 Resource Control during Transmission

During operation of one or more TCHs, one MP may wish to turnaround one TCH, or it may wish to initiate TCH reservation to reserve more TCHs. Some parameters are used in the algorithm shown in Figure 3-29 that applies to unicast links:

N_{RPDU}^{r}, N_{RPDU}^{T} The number of pending real-time RPDUs destined to my partner; r = real-time, T = total

N_{RPDU}^{P}: The number of pending RPDUs of my partner.

N_{TCH}^{P}: The number of TCHs in a TDMA frame used by my partner for transmitting with me.

N_{TCH}^{M}: The number of TCHs in a TDMA frame used by me to transmit with my partner

N_{TCH}^{F}: The number of free TCHs in a TDMA frame observed by me

Thr_i $(1 \leq i \leq 6)$: The threshold values, implementation dependent

Variables N_{RPDU}^{r}, N_{RPDU}^{T}, N_{TCH}^{M} and N_{TCH}^{F} are maintained by each MP, whilst N_{TCH}^{P} and N_{RPDU}^{P} are carried in data RPDUs.

If an MP has zero N_{RPDU}^{T} or its N_{TCH}^{M} can satisfy the current needs, it quits the algorithm (lines 1-2). If it has no TCH for transmission but the number of its pending PPDUs < *Thr_2* whilst $N_{TCH}^{P} > 0$, then it requests TCH turnaround (lines 3-4). If its partner MP uses > 1 TCHs for transmitting and can handle its transmission with less TCHs, the MP shall request TCH turnaround of one TCH (lines 5-6). If the MP has pending real-time RPDUs and some free TCHs in a TDMA frame exist, it initiates TCH reservation (lines 7-9). If the MP finds > *Thr_5* free TCHs existing, if it has not enough TCHs for transmitting its pending RPDUs, it shall initiate TCH reservation (lines 10-12).

```
1  If    N_TCH^F < 0.1 × NUM(TCH) and Sum(N_TCH^M) > 0
2        Then If    find a reserved TCH in the hang-on state
3                   Then release the TCH
4             Else  check all maintained serivce links one-by-one
5                   If   N_TCH^M(i) == 1 and N_RPDU^r(i) == 0
6                        Then A(i) = 0
7                             B(i) = N_RPDU^P(i) / N_TCH^M(i)
8                   If   N_TCH^M(i) > 1
9                        Then A(i) = N_RPDU^r(i) / (N_TCH^M(i) - 1)
10                            B(i) = N_RPDU^P(i) / N_TCH^M(i)
11            If    find k whose A(k) < Thr_1
12                  and B(k) is the smallest
13                  Then release a TCH in use for
14                       transmission with station k
```

Figure 3-30. Forced release a TCH.

3.3.4.4 Forced Release of TCHs

One advantage of MDCF is that the short-term traffic situation in an area can be derived by an MP by monitoring the TCH usage. When an MP finds that the TCHs in a TDMA frame are close to be fully reserved at a time, it knows that the network is highly loaded. When this happens, the MP shall check whether it can forced release a reserved TCH in order to ensure that there are free TCHs in a TDMA frame available for forthcoming real-time traffic.

The following definitions are extended from those given in Section 3.3.4.3:

$N_{RPDU}^{r}(i)$: The number of pending real-time RPDUs destined to my adjacent MP *i*

$N_{RPDU}^{T}(i)$: The number of pending RPDUs destined to my my adjacent MP *i*

$N_{TCH}^{M}(i)$: The number of TCHs used by me for transmitting with my adjacent MP *i*

$Sum(N_{TCH}^{M})$: The sum of number of TCHs used by me for transmitting

Thr_1: A threshold, implementation dependent

Figure 3-30 shows the algorithm for forced releasing a TCH. On detecting the free TCHs in a TDMA frame is less than a predefined threshold, an MP having reserved TCHs for use shall perform this algorithm (Line 1). In this example, the predefined threshold for judging the congestion situation is 10% of the number of the TCHs in a TDMA frame. It is implementation dependent. If the MP finds one of its reserved TCHs in the hang-on state, it releases the TCH and quits the algorithm (Lines 2-3). Otherwise, it checks its maintained links having reserved TCHs one by one. The MP evaluates whether it is able to timely deliver the pending real-time RPDUs with one reduced number of TCHs to a destination. If it finds more than one of those links, it shall choose one whose $N_{RPDU}{}^{T}(i)/N_{TCH}{}^{M}(i)$ is the smallest, and release one TCH reserved for the link (Lines 4 -14).

Upon forced releasing a TCH, an MP shall perform the algorithm again after a certain period when necessary.

3.4 Mesh Routing and Security

The Mesh Routing is responsible for discovering and maintaining the mesh topology, and determining the optimal route for packet delivery. The Security part is for securing information exchange between MPs over the shared medium.

An MACF network is formed in a fully distributed manner. The mesh topology knowledge can be built up in the routing discovery stage of running a routing protocol at each MP. The mesh topology knowledge includes status and quality of mesh links between MPs. A routing protocol also takes care of the topology knowledge refreshment during operation.

Routing protocols [74]-[78] have been extensively studied in the scope of Mobile Ad Hoc Networks (MANET) [73] working group in the Internet Engineering Task Force (IETF). The mesh routing protocol used for MDCF networks can be any accepted MANET protocol or any recently proposed mesh routing scheme. Advanced routing protocols appear possible to realize when considering the special feature of MDCF, e.g. existence or non existence of TCHs for a given link. A route might be selected that has already reserved TCHs, compared to any other route. This might contribute to extent the lift time of TCHs and reduce overhead for reestablishment of TCHs. However, routing protocol development is out of scope of the thesis.

The IEEE 802.11i [20] security mechanisms have been well developed for the WLAN application. The mesh security for MDCF adopts the mechanisms including their future extensions.

CHAPTER 4

Modeling and Performance Analysis

A WMN tends to be highly loaded, since multi-hop relaying increases traffic: An n-hop transmission leads to n times higher overall network traffic than a one-hop transmission. This also causes much more contention for channel access. Hence, how well MDCF handles the situation is of great interest. Besides this, as MDCF is a TDMA based protocol aiming at supporting QoS in mesh, it is of importance to find out the optimal frame parameter settings for achieving a high possible network throughput as well as a low possible end-to-end delay meeting QoS requirements. The above reasons motivate the analytical study presented here.

This Chapter uses mathematical analysis to reveal the two key performances of MDCF: the elimination performance of the channel access scheme (Section 4.1) and the traffic performance of MDCF in mesh (Section 4.2). The traffic performance here means the throughput and end-to-end delay performance. To study the traffic performance of MDCF in mesh, a simple yet highly accurate analytical model is established based on the theory of queueing network [81]. The accuracy of the model is verified by simulations. To the best of our knowledge, this is the first analytical model used to study the traffic performance of a specific system in mesh environments. After that, the impact of the key frame parameters on the results gained is investigated by using the model. Based on this, the optimal frame parameter settings accounting for supporting QoS in mesh can be precisely determined.

4.1 Elimination Performance

4.1.1 Background and Motivation

As introduced, contention for channel access in a WMN is much more serious than that in a single hop network. To handle this and hence avoid collisions, the channel access scheme for WMNs should be highly eliminating, namely, ensuring only one winner in each contention even where a large number of MPs contend at the same time.

Channel access in MDCF is performed in the ACH, which consists of three phases: PP, FEP and TP. The PP is the prioritized contention phase in favor of high QoS level traffic, while the FEP is used to ensure a highly eliminating and fair channel access. Both the PP and FEP comprise a number of contention slots, in each of which a contending MP either transmits an AES or listens the channel. Figure 3-4 shows the structure of the ACH. A contention level is represented by a binary number whose bits correspond to the contention slots one by one. The higher a binary number, the higher a contention priority level. Section 3.2.2 describes the contention scheme in detail. The contention levels in the PP and FEP are called PPCLs and FEPCLs, respectively. The way to determine the PPCL at a contending MP is introduced in Section 3.2.2.2. This section focuses on studying the elimination performance of the channel access scheme.

Let n denote the number of contention slots in the FEP. Obviously, the amount of FEPCLs is 2^n. To implement a fair channel access, the amount of FEPCLs 2^n is divided into K equal-size non-overlapping CNGs ordered as: [0, ($2^n/K$) -1], [$2^n/K$, ($2 \times 2^n/K$) -1], ..., [(K-1) $\times 2^n/K$, 2^n -1]. The last one is the highest CNG. Each CNG contains $2^n/K$ contention levels. After winning the contention in the PP, a contending MP determines a CNG to select a FEPCL number. The fairness mechanism ensures that the more often an MP loses the contention, the higher CNG level it will use to select a FEPCL. Obviously, the more CNGs exist, the better the short term fairness performance would be. With a big K, an MP that lost a contention is able to stepwise increase its FEPCL as the number of lost contentions for the same packet. This enables an MP to win a future contention soon compared to MPs starting to contend later for a transmission via the ACH. However a big K results into a small $2^n / K$, the amount of contention levels in each CNG. If $2^n / K$ is small, a good elimination performance cannot be guaranteed. The numbers n and K should be well selected so that a fair elimination can be ensured with a lowest possible overhead.

4.1.2 Elimination Performance

Suppose that N MPs contend at the same time with the same PPCL. Let $p(N, n)$ be the probability of only one winner in the contention given the number of contention slots in the FEP is n. Assume that after a contending MP wins the contention in the PP, it randomly select a FEPCL $l \in [0, 2^n -1]$ for the contention in the FEP. The probability that it wins the contention in the FEP over the other $N-1$ MPs is: $p(L=l) \times p(L<l)^{N-1}$, where $p(L=l)$ and $p(L<l)$ denote the probabilities that the FEPCL is equal to l and smaller than l, respectively, given $l \in [0, 2^n -1]$. Obviously, $p(N, n)$ is given by,

$$p(N,n) = \binom{1}{N} \sum_{l=1}^{2^n} p(L=l) \times p(L<l)^{N-1} \tag{4.1}$$

Where

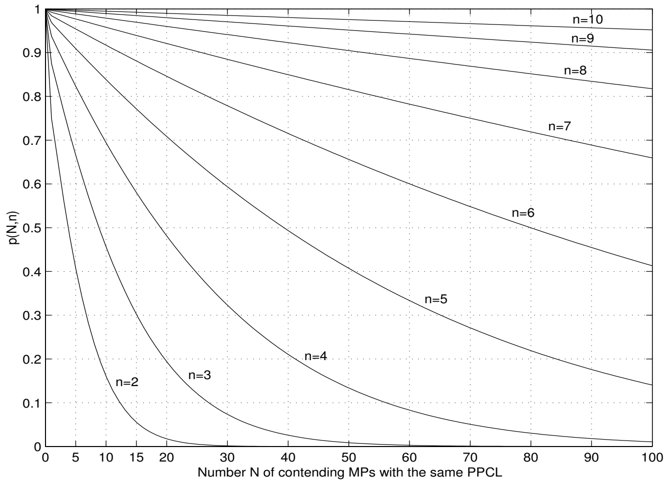

Figure 4-1. p(N, n) vs. N - the number of contending MPs with the same PPCL.

$$p(L = l) = \frac{1}{2^n} \tag{4.2}$$

$$p(L < l) = \frac{l-1}{2^n} \tag{4.3}$$

Inserting Eq. (4.2) and Eq. (4.3) into Eq. (4.1) yields

$$p(N, n) = N \sum_{l=1}^{2^n} \frac{1}{2^n} \times \left(\frac{l-1}{2^n}\right)^{N-1} \tag{4.4}$$

Assume that *N’* of *N* MPs generate their FEPCLs from the same CNG. Let *p’(N’, n, K)* be the probability of only one winner in the contention given 1) the number of contention slots in the FEP is *n* and 2) the number of CNGs is *K*. Similarly, it can be derived:

$$p'(N', n, K) = N' \sum_{l=1}^{Int(2^n/K)} \frac{1}{Int(2^n/K)} \times \left[\frac{(l-1)}{Int(2^n/K)}\right]^{N'-1} \tag{4.5}$$

Where the function Int(·) returns the integer of a value.

As introduced in Chapter 3, when a contending MP wants to send beacons via the ACH it generates the FEPCL from [0, 2^n-1], whilst for the other cases, it generates the FEPCL from a CNG (the number of contention levels is $2^n/K$). Therefore, *p(N, n)* and *p’(N’, n, K)* are the elimination probabilities of contending for sending beacons and other packets, respectively.

The relation of *p(N, n)* and *N* is plotted in Figure 4-1. It is clear that *n* should be big enough to ensure a high elimination performance to avoid collision and hence the waste of the scare bandwidth. As to be seen from the graph, when *N* is 5 and the values of *n* are 2, 3 and 4, respectively, the elimination probabilities are 0.4, 0.66 and 0.82. When *N* is

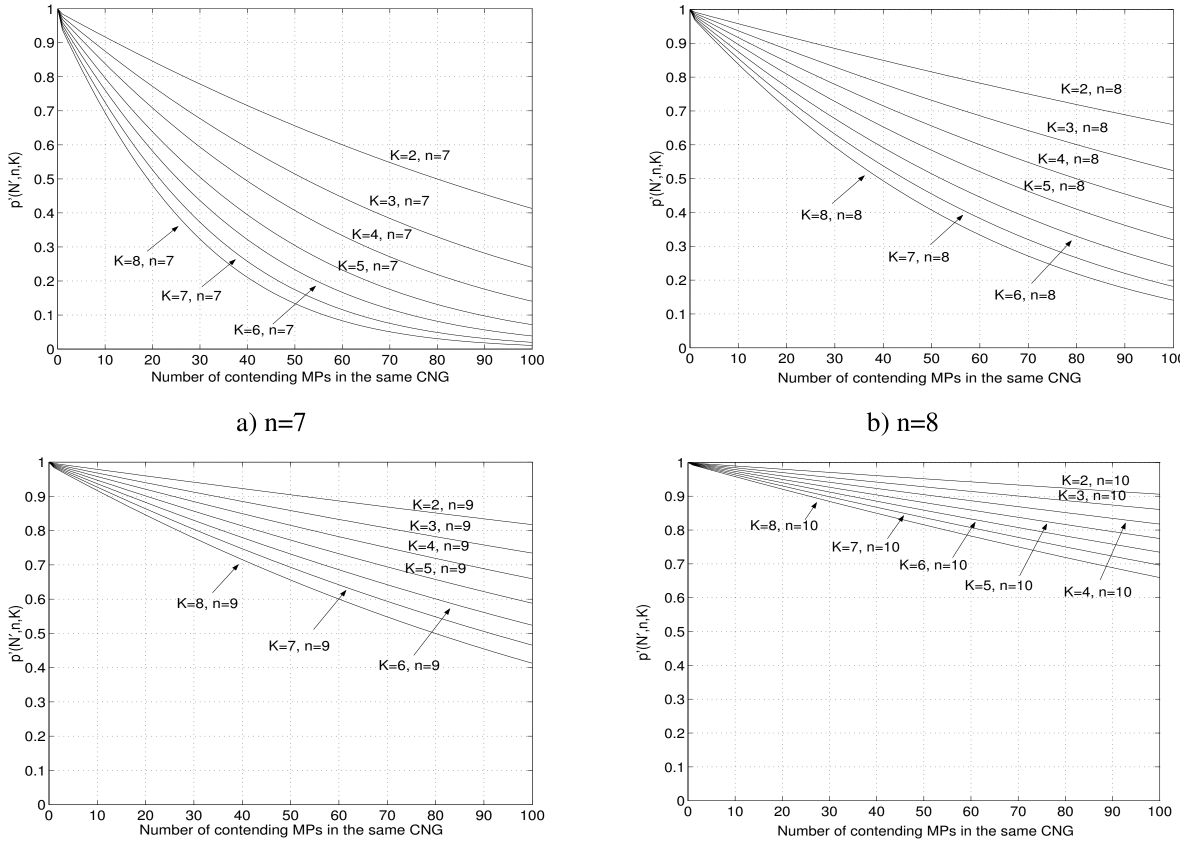

a) n=7 b) n=8

c) n=9 d) n=10

Figure 4-2. p'(N',n, K) vs. N' - the number of contending MPs in the same CNG.

increased to 15, the elimination probabilities are reduced to 0.05 (n = 2), 0.3 (n = 3) and 0.58 (n = 4). However a slight increase of n results in significantly improving the elimination performance. Even if N is 30, when the values of n are 7 and 8, the elimination probabilities reach 0.88 and 0.95, respectively. Note that in TG "s" of the 802.11 project, the working assumption for the maximum number N of MPs is 32. As shown in Table 4-1, we assume m = 2 as a reasonable assumption in this thesis.

Figure 4-2 shows the relation of $p'(N', n, K)$ and N'. As indicated in Figure 4-2a & b, when N' is 10 and the values of n are 7 and 8, in case K is 8, the elimination probabilities are 0.69 and 0.83, respectively. As N' increases, the elimination performance decreases sharply: When N' is 20, the elimination probabilities go down to 0.48 (n = 7, K = 8) and 0.70 (n = 8, K = 8). The elimination performance can be improved at the cost of reducing K: When K is 3, in case N' is 20, the elimination probabilities are 0.77 and 0.88 if the values of n are 7 and 8, respectively. As aforementioned, a small K cannot ensure a short-term fairness. In order to achieve a satisfactory short-term fairness performance while ensuring a high elimination performance in a middle-scale multi-hop network, n should be big enough. As shown in Figure 4-2c & d, when the values of n are 9 and 10, respectively, even if N' = 40 and K=8, the elimination probabilities still reach 0.72 and

0.85. When N' =100 and K = 8, in case that n is 10, the elimination probability is still around 0.65.

It should be noted that in an MDCF multi-hop network, MPs contending with each other for channel access may spread up to 4 hops, see Section 3.2.5. Hence, to ensure a high elimination performance ($p'(N', n, K) > 0.9$) in small scale mesh networks (like $N < 32$ and $N' < 10$), n can be 8 if K is smaller than 5. While for medium scale mesh networks ($N \in [0, 50]$, $N' \in [0, 30]$), n should be at least 9 or 10. This also allows that K can be over 6.

4.2 Analysis of Traffic Performance in Mesh

4.2.1 Related Work

The study of throughput and delay performance of MDCF in mesh is the main concern of the Chapter. The throughput-delay characteristics of non- and p-persistent carrier sense multiple access (CSMA) are analyzed in [48] based on the renewal theory. Similar approaches are widely used to analyze the traffic performance of packet-oriented protocols. In [50], an analytical model is proposed to compute the single-hop saturation throughput of the 802.11 DCF, which is packet-oriented based on CSMA with collision avoidance (CA) with binary slotted exponential backoff. In the above mentioned packet-oriented systems, a station contends for channel access to gain a single packet transmission chance, different from MDCF where a TCH is reserved instead. Accordingly, the analytical approaches proposed in those papers cannot be used here. The performance of TDMA-based cellular networks has been extensively analyzed like in [51]. The methods used there also cannot be borrowed since MDCF is distributed in nature for mesh networks, which is significantly different from the centralized protocols of cellular radio networks. This Section presents a simple yet highly accurate analytical model based on the theory of queueing network [81], [80], to study the traffic performance of MDCF in both single-hop and mesh environments. To the best of our knowledge, this is the first analytical model used to study the traffic performance of a a TDMA based mesh network.

4.2.2 System Model: Scenario and Assumptions

Multi-hop mesh networks differ in topology from scenario to scenario. It is, therefore, difficult to develop an analytical model generally applicable for any multi-hop network topology. We focus here on the free space multi-hop scenario shown in Figure 4-3, where spatial reuse is impossible. It is worth noting that since MDCF is able to inhibit hidden stations in multi-hop environments (see Secion 3.2.5), the traffic performance of MDCF mesh networks with spatial channel reuse (like in indoor scenarios) is better than calculated for the scenario considered here. In this sense, this Section studies a worst case scenario. Moreover, the evaluation on the scenario provides an insight in the

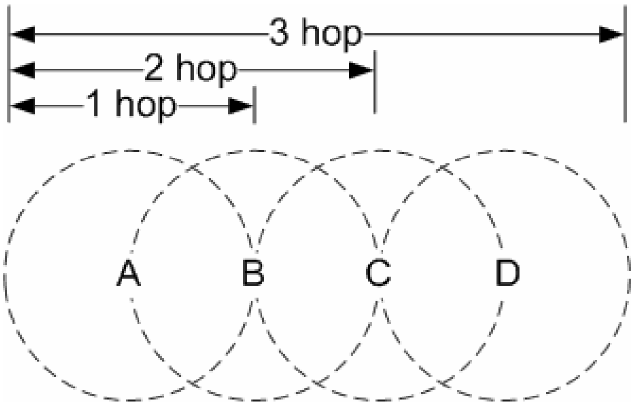

Figure 4-3. Study scenario: a free space multi-hop network.

multi-hop capability of MDCF. Based on that, the impacts of frame parameters are investigated, and the optimal frame settings can be determined.

The analysis is split into two parts. First, we establish an open queueing network model to study the behavior of single-hop MDCF networks. Based on that, we then extend the model to study the performance of multi-hop MDCF networks.

Figure 4-3 shows the network used for evaluation. The detailed description of the scenario and the assumptions made for deriving the analytical model are as follows:

1) MPs are in a free space area that is divided into four clusters: A, B, C and D. Only one, two, and three hop transmissions are under consideration. All MPs are identical in transmission and reception capabilities. Assuming that the carrier sense range is 2 times the transmission range, the spatial reuse distance is 4 hops away in a free space MDCF mesh network (see Secion 3.2.5). Hence, no spatial reuse is possible in this scenario.

2) Each MP generates packet trains, all with the same QoS level. A *packet train* contains g MPDUs, as shown in Figure 4-4. The MPDUs in a packet train are generated at the same time. All packet trains in a given scenario have the same number of MPDUs.

3) The traffic source consists of a large number of MPs and stations associated in one-hop distance to an MP which collectively form an independent Poisson source with a mean packet train generation rate of λ_{PT} packet trains/s. Obviously the aggregate mean MPDU generation rate λ_{MPDU} is $g\lambda_{PT}$.

4) The number of ACH and TCHs in a TDMA frame is 1 and N, respectively.

5) Channel access is assumed to be absolutely eliminative, with only one winner in each ACH contention. This is close to what is achieved in MDCF, see last Section.

6) Transmissions are under the Unacknowledged Mode (UM). No packet is lost during transmission. On-demand-TDD TCH turnaround (see Section 3.2.4) and packet

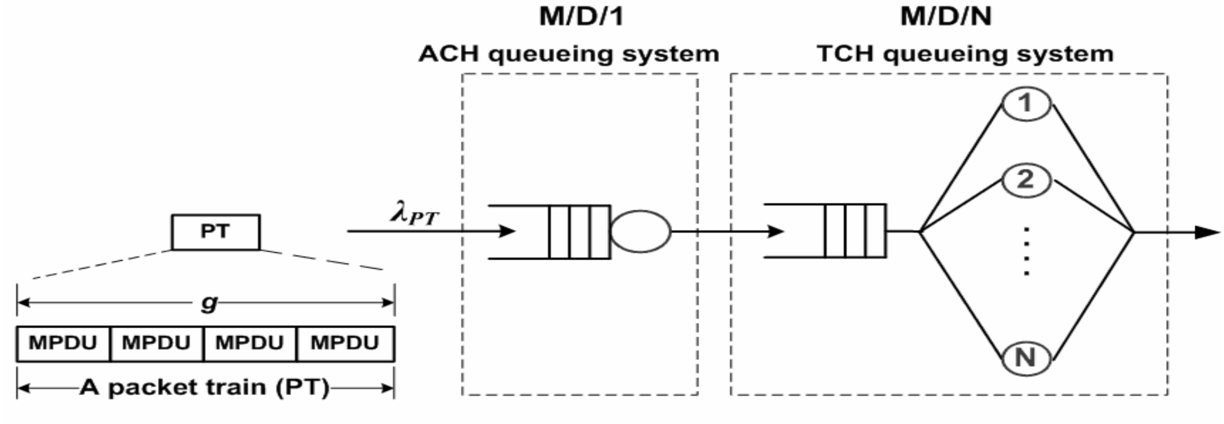

Definitions:
g – number of MPDUs in a packet train (PT)
h – hang on time of a TCH (unit: TDMA frames)
λ_{PT} – generation rate of PTs
N – number of TCHs in a TDMA frame (= number of servers in TCH queueing system)

Note:
- Input of the open queueing network is packet trains (PT), each containing g MPDUs.
- Service rate of the ACH queue server depends on availablity of at least one free server in TCH queueing system
- Service rate of a TCH queue server is $1/(g+h)$ (unit: 1 PT/TDMA frame)

Figure 4-4. A queueing model for single-hop MDCF networks.

multiplex (see Section 3.2.7) are not enabled.

7) The hang-on count is started on the completion of transmission of the last MPDU in a packet train on a TCH. The TCH is considered free on the expiration of the hang-on time, which is h TDMA frames and same at each MP.

8) For simplicity, the evaluation scenarios are: a) all transmissions span single hop; b) all transmissions span two-hop; c) all transmissions span three-hop.

4.2.3 Analytical Model

4.2.3.1 Introduction of the Model

We simply review a transmission process in MDCF assuming that only one TCH is needed for such a packet train: An MP having pending MPDUs checks whether there is a free TCH in a TDMA frame. If so, it contends in the ACH to reserve a TCH for transmission, or otherwise it waits until a free TCH appears. If the MP succeeds in an ACH contention, it thereafter transmits its g pending MPDUs on the reserved TCH. After that, the MP starts to hang on. On expiration of the hang-on time, the reserved TCH is freed.

Unlike in 802.11 DCF [50] and with non- and p-persistent CSMA [48], the level of contention for channel access in MDCF does not contribute a significant load to the network since channel access is highly eliminative. The loss caused by collision is very small. Instead, the ratio of the average number of pending MPDUs at MPs to the hang-on time mostly affects the TCH utilization and in turn the achievable network throughput. However, the contention level impacts on the packet delay significantly: When contention in a network is heavy, only one ACH per TDMA frame may result in a bottleneck. When all TCHs in a TDMA frame are occupied, an MP wishing to transmit must wait until a free TCH appears.

A model is proposed to simulate the above described transmission process: Use *packet trains* (see Assumption 2) as input traffic to go through an open queueing network, which consists of 1 ACH queuing system and 1 TCH queueing system with *N* servers. The performance of a network can be characterized by the throughput and delay performance of MPDUs, contained in packet trains. This model considers the impact of the contention level and the number of pending MPDUs for a TCH on the performance. Figure 4-4 shows the model for single-hop networks. It works as follows:

MPs having pending packet trains first contend in the ACH if at least one free server in the TCH queueing system is available. In the following, we call the server ACH and TCH with its related queues, ACH queue and TCH queue, respectively. The ACH queue represents the number of pending packet trains waiting decentrally in the buffer of the MPs. Clearly, the arrival rate of packet trains to the ACH queue is a Poisson process with rate λ_{PT} packet trains/s. Since no collision happens in the TP of the ACH (Assumption 5), a packet train is served successfully per TDMA frame, i.e. the service rate of the ACH queue is 1 packet train/TDMA frame if free TCHs exist. However, the ACH queue stops handling packet trains if no free TCH is available. When this situation ever happens, the overall service rate of the ACH is below 1 packet train/TDMA frame. Based on above analysis, the ACH can be modeled as M/D/1 queue, whose service rate is dependent on the availability of at least one free server in the TCH queueing system.

After being served by the ACH queue, a packet train is transferred into the TCH queueing system. Then, the arrival rate of packet trains to the TCH queueing system equals to λ_{PT} when $\lambda_{PT} \leq$ service rate of the ACH queue or otherwise the service rate of the ACH queue. Under Assumption 6, it is clear that the service rate of a TCH is 1 packet train per $g+ h$ TDMA frames: A TCH needs g TDMA frames to complete the service for a packet train. After that, the TCH starts to hang on h TDMA frames and will not serve for any MPDU before it is freed. Since the number of TCHs in a TDMA frame is *N*, clearly, those TCHs can be modeled as M/D/N queue.

The following definitions are used:

$\boldsymbol{D_M^{j\text{-}hop}}$: j-hop mean end-to-end MPDU delay, $j \in \{1, 2, 3\}$

$\boldsymbol{D^i}$: End-to-end delay of the i^{th} MPDU in a packet train, $i \in [1, g]$

$\boldsymbol{g}$: The number of MPDUs in a packet train

$\boldsymbol{h}$: The hang-on time of a TCH counted in number of TDMA frames

max(x): Upper bound of an uncertain value x

N: The number of TCHs in a TDMA frame

P_{TDMA}: The length of a TDMA frame in ms

$Q_{Acc}{}^{j\text{-}hop}$: Access delay of a packet train at the jth hop. It is the sum of the service time and waiting time in the ACH queue

T_{ACH}, T_{TCH}, T_{ECH}: Duration of a (ACH, TCH, ECH) slot

$Th_{PT}{}^{j\text{-}hop}$, $Th_{MPDU}{}^{j\text{-}hop}$, $N(Th_{MPDU}{}^{j\text{-}hop})$: *j*-hop (packet train, MPDU, normalized MPDU) throughput, j ∈ {*1*, 2, 3}

T_{Tran}: Transmission delay of an MPDU on a TCH

W^{i}_{TCH}: Waiting time of the i^{th} MPDU in a packet train at a TCH, $i \in [1, g]$

X_{ACH}: Service time of the ACH queue

ρ_{ACH}: Utilization factor of the ACH server

Λ: Time difference between the start of the ACH and start time of a TCH in a TDMA frame

4.2.3.2 Performance Analysis of Single-hop Network

From the queueing model shown in Figure 4-4, it is clear:

$$D^i = Q_{Acc} + W^i_{TCH} + \Lambda + T_{Tran} \qquad i \in [1, g] \tag{4.6}$$

Assuming an MP wins an ACH contention at the n^{th} TDMA frame, it shall transmit the first MPDU on a TCH in the $(n+1)^{th}$ TDMA frame. The term Λ reflects the time differences between the start of the ACH and the start of a TCH in a TDMA frame that is randomly selected. Obviously, the waiting time W^{i}_{TCH} is:

$$W^i_{TCH} = i \times P_{TDMA} \qquad i \in [1, g] \tag{4.7}$$

The one-hop mean MPDU delay $D_M{}^{i\text{-}hop}$ is given by:

$$\begin{aligned} D_M^{1-hop} &= \frac{1}{g} \times \sum_{i=1}^{g} D^i \\ &= \frac{1}{g} \times \left[g \times (Q_{Acc} + T_{Tran} + \Lambda) + P_{TDMA} \times \sum_{i=1}^{g} i \right] \\ &= Q_{Acc}^{1-hop} + T_{Tran} + \Lambda + P_{TDMA} \times \frac{g+1}{2} \end{aligned} \tag{4.8}$$

As the ACH can be modeled as M/D/1 queue, hence Q_{Acc} is given by [79]:

$$Q_{Acc}^{1-hop} = X_{ACH} \times \left[1 + \frac{\rho_{ACH}}{2 \times (1 - \rho_{ACH})} \right] \tag{4.9}$$

Transfer of a packet train (g MPDUs) on a TCH needs $g+h$ TDMA frames (taking the hang-on time into account), whilst reservation of N TCHs to serve N packet trains in parallel needs N TDMA frames. Then, if $g+h \leq N$, even when the ACH server is fully utilized, there are still N-g-h free TCHs. Under this, the service time of the ACH is 1 TDMA frame. But if $g+h > N$, when the arrival rate of packet trains is high enough, all N TCHs may be occupied at a time. If so, the ACH stops working until one free TCH appears again. Under this condition, the service time of the ACH can be looked as $(g+h)/N$ TDMA frames to match the processing capability of the N TCHs. Hence, we have,

$$\begin{cases} X_{ACH} = P_{TDMA} & g + h \leq N \\ X_{ACH} = \dfrac{g+h}{N} \times P_{TDMA} & g + h > N \end{cases} \tag{4.10}$$

from [79], the ACH utilization is:

$$\rho_{ACH} = \lambda_{PT} \times X_{ACH} \tag{4.11}$$

Substituting Eq. (4.10) and Eq. (4.11) into Eq. (4.9) yields:

$$\begin{cases} Q_{Acc}^{1-hop} = P_{TDMA} \times \left[1 + \dfrac{\lambda_{PT} \times P_{TDMA}}{2 \times (1 - \lambda_{PT} \times P_{TDMA})} \right] & g + h \leq N \\ Q_{Acc}^{1-hop} = \dfrac{g+h}{N} \times P_{TDMA} \times \left[1 + \dfrac{\lambda_{PT} \times ((g+h)/N) \times P_{TDMA}}{2 \times (1 - \lambda_{PT} \times ((g+h)/N) \times P_{TDMA})} \right] & g + h > N \end{cases} \tag{4.12}$$

The delay performance is jointly described by Eq. (4.8) and Eq. (4.12).

Since no packet train is lost in the queueing network (Assumption 6), $Th_{PT}^{1\text{-}hop}$ is equal to λ_{PT}:

$$Th_{PT}^{1-hop} = \lambda_{PT} \qquad when \quad \lambda_{PT} < 1 / X_{ACH} \tag{4.13}$$

From Eq. (4.11), the $max(\lambda_{PT})$ = $1/X_{ACH}$. Then,

$$\max(Th_{pg}^{1-hop}) = \begin{cases} \dfrac{1}{P_{TDMA}} & g + h \leq N \\ \dfrac{N}{(g+h) \times P_{TDMA}} & g + h > N \end{cases} \tag{4.14}$$

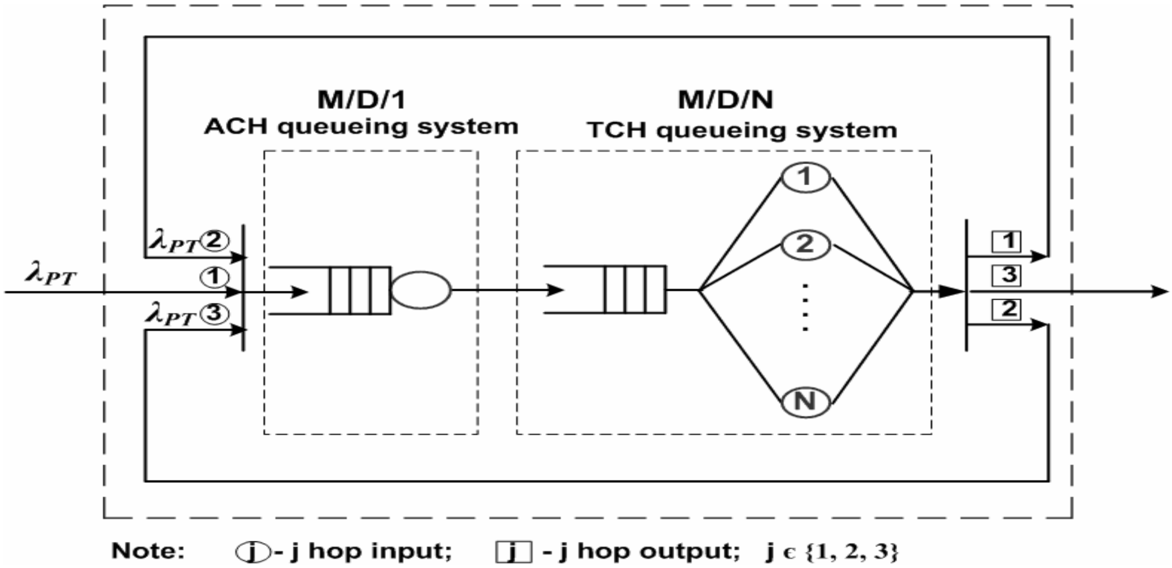

Figure 4-5. A queueing model for multi-hop MDCF networks. It is an open queueing network, shown inside the dotted box. Specifically, this model is for a 3-hop MDCF network, where no spatial reuse is possible.

4.2.3.3 Performance Analysis of Multi-hop Network

Since spatial reuse is not possible in the evaluated scenario (Assumption 1), source and relaying MPs must share using the radio resource. Figure 4-5 depicts the queueing model proposed for such multi-hop networks, which is also an open queueing network. Beside an external input, there are two internal inputs to the ACH queue. The two internal inputs come from the outputs of relaying MPs. The 1-hop output of a TCH at an MP is the 2^{nd} -hop input to the ACH, and in turn the 2-hop output of a TCH becomes the 3^{rd} -hop input to the ACH. The ACH queueing system and TCH queueing system together forms a one-hop queueing network. A 3-hop transmission needs to go through the one-hop queueing network 3 times. The output port 3 of the TCH queueing system in Figure 4-5 is the output of the entire queueing network. Note this model is valid only when no spatial reuse is possible. Otherwise, source and relaying MPs may not contend in the same ACH queue, and the number of TCH queue servers available at each MP may be different.

Based on the model, it is easy to have:

$$\begin{aligned} D_M^{j-hop} &= j\times(Q_{Acc}^{j-hop}+T_{Tran}+\Lambda+P_{TDMA}\times\frac{g+1}{2})-(j-1)\times P_{TDMA}\times\frac{(g+2)\times(g-1)}{2\times g} \\ &= j\times(Q_{Acc}^{j-hop}+T_{Tran}+\Lambda)+\frac{P_{TDMA}\times(g^2+g-2+2\times j)}{2\times g} \qquad j\in\{1,2,3\} \end{aligned} \tag{4.15}$$

where j is the number of hops. The term $(j\text{-}1)P_{TDMA}(g+2)(g\text{-}1)/(2g)$ takes into account that the 2^{rd} to g^{th} MPDUs in a packet train do not need to wait for a duration of $Q_{Acc}^{j\text{-}hop}$ as the 1st MPDU does at a relaying MP. This is because MPDUs in a packet train arrive at a relaying MP every TDMA frame one after another, and a relaying MP starts to contend for channel access for relaying as long as the 1st MPDU is received. Its delay contribution is $(j\text{-}1)P_{TDMA}\Sigma i$, $i \in [2, g]$. Averaging the value over the train length g gives $(j\text{-}1)P_{TDMA}(g+2)(g\text{-}1)/(2g)$.

Since no packet is lost during transmission or owing to overflow of a queue, the traffic output (throughput) of each one-hop queueing network is same as its traffic input. Given an external traffic load of λ_{PT}, the traffic load to the ACH queue is $j\lambda_{PT}$, where j is the number of hops. Therefore, $Q_{Acc}{}^{j\text{-}hop}$ is given by:

$$\begin{cases} Q_{Acc}^{j-hop} = P_{TDMA} \times \left[1 + \dfrac{j \times \lambda_{PT} \times P_{TDMA}}{2 \times (1 - j \times \lambda_{PT} \times P_{TDMA})} \right] & g+h \le N,\ j \in \{1,2,3\} \\ Q_{Acc}^{j-hop} = \dfrac{g+h}{N} \times P_{TDMA} \times \left[1 + \dfrac{j \times \lambda_{PT} \times ((g+h)/N) \times P_{TDMA}}{2 \times (1 - j \times \lambda_{PT} \times ((g+h)/N) \times P_{TDMA})} \right] & g+h > N,\ j \in \{1,2,3\} \end{cases} \tag{4.16}$$

X_{ACH} is same as in the single-hop case, see Eq. (4.10). Similarly,

$$Th_{PT}^{j-hop} = \lambda_{PT} \qquad when \quad \lambda_{PT} < 1/(j \times X_{ACH}) \tag{4.17}$$

As stated, given an external traffic load of λ_{PT}, for a $j \in (1, 2, 3)$ hop network, the traffic load for the ACH queue is $j\lambda_{PT}$. From Eq. (4.11), we have $max(\lambda_{PT}) = 1/(jX_{ACH})$. Thus,

$$\max(Th_{PT}^{j-hop}) = \begin{cases} \dfrac{1}{j \times P_{TDMA}} & g+h \le N,\ j \in \{1,2,3\} \\ \dfrac{N}{j \times (g+h) \times P_{TDMA}} & g+h > N,\ j \in \{1,2,3\} \end{cases} \tag{4.18}$$

Clearly, $\lambda_{MPDU} = g\lambda_{RP}$. Applying this into Eqs. (4.17) - (4.18) yields,

$$Th_{MPDU}^{j-hop} = \begin{cases} \lambda_{MPDU} & \lambda_{MPDU} < \max(Th_{MPDU}^{j-hop}) \\ \max(Th_{MPDU}^{j-hop}) & \lambda_{MPDU} \ge \max(Th_{MPDU}^{j-hop}) \end{cases} \tag{4.19}$$

where

$$\max(Th_{MPDU}^{j-hop}) = \begin{cases} g/(j \times P_{TDMA}) & g+h \le N,\ j \in \{1,2,3\} \\ (N \times g)/(j \times (g+h) \times P_{TDMA}) & g+h > N,\ j \in \{1,2,3\} \end{cases} \tag{4.20}$$

The unit of $Th_{MPDU}{}^{j\text{-}hop}$ is MPDUs/s. Hence, $T_{TCH}Th_{MPDU}{}^{j\text{-}hop}$ is a throughput with the unit of MPDUs/TCH. Since an MPDU is one TCH slot in length, obviously, $T_{TCH}Th_{MPDU}{}^{j\text{-}hop}$ is the normalized MPDU throughput. We have,

$$N(Th_{MPDU}^{j-hop}) = T_{TCH} \times Th_{MPDU}^{j-hop} = g \times T_{TCH} \times Th_{PT}^{j-hop} \qquad j \in \{1,2,3\} \tag{4.21}$$

Table 4-1. Key parameter settings used for performance analysis.

Number of contention slots in the PP (ACH) *m*	2
Number of contention slots in the FEP (ACH) *n*	10
Duration of a contention slot used in the ACH	6 µs
Duration of the TP in an ACH	28 µs
Duration of a TCH	45 µs
Duration of an ECH	6 µs
Number of TCHs/ECHs in a TDMA frame	16
Duration of a TDMA frame	916 µs
Hang on period (unit: TDMA frames)	6

4.2.4 Performance Results

4.2.4.1 Evaluation Environment

The IEEE 802.11a PHY [3] working at 5.2 GHz is assumed. For validation purpose, the analytical results are compared with the results achieved in a simulator, which is built up based on the system assumptions (see Section 4.2.2). Table 4-1 shows the parameter settings used for analysis. The number of contention slots in the PP is 2, corresponding to $2^2 = 4$ PPCLs. The PPCL of each newly generated packet train at a source MP is 1. As long as the increased delay of the first MPDU in a packet train at an MP is more than 20 ms, the PPCL used for contention for the packet train shall be incremented by 1. Note that Assumption 5 is relaxed in simulation, since the number of contention slots in the FEP is 10, which guarantees a highly but not fully eliminative channel access.

4.2.4.2 Throughput and Delay Performance in Mesh

The terms "throughput" and "delay" presented in this Section signify the normalized MPDU throughput and end-to-end mean MPDU delay, respectively.

Note:1) in the following graphs, analytical results are plotted with solid lines while simulation results are represented by points; 2) transmissions in single-, two- and three-hop networks span one hop, two hops and three hops, respectively; 3) Simulation results are gained applying the batch mean method with a level of confidence of 95%.

4.2.4.2.1 Impact of the traffic load by packet trains

The throughput vs. the traffic load of packet trains in single-, two-, and three-hop networks is depicted in Figure 4-6a, c and e, respectively. In all networks, under a given *g*, the throughput increases lineally with the traffic load until reaching its saturation value

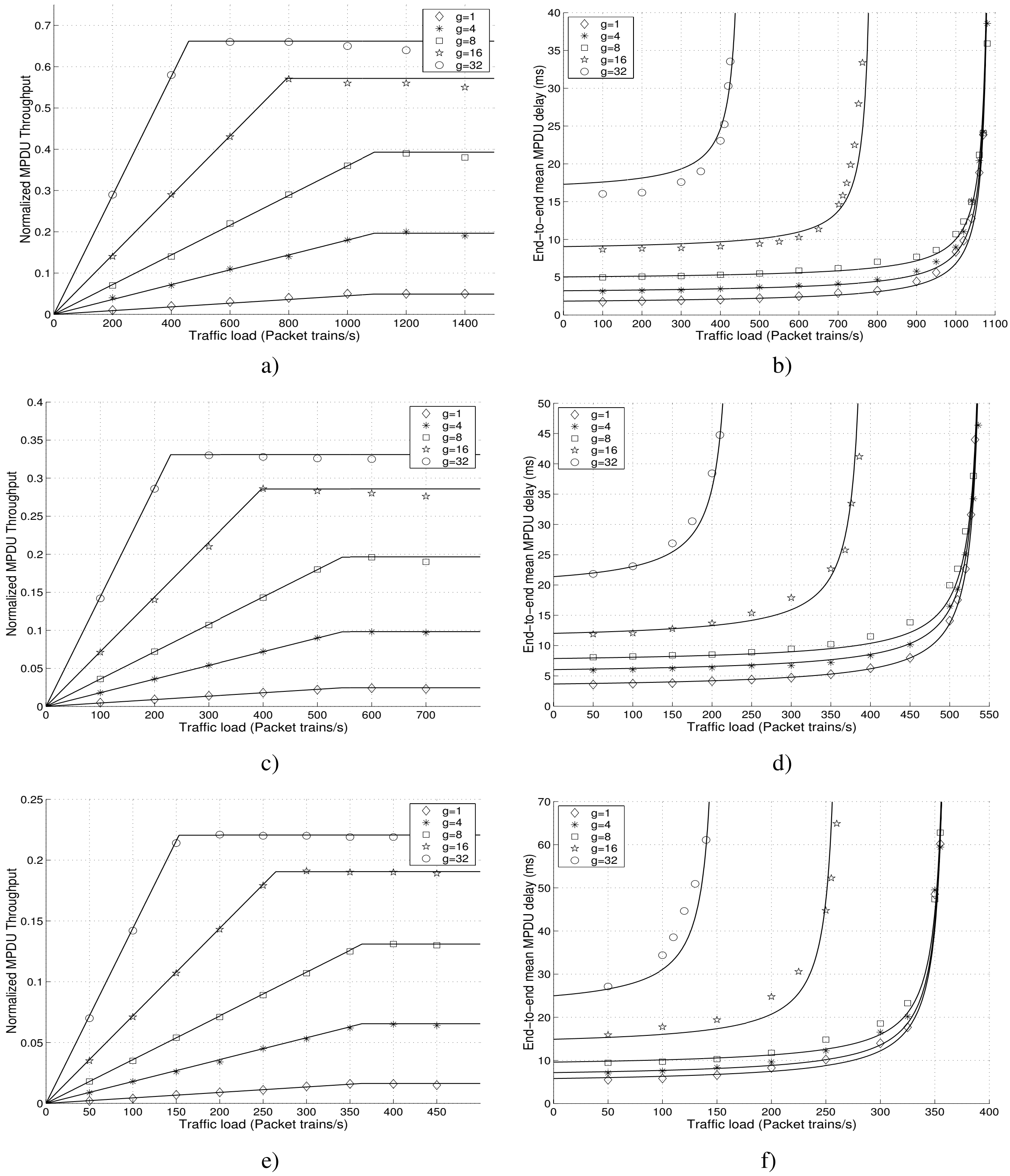

Figure 4-6. Impact of the traffic load of packet trains, N = 16, T_{TCH} = 45 μs: a) Throughput in single-hop network; b) Delay in single-hop network; c) Throughput in two-hop network; d) Delay in two-hop network; e) Throughput in three-hop network; f) Delay in three-hop network. *Note: Throughput and delay here mean normalized MPDU throughput and end-to-end MPDU delay, respectively.*

and thereafter stays the same irrespective of any further increase of the traffic load. The latter performance is mainly owing to the highly eliminative channel access scheme: Even when a network is highly loaded and a large number of MPs contend at the same time, only one MP wins. The loss caused by collision is very small. It also can be seen that in a given j-hop network, for a given traffic load, a higher g leads to a higher throughput. The reason for this is obvious: On completion of transmitting g MPDUs, an MP starts to hang on for h TDMA frames before releasing the reserved TCHs. Therefore, the smaller g, the higher the overhead contribution resulting from h and the smaller the TCH utilization. Note that setting the hang-on time for a TCH helps to increase the channel utilization in mesh networks when packet multiplexing is enabled, see Section 3.2.9. This however is not the case here.

By comparing the results obtained for j-hop networks (j = 1, 2, 3), it can be found that under a given g, the highest achievable saturation throughput of single-hop networks is 2 and 3 times larger than that of two-hop and three-hop networks, respectively. This is understandable since an n-hop transmission brings n times network traffic, saturating a network faster.

Figure 4-6b, d and f show the delay performance in single-, two- and three-hop networks, respectively. As to be seen, in all networks, a smaller g leads to a smaller delay under the same traffic load. The reason is clear: An MP needs at least g TDMA frames to transmit g MPDUs on a TCH. The more MPDUs in a packet train, the higher the queueing delay.

Under a given m, when λ_{PT} is smaller than a certain value L, the delay is almost the same irrespective of λ_{PT}. A network under this situation can be considered lightly loaded where the packet delay is mainly resulting from the queueing delay: $P_{TDMA}(g+1)/2$. In a lightly loaded network, the end-to-end delay is small: e.g when g = 16, the delays in single, two and three hop networks are 9 ms, 13 ms and 15 ms, respectively, well under the QoS delay requirements for real-time traffic [9]. In contrast, when λ_{PT} is higher than L, the delay shall increase sharply. When this happens, a network is considered highly loaded where the delay is mainly due to the access delay: $Q_{Acc}^{j\text{-}hop}$. It can be seen that single-hop, two-hop and three-hop networks are lightly loaded when $\lambda_{PT} < 0.8max(Th_{PT}^{1\text{-}hop})$, $\lambda_{PT} < 0.7max(Th_{PT}^{2\text{-}hop})$ and $\lambda_{PT} < 0.6max(Th_{PT}^{3\text{-}hop})$, respectively. As to be seen, the saturation throughput $max(Th_{PT}^{j\text{-}hop})$ is highly dependent on g and j: a higher g or a small j leads to a larger $max(Th_{PT}^{j\text{-}hop})$.

To sum up, a larger g results into a higher $max(Th_{PT}^{j\text{-}hop})$ but a longer mean delay. With a higher $max(Th_{PT}^{j\text{-}hop})$, a network is more likely to be in the lightly loaded situation, only under which the QoS delivery in mesh is possible. Besides, a multi-hop network tends to be highly loaded: the more hops are being passed by a packet, the higher the delay would be.

4.2.4.2.2 Impact of the traffic load by MPDUs

The traffic load of packet trains cannot really reflect the load situation in a network, which is measured by the traffic load resulting from MPDUs. This sub-section reveals the impact of the traffic load by MPDUs on the traffic performance.

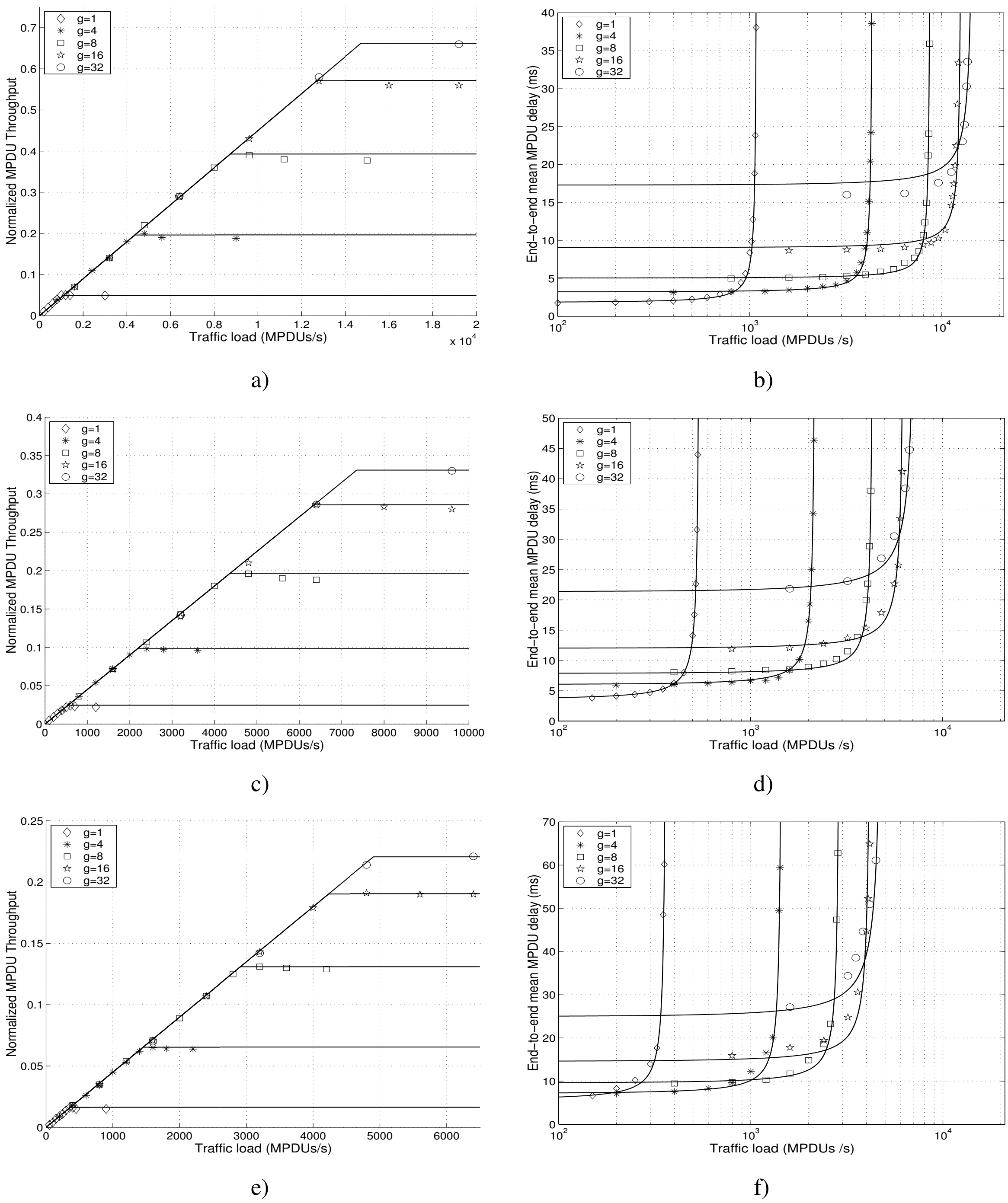

Figure 4-7. Impact of the traffic load of MPDUs, N = 16, T_{TCH} = 45 μs: a) Throughput in single-hop networks; b) Delay in single-hop networks; c) Throughput in two-hop networks; d) Delay in two-hop networks; e) Throughput in three-hop networks; f) Delay in three-hop networks. *Note: Throughput and delay here mean normalized MPDU throughput and end-to-end MPDU delay, respectively.*

The normalized throughput $Th_{MPDU}^{j\text{-}hop}$ for j = 1, 2 and 3 is plotted in Figure 4-7a, c and e, respectively. It is clear to see that the simulation results match well with the analytical results plotted by using Eqs. (4.19) - (4.21). Same as the result shown in Figure 4-6a, c and e, in all networks, a larger g leads to a higher maximum throughput: E.g. in two-hop networks, when $g = 1$ and $g = 32$, the maximum throughput is 0.025 and 0.33, respectively. However, given a traffic load, the throughputs under different g values are same as long as the load is not high enough to saturate a network. This is different from the result shown in Figure 4-6a, c and e. Moreover, a smaller g value tends to saturate a network under low load which is also different from that shown in Figure 4-6a, c and e.

The delay performance is shown in Figure 4-7b, d and f. When a network is lightly loaded, under a given λ_{MPDU}, a higher g causes a higher delay. However, with a smaller g, a network is saturated with a low load, under which the delay is significantly high. This is different from the results shown in Figure 4-6b, d and f, where under a given λ_{PT}, a higher g is prone to get a network saturated. As shown in Figure 4-7b, when $g = 1$, a single-hop network is highly loaded where the delay is 9 ms, given $\lambda_{MPDU} = 10^3$ MPDUs/s. In contrast, under the same λ_{MPDU}, when $g = 4$ and $g = 8$, the network is lightly loaded, where the delay is 3 ms and 5 ms, respectively. A higher g results into a wider range of λ_{MPDU}, under which a network is in lightly loaded situations. It is worth pointing out that under a given g, the delays in single-, two- and three-hop networks are close as long as those networks are lightly loaded: E.g. when $g = 8$, given $\lambda_{MPDU} = 10^3$ MPDUs/s, the single-, two- and three- hop delays are 5 ms, 8 ms and 10 ms, respectively. This is important for ensuring QoS in mesh.

From the above analysis, it is clear to see that g has a great impact on the achievable throughput, delay and range of the λ_{MPDU}, under which a network is considered lightly loaded. In order to obtain a better performance in the first and third aspects, g should be as high as possible, which is however adverse to the delay performance. It can be found that a good trade-off is achieved when $g = 16$. With this value, the $max(Th_{MPDU}^{j\text{-}hop})$ is close to its maximum value $N/(jP_{TDMA})$ as indicated in Eq. (4.20). As a result, the range of λ_{MPDU} leading to a lightly loaded network is wide. At the same time the delays in single-, two- and three-hop networks are only 9 ms, 13 ms and 15 ms, respectively, when networks are lightly loaded.

4.2.4.2.3 Impact of number of TCHs in a TDMA frame

The number N of TCHs in a TDMA frame impacts the throughput and delay performance: With a larger N, MDCF is able to serve for transmitting more packet trains (or MPDUs) in parallel, resulting in a higher throughput. Moreover, the probability that one-hop transmissions of a multi-hop connection take place in parallel in a TDMA frame is higher, see Figure 3-12. As a consequence, the end-to-end packet delay is lower. On the other hand, a larger N leads to a longer TDMA frame, which in turn results in a longer access delay and in a lower throughput as well as a larger packet delay, too.

The correctness of the analytical model has been validated by simulation in the last two sub-sections. In the following, the analytical model is used to study the above mentioned impact. This helps to find out the optimal frame length for QoS support in mesh.

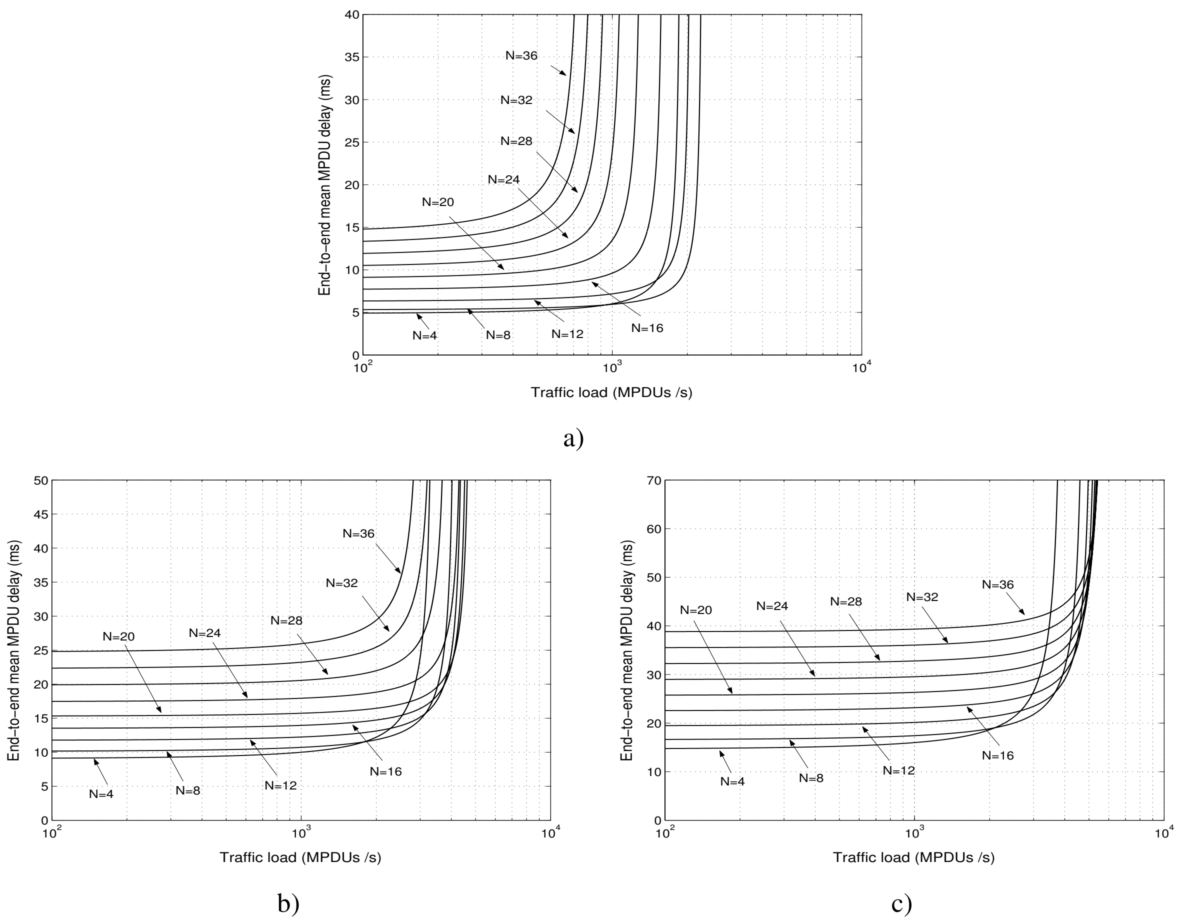

Figure 4-8. Impact of N in three hop networks, where T_{TCH} = 45 μs: a) g = 4; b) g = 16; c) g =32.

To save the space, only the delay under different N values in three-hop networks is plotted, according to Eqs. (4.15) - (4.16). The saturation throughput $max(Th_{MPDU}^{3\text{-}hop})$ can be derived by observing the delay: in a given condition, a λ_{MPDU} value causing a significant high delay is almost equal to the $max(Th_{MPDU}^{3\text{-}hop})$, see Eq. (4.19).

Figure 4-8a, b and c exhibit the impact of N on the delay performance in three-hop networks when g is 4, 16 and 32, respectively. As can be seen, a larger N causes a higher delay under a given g. This is obvious: given a T_{TCH}, a larger N results into a longer P_{TDMA} and accordingly a higher delay. When g is small (g = 4), high $max(Th_{MPDU}^{3\text{-}hop})$ is obtained when N is small, whilst when g is increased to 16, the highest $max(Th_{MPDU}^{3\text{-}hop})$ appears at when N = 16. In contrast, when g = 32, the $max(Th_{MPDU}^{3\text{-}hop})$ increases with N and are almost same when N > 8. In real network runs, g can be either small or big. Accounting for this, to ensure a high network throughput and a low delay in mesh, N should be between [8, 20].

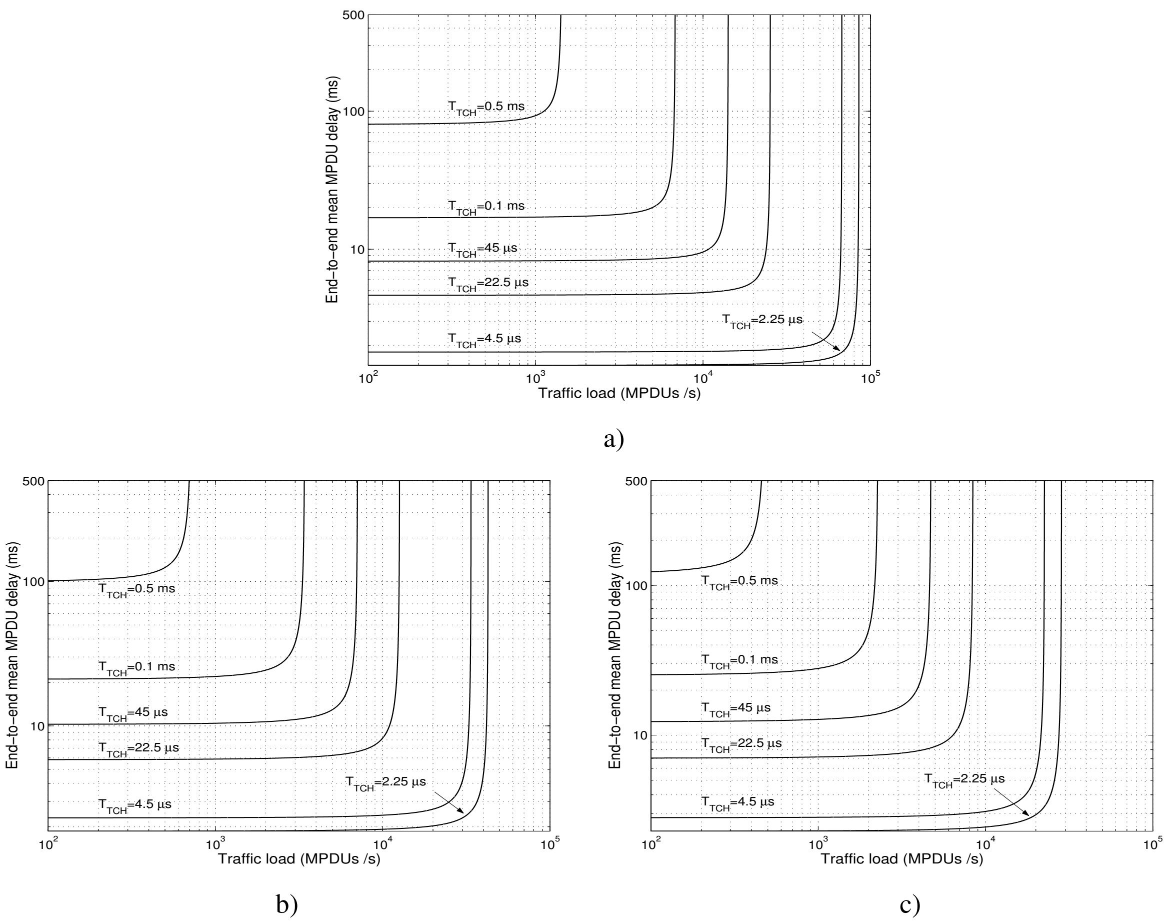

Figure 4-9. Impact of T_{TCH}, where g = N = 16: a) in single hop networks; b) in two hop networks; c) in three hop networks.

4.2.4.2.4 Impact of the duration of a TCH slot

Clearly, T_{TCH} depends on the PHY data rate. Given a predefined maximum MPDU size, the higher the PHY data rate, the shorter T_{TCH}. The impact of T_{TCH} on the delay in single-hop, two-hop and three-hop networks is depicted in Figure 4-9a, b and c, respectively. It is shown that a short T_{TCH} leads to a lower delay as well as a higher $max(Th_{MPDU}^{j\text{-}hop})$, derived by observing the delay change. When T_{TCH} = 4.5 µs, the delay in a lightly loaded three-hop networks is 0.9 ms while the $max(Th_{MPDU}^{3\text{-}hop})$ is 2.1 × 10^4 MPDUs/s. Note this performance can only be achieved on a PHY supporting a very high data rate. Assuming a MPDU is 100 bytes long, the PHY data rate should be over 100 bytes /4.5µs = 177 Mbps. On the contrary, when T_{TCH} = 0.5 ms, the single-hop delay under lightly loaded situations and $max(Th_{MPDU}^{1\text{-}hop})$ are 80 ms and 1.5 × 10^3 MPDUs/s, respectively. Similarly, given a MPDU is 100 bytes long, the required PHY data rate in this scenario is 100 bytes /0.5 ms = 1.6 Mbps. To obtain a better delay performance under this PHY, *N* should be small. This however leads to a smaller $max(Th_{MPDU}^{j\text{-}hop})$.

In short, to achieve a high traffic performance, T_{TCH} should be set as short as possible as long as a PHY allows.

4.2.4.2.5 A short summary

In Section 4.2.4, the throughput and delay performance of MDCF in the mesh environment is investigated using the analytical model established in Section 4.2.3. The accuracy of the analytical result is examined and proven by simulation. Further, the impacts of the following parameters are studied using the analytical model: 1) The number of MPDUs in a packet train: g; 2) The number of TCHs per TDMA frame: N; 3) The duration of a TCH slot: T_{TCH}. The evaluation result of the impact of g can be utilized to design the TCH scheduling policy, and the results of the impacts of N and T_{TCH} can be used to optimize the TDMA frame structure.

Please note that the hang-on time h also impacts the throughput and delay performance. However, h is selected in an environment mainly by considering traffic patterns and the estimated multiplexing factor, as already described in Section 3.2.9.1. Hence, we do not investigate the impact of h here.

4.2.5 Performance Evaluation with the Erlang-C (M/M/N) System

4.2.5.1 Introduction

The Erlang-C (M/M/N) system [82] is widely applicable to systems found in our daily life, where

- A large number of customers jointly generate requests, modeled with a Poisson arrival process, to a number of N ($N > 1$) servers.
- Service times are exponentially (geometrically for a discrete random variable) distributed.
- An arriving request is queued when all the servers are busy.
- The resource is allocated exclusively to serve one request for the specified (random) time period.

An example of the system is the call centre, which is a centralized office used to receive and transmit a large volume of requests by telephone. The behavior of the system can be modeled by M/M/N. Similar to an Erlang-C system, an MDCF system provides the transmission service with N ($N > 1$) servers (N - the number of TCHs per TDMA frame). Hence, it is of interest to see how well the performance of an MDCF system can be described by an Erlang-C system, given that they work under the same conditions, i.e. the same server number N, same traffic input process and same service time distribution function.

Figure 4-10a and b show the queueing models of single- and multi-hop Erlang-C networks, respectively. The input of the system is one packet train per request and each

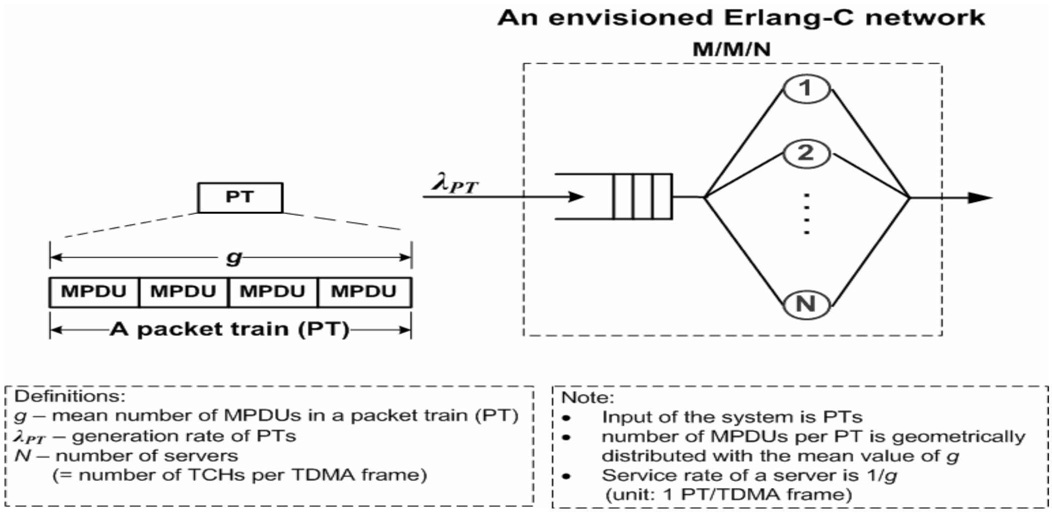

a)

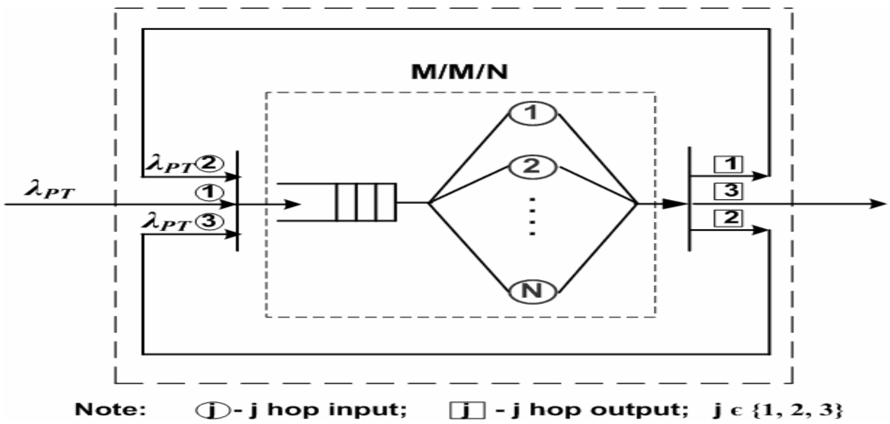

b)

Figure 4-10. Queuing models of the envisioned Erlang-C transmission system: a) Single-hop networks; b) Multi-hop networks – Note that this model is for 3-hop networks, where no spatial reuse is possible.

server is occupied for the duration needed to transmit a packet train. In the following, unless otherwise stated, the term *Erlang-C network* refers to the system of Figure 4-10.

The following performance study adopts the assumptions described in Section 4.2.2 except that

1): *A TCH in transmission is considered free on the expiration of the hang-on time* (see Assumption 7)

2): *All packet trains in a given scenario have the same number of MPDUs* (see Assumption 2)

3): *The number of ACH per TDMA frame is 1* (see attachment 4).

Instead, we assume:

- After completion of transmission of a packet train, a TCH is available for use again.
- In a given scenario, the number of MPDUs in a packet train is geometrically distributed with a mean value of g.
- In an Erlang-C network, no ACH exists (representing collision free channel access in zero time duration).

Clearly, under these conditions, the service time of a server is geometrically distributed, enabling application of Erlang-C. The following definitions are used:

$\boldsymbol{D_M^{j\text{-}hop}}$: j-hop mean end-to-end MPDU delay, $j \in \{1, 2, 3\}$

$\boldsymbol{D^i}$: End-to-end delay of the ith MPDU in a packet train

$\boldsymbol{g}$: Mean number of MPDUs in a packet train

$\boldsymbol{N}$: Number of servers (TCHs per TDMA frame) in an Erlang-C network

$\boldsymbol{p}$: Probability of only 1 MPDU in a packet train ($p \in [0, 1]$)

$\boldsymbol{P(X= k)}$: Probability of k MPDUs in a packet train, $k \in \{1, 2, 3, \ldots\}$

$\boldsymbol{P_{TDMA}}$: The length of a TDMA frame in ms

$\boldsymbol{W_{PT}}$: Mean one-hop waiting time of packet trains at an Erlang-C network

$\boldsymbol{\lambda_{PT}}$: Packet train arrival rate to an Erlang-C network

$\boldsymbol{\mu}$: Mean service rate per server

$\boldsymbol{\rho}$: Utilization of the Erlang-C queue, $\rho = \lambda_{PT} /(N\mu)$

4.2.5.2 Performance Analysis of Erlang-C Networks

The number of MPDUs in a packet train is geometrically distributed, i.e.,

$$P(X = K) = p \times (1 - p)^{K-1} \qquad k \in \{1,2,3,\ldots\} \tag{4.22}$$

Accodingly, g is given by [79],

$$g = E(X) = \frac{1}{p} \tag{4.23}$$

Using expressions in [82], we have,

$$W_{PT} = P_q \times \frac{1}{N \times \mu - \lambda_{PT}} \tag{4.24}$$

where

$$P_q = \frac{\pi_0 \times (N \times \rho)^N}{N! \times (1-\rho)}$$

and

$$\pi_0 = \left[\sum_{n=0}^{N-1} \frac{(N \times \rho)^N}{n!} + \frac{(N \times \rho)^N}{N! \times (1-\rho)} \right]^{-1}.$$

The utilization ρ for a queueing system with multiple servers is [79]:

$$\rho = \frac{\lambda_{PT}}{N \times \mu} \tag{4.25}$$

By definition,

$$\mu = \frac{1}{g \times P_{TDMA}} \tag{4.26}$$

Hence, the mean one-hop delay of packet trains is $W_{PT} + 1/\mu$, and $D_M^{1\text{-}hop}$ is:

$$\begin{aligned} D_M^{1-hop} &= \frac{1}{g} \times \sum_{i=1}^{g} D^i = \frac{1}{g} \times \left[g \times W_{PT} + P_{TDMA} \times \sum_{i=1}^{g} i \right] \\ &= W_{PT} + P_{TDMA} \times \frac{g+1}{2} \end{aligned} \tag{4.27}$$

The queueing model for multi-hop Erlang-C networks is shown in Figure 4-10b. From the model, it is easy to derive,

$$\begin{aligned} D_M^{j-hop} &= j \times (D_M^{1-hop}) - (j-1) \times P_{TDMA} \times \frac{(g+2) \times (g-1)}{2 \times g} \\ &= j \times W_{PT} + \frac{P_{TDMA} \times (g^2 + g - 2 + 2 \times j)}{2 \times g} \qquad j \in \{1,2,3\} \end{aligned} \tag{4.28}$$

where j is the number of hops. In mesh environments, a relaying MP starts to contend for channel access for relaying when the 1st MPDU in a packet train is received, i.e. the ith MPDU ($i \geq 2$) in a packet train does not need to wait for a period of iP_{TDMA} until being transmitted by the relaying MP. Hence, in Eq. (4.28), this part of the time is deduced: The sum of the time for the 2rd to gth MPDUs is $(j-1)P_{TDMA}\Sigma i,\ i \in [2, g]$. Averaging the value over the mean train length g yields $(j-1)P_{TDMA}(g+2)(g-1)/(2g)$.

Given an external traffic arrival rate of λ_{PT}, for a $j \in (1, 2, 3)$ hop network, the traffic load for the queueing system is $j\lambda_{PT}$. From Eq. (4.25), we have $\rho = (j\lambda_{PT})/(N\mu) \leq 1$, i.e.,

$$\lambda_{PT} \leq \frac{N \times \mu}{j} = \frac{N}{j \times g \times P_{TDMA}} \qquad j \in \{1,2,3\} \qquad (4.29)$$

where j is the number of hops. The above equation specifies the upper limit of $\lambda_{PT.}$

4.2.5.3 Performance Comparison Results

In this sub-Section, the performance result of MDCF networks is compared to that of the Erlang-C network working under the same conditions. The performance of MDCF networks is studied using both the simulation and analytical model described in Section 4.2.3, whilst the performance of Erlang-C networks is studied using the analytical model presented in Section 4.2.5.2. For fair comparison with Erlang-C networks, both simulation and analytical results of MDCF networks are taken assuming a *hang-on time h = 0.* Simulation results of MDCF networks, *where packet trains with the number of MPDUs geometrically distributed with mean g,* have been generated.

Figure 4-11 shows the results. Please note that the MDCF analytical model presented in Section 4.2.3 is derived assuming that *packet trains comprise a fixed number of MPDUs g*. It is visible that the MDCF simulation result matches the MDCF analytical result very well. This implies that the MDCF analytical model appears to be more generally applicable and is not limited to fix length packet trains.

For a network with a given number of hops, the smaller g, the larger the difference of the saturation throughput is (Note that the saturation throughput can be derived from the pole of the delay curve, see Caption of Figure 4-11). As plotted in Figure 4-11a, b and c, in case of single-hop networks, when g = 1, the saturation throughput of the Erlang-C model is 17000/1400 ≈ 12 times higher than that gained from the MDCF analysis and simulation, whilst when g = 8, the saturation throughput of Erlang-C networks is only 2100/1050 = 2 times higher than that of MDCF. Further, when g = 32, the saturation throughput of MDCF single-hop networks is very close to that of the Erlang-C single-hop network.

The same trends applies for two- and three-hop networks, see Figure 4-11d, e, f, g, h and i. There is a reason for this: An ACH server exists in an MDCF network that is not contained in an Erlang-C network. As a consequence, in an MDCF network, no matter how many TCHs are free, only one packet train can be put into a free TCH for to be served per TDMA frame. In contrast to this, any number of newly arriving packet trains can be put into free TCHs per TDMA frame in the Erlang-C model, as long as there are free servers available. When g is small, the ACH server in MDCF networks is a bottleneck since the service time of a request is one TCH time slot only. That is why the saturation throughput of Erlang-C networks is much higher than that of MDCF networks in that case. Since the service duration of a request increases with increased length g of the packet trains, the ACH queue in MDCF networks is unloaded then and the bottleneck disappears - the more, the higher g is. Under larger g, the saturation

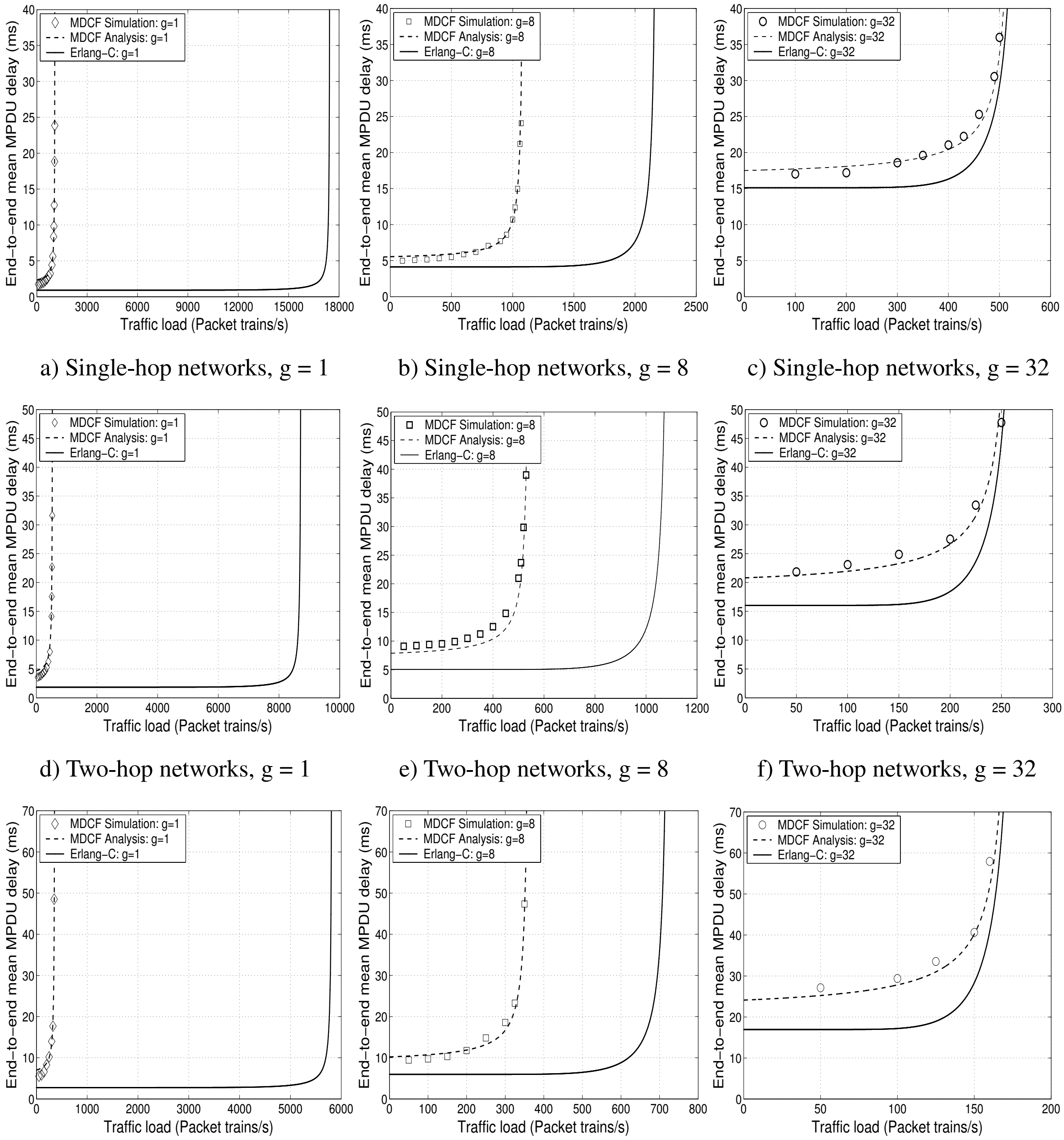

a) Single-hop networks, g = 1 b) Single-hop networks, g = 8 c) Single-hop networks, g = 32

d) Two-hop networks, g = 1 e) Two-hop networks, g = 8 f) Two-hop networks, g = 32

g) Three-hop networks, g = 1 h) Three-hop networks, g = 8 i) Three-hop networks, g = 32

Figure 4-11. Performance comparison between MDCF networks and Erlang-C networks. Only the delay performance is given. The saturation throughput can be derived from the pole traffic load volume.

throughput of MDCF is close to that of the Erlang-C model.

The above result motivates to improve the performance of MDCF: An adaptation of the number of ACH slots per TDMA frame according to traffic volume in a network would remove the ACH bottleneck. In case of light load that might result from small g, put in use > 1 ACH slots per TDMA frame in order to speed up the channel access in a network, whilst in case of high load (larger g), use one ACH slot per TDMA frame only, to have as much TCH available as possible per TDMA frame. A similar scheme is proposed in [95]. However, implementation of such a scheme under decentral control in mesh is not trivial.

Comparing the results obtained for j-hop networks (j = 1, 2, 3), it can be found that under a given g, the saturation throughput of single-hop networks is 2 and 3 times larger than that of two-hop and three-hop networks, respectively, both when using MDCF and Erlang-C. This is understandable since an n-hop transmission brings n times network traffic, saturating a network faster.

Another notable result is that under a given g and a given λ_{PT} causing a lightly loaded network, the delay difference between when using MDCF and Erlang-C increases with the number of hops: E.g., given g = 8 and λ_{PT} = 100 packet trains/s, the delay under single-, two- and three-hop MDCF networks is 2 ms, 3.5 ms and 5 ms longer than that under single-, two- and three-hop Erlang-C networks, respectively. This is also owing to the existence of the ACH server in an MDCF network: A packet train in MDCF networks needs to go through the ACH queue and TCH queue to complete a one-hop transmission, whilst a packet train in Erlang-C networks only needs to go through the TCH queue per one-hop transmission. Obiviously, the more hops that a transmission needs to go through, the larger delay the difference of the two models is.

CHAPTER 5

Simulation Performance Evaluation

In this Chapter, the performance of MDCF is extensively studied by simulation. For comparison reason, simulation is also performed on the same scenarios by using the 802.11 DCF or EDCA. Section 5.1 introduces the simulation tool and key parameter settings used. The performance evaluation of MTSF for synchronizing MPs for TDMA operation in MDCF multi-hop networks is presented in Section 5.2. The performance analysis of MDCF networks is performed in Chapter 4 assuming a specific scenario. Section 5.3 uses simulation to reveal the performance of MDCF networks in more realistic scenarios. MDCF can be used to interconnect Access Points (APs) of individual 802.11 Basic Service Set (BSS) networks to form an 802.11 ESS mesh network. Section 5.4 presents the performance of an ESS mesh network using MDCF.

5.1 Simulation Tool

To evaluate the performance of MDCF in multi-hop mesh environments, an event-driven simulator is developed based on Specification and Description Language (SDL) Performance Evaluation Tool Class Library (SPEETCL) [83] in C++. The structure and main components of the simulator is shown in Figure 5-1. Note that Internet Protocol (IP) and LLC protocol are not included in the simulator, since the evaluation focus is on the performance of the MAC protocol where the impact of above two protocols can be ignored.

The simulator comprises 6 parts: traffic generators, transport protocols, MAC protocols, PHY layer (the IEEE 802.11a PHY), location & mobility management and radio channel. In the remainder of the Section, each part will be introduced in detail.

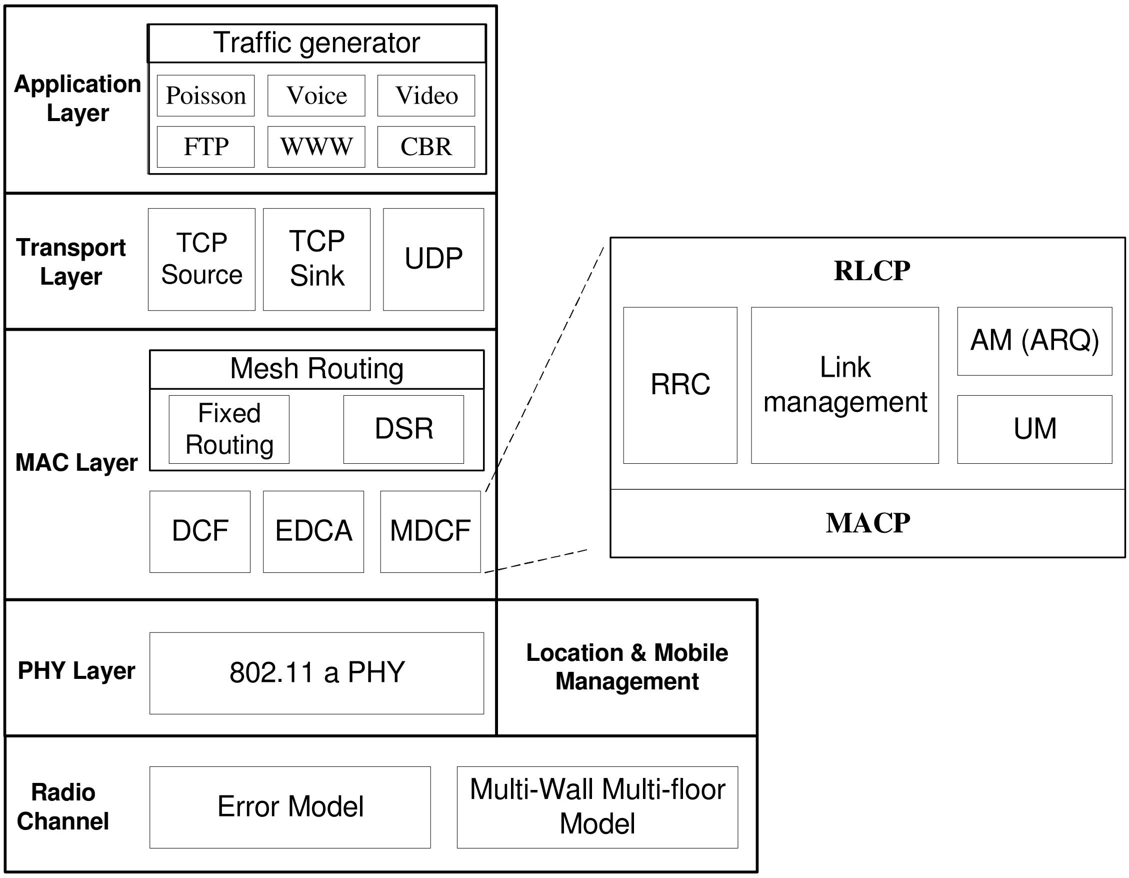

Figure 5-1. The structure and components of the MDCF simulator.

5.1.1 Radio Channel Model

Two channel models are implemented in the simulator: error model and multi-wall multi-floor model [84].

5.1.1.1 Error Model

The error model can provide the packet error information. Errors are generated according to a predefined probability distribution. The error information (correct or not in future) can be specified in terms of packets or time interval. The error model is simple yet able to represent the quality of a channel. For instance, given a targeted packet error ratio and an error generation statistical model, the lossy nature of the wireless channel in a given scenario can be simulated. However, the error model cannot reflect the path loss behavior of an actual radio channel. Moreover, interference, which usually appears in a wireless network, cannot be simulated using this model.

5.1.1.2 Multi-Wall Multi-Floor Model

To precisely simulate the indoor radio channel, the multi-wall multi-floor model is

Table 5-1. The MPDU lengths used in MDCF and the minimum receiving sensitivities under different PHY modes on the IEEE 802.11a PHY.

Modulation	Bit rate [Mbps]	MPDU lengths (Bytes)	Minimum sensitivity at receiver (dbm)
BPSK ½	6	27	-82
BPSK ¾	9	40.5	-81
QPSK ½	12	54	-79
QPSK ¾	18	81	-77
16QAM ½	24	108	-74
16QAM ¾	36	162	-70
64QAM ¾	54	243	-65

adopted as the path loss model [84]:

$$L_{MWF} = 20\log(\frac{4\pi}{\lambda}) + 10n\log(d) + \sum_{i=1}^{I}\sum_{k=1}^{K_{wi}} L_{wik} + \sum_{j=1}^{J}\sum_{k=1}^{K_{fj}} L_{fjk} \tag{5.1}$$

Where L_{MWF} is the path loss between the sender and receiver, L_{Wik} the attenuation due to wall type i and k^{th} traversed wall, L_{fjk} the attenuation due to floor type j and k^{th} traversed floor, d the distance between the transmitter and receiver, I the number of wall types, J the number of floor types, K_{wi} the number of traversed walls of category i, K_{fi} the number of traversed floors of category j, n the path loss exponent.

The received power P_R in dBm is given by:

$$P_R = P_T - L_{MWF} + G \tag{5.2}$$

Where P_T is the transmitted power; L_{MWF} is path loss between sender and receiver; G is the amount of receive and transmit antenna gains. It is assumed that omni directional antennas are used and the amount of the transmit and receive antenna gains is 6 dBi.

5.1.2 Physical Layer

The PHY layer is the OFDM-based IEEE 802.11a PHY working at 5.2 GHz. A TCH slot fits into 9 OFDM symbols. Table 5-1 shows the MPDU length per TCH and the minimum sensitivity levels of a receiver under each modulation scheme [3].

The *SINR* values of energy signals and MPDUs are calculated by using Eq. (2.2). The receive noise floor is assumed as -93 dBm. In the simulator, an MPDU may be decoded at a receiver only if the received SINR is over the minimal sensitivity level under a given PHY mode.

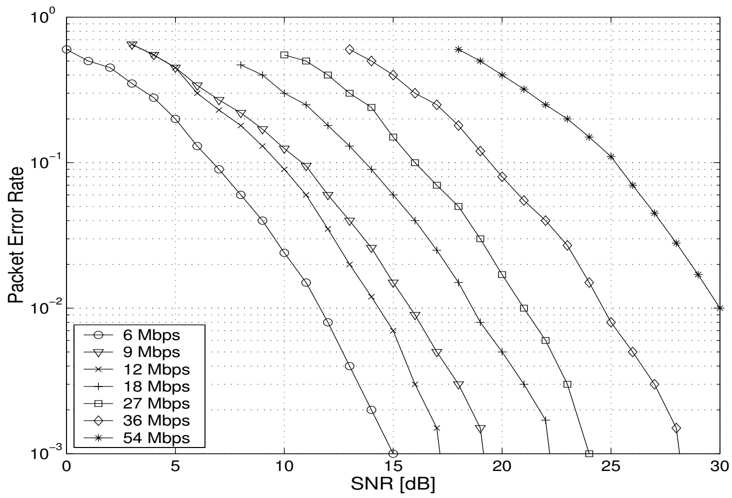

Figure 5-2. Packet loss rate vs. SNR on Hiperlan/2 PHY.

In [87], J. KunJush et al. study the relation of *SINR* and packet error rate (PER) at the example of the Hiperlan/2 PHY [37], which is based on the same OFDM technology as 802.11a is. Figure 5-2 shows the relation. User protocol data units in Hiperlan/2 have a fixed length of 54 bytes irrespective of the PHY mode.

The implemented simulator utilizes the reported results. Unlike in Hiperlan/2, the lengths of MPDUs used in MDCF on the IEEE 802.11a PHY vary from 27 bytes (BPSK 1/2) to 243 bytes (64QAM 3/4) as shown in Table 5-1. As packet - oriented schemes, the 802.11 DCF/EDCA use different lengths of MPDUs for transmission. In the simulator, given a *SINR* at a receiver, the PER of an MPDU P_{MPDU} is calculated from:

$$P_{MPDU} = 1 - (1 - p)^{\frac{L_{MPDU}}{54}} \tag{5.3}$$

where p is the PER corresponding to a given *SINR* reported in [87], and L_{MPDU} is the length of an MPDU in bytes.

5.1.3 Location & Mobility Management

Stations and MPs in each simulation run are assumed to be in a two dimensional topology and be movable inside the topology. Each station or MP has X, Y coordinates that can be continuously adjusted as it moves.

Two mobility models are implemented in the simulator. The first one is the fixed speed move model. Each MP in this model moves with a fixed speed until reaching its predefined destination. The second model is called random waypoint [88], where the level of movement is related to the predifined pause time: Each station or MP remains stationary for a pause time since it is actived. It then selects a random destination in the

Table 5-2. The TDMA frame settings of MDCF used in simulation.

Parameter settings in a TDMA frame	
Number m of contention slots in the PP of the ACH	3
Number n of contention slots in the FEP of the ACH	9
Duration of the TP in the ACH	28 µs
Duration of a TCH	45 µs
Duration of an ECH	6 µs
Number of TCHs/ECHs in a TDMA frame	16
Duration of a TDMA frame	916 µs

Table 5-3. Key parameter setting of DCF and EDCA used in simulation.

Key parameter settings of the DCF and EDCA in the simulator				
DCF	CWmin			15
	CWmax			1023
	Retry time			7
EDCA	Parameters	AC_VO	AC_VI	AC_BK
	CWmin	7	15	31
	CWmax	15	31	1023
	AIFSN	2	2	3
	Retry time	7	7	7

specified topology and moves to that destination at a speed uniformly distributed between 0 and a maximum speed value. Upon reaching the destination, the station or MP pauses again, selects another destination, and moves towards the new destination. It repeats this behavior during a simulation run.

5.1.4 MAC Layer

In the MAC layer, MDCF, 802.11 DCF, 802.11 EDCA and two mesh routing schemes are implemented, see Figure 5-1. All the features of MDCF are implemented. Table 5-2 describes the TDMA frame parameter settings used in the simulator. DCF is implemented by applying modified code from ns-2 [86], and EDCA is implemented on top of DCF. Important settings of DCF and EDCA are listed in Table 5-3.

The mesh routing algorithms used in the simulator include the fixed routing scheme and Dynamic Source Routing (DSR) [76]. Fixed routing is used to manually configure the transmission routes in a given scenario. DSR is a known wireless routing protocol that establishes and maintains mesh routes in an on-demand manner. The performance of the MAC protocols can be evaluated for both algorithms.

5.1.5 Transport Layer

User Datagram Protocol (UDP) and Transport Control Protocol (TCP) are also implemented using modified code from ns-2. The TCP version implemented is Reno.

UDP is one of the core protocols of the Internet protocol suite. It does not provide reliable transfer and re-ordering of data packets delivered by the protocol. Packets may arrive out of order or go lost. Since no packet retransmission is used, delivered UDP packets experience small delays. Accordingly, UDP is used to transfer time-bounded services like voice and video traffic that tolerate a certain level of PLR.

TCP is one of the prevalent transmission protocols in the Internet, offering reliable in-sequence data transfer to the upper layer. It adapts its traffic load to the network condition and performs congestion control. File Transfer Protocol (FTP) traffic and World Wide Web (WWW) traffic are transferred by using TCP. A TCP connection needs to be established between a TCP source and a TCP sink for transmission before user data can be transmitted. The TCP source and TCP sink are separately implemented in the simulator.

5.1.6 Application Layer

Six types of traffic sources are implemented in the simulator: Poisson, voice, video conference, FTP, WWW and CBR traffic. They are used for different evaluation purposes. FTP and WWW traffic are best effort traffic, whilst voice and video conference traffic are real-time traffic. Poisson and CBR traffic can be real-time, background or best effort traffic dependent on the evaluation intention. The PPCLs of various traffic classes are given in Table 2-1.

5.1.6.1 Poisson Traffic

Due to its attractive theoretical properties [79], the Poisson process is often used to model network traffic behavior and packet arrivals.

The Poisson and exponential distributions are related: If the packet generation process is a Poisson with rate λ, then the inter-arrival times of successive packets are exponentially distributed with mean $1/\lambda$ [79]. A Poisson traffic flow is generated by making use of this relation in the simulator.

However, a Poisson traffic flow in many cases is not suitable as a realistic model for performance evaluation. Instead statistically self-similar processes, which much differ from the Poisson process, should be used [89]. This is the reason why 5 other types of traffic generators are implemented and used for evaluation.

5.1.6.2 Voice Traffic

The voice traffic (G. 711 coder) is modeled by the known two-state on-off model [59] with exponentially distributed duration of voice spurts and silence gaps. A G.711 vo-coder operates at 64 kbps by using the Pulse Code Modulation (PCM) scheme. In the simulator, the time intervals spent in the On (talk spurt) and off (silent gap) states are geometrically distributed. The mean periods of the On and Off states are 0.35 s and 0.65 s, respectively. As a result, a voice source generates data with a mean bit rate of 22.4 kbps. The voice payload is 160 bytes [60]. Accordingly, the mean inter-arrival time of voice packets is $(160 \times 8) / (64 \times 10^3) = 20$ ms.

Assume that the Packet Loss Concealment (PLC) technique is used. Based on that, to preserve voice quality [90], the maximum delay and PLR should be lower than 60 ms and 6% [9], respectively. When the MAC protocol is MDCF, it is clear that the RLCP service mode can be the UM if voice transmissions are within one-hop. However, for multi-hop voice transmissions, the service mode should be the AM in order to ensure a PLR under 6%. The detailed explanation for this is given in Section 3.3.1.3.

5.1.6.3 Video Conference Traffic

The on-off minisources model [54] is used to generate high bit rate video conference (H. 263 codec) streams. A video conference stream is the aggregated output of N independent On-Off minisources. An On minisource produces a constant bit-rate of λ bit/s. The time intervals on the On and off states are geometrically distributed with mean values of α and β, respectively. The minisource activity factor is given by $p = \alpha / (\alpha + \beta)$. It is clear that the mean bit rate of a video conference source is $N\lambda p$ bit/s and the maximum bit rate is $N\lambda$.

In the simulator, we let $N = 5$, $\lambda = 256$ kbps, $\alpha = 1250$ s^{-1} and $\beta = 5000$ s^{-1}. Accordingly, the mean and highest bit rates of a video conference source are 256 kbps and 1.28 Mbps, respectively. The video payload is 512 bytes [9]. The tolerable delay and PLR for video conference traffic are 100 ms and 0.1% [9], respectively. Note the required PLR is extremely low. Therefore, when the MAC protocol is MDCF, the AM should be used to perform the delivery service even if transmissions are in one-hop.

Both voice and video traffic are extremely delay-sensitive. Real-time Transport Protocol (RTP) is used on top of UDP to deliver the traffic. The RTP/UDP/IP introduces an overhead of 40 bytes. A real-time MPDU is dropped if its experienced delay is higher than the tolerable delay value.

5.1.6.4 FTP Traffic

FTP is the protocol used for exchanging files over a network based on the TCP/IP protocol. The transport protocol for it is TCP. Accordingly, its transmission behavior is dependent on the behavior of TCP. In the simulator, the FTP performance is equivalent to the TCP performance. The TCP traffic and FTP traffic are used interchangeable in this thesis. FTP is located in the application layer. It specifies file sizes, from which TCP derives the number of FTP packets that should be transmitted. A TCP connection for transmission is released when the amount of transferred FTP packets reaches the predefined number.

TCP is designed for wired networks assuming that packet losses are almost solely owing to network congestion. Using TCP directly over the lossy radio link shall lead to a very low transmission efficiency. One solution for this is to adapt TCP itself suitable for the wireless environment. Another one is to utilize the error control scheme provided by the link layer. The error control protocol in the link layer retransmits lost packets when necessary. It seems to TCP that there is no packet loss as long as no buffer overflow occurs in the link layer and the Round Trip Time keeps small. As a result, TCP is able to perform well over the wireless medium. When the MAC protocol is MDCF, the AM should be used to deliver TCP protocol data units.

5.1.6.5 WWW Traffic

Another highly bursty WWW traffic class is simulated using the model specified in [55]. A WWW source switches between the packet call state and reading time state. In the packet call state, a source generates a number of packets according to the geometric distribution with mean value of 25 s. The interarrival time of packets is exponentially distributed with mean value of 0.0104 s. In the reading time, no traffic is generated. The generated packets are with a mean packet length of 480 bytes, while the longest packet length reaches 66666 bytes. The average requested file size is 12 kBytes.

The WWW traffic has no delay requirement but requires zero PLR. The transport protocol for it is TCP.

5.1.6.6 CBR Traffic

The constant bit rate (CBR) traffic is a simple and ideal traffic. A CBR source generates data packets of a fixed length at a predefined constant rate. Some multi-media contents are streamed as CBR traffic.

In addition to its simplicity, another advantage of the traffic is that its generation behavior is predicable. The packet size, packet generation interval and stream duration of a given flow are fixed. Owing to this, the CBR traffic is often used to analyze the performance of a network.

For different evaluation purposes, the transport protocol serving for the CBR traffic can

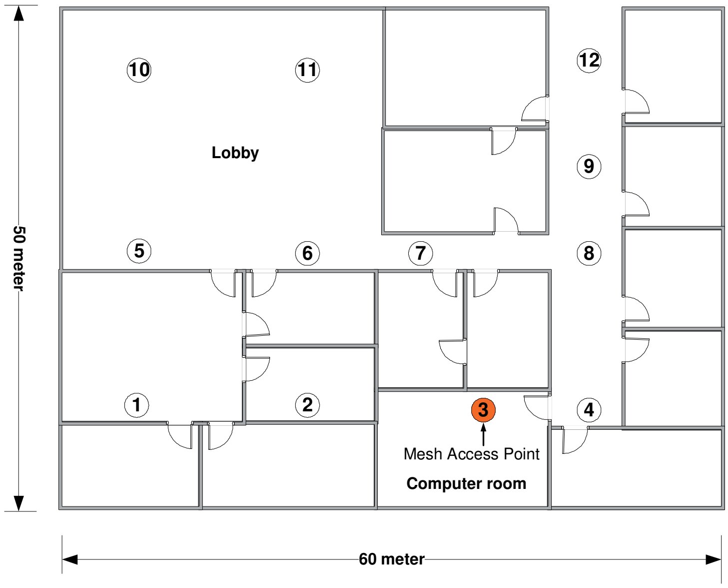

Figure 5-3. An indoor scenario (office): Assuming the IEEE 802.11a PHY, the path loss caused by a wall is 16 dB [84]. Transmit power of each MP is 80 mW. 16QAM 1/2 is used to transmit beacons,see Table 5-1. The beacon transmission ranges from a given MP across free space, one wall and two walls are > 60 m, 36 m and 7 m, respectively. 12 MPs are deployed to assure service connectivity in each room. MP 3 is the only AP in the scenario, providing Internet access for the mesh network. The maximal hop count for packet relaying between two farthest located MPs is 3 hops. Any MP can be Type 1 MP (see Section 3.2.13.3).

be either UDP or TCP. Accordingly, when the MAC protocol is MDCF, both the AM and UM can be used in RLCP to deliver the traffic.

5.2 Synchronization Performance

5.2.1 Simulation Scenarios

An indoor and an outdoor scenario are used to evaluate the performance of MTSF - the synchronization algorithm is described in Section 3.2.13.

An indoor scenario (50 m × 60 m) shown in Figure 5-3 represents a typical office environment using mesh technology. When the IEEE 802.11a PHY is used, walls between adjacent rooms cause serious signal attenuation: 16 dBm/wall at 5.2 GHz [84]. In order to assure connectivity in every room in the scenario, 12 mesh points are deployed as shown in Figure 5-3. Note MPs 10 and 11 are for providing connectivity to the area outside the office building but near the lobby. In this scenario, the transmission ranges of a given MP in different directions are different. See the caption of Figure 5-3 for details. Hidden MPs widely exist in the scenario. For instance, when MP10 or 11 is transmitting to MP 5 or 6, MPs 7 and 8 are potential hidden MPs.

A 5 × 5 grid topology network depicted in Figure 5-4 is used to simulate an interfer-

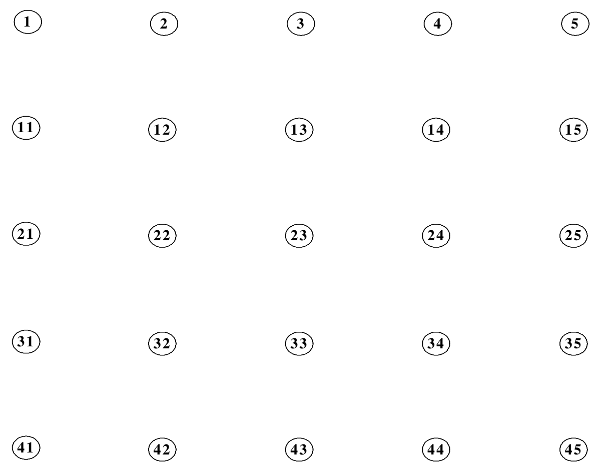

Figure 5-4. An outdoor scenario: Adjacent MPs are evenly apart from each other. The distance between adjacent MPs is different for different evaluation purposes. 16QAM 1/2 is used to transmit beacons. The transmit power is selected in a way to guarantee that the beacon transmission range is a bit larger than the distance between two adjacent MPs, but smaller than twice the value of the distance. Parts of the topology are also used for evaluation. Clearly when the used topologies are 1 × 2, 2 × 2, 2 × 3, 3 × 3, 3 × 4, 4 × 4, 4 × 5 and 5 × 5, the maximum hop count for packet relaying between two farthest located MPs in the related topology are 1, 2, 3, 4, 5, 6, 7 and 8, respectively. Any MP can be Type 1 MP (see Section 3.2.13.3).

ence-prone outdoor environment, where hidden and exposed MPs widely exist. See the caption of Figure 5-4 for a detailed scenario description.

5.2.2 Evaluation Results

The metric used to measure the synchronization performance is *global time error* (GTE), which is defined as the maximum clock difference between any pair of MPs in a network. Firstly, the GTE in the indoor scenario is traced over time to show how the synchronization algorithm works. Then the mean GTE value and its respective standard devition are plotted as error bar graphs to show the synchronization performance under the impacts of the physical clock drift rate, the beacon interval, the network size (in terms of number of the maximum relaying hops) and the maximum transmission range.

5.2.2.1 Trace of GTE over Time

Figure 5-5 shows the trace of the GTE over time and traces of compensated clock drift rates of 6 randomly selected MPs in the indoor scenario. It is easy to see that the compensated clock drift rate at each MP gets close with time. As a result, the GTE gets small over time. As indicated by the figure, at the beginning of the simulation, the maximum difference of clock drift rates of sampled MPs is up to 0.02 - (-0.02) = 0.04 µs/TDMA frame. Consequently, the GTE is 4 µs. The period [0, 3] (s) is the fast compensation phase, during which the synchronization function at each MP quickly adjusts the compensation factor d_i (see Section 3.2.13.6.3). At the end of the stage, the maxi-

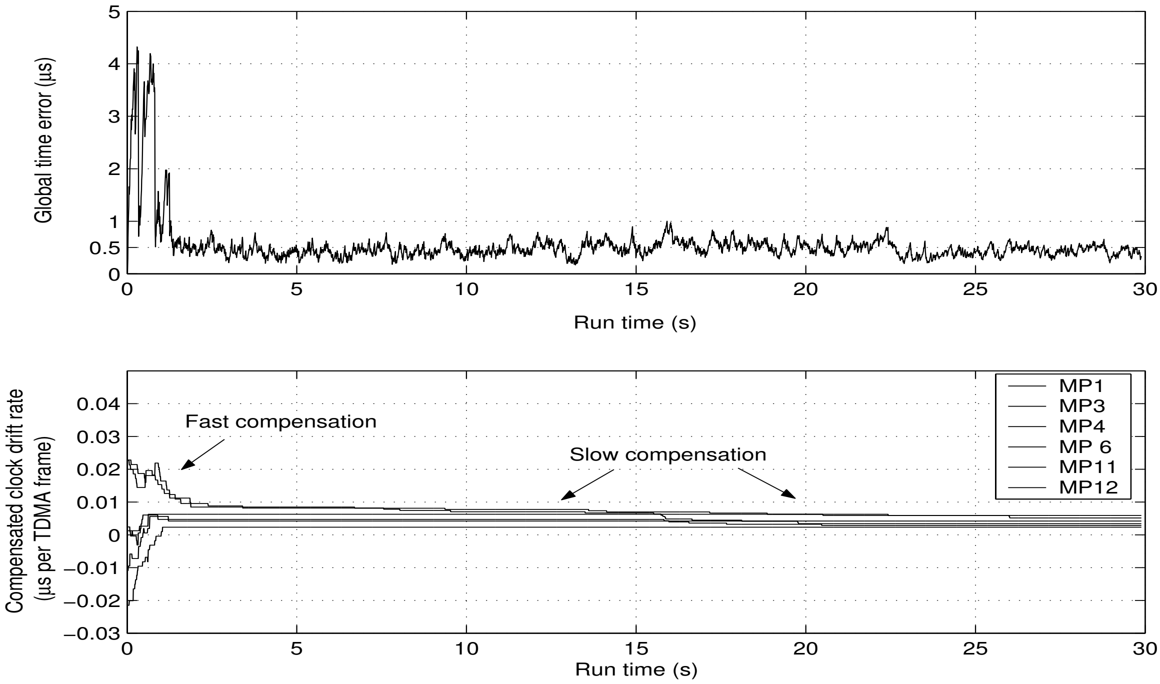

Figure 5-5. The trace of global time error (GTE) over time and related traces of compensated clock drift rates of 6 selected MPs in the indoor scenario, where the beacon interval is 20 TDMA frames and the maximum physical clock drift rate is 50 ppm.

mum difference of clock drift rates is reduced to 0.01 – 0.002 $\approx$ 0.01 μs/TDMA frame and the related GTE is reduced to 0.7 μs. After that, the synchronization function at each MP slowly adjusts d_i. The maximum difference of clock drift rates at sampled MPs keeps getting close with time. In the period [25, 30] (s), the maximum difference is less than 0.005 μs/TDMA frame and corresponding GTE is around 0.5 μs. Obviously, the distributed synchronization function works effectively in the indoor mesh environment. It is worth noting that the compensation algorithm is important for achieving a high synchronization precision and is helpful to reduce the overhead used to send beacons. Only when differences of clock drift rates between MPs are small enough, a larger beacon interval is possible to be used, as shown in the following.

5.2.2.2 Impact of Physical Clock Drift Rate on Beacon Interval

Figure 5-6 shows the relations of the GTE and maximum physical clock drift rate under various beacon intervals in the indoor (a) and 5 × 5 outdoor scenarios (b), respectively. It is clear that a shorter beacon interval helps to achieve a higher synchronization precision, as proven in both Figure 5-6a and b. But this incurs a higher overhead for beacon transmission and requires a higher energy consumption. Under a given beacon interval, a smaller physical clock drift rate leads to a higher synchronization precision, but this results in a bit higher hardware cost. Given that the tolerable GTE is 1.25 μs, in the indoor scenario, the maximum physical clock drift rate can be up to 80 ppm if the

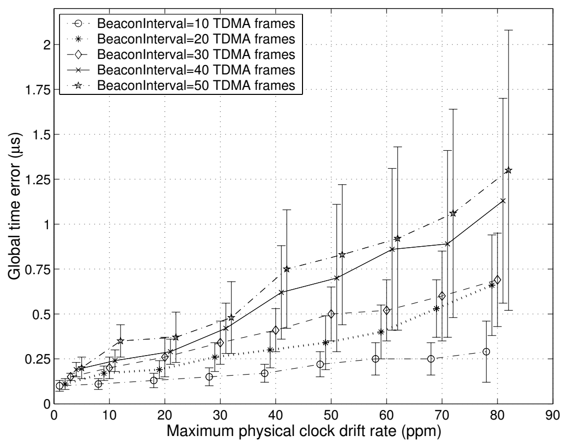

a) GTE in the indoor environment.

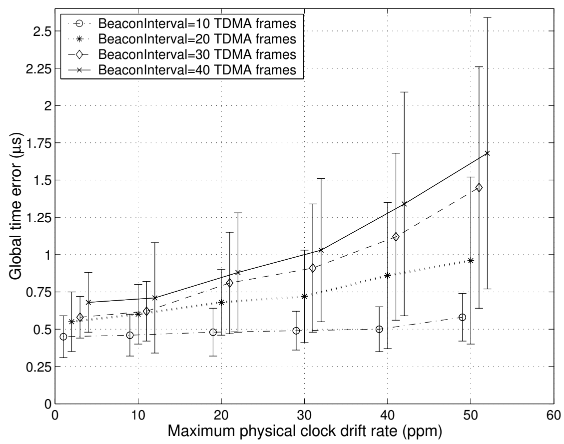

b) GTE in the 5 × 5 outdoor environment.

Figure 5-6. GTE vs. maximum physical clock drift. Key parameter settings for the indoor environment is introduced in Figure 5-3. The settings for the 5 × 5 outdoor environment are: distance between adjacent MPs is 120 m; transmit power at each MP is 100 mW; beacon transmission range is 140 m. Packet relaying between two farthest located MPs, like from MP 1 to MP 45, needs 8 hops. Note that in order to avoid overlapping error bar lines in the figure, the physical clock drift rates used for plotting are -2 ppm to 2 ppm deviated from the values used in the simulation, which are 2 ppm, 10 ppm, 20 ppm, 30 ppm, 40 ppm, 50 ppm, 60 ppm, 70 ppm and 80 ppm. *Note that GTE is sampled per 2 ms.*

beacon interval is no more than 30 TDMA frames, or beacon intervals can be up to 50 TDMA frames if the maximum physical clock drift rate is less than 50 ppm, as indicated in Figure 5-6a. under the same constraints, in the outdoor scenario, when the maximum physical clock drift rate is 50 ppm, the beacon interval should be 10 TDMA frames (9.16ms), or the beacon interval can be 40 TDMA frames given that the maximum physical clock drift rate is under 20 ppm, as suggested by Figure 5-6b.

It appears that under a given physical clock drift rate and a given beacon interval, the indoor network achieves a higher synchronization precision than in the outdoor network. The reason for this is that the maximum beacon transmission range in the indoor network is < 50 m, whilst that in the outdoor network is 120 m. The impact of the maximum beacon transmission range on the synchronization precision will be studied later.

5.2.2.3 Impact of Network Size

MTSF operates nicely in the multi-hop environment studied before. This sub-section studys the impact of the network size measured in terms of the maximum number of relaying hops on the synchronization precision. For simplicity, in the following, a network is called n-hop network to indicate its size. As shown in Figure 5-7, in the one hop network, even when the physical clock drift rate is 30 ppm and the beacon interval is 40 TDMA frames, the GTE is small: The mean value is 0.2 µs and the standard deviation is 0.15 µs. Under the same condition, the six hop network achieves a mean GTE of 0.75 µs with standard deviation of less than 0.25 µs. In contrast, in the eight

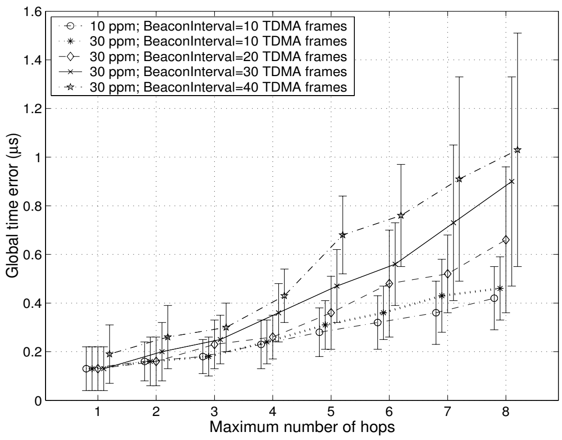

Figure 5-7. Impact of network size, which is measured in terms of the maximum relaying hops. Parts of the 5 × 5 outdoor grid topology shown in Figure 5-4 are used to simulate different network size. In details, topologies 1 × 2, 2 × 2, 2 × 3, 3 × 3, 3 × 4, 4 × 4, 4 × 5 and 5 × 5 are used to simulate the networks where packet relaying between two farthest located MPs needs 1, 2, 3, 4, 5, 6, 7 and 8 hops, respectively. Distance between adjacent MPs, transmit power at each MP and beacon transmission range are 120 m, 100 mW and 140 m, respectively. Note that to avoid overlapping error bar lines in the figure, the maximum number of hops used for plotting deviate a bit from the values used in simulation, which are 1, 2, 3, 4, 5, 6, 7 and 8 hops. *Note that GTE is sampled per 2 ms.*

hop network, given that the tolerable GTE is 1.25 μs, the beacon interval should be no more than 20 TDMA frames if the physical drift rate is 30 ppm. In the multi-hop environment, MPs which are not in the mutual beacon transmission range need multiple times the beacon interval to exchange the synchronization information. Accordingly, the network wide GTE is increased with the network size. Clearly, the guard time internal to time slots for avoiding synchronization errors should match the network size as well.

5.2.2.4 Impact of Maximum Beacon Transmission Range

As suggested in Eq. (3.13), the synchronization precision is highly dependent on the maximum beacon transmission range. This is confirmed by the simulation result shown in Figure 5-8. When the maximum beacon transmission range is 40 m, even if the physical clock drift rate is 30 ppm and beacon interval is 40 TDMA frames, the mean GTE plus its standard deviation is less than 0.75 μs. With the incrase of the maximum beacon transmission range, the GTE performance including both the mean value and standard deviation value decreases. When the maximum beacon transmission range is 240 m, if the physical clock drift rate is 30 ppm and the beacon interval is 40 TDMA frames, the mean and standard deviation GTEs are 1.6 μs and 0.8 μs, respectively, almost 5 times that of the case with maximum beacon transmission range 40 m. It is worth noting that the signal propagation delay (3.3 μs/km) is 0.8 μs over 240 m and the round trip propagation delay is twice that value. As indicated in Eq. (3.15), the design of the guard time to avoid synchroniazion errors should account for the maximum beacon

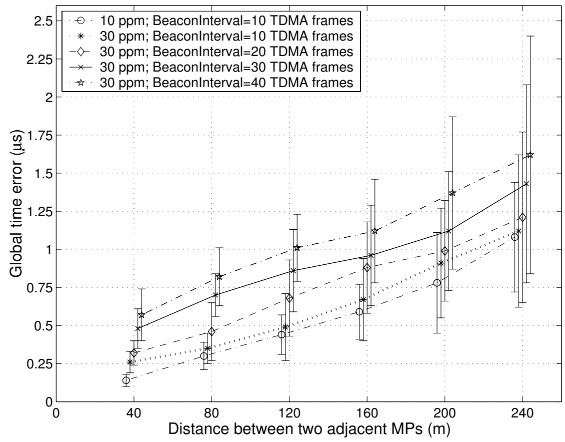

Figure 5-8. Impact of the maximum beacon transmission range on GTE. The 5 × 5 outdoor grid topology shown in Figure 5-4 is used for evaluation. Transmit powers are 10 mW, 40 mW, 100 mW, 260 mW, 400 mW and 600 mW when the set distances between adjacent MPs are 40 m, 80 m, 120 m, 160 m, 200 m and 240 m, respectively. Beacons transmitted from an MP can be only decoded by its adjacent MPs. Note that to avoid overlapping error bar lines in the figure, the distances between adjacent MPs used for plotting deviate a bit from the values used in simulation, which are 40, 80, 120, 160, 200 and 240 m. *Note that GTE is sampled per 2 ms.*

transmission range and distance between adjacent MPs.

5.3 Performance of MDCF Networks

In this Section, the traffic performance of MDCF networks is extensively investigated. How well MDCF performs in mesh environments to fulfill QoS commitments is the main concern. To clearly reveal this, several evaluation scenarios are used step by step. Section 5.3.1 first describes the simulation scenarios and important simulation settings. After that, the performances of single-hop and multi-hop MDCF networks are studied in Section 5.3.2 and Section 5.3.2, respectively. Finally, the QoS performance of MDCF is intensively examined in Section 5.3.4. The evaluation results obtained in an MDCF network are compared to the results when using DCF or EDCA in the same scenario.

5.3.1 Important Settings and Simulation Scenarios

Table 5-4 lists important settings used for the simulation. It can be computed from the presented information that the transmission range of MPDUs is 120 m whereas the carrier sense ranges of MPDUs, BESs and AESs are about 280, 280 and 370 m, respectively. Unless otherwise stated, the PHY data rate is 24 Mbps and the multi-wall multi-floor channel mode is used. *Note that in this Section, when the evaluation is on single-hop networks, "stations" are used instead of "MPs".*

Five scenarios are used for evaluation:

- Point-to-point (PTP) transmission – transmissions between two MPs, which are in

Table 5-4. Important simulation settings in PHY, ARQ and TCP.

Important settings in PHY, ARQ and TCP	
Transmission power for MPDUs & BESs	80 mW
Transmission power for AESs	160 mW
Carrier sense threshold	- 83 dBm
Minimal receiving sensitivity	- 74 dBm
PHY mode and rate	16QAM½, 24 Mbps
Length of a MDCF MPDU	108 bytes
ARQ poll period (only in MDCF)	20 MPDUs
TCP window sizes	20 TCP packets

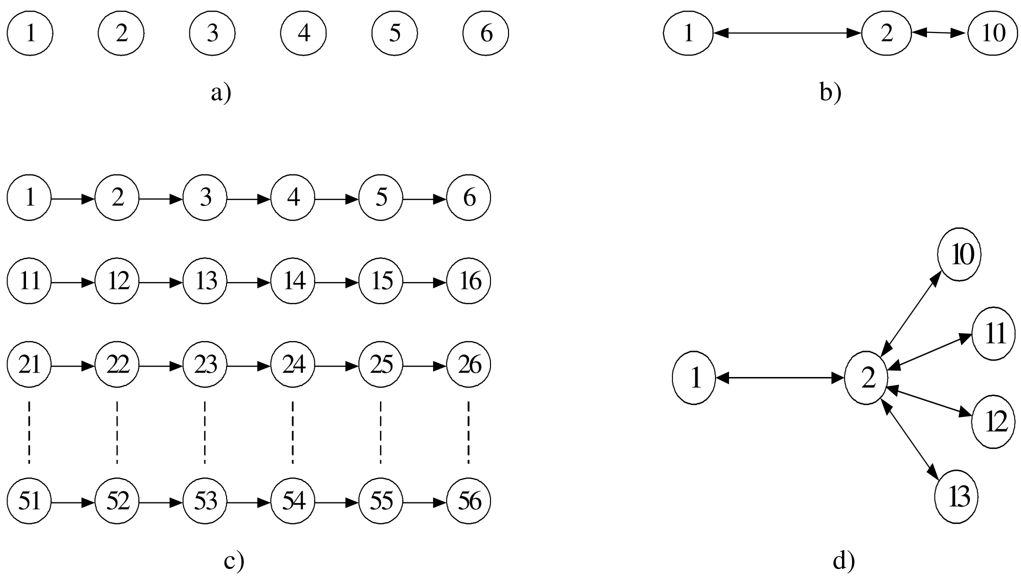

Figure 5-9. Simulation scenarios: a) a string topology; b) capture topology; c) a 6 × 6 grid topology; d) a two-hop tree topology.

mutual transmission range. No competing MPs exist. The system efficiency i.e. the maximum one-hop throughput under ideal channel condition, and the basic throughput and delay performances under UM and AM, respectively, are evaluated using the scenario. The impact of the PHY mode and the size of MAC Service Data Unit (MSDU) on throughput is studied as well.

- Single hop network –50 stations under an MP are randomly distributed in an area (80 m × 80 m), each in mutual transmission range. The single-hop saturation performance and basic QoS performance are evaluated there.
- String topology – 6 MPs make up a string topology, each 100 m apart from its adjacent MPs, as shown in Figure 5-9a. Clearly, each MP is in the transmission

range of its adjacent MPs only. It needs 5 hops to deliver packets from MP 1 to MP 6. The string topology is used to simulate a simple environment with hidden and exposed MPs. Accordingly, the capability of MDCF to handle hidden and exposed MPs in mesh environments can be clearly observed there. Besides, the traffic performance of the string multi-hop network is studied, the results of which are used to analyze the performance achieved in more complicated multi-hop mesh scenarios.

- Capture topology – as depicted in Figure 5-9b, MP 1 and 2 are 100 m apart, whilst MP 2 and 10 are 40 m apart. When MP 1 and 10 simultaneously transmit to MP 2, MP 2 can decode packets from MP 10 in presence of interference from MP 1. The performance of MDCF in the capture environment is studied in the scenario.
- Grid topology – a 6 × 6 grid topology to connect MPs as shown in Figure 5-9c. Adjacent MPs are 100 m apart from each other. This scenario is used to simulate a highly interference-prone multi-hop environment.
- A two hop tree topology – as shown in Figure 5-9d, MP1, 10, 11, 12 and 13 are about 100 m away from MP2, which is the relay MP for the end-to-end links MP1-10, MP1-11, MP1-12 and MP1-13. The scenario is used to evaluate the performance of MDCF when multiplexing packets along multi-hop routes.

5.3.2 Performance in Single Hop Networks

5.3.2.1 System Efficiency

MDCF is a fully distributed protocol for mesh networks with QoS guarantee. To do so, a significant amount of control time slots (ACH and ECHs) are used in MDCF per TDMA frame to implement an efficient prioritized channel access scheme and properly handle hidden MPs, exposed MPs and capture in mesh environments. Then, a question arises: how is the system efficiency?

A study is performed on the PTP scenario to answer the question.

5.3.2.1.1 Maximum throughput (MT)

MT is defined as the highest throughput that can be achieved in a network. Cleary, in the mesh environment, MT is a single-hop throughput which is achieved with an error-free channel without any competing station, i.e., it is achieved in the PTP transmission scenario described in Section 5.3.1.

CBR traffic is used and the load of it at the sending station is high enough to saturate the network. The radio channel model uses the error model and the channel packet error rate is set as 0. For fair comparison between MDCF and DCF, the AM is selected as the service model in MDCF.

Figure 5-10a and b show the normalized and actual MT, respectively, accounting for the impacts of the MSDU size and PHY mode. When using DCF, both the normalized and

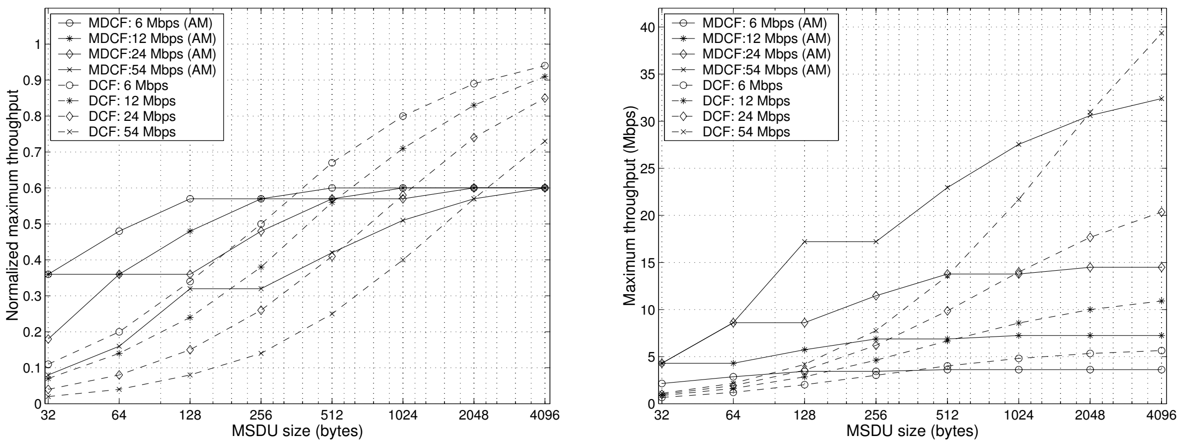

a) b)

Figure 5-10. Maximum single-hop throughput: a) normalized throughput; b) actual throughput. In MDCF, an MSDU is fragmented into one or several MPDUs. In DCF, MAC layer fragmentation is not used: An MPDU is formed by adding the MAC layer header and tail (FCS) before and after an MSDU, respectively. CBR traffic is used for evaluation. Please note that only the MT values when the MSDU sizes are 32, 64, 128, 256, 512, 1024, 2048 and 4096 bytes, respectively, are shown. Solid lines represent MDCF results.

actual MTs under a given PHY mode increase with the MSDU size. The actual DCF MTs well match the results reported in [91]. When using MDCF, the MT under a given PHY mode increases with the increased MSDU size until saturation and then stays unchanged. The highest normalized MDCF MT under all the PHY modes is 0.6, which is very close to TH^{O}_{TMT} (0.626) obtained from applying the relevant values shown in Table 5-2 into Eq. (3.3). Note TH^{O}_{TMT} differs from the normalized MT in that it does not consider ARQ overhead. Under a given PHY mode, MDCF performs better than DCF as long as the MSDU size is not large. E.g. DCF MT is higher than with MDCF only, if the MSDU sizes are larger than 400, 512, 1200 and 2400 bytes when using 6, 12, 24 and 54 Mbps PHYs, respectively. As suggested in [9], in most applications, APDU sizes are smaller than 512 bytes. Then, it can be said that, MDCF outperforms DCF in terms of the throughput capacity.

In MDCF, an MSDU needs to be fragmented before transmission, if the MSDU size exceeds the maximum allowed MPDU size that depends on the PHY mode, see Table 5-1. If the size of an MSDU is not multiple of the used fragmentation threshold, the last MPDU shall be padded, causing fragmentation loss. This is the reason why the MSDU size impacts MDCF MTs (note that Figure 5-10a and b only show the MT values corresponding to several MSDU sizes, see caption of Figure 5-10). However, as indicated in Figure 5-10a and b, the level of the impact of fragmentation loss in MDCF is much smaller than in DCF: Under a given PHY mode, the increasing rate of the MT value with increased MSDU size when using MDCF is much smaller than using DCF. Moreover, under all the PHY modes, when using MDCF, the MT is close to saturation when the MSDU size is larger than 512 bytes. In contrast to this, there is no saturation MT with

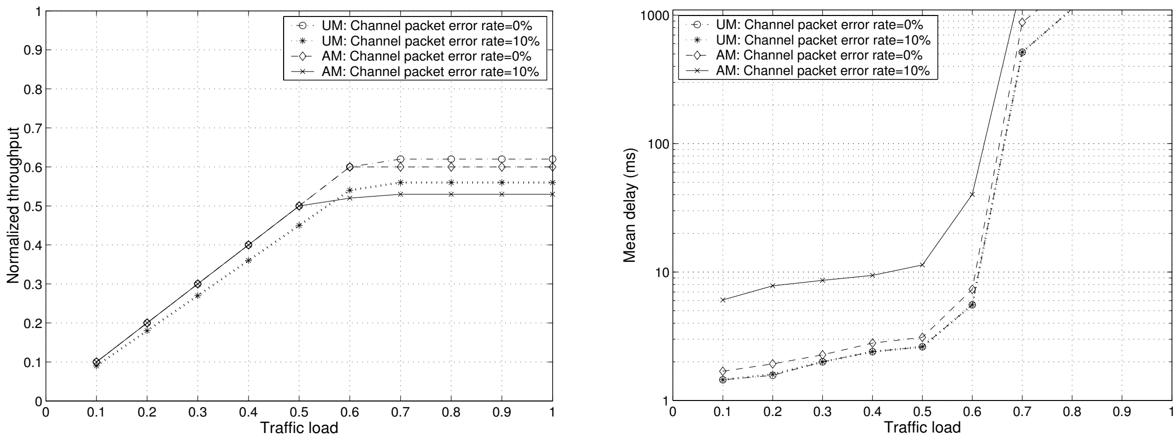

a) b)

Figure 5-11. Basic one-hop traffic performance under the UM and AM: a) throughput performance; b) delay performance. CBR traffic is used for evaluation. Key ARQ parameters for the AM: the polling timer is 5 TDMA frames; both the transmitting and receiving window sizes are 300 RPDUs. The PHY data rate is 24 Mbps and the MSDU size is 512 bytes.

increased MSDU sizes when using DCF: the larger the MSDU size, the higher the MT.

It is worth noting that due to the fragmentation loss, using an n-times higher bit rate PHY does not necessarily generate an n-times higher MDCF MAC throughput as shown in Figure 5-10b. E.g when the MSDU size is 256 bytes, the actual MT differences between using 6 Mbps PHY and 24 Mbps PHY are (11.47 / 3.44 = 3.3) < (24 / 6 = 4). The reason is clear: A lower bit rate PHY only supports a smaller maximum MPDU size (see Table 5-1), resulting in a smaller fragmentation loss. Hence, the transmission efficiency of MDCF when using a lower bit rate PHY is relatively higher than with DCF.

5.3.2.1.2 One-hop throughput and delay performance under UM and AM

The PTP scenario is used to study the one-hop traffic performance of MDCF under UM and AM, respectively. CBR traffic and the error channel model are used. Figure 5-11a and b show throughput and delay performance, respectively, for 0 and 10% channel packet error rate.

The throughput under both UM and AM, increases with the traffic load until reaching saturation. When the channel packet error rate is 0, the network is saturated when the traffic loads are over 0.62 and 0.6 under UM and AM, respectively. Accordingly, the throughput under UM is a bit higher than under AM, since AM introduces some overhead for ARQ operation. When the traffic load is not saturating the system, the throughput equals the traffic load under both, UM and AM. When the channel packet error rate is 10%, the network becomes saturated when the traffic loads are over 0.56 and 0.52 under UM and AM, respectively. It is worthy noting that when traffic load is not saturating the system, the UM throughput is smaller than the traffic load since some

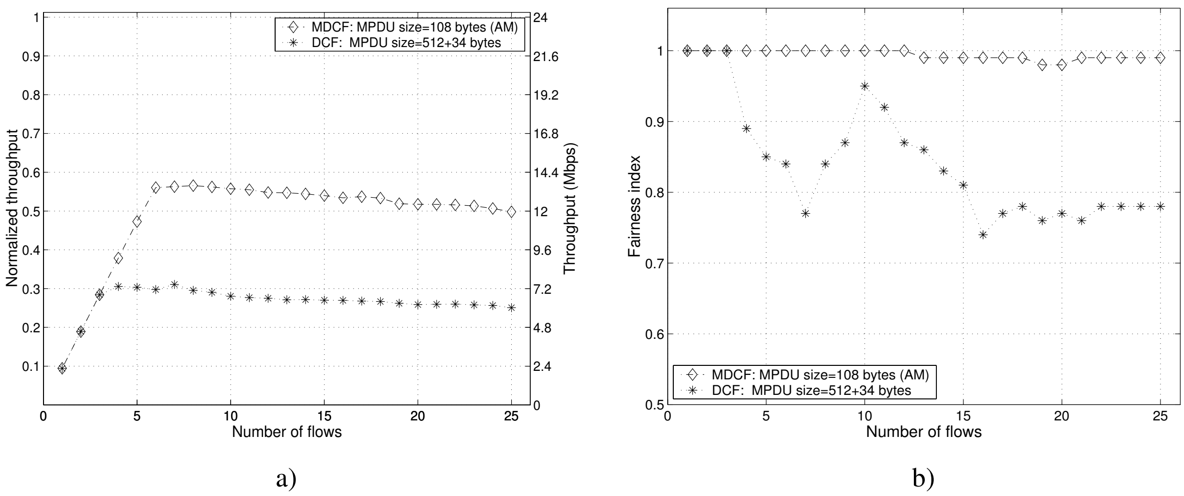

Figure 5-12. The saturation performance: a) throughput performance; b) fairness index. The MSDU size is 512 bytes. The single hop scenario is used. Each sending station generates CBR traffic at a rate of 555 MSDU/s (2.27 Mbps). Each flow is between two different stations.

packets are lost, whilst the AM throughput equals the traffic load.

One benefit of using UM for transmission is that packet delay is lower than under AM, see Figure 5-11b. When traffic load is smaller than 0.5, packet delay under UM is smaller than 2 ms regardless of the channel packet error rate. The packet need not wait and delay is mainly owing to the transmission delay. The delay is increased significantly when the traffic load is 0.6 or higher, since the network becomes saturated and the queuing delay dominates. The delay under AM is highly dependent on the channel packet error rate. As shown in Figure 5-11b, when the channel packet error rate is 10%, packet delay under AM is between 6 to 11 ms even under low load.

5.3.2.2 Saturation Throughput under Multiple Competing Stations

In a distributed network, saturation throughput under multiple competing stations, each always having available packets for transmission, reveals the highest load that the network can deliver in stable conditions, see [50] for an example. In the following evaluations, the multi-wall multi-floor channel model is used. 50 stations are randomly located in a single-hop network. Each flow is between two stations and the sending station generates CBR traffic at a rate of 2.27 Mbps. The network traffic load is varied by changing the number of flows. The performance metrics are aggregate throughput and fairness index, see Eq. (2.7).

Figure 5-12a shows the throughput performance. The DCF network becomes saturated when the number of flows is 3, whilst the MDCF network is saturated when the number of flows is over 6. The saturation throughput of MDCF is almost two times that of DCF. After reaching saturation, the aggregate throughput of both protocols reduces with increased number of flows, owing to collision related overhead.

The fairness performance is shown in Figure 5-12b. MDCF performs well in fairly distributing the bandwidth under the contending flows, resulting in a fairness index always very close to 1. In contrast, the fairness index in the DCF network decreases and substantially varies with the number of flows. When the number of flows is over 15, the fairness index is below 0.8, meaning that some stations suffer from starvation in using the channel for transmission. Although the throughput degradation in the DCF network with increased number of flows is limited (to 18%), the fairness performance degrades significantly.

Obviously, MDCF performs much better when multiple stations contend for channel access than DCF.

5.3.3 Performance in Multi Hop Networks

As pointed out in Section 2.2, a MAC protocol for mesh networks should be able to properly handle hidden MPs, exposed MPs, capture and high load situations. In this Section, two string topologies (Figure 5-9a and b) are used to study the performance of MDCF in hidden MPs, exposed MPs and capture environments, respectively. In addition, the performance of MDCF operating in multi-hop mesh environments is studied on a grid topology. One property of MDCF mesh networks is that any one-hop MDCF link may multiplex any packets transmitted on that route, see Section 3.2.7. The last part of the Section studies the benefits of using packet multiplexing in mesh networks.

5.3.3.1 Fundamental Study

The string networks shown in Figure 5-9a and b are used for evaluation. Please see Section 5.3.1 for a detailed description of topology parameters. Both the performances under CBR and TCP traffic are studied. When CBR traffic is used, the CBR rate at a sending MP is set as 9 Mbps. When TCP traffic is used, the TCP window size is set as 20 TCP PDUs. Unless otherwise stated, the MSDU size is 512 bytes, whilst the MPDU sizes when using DCF and MDCF are 512+34 (DCF MAC header) = 546 bytes and 108 bytes, respectively.

5.3.3.1.1 Hidden MP environment

In the string topology shown in Figure 5-9a, when MP 1 is transmitting to MP 2, MP 4 is a hidden MP to the transmission pair (see Section 2.2 for details).

- Evaluation scenario - MP 1 starts to transmit to MP 2 at t = 1 s (Flow 1), whilst MP 4 starts to transmit to MP 5 at t = 6 s (Flow 2).

Figure 5-14 shows the throughput traces for CBR traffic. In the DCF network, when MP 4 starts to transmit, the throughput of Flow 1 is significantly reduced and almost 3 times lower than that of Flow 2. Moreover, the aggregate throughput when 2 flows exist is lower that that when only Flow 1 exists. Obviously, from t = 6 s on, MP 2 is interfered by MP 4 when it is receiving from MP 1. DCF cannot inhibit hidden MPs in the multi-hop

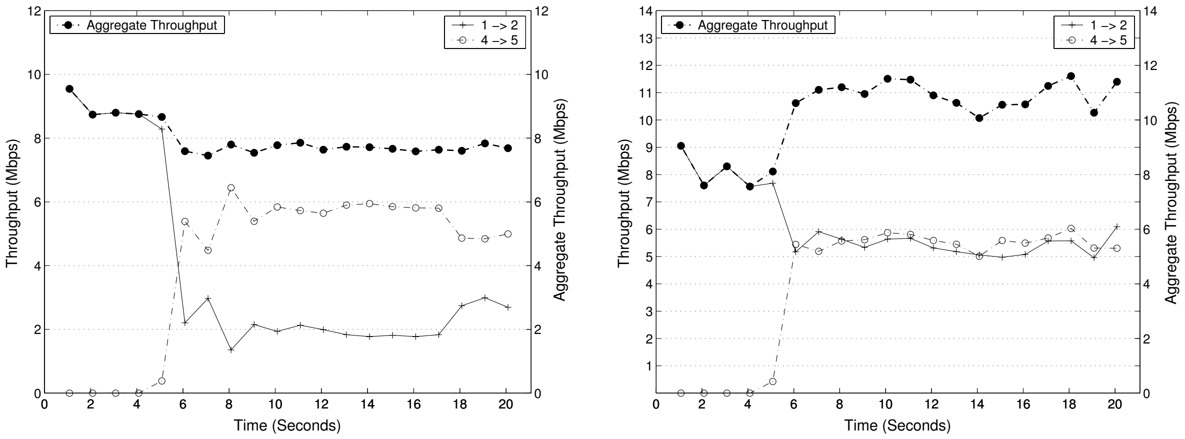

a) DCF b) MDCF

Figure 5-14. Throughput trace in the hidden MP scenario under CBR traffic input: a) trace in the DCF network; b) trace in the MDCF network. The fairness index from 6 to 20 seconds in the DCF network is 0.838, whilst that in the MDCF network is 1.

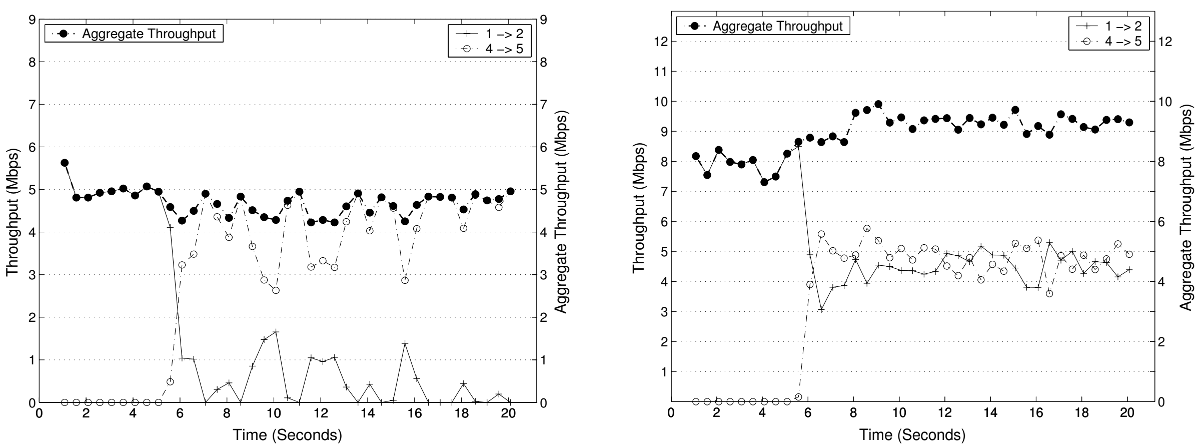

a) DCF b) MDCF

Figure 5-13. Throughput trace in the hidden MP scenario under TCP traffic input: a) trace in the DCF network; b) trace in the MDCF network. The fairness index from 6 to 20 seconds in the DCF network is 0.614, whilst that in the MDCF network is 1.

environment. On the contrary, in the MDCF network, when MP 4 starts to transmit, two flows equally share the bandwidth and the aggregate throughput of two flows is higher than when only Flow 1 exists. Further, it can be found that the aggregate throughput when two flows exist is close to the single-hop MT shown in Figure 5-10. The reason for this is that MP 4 uses TCHs for transmission other than those being used between MP 1 and 2 since it is able to sense BESs from MP 2.

The TCP throughput traces are shown in Figure 5-13. In the DCF network, after the start of Flow 2, the transmission of Flow 1 looks like being stopped. With TCP, the source cannot increase the transmission window size unless receiving acknowledgments from the sink in due time. When MP 4 transmits, since MP 2 is interfered, it cannot acknowledge the reception to MP 1. Without receiving acknowledgments from MP 2, MP 1 assumes the network is congested and reduces the window size. Accordingly, the throughput of Flow 1 is very low. In contrast, in the MDCF network, two flows equally share the bandwidth from t = 6 s on.

It is easy to see that MDCF can effectively handle hidden stations to avoid performance degradation in the multi-hop environment, which is not possible when using DCF.

5.3.3.1.2 Exposed MP environment

In the string topology shown in Figure 5-9a, MP 2 and 4 are in mutual carrier sense range. When MP 2 wants to transmit to MP 1 and MP 4 wants to transmit to MP 5, they are exposed MP pairs (see Section 2.2 for details).

- Evaluation scenario - MP 4 starts to transmit to MP 5 at t = 1 s (Flow 1), whilst MP 2 starts to transmit to MP 1 at t = 6 s (Flow 2).

Figure 5-15 and Figure 5-16 show the throughput traces when using CBR and TCP traffic, respectively. MP 1 and 5 are out of the carrier sense range of MP 4 and 2, respectively. Therefore, transmissions of two flows can take place in parallel without causing interference to each other. In the DCF network with CBR traffic, after Flow 2 appears, the aggregate throughput degrades from 9 Mbps to 8 Mbps. Though the long-term fairness index (from 6 to 20 seconds) in the DCF network is close to 1, the short-term fairness performance is bad: in most of the run time when two flows exist, the bandwidth cannot be equally shared by two flows as shown in Figure 5-15a. When traffic is TCP, the situation is even worse: in most of the run time since t = 6 s on, only one flow can use the radio for transmission as indicated in Figure 5-16a. The main reason for the DCF performance under CBR traffic is that when MP 2 and 4 sense transmissions from each other, they postpone their own transmissions (stopping the decrement of backoff slots). When traffic is TCP, MP 1 needs to send TCP acknowledgments from time to time. If MP 2 senses the transmission from MP 4, it will not reply a CTS when receiving a RTS from MP 1. Without receiving CTS feedback from MP 2 timely, MP 1 shall increase its contention window size. If the TCP transmission window size at MP 4 is large at the time, clearly, Flow 1 will be starved. Flow 2 might be starved under the similar situation.

In the MDCF network, no matter which traffic is used, after the second flow appears, two flows can equally share the bandwidth as shown in Figure 5-15b and Figure 5-16b. The reason is already stated in Section 3.2.6. Like the situation described in Section 3.2.5, the spatial reuse distance of the MDCF network is 4 hops. No parallel transmission between an exposed MP pair is possible in DCF networks as in parallel in MDCF networks. Therefore, the aggregate throughput for two flows is close to the single-hop MT shown in Figure 5-10. All flows in the scenario can fairly share the bandwidth, which is not possible to achieve in the DCF network.

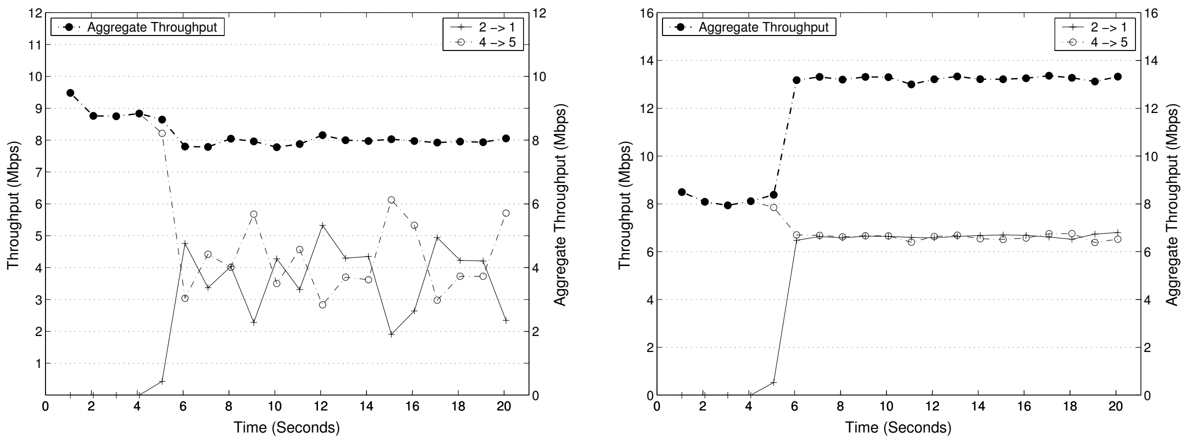

a) DCF b) MDCF

Figure 5-15. Throughput trace in the exposed MP scenario under CBR traffic input: a) trace in the DCF network; b) trace in the MDCF network. The fairness index from 6 to 20 seconds in the DCF network is 0.99, whilst that in the MDCF network is 1.

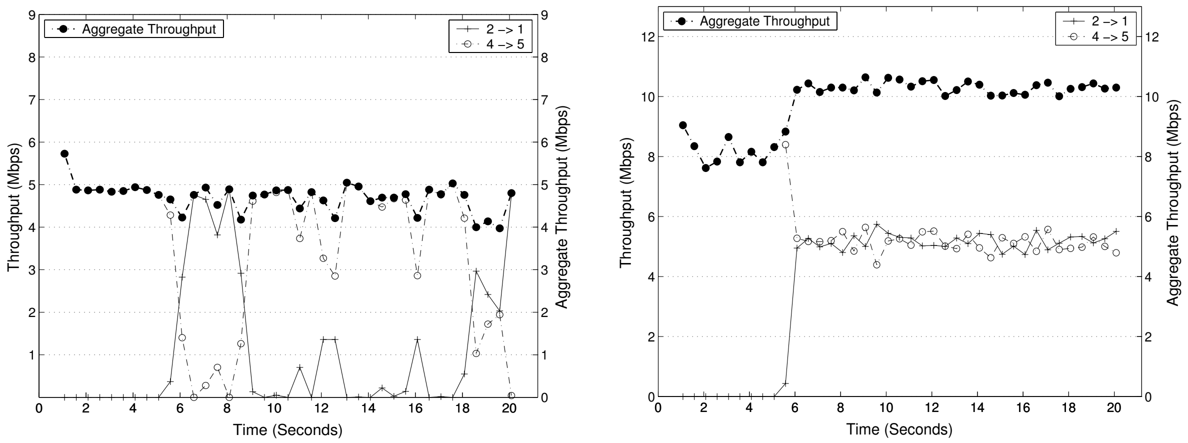

a) DCF b) MDCF

Figure 5-16. Throughput trace in the exposed MP scenario under TCP traffic input: a) trace in the DCF network; b) trace in the MDCF network. The fairness index from 6 to 20 seconds in the DCF network is 0.88, whilst that in the MDCF network is 1.

5.3.3.1.3 Capture environment

Figure 5-9b shows the topology used for evaluation, where the channel capture may-happen, when MP 1 and MP 10 transmit simultaneously to MP 2 (see Section 2.2 for details).

- Evaluation scenario - MP 1 starts to transmit to MP 2 at t = 1 s (Flow 1), whilst MP 10 starts to transmit to MP 2 at t = 6 s (Flow 2).

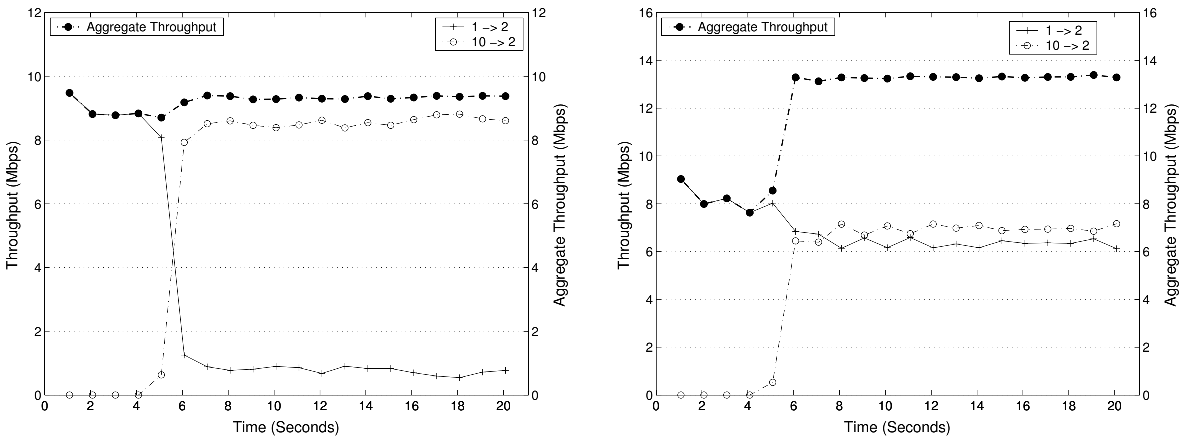

a) DCF b) MDCF

Figure 5-17. Throughput trace in the capture scenario under CBR traffic input: a) trace in the DCF network; b) trace in the MDCF network. The fairness index from 6 to 20 seconds in the DCF network is 0.59, whilst that in the MDCF network is 1.

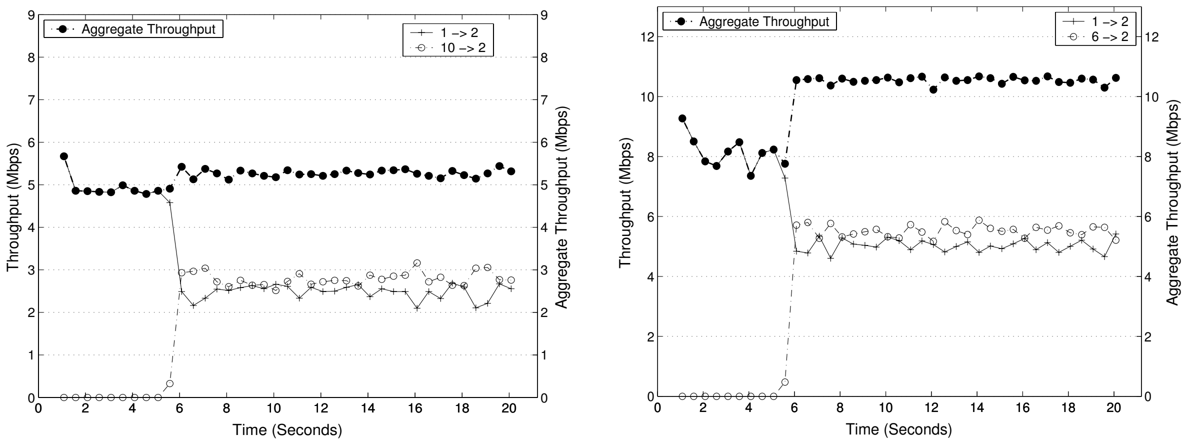

a) DCF b) MDCF

Figure 5-18. Throughput trace in the capture scenario under TCP traffic input: a) trace in the DCF network; b) trace in the MDCF network. The fairness index from 6 to 20 seconds in the DCF network is 1, whilst that in the MDCF network is 1.

Figure 5-17 and Figure 5-18 show the throughput trace in the capture scenario under CBR and TCP traffic, respectively. In the DCF network, when traffic is CBR, after Flow 2 appears, the chance of Flow 1 to use the channel is significantly reduced. On the contrary, Flow 2 almost monopolizes the channel. In other words, the radio channel is captured by Flow 2. Since MP 10 locates very close to MP 2 compared to MP 1, MP 2 can decode packets from MP 10 even when MP 1 transmits simultaneously. On the other hand, packets from MP 1 to 2 will be corrupted if MP 10 transmits in parallel with MP 1.

Therefore, when MP 1 and 10 happen to contend in the channel to send out RTS to MP 2, the one from MP 10 will be understood by MP 2. Afterwards, MP 1 invokes the back-off procedure since it fails to receive CTS from MP 2, whilst MP 10 reset its contention window after successfully delivering an MPDU to MP 2. Accordingly, Flow 2 captures the channel. However, when TCP traffic is used, the channel capture in the DCF network disappears as shown in Figure 5-18a. This is attributed to the TCP traffic control. After receiving TCP data packets, the TCP sink at MP 2 needs to send TCP an acknowledgment packet, without which the TCP source cannot generate more traffic. MP 2 can manage transmitting acknowledgment packets to MP 1 and 10, subsequently, without in favor of either MP 1 or 10. As a result, the channel capture is avoided.

In the MDCF network, no matter which traffic is used, no flow captures the channel at any time. Instead, two flows equally share the bandwidth. This proves the statements given in Section 3.2.6.

5.3.3.1.4 Impact of the number of hops on throughput

Evaluation is performed on the string network shown in Figure 5-9a. Both CBR and TCP traffic are used. MP 1 works as sources, while 2, 3, 4, 5 and 6 are sinks for the 1, 2, 3, 4 and 5 hop simulation runs, respectively. The service mode of MDCF is AM.

Figure 5-19a shows the maximum throughput vs. the different number of hops when traffic is CBR. In the MDCF network, the 2, 3, 4 and 5 hop throughputs are 1/2, 1/3, 1/4 and 1/5 of the single hop throughput, respectively. Like in Figure 3-10, the spatial reuse distance of the topology is 4 hops. Hence the total bandwidth is shared by ARQ flows within 4 hops, leading to a channel utilization of 1/4. For the 5 hop transmission, the increased ARQ control overhead reduces the channel utilization to 1/5. In contrast, 2, 3,

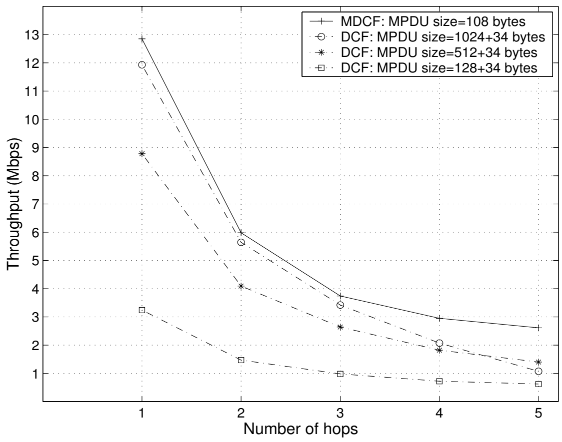

a)

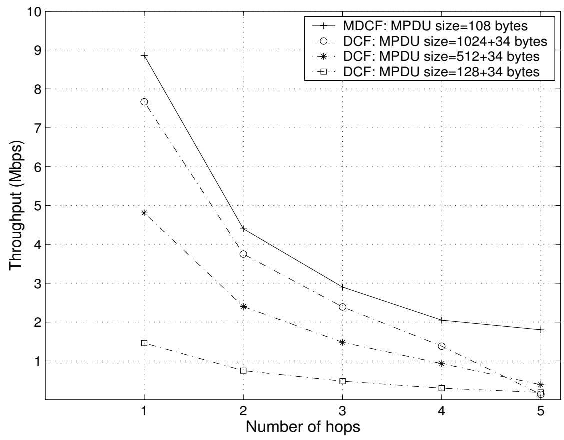

b)

Figure 5-19. Throughput vs. the number of hops: a) with CBR traffic input; b) with TCP traffic input. When CBR traffic is used, MP 1 generates CBR traffic at rates of 13, 6.5, 4.5, 3.5 and 3 Mbps when the numbers of hop in simulation are 1, 2, 3, 4 and 5, respectively.

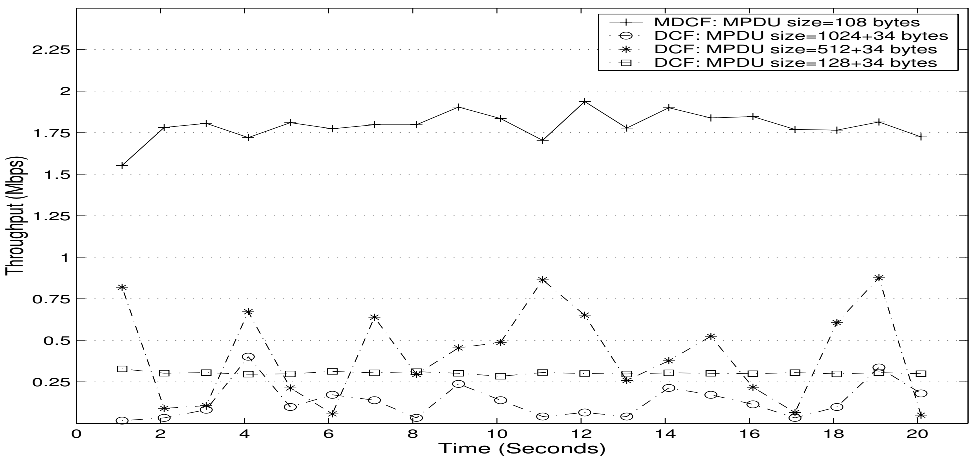

Figure 5-20. Throughput trace of the 5-hop TCP transmission over the string topology.

4 and 5 hop throughputs in the DCF network are 1/2, 1/3, 1/5 and 1/10 of the single hop throughput when the DCF MPDU size is 1024 + 34 bytes. MDCF using an MPDU size of 108 bytes generates a higher throughput than DCF even using a larger DCF MPDU size (1024 bytes) that is much better to reach high performance than smaller MPDU sizes under DCF. The 5 hop CBR throughput in the MDCF network is 2.61 / 1.07 = 2.44, 2.61 / 1.7 = 1.87 and 2.61 / 0.62 = 4.23 times that of the DCF network when the DCF MPDU sizes are 1024 + 34, 512 + 34 and 128 + 34 bytes, respectively.

The TCP throughput vs. the number of hops is shown in Figure 5-19b. The trend of the throughputs degradation with increased number of hops is similar to that when using CBR traffic for both the DCF and MDCF networks. However, the 5 hop throughput differences between the MDCF network and DCF network is even larger than that when using CBR traffic: The 5 hop TCP throughput in the MDCF network is 1.8 / 0.14 = 12.8, 1.8 / 0.39 = 4.65 and 2.41 / 0.19 = 9.73 times that of the DCF network when the DCF MPDU sizes are 1024 + 34, 512 + 34 and 128 + 34 bytes, respectively.

To clearly show how DCF and MDCF behave in an interference-prone multi-hop environment, the 5-hop TCP throughput trace is plotted in Figure 5-20. It can be seen that the throughput in the MDCF network is very stable during all the sample time. The highest (1.9 Mbps) recorded throughput is about 16% larger than the lowest (1.58 Mbps) recorded throughput. In contrast, in the DCF network, the 5-hop throughput is stable and very low only when the MPDU size is 128 + 34 bytes. When the MPDU sizes are 1024 + 34 and 512 + 34 bytes, the throughputs oscillate sharply and often: the highest throughputs are 95% and 88% than the lowest ones when the MPDU sizes are 1024 + 34 and 512 + 34 bytes, respectively. It is worth noting that the 5-hop DCF throughput with MPDU size 128 +34 bytes is much higher than the throughput with MPDU size 1024 + 34 bytes.

The reason for the significant performance difference between MDCF and DCF is that

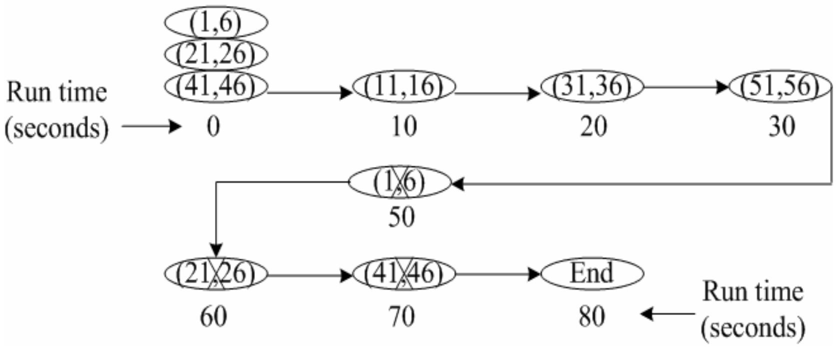

Figure 5-21. Start and stop times of 6 TCP connections in the grid network.

DCF cannot effectively handle hidden and exposed stations that MDCF can. MDCF also performs well with small size MPDUs, which is not the case with DCF.

5.3.3.2 Highly Interference-prone Multi-hop Environment

The grid topology shown in Figure 5-9c represents a very interference-prone multi-hop environment. MPs 1- 6, 11-16, 21-26, 31-36, 41-46 and 51-56 make up 6 multi-hop routes for six 5-hop TCP connections. MPs 1, 11, 21, 31, 41 and 51 are TCP sources, while MPs 6, 16, 26, 36, 46 and 56 are TCP sinks. For simplicity, we use notations (1, 6), (11, 16), (21, 26), (31, 36), (41, 46) and (51, 56) to represent above 6 MP pairs, each connected by a 5-hop TCP connection.

The TCP connections are started and terminated at different time instants during simulation. Figure 5-21 shows the details. Pairs (1, 6) (21, 26) and (41, 46) start to transmit at t = 0 second. Pairs (11, 16), (31, 36) and (51, 56) start transmissions one after the other at time instants 10, 20 and 30 seconds, respectively. Pairs (1, 6), (21, 26) and (41, 46) tear down their TCP connections at time instants 50, 60 and 70 seconds, respectively.

Figure 5-22a presents throughput traces achieved in the MDCF network. In time period [0, 10] the throughput of each active connection is about 0.45 Mbps, and aggregate throughput of three connections amounts to 1.4 Mbps. This value is 0.4 Mbps lower than that of the string topology at 5-hop, which is 1.8 Mbps in Figure 5-20. By opening three more connections one by one at t = 10, 20 and 30 seconds, the throughput of each active connection goes down to 0.2 Mbps. The aggregate throughput is reduced to 1.2 Mbps, since the amount of ARQ control overhead is increased with increased number of active TCP connections. Note each TCP connection needs 5 underlying ARQ connections established for it. As indicated in Table 5-4, each ARQ transmit entity polls every 20 MPDUs.

It can be concluded that MDCF effectively handles highly loaded situations, hidden and exposed MPs, since the level of throughput degradation caused by any of those can be expected to be very large in this scenario. From t = 50 second, the gradual termination of

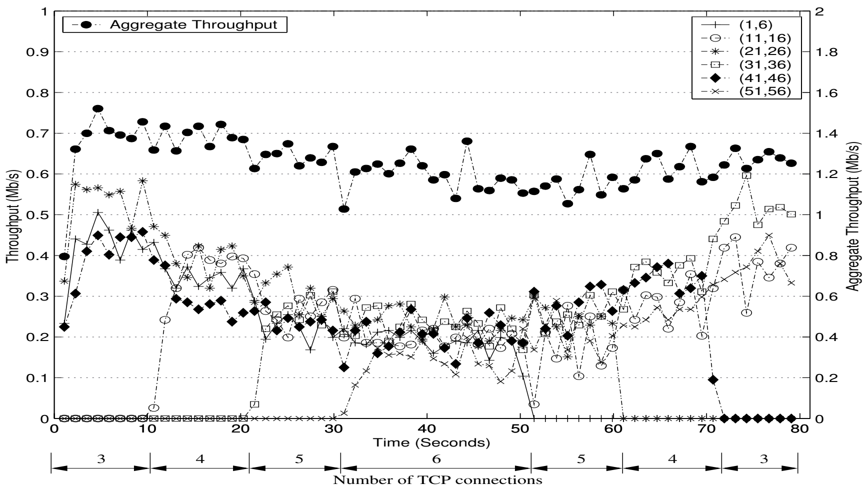

a) Throughput trace in the MDCF network.

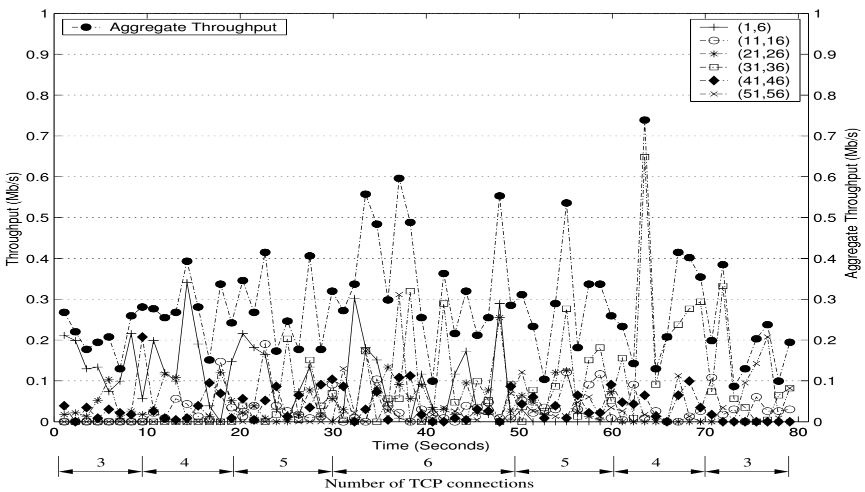

b) Throughput trace in the DCF network.

Figure 5-22. Throughput trace of each TCP connection and aggregate throughput of the grid network. The start and stop times of 6 TCP connections are given in Figure 5-21. The throughput is sampled per 1.2 s. The MPDU size used by DCF is 512 + 34 bytes, whereas the MPDU size used by MDCF is 108 bytes.

connections established in pairs (1, 6), (21, 26) and (41, 46) causes both throughput of remaining connections and aggregate throughput to return to previous levels. Transmission service is very stable during all the periods with some degradation under overload. A notable result is that each active connection achieves almost the same throughput at any time period, underlining that a fair share of the bandwidth is achieved in this heavy loaded multi-hop network.

In comparison, the throughput trace achieved in the DCF network is shown in Figure 5-22b for an MPDU size of 512 bytes. One can hardly find a period where the bandwidth is fairly shared among active connections. The aggregate throughput varies significantly over time and is mostly between 0.2 to 0.55 Mb/s, which is 1/2 to 1/5 of that

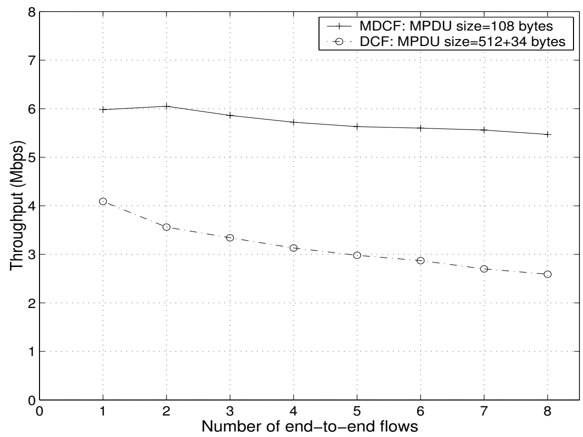

Figure 5-23. Impact of packet multiplexing in mesh environment. CBR traffic is used. The MSDU size is 512 bytes. In each simulation run, each traffic source generates the same amount of CBR traffic and the aggregate traffic load is 6.5 Mbps.

achieved under MDCF control.

5.3.3.3 Packet Multiplexing

MDCF is a channel oriented protocol. In mesh environments, a TCH reserved for any one-hop link is used to multiplex any MPDUs transmitted on the link. This feature is very useful in mesh networks as already stated in Section 3.2.7. This Section studies the benefit of using packet multiplexing in the mesh environment.

The two-hop tree topology shown in Figure 5-9d is used for evaluation. A detailed description of the topology is given in Section 5.3.1. The aggregate two-hop throughput with increased number of end-to-end CBR flows is of interest here. Up to 8 flows are produced: MP 1 generates a CBR traffic flow one-by-one destined to MP 10, 11, 12 and 13, respectively, and each of MP 10, 11, 12 and 13 generates a CBR flow destined to MP 1, respectively. MP 2 works as a relay MP for each end-to-end connection.

The aggregate end-to-end throughput vs. the number of flows is shown in Figure 5-23. When DCF is used, the aggregate throughput is decreased with increased number of flows. This is understandable since the number of MPs wishing to transmit MPDUs is increased with the number of flows. Accordingly, the number of competing MPs is increased as well. This leads to the throughput degradation: the throughput in the DCF network degrades more than 36% when the number of flows increases from 1 to 8 (from 4.1 Mbps to 2.6 Mbps).

In contrast, when MDCF is used, the aggregate throughput degrades very slightly as the number of flows increases: the throughput when the number of flows is 8 (5.47 Mbps) is 8.3% lower than that when only 1 flow exists (6 Mbps). This result is attributed to packet multiplexing on the link between MP 1 and MP 2 that is a necessary path for all the flows. Once some TCHs are reserved for that link, MPDUs of each flow, either from

MP 1 to {10, 11, 12, 13} or from MP {10, 11, 12, 13} to 1, shall be transmitted on these TCHs. MP 1 and 2 do not need to contend for channel access for each flow. Accordingly, the throughput is increased since the contention is significantly reduced. Similarly, packet multiplexing takes place also in one-hop links between MP 2 and 10, MP 2 and 11, MP 2 and 12, and MP 2 and 13.

It is worth noting that in a mesh network, usually a lot of one-hop links exist on which MPDUs destined to different final MPs need to go through. Packet multiplexing exploits this in mesh networks and contributes a lot to improve the QoS and capacity of MDCF multi-hop networks. The simulation evaluation of an indoor ESS mesh network created by using MDCF presented in Section 5.4 will also confirm this.

5.3.4 QoS Performance in Single-hop Networks with Background Traffic

Implementation of QoS in a wireless network requires that high QoS-level traffic is served with higher priority than low priority traffic. This is much more difficult to achieve in networks with decentral control than in networks with central control. 802.11 EDCA attempts to do that by prioritizing the channel access according to the QoS-level of pending MPDUs at a station. Each station wishing to transmit contends in the radio channel without considering the congestion situation in its area at a time. Accordingly, the PLR of real-time traffic sometimes can hardly be guaranteed even though the packet delay is very small as is shown in Section 5.3.4.1. To support QoS in a distributed manner, MDCF prioritizes the channel access like EDCA. Besides that, an MDCF station intending to transmit takes the available channel resources into account by observing the TCH utilization before contending for TCHs. If necessary, a station may apply forced release of some of its reserved TCHs (see Section 3.3.4.4).

This Section studies how MDCF performs under distributed control to support QoS. The single-hop network introduced in Section 5.3.1 is used for evaluation. The results are compared to that when using EDCA. Two issues are of concern: 1) How does a network perform when there exist flows of different types; 2) How many real-time traffic flows can be supported simultaneously in a single-hop network? To address these, two studies are performed: at first, given 1 TCP flow pre-exists in a network, the impact of the number of concurrent video flows on the network performance is investigated; then, given 1 TCP flow and several video flows pre-exist in a network, the impact of the number of concurrent voice flows is examined. Metrics of the network performance includes throughput, delay and PLR.

5.3.4.1 Impact of Number of Concurrent Video flows

TCP is a widely used application in the IP world. It is a best effort traffic and able to adapt its traffic load according to the network condition [92]. It is of interest to see how MDCF is able to support QoS when such traffic exists as background traffic.

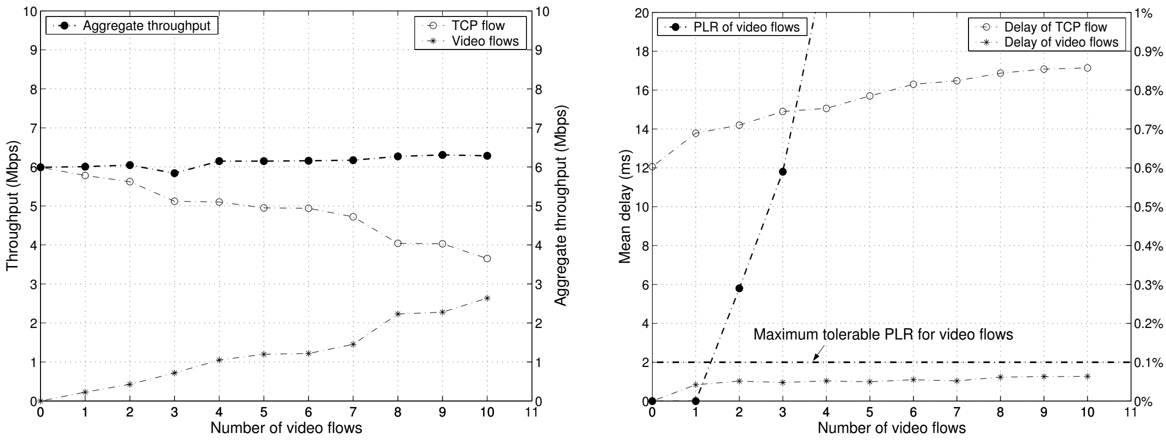

a) b)

Figure 5-24. QoS performance of single-hop EDCA networks when 1 TCP flow pre-exists: a) throughput vs. the number of concurrent video flows; b) delay and PLR vs. the number of concurrent video flows. Please note that the PHY data rate is 24 Mbps.

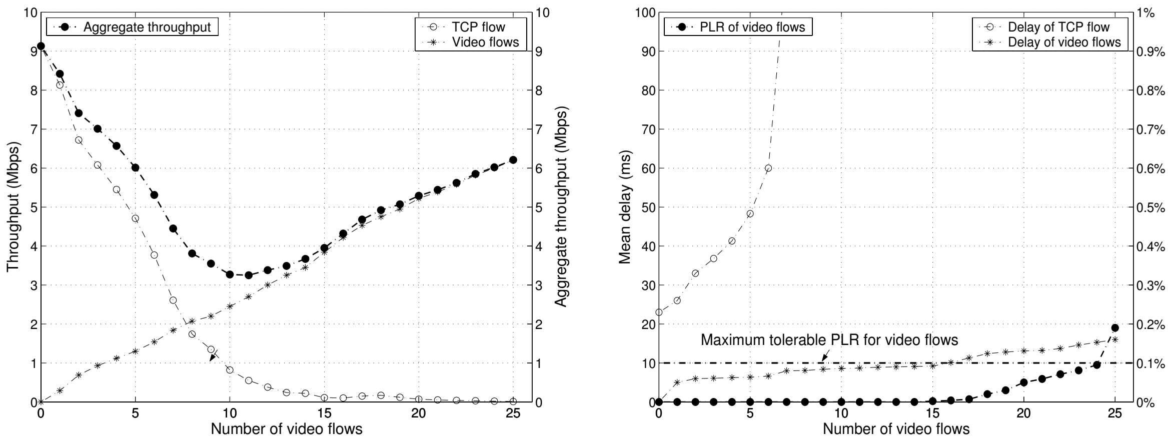

a) b)

Figure 5-25. QoS performance of single-hop MDCF networks when 1 TCP flow pre-exists: a) throughput vs. the number of concurrent video flows; b) delay and PLR vs. the number of concurrent video flows. Please note that the PHY data rate is 24 Mbps.

- Evaluation scenario – After a TCP connection is established between a station and the AP of the single-hop network, a number of long-lived video conference flows are initiated. Each video flow is between the AP and a different station.

Figure 5-24 presents the QoS performance of the EDCA network. As indicated in Figure 5-24a, an increase of the number of concurrent video flows in the EDCA network causes TCP throughput to decline gradually, but the aggregate throughput is increased. Figure 5-24b shows that the delay of the TCP flow increases with the number of concurrent video flows, whilst the mean delay of video flows is below 2 ms even when the number of concurrent video flows is 10. Obviously, EDCA performs well in achieving a high possible network throughput and ensuring a low packet delay for video traffic. However, it can be found from Figure 5-24b that the PLR of video flows increases sharply with the number of concurrent video flows. When there are 2 video flows active, the PLR of video flows is around 0.3%. As suggested in Table 2-1, QoS cannot be guaranteed under this condition. The reason for this is that the TCP source station does not consider the congestion situation that it may cause, and then refrain to contend in the channel. This causes much collisions when contending for channel access so that video MPDUs are dropped at the sender when failing to transmit an MPDU after 7 attempts. *In summary, given 1 TCP flow exists, a single-hop EDCA network is able to support only 1 video flow when the PHY data rate is 24 Mbps.*

The throughput performance of the MDCF network is shown in Figure 5-25a. Different from the trend shown in the EDCA network, the throughput of the TCP flow in the MDCF network reduces significantly with the number of video flows. When the number of video flows is 10, the throughput of TCP flow is less than 1 Mbps, 9 times lower than without any video flow. The aggregate throughput first declines substantially then ascends with the increase of the number of video flows. As described in Section 3.3.4.4, an MDCF station shall apply forced release to it's reserved TCHs that are transmitting non-real-time MPDUs when it observes that the TCH load in a TDMA frame approaches saturation. It will not contend to reserve TCHs for best effort traffic unless the number of free TCHs in a TDMA frame is sufficiently high again. This implies that only real-time MPDUs are considered for transmission when free TCHs in a TDMA frame become rare. Accordingly, the TCP throughput degrades substantially with increased number of video flows. The aggregate throughput declines as well with the number of video flows when the number is small. This is because some of the TCHs in a TDMA frame are left free for being used by forthcoming real-time traffic. When the number of video flows is over 10 (equivalent mean load: 2.56 Mbps, see Table 2-1), the aggregate throughput increases with the number of video flows.

Figure 5-25b shows the delay and PLR performance of the MDCF network. The delay of the TCP flow increases sharply with increased number of video flows, while that of video flows increases slightly only. Clearly, MDCF does well in ensuring that video MPDU being transmitted with priority: the mean delay of 25 concurrent video flows is 20 ms, well below the QoS delay requirement. More important, the PLR performance of video flows is very good: the PLR is 0.09% when the number of video flows is 24. This is attributed to two issues: 1) an effective fair eliminative channel access mechanism; 2) guarantee by the RRC algorithms that only real-time MPDUs are considered for transmission when an MDCF network is highly loaded. *In summary, given 1 TCP flow exists, a single-hop MDCF network is able to support up to 24 video flows when the PHY data rate is 24 Mbps.*

5.3.4.2 Impact of Number of Concurrent Voice Flows

Voice traffic is characterized by low traffic volume and the most restrictive QoS delay

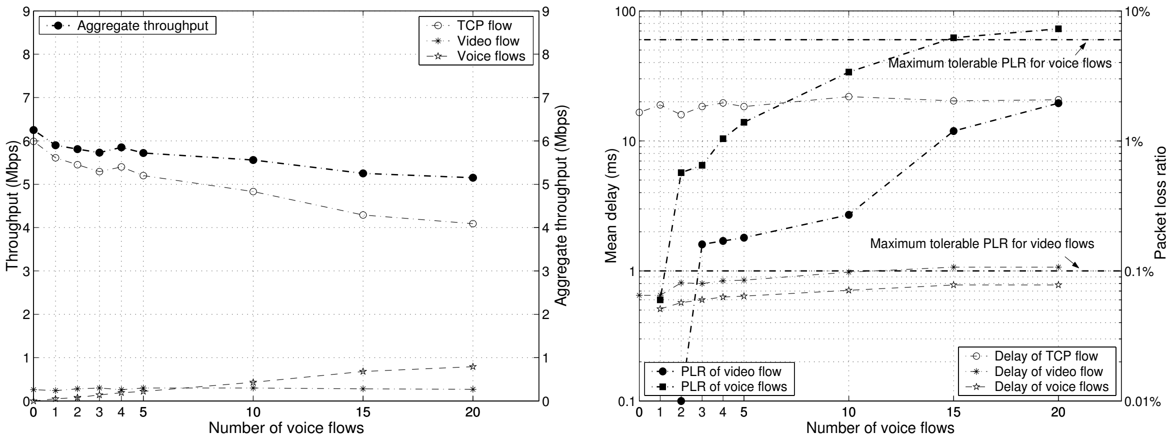

a) b)

Figure 5-26. QoS performance of single-hop EDCA networks when 1 TCP flow and 1 video flows pre-exist: a) throughput vs. the number of video flows; b) delay and PLR vs. the number of voice flows.

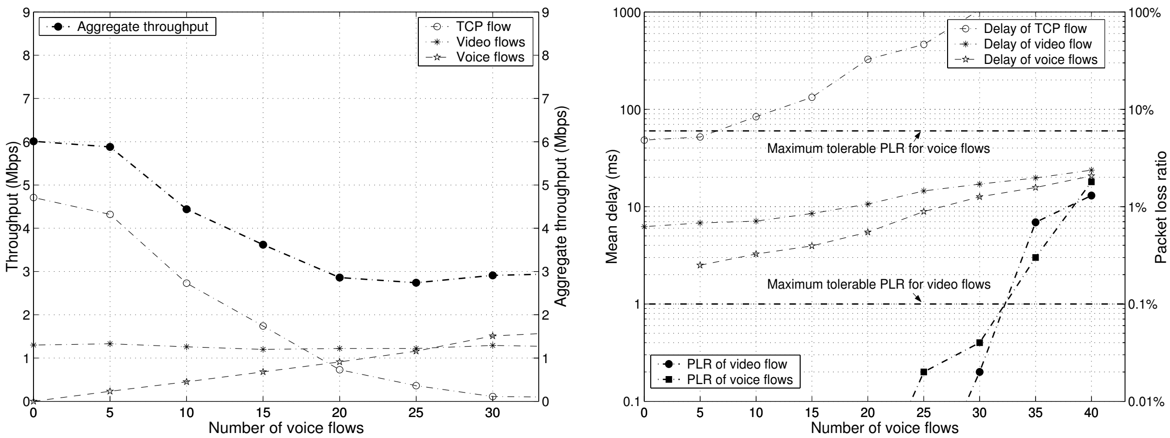

a) b)

Figure 5-27. QoS performance of single-hop MDCF networks when 1 TCP flow and 5 video flows pre-exist: a) throughput vs. the number of video flows; b) delay and PLR vs. the number of voice flows.

requirement (< 60 ms, see Table 2-1). Owing to this, voice traffic is assigned the highest channel access priority among all supported traffic classes, both in EDCA and MDCF. This Section investigates the impact of the number of concurrent voice flows given 1 TCP flow and several video flows pre-exist as background traffic.

- Evaluation scenario – After a TCP connection is established and one or several long-lived video conference flows are initiated, a number of long-lived voice flows are launched. Each flow or stream is between the AP of the single-hop network and a different station.

Figure 5-26 shows the QoS performance of the EDCA network given 1 TCP flow and 1 video flow pre-exist. When the number of voice flows increases in the EDCA network, the throughput of the video flow stays the same, while the throughput of the TCP flow

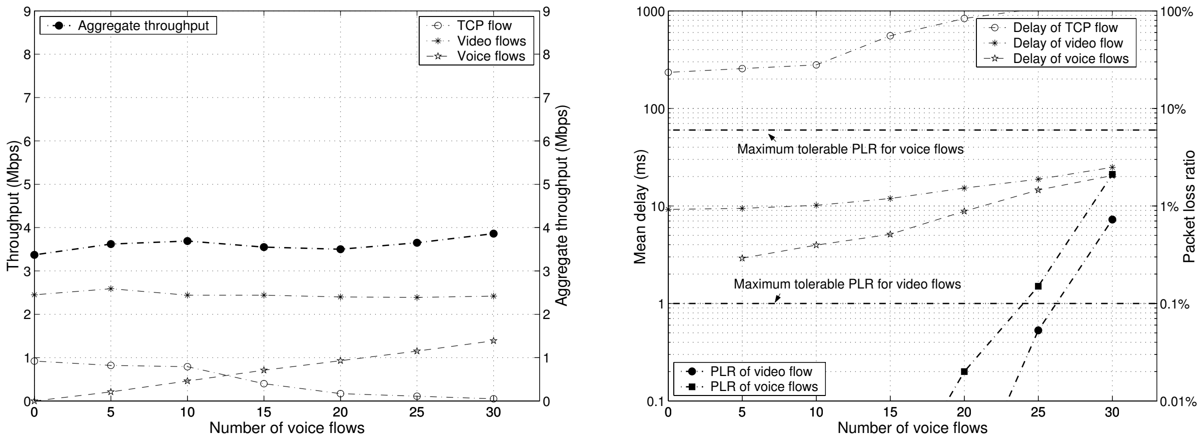

a) b)

Figure 5-28. QoS performance of single-hop MDCF networks when 1 TCP flow and 10 video flows pre-exist: a) throughput vs. the number of video flows; b) delay and PLR vs. the number of voice flows.

and aggregate throughput degrade gradually. The mean TCP delay, video delay and voice delay are very in-sensitive to an increased number of voice flows as shown in Figure 5-26b. The mean TCP delay is around 20 ms, whilst the mean video and voice delay is below 1 ms, well under the QoS requirements. However, EDCA performs badly in controlling the PLRs of the video flow and the voice flows when the number of voice flows increases: when the number is 2, the PLR of the video flow is higher than 0.1%, (the maximum tolerable value to guarantee QoS of video traffic, see Table 2-1); when the number is 15, the PLR of voice flows is 6% (the maximum tolerable value to guarantee QoS of voice traffic, see Table 2-1). The reason for this is the same as explained earlier. *In summary, a single-hop EDCA network is able to support 1 TCP flow, 1 video flow and 2 voice flows simultaneously or 1 TCP flow and 15 voice flows simultaneously when the PHY data rate is 24 Mbps.*

Figure 5-27 presents the QoS performance of the MDCF network given 1 TCP flow and 5 video flows pre-exist. When the number of voice flows increases, the video throughput stays the same, whilst the TCP throughput declines sharply. When there are 30 voice flows in the MDCF network, the TCP throughput is close to 0 and the aggregate throughput is around 3 Mbps. It is indicated by Figure 5-27b that the mean delay of video flows and voice flows increases with the number of voice flows. However even when 40 voice flows exist in the MDCF network, the mean video and voice delays are around 25 ms and 20 ms, respectively, both well under the QoS delay requirement. The capability of the MDCF network to control PLRs of real-time traffic is well demonstrated: when the number of voice flows is 32, the PLR of video flows is approaching its maximum tolerable value (0.1%), and the PLR of voice flows is below its maximum tolerable value (6%,). Even when the number of voice flows is 40, the PLR of voice flows is still below 6%.

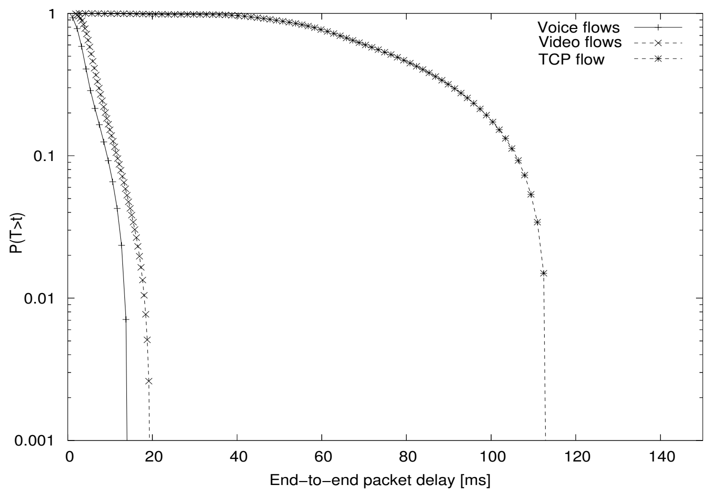

Figure 5-29. Complementary CDF of packet delay for concurrent traffic in a single hop MDCF network: 1 TCP flow, 5 video flows and 10 voice flows are running in parallel.

Figure 5-28 presents the QoS performance of the MDCF network given 1 TCP flow and 10 video flows pre-exist. Once again the figure shows that the MDCF is able to support a large number of real-time traffic with existing TCP background traffic. *In summary, a single-hop MDCF network is able to support 1 TCP flow, 5 video flows and 30 voice flows simultaneously or 1 TCP flow and 10 video flows and 23 voice flows simultaneously when the PHY data rate is 24 Mbps.*

Figure 5-29 shows the complementary Complementary Distribution Function (CDF) of packet delay in a single hop MDCF network when 1 TCP flow, 5 video flows and 10 voice flows are running in parallel. The figure clearly shows that all the video and voice packets are delivered within 20 ms. In contrast, TCP packets are highly delayed: the delays of more than 20% packets are above 100 ms.

From the presented simulation results, it is clear to see that MDCF significantly outperforms EDCA in providing QoS support in distributed networks. In the following Section, the QoS performance of MDCF-based ESS mesh networks will be presented.

5.4 Performance of MDCF based ESS Mesh Networks

Previous evaluations have shown that MDCF is able to perform efficiently in multi-hop environments and support QoS well in single-hop networks under distributed control. As stated throughout the thesis, MDCF is well suited for mesh networks supporting QoS. Hence the real interest of the evaluation work lies in: how is the QoS performance and capacity of mesh networks created by using MDCF? This section examines this issue in two example ESS mesh networks: one open space ESS mesh network and one indoor ESS mesh network.

5.4.1 Open Space Scenario

The grid topology shown in Figure 5-9c is used for evaluation where MPs in a row (or column) are 100 m apart. Each MP in the figure is assumed an AP of a BSS. MPs are using same transmit power: 120 mW for MPDUs and BESs; 200 mW for AESs. It can be calculated that the transmission range of MPDUs is 150 m whereas the carrier sense ranges of MPDUs, BESs and AESs are about 330, 330 and 400 m, respectively.

MPs form a multi-hop network on a frequency channel whilst BSSs are assumed to operate on other frequency channels. MP 24 is assumed to be the only MP with Internet access. This scenario is a typical ESS mesh network. All communications in this scenario are from a station in a BSS to its close by MP and from there to an Internet terminal. Hence, transmissions in the ESS network are between MP 24 and a station in a BSS. MPs perform multi-hop relaying to or from MP 24, which is the bottleneck MP. MPDUs from the farthest MP need 3 hops to reach MP 24. We evaluate the network performance in delivering QoS traffic assuming that each BSS is lightly loaded. The packet delay from a station to its AP (less than 1 ms in a lightly loaded BSS) and packet delay from MP24 to an Internet terminal are neglected. Hops in Figure 5-30 and Figure 5-31 are counted from source/destination MP to/from MP 24. Note that another hop is in fact needed to connect a station in a BSS to its serving MP

5.4.1.1 Supported Number of Homogenous Real-time Flows in Parallel

The first study of interest is to investigate the number of real-time traffic flows that can be served in parallel for a given traffic type and given number of hops. The results obtained by using MDCF and EDCA, to form a multi-hop mesh network are compared.

- Evaluation scenario –A number of homogenous real-time flows spanning a given number of hops are initiated in parallel in a simulation run.

According to Figure 5-30a, MDCF is able to support 120 × 1-hop, 45 × 2-hop, and 18 × 3-hop concurrent voice flows with PLR $\leq$ 6%. The delay performance is shown in Figure 5-30b. Under EDCA, end-to-end delay is much lower than with MDCF. Transmission of a voice packet in a 1-hop EDCA network needs less than 0.4 ms under light load, where an MP can seize the channel and finish its transmission much faster than with MDCF. However, with an increased traffic load, the performance of the EDCA based ESS mesh network deteriorates sharply, see Figure 5-30a, it is able to support 30 × 1-hop, 14 × 2-hop and 5 × 3-hop concurrent voice flows with PLR $\leq$ 6%. An EDCA MP drops a packet when it fails to retransmit the same packet more than 7 times. A relative small contention window (CW) results in considerable collision. Increasing the retry time does not help to reduce the PLR but just increases the delay. EDCA cannot perform well in a highly loaded network. The only way to reduce the PLR is to increase the CW size for voice packets, which however leads to longer delay and a low efficiency for delivering video and background traffic, because CW sizes for those traffic classes should be increased accordingly. In contrast, MDCF can support much more concurrent

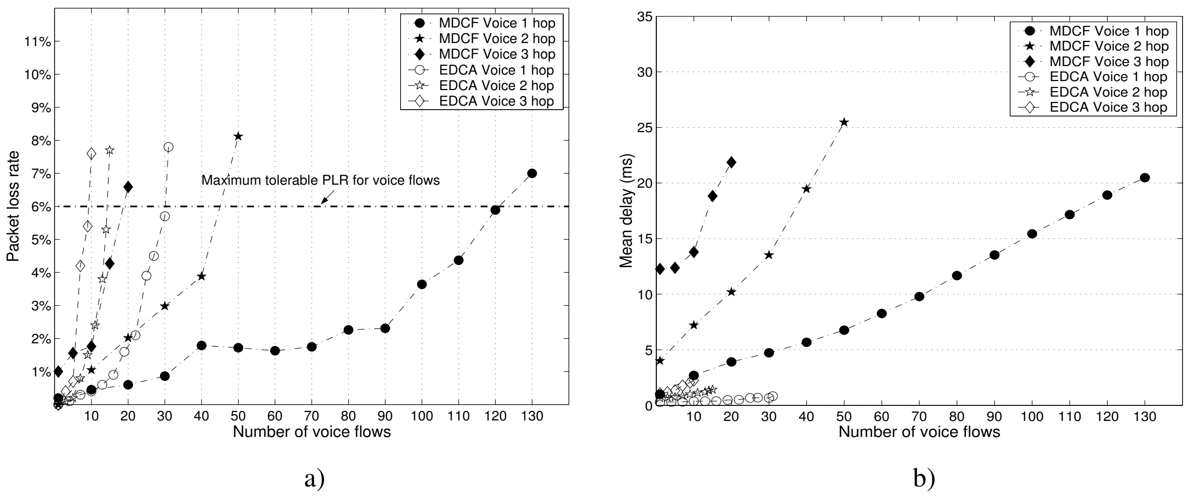

Figure 5-30. QoS performance of the open space ESS mesh network when delivering voice traffic: a) PLR vs. the number of voice flows; b) mean end-to-end delay vs. the number of voice flows.

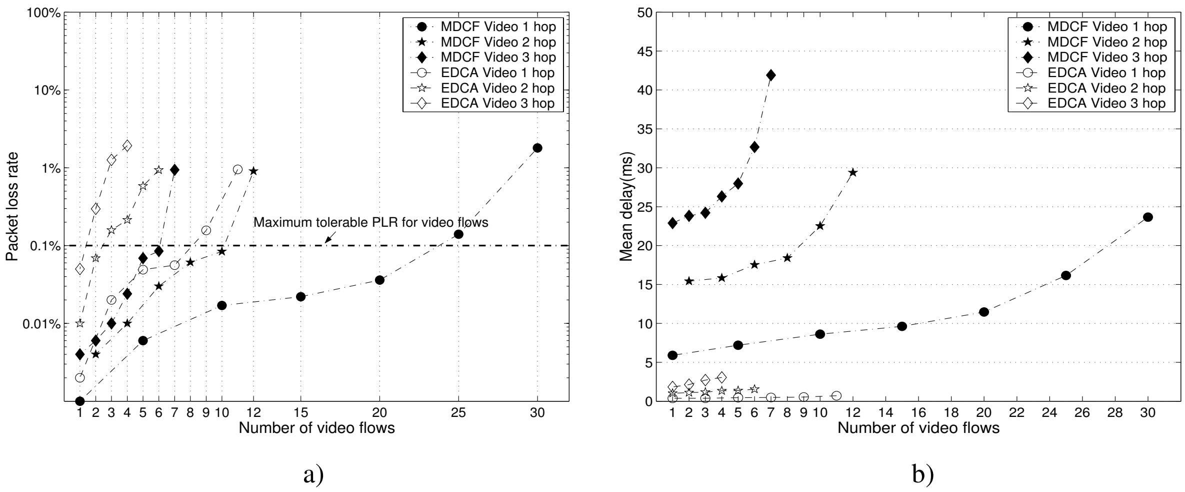

Figure 5-31. QoS performance of the open space ESS mesh network when delivering video traffic: a) PLR vs. the number of video flows; b) mean end-to-end delay vs. the number of video flows.

voice flows than EDCA with a higher delay that is well below the delay requirement.

A video conference source generates highly bursty traffic. Given that the tolerable PLR is 0.1%, the supported number of concurrent 1, 2 and 3 hop video flows in the ESS mesh network when using MDCF are 24, 10 and 6, respectively, see Figure 5-31a. In contrast, the ESS mesh network when using EDCA, only can support 8 × 1-hop, 2 × 2-hop and 1 × 3-hop concurrent video flows, respectively, 1/3, 1/5 and 1/6 of that under MDCF. A video flow offers a much higher traffic load than a voice flow does, resulting in a more serious contention. Though the packet delay is very small with EDCA, the PLR is quite high. EDCA cannot make a trade-off between the low delay and high PLR.

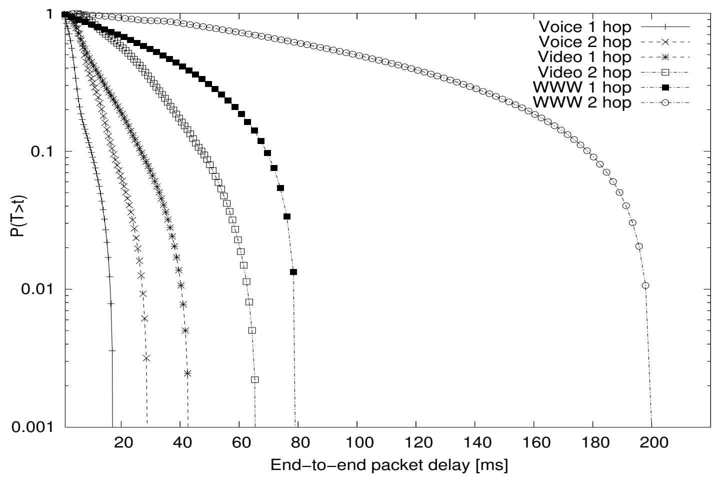

Figure 5-32. Complementary CDF of end-to-end delay for concurrent traffic groups in the open space ESS mesh network (grid topology). Seven 1-hop voice, seven 2-hop voice, three 1-hop video, three 2-hop video, fourteen 1-hop WWW and fourteen 2-hop WWW services are running in parallel.

5.4.1.2 Capability of Handling Mixed Traffic Services in Mesh

The second study is to show the QoS performance of the ESS mesh network when using MDCF to handle mixed traffic services in the network. Since EDCA cannot support even 3 concurrent 2-hop video flows, see Figure 5-31ac, no comparison is possible here.

- Evaluation scenario – 7 × 1-hop voice, 7 × 2-hop voice, 3 × 1-hop video, 3 × 2-hop video, 14 × 1-hop WWW and 14 ×2-hop WWW flows are served in parallel.

The traffic flows are assumed in 6 groups. Flows generated from a given traffic type spanning a given number of hops constitute a group. Figure 5-32 shows the Complementary CDF of end-to-end delay for each group. For a given number of hops, voice and video flows achieve the lowest and second lowest delay. For a given traffic type, the delay of 1-hop transmission is almost half that of 2 hop transmissions. It can be concluded that the ESS mesh network is able to serve 48 mixed end-to-end traffic flows in parallel, meeting the particular QoS requirements. The QoS support of MDCF works efficiently in an ESS mesh network.

5.4.2 Indoor Office Scenario

An indoor office ESS mesh network shown in Figure 5-3 is used for evaluation. Please see the caption of Figure 5-3 and Section 5.2.1 for a detailed network description. Important simulation settings like the transmission powers, carrier sense threshold and PHY mode are described in Table 5-4. From those parameters, the transmission and carrier sense ranges can be computed and are listed in Table 5-6. The PHY data rate is 24 Mbps.

Each MP appearing in Figure 5-3 is also an AP of a BSS. MPs forming a multi-hop

Table 5-6. Transmission and carrier sense ranges in the indoor ESS mesh network.

	In free space	Across one wall	Across two walls
Transmission range of MPDUs	> 60 m	36 m	7 m
Carrier sense range of MPDUs & BESs	> 60 m	> 60 m	18 m
Carrier sense range of AESs	> 60 m	> 60 m	24 m

Table 5-5. Mesh Routes in the indoor ESS mesh network.

Source MP	Next-hop MP	Destination MP	Number of hops
1	2	3	2
2	3	3	1
4	3	3	1
5	1	3	3
5, 6, 7,	8	3	3
8, 9, 12	4	3	2
10, 11	1	3	3

network operate on a frequency channel whilst BSSs operate on other frequency channels. MP 3 is the only MP with Internet access. All communication in this simulation study is from a station in a BSS to an Internet terminal. Hence, transmissions in the ESS network are between a station in a BSS and MP 3. MPs perform multi-hop relaying to or from MP 3. MPDUs from the farthest MP need 3 hops to reach MP 3. The mesh routes are described in Table 5-5. Obviously, the volume of traffic exchanged in the one-hop links MP 3 - 4, MP 3 - 2, MP 8 - 4 and MP 1 - 2 are much higher than those in other links since these are carrying multiplexed packets coming from farther away MPs, like MP 9, 12 or 1, 6, 5, 10, 11. When the network is highly loaded, those one-hop links tend to become highly loaded and MP 3 is the bottleneck then.

Each BSS is assumed lightly loaded. Therefore, the packet delay from a station to its AP (less than 1 ms in a lightly loaded BSS) and packet delay from MP 3 to an Internet terminal are being neglected. The hops appearing in the following figures are counted from any MP to MP 3.

The investigation is intended to reveal the QoS capacity of MDCF-based ESS mesh networks working in an indoor office environment. To do so, it is first assumed that each MP in the network serves a voice connection with a terminal in the Internet. Based on that, the impact of the number of concurrent video flows spanning a given number of hops is studied. Further, the impact of the number of concurrent WWW flows spanning a given number of hops is examined given that the above mentioned voice flows and

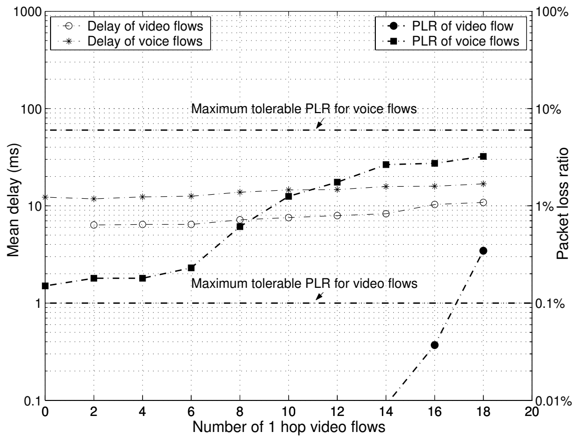

a)

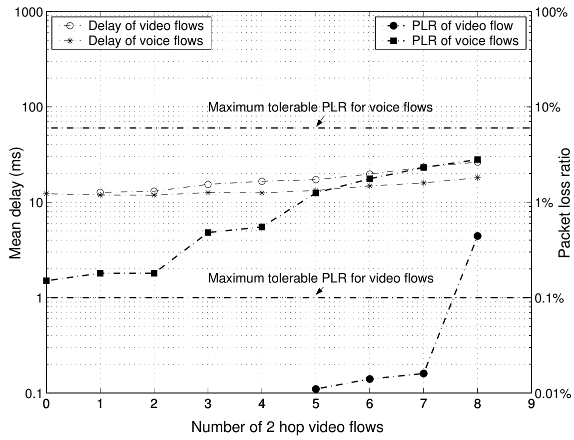

b)

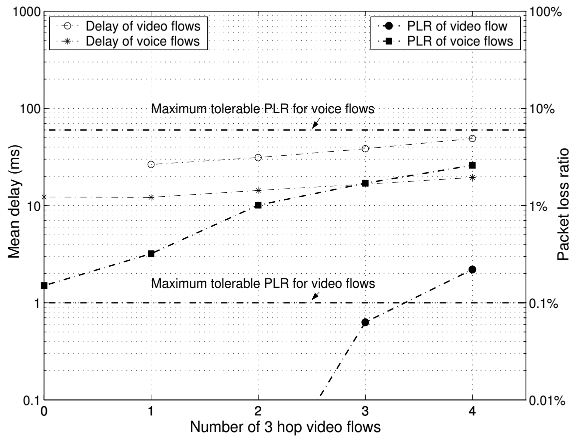

c)

Figure 5-33. Impact of the number of given-hop video flows when 2 × 1-hop, 4 × 2-hop and 5 × 3-hop voice flows exist: a) 1 hop video flows; b) 2 hop video flows; c) 3 hop video flows.

some video flows exist. Delay of different types of traffic spanning different number of hops when the network is highly loaded is investigated, too. Note that since EDCA cannot support even 3 concurrent 2-hop video flows in a grid network, see Figure 5-31a, no comparison is made here.

5.4.2.1 Impact of the Number of Concurrent Video flows

- Evaluation scenario of Figure 5-3 – Each MP in the network has a voice connection with a terminal in the Internet. This means that between MP 3 and each of the other MPs, there exists a voice flow. Hence, in the evaluation 2 × 1-hop, 4 × 2-hop and 5 × 3-hop voice flows exist. Further, a number of video conference flows spanning a given number of hops are operated in parallel. All flows are assumed long-lived.

Figure 5-33a, b and c show the impact of the number of concurrent 1, 2 and 3 hop video flows, respectively, on both the mean end-to-end delay and PLR. With 1-hop video flows only, all video MPDUs in the MDCF multi-hop network are transferred between either MP 3 - 4 or MP 2 -3. As indicated in Figure 5-33a, both the mean voice and video packet delays increase slightly with the number of 1-hop video flows. When the number is 18, the mean voice and video packet delays are 16 ms and 10 ms, respectively, both well under the respective QoS delay requirements as described in Table 2-1. Under a given number of 1-hop video flows, the video packet delay is even lower than the voice packet delay. The reason for this is that the mean voice packet delay is an average of 1, 2 and 3 hop end-to-end delays, whilst the mean video packet delay is only 1-hop delay. Moreover, owing to the packet multiplexing feature of MDCF, video packets of a flow can be transmitted on TCHs reserved by other flows like a voice flow or a video flow. As suggested in Table 5-5, all flows need to go through either the link MP 2 - 3 or the link MP 3 - 4. Hence, the increase of the number of 1-hop video flows does not result in an increase of ACH contention. Instead, the utilization of reserved TCHs is greatly improved. This leads to that both, voice and video packets experience low packet delay as shown in the figure.

The PLR of voice flows increases with the number of 1-hop video flows as indicated in Figure 5-33a. When 18 ×1-hop video flows exist, the PLR of voice flows is 3%, still lower than the tolerable value (6%) for voice traffic. The PLR of 1-hop video flows is lower than 0.01% when the number of 1-hop video flows is smaller than 14, while the PLR is rapidly increased to 0.03% and 0.3% when the numbers of 1-hop video flows are 16 and 18, respectively. It can be calculated using the information given in Table 2-1 that 16 1-hop video flows aggregated generate a mean rate of 4.09 Mbps and a peak rate of 20.48 Mbps. Obviously, the one-hop links MP 2-3 and MP 3-4 are highly loaded especially when some video flows happen to be at their peak rate at the same time. It is therefore understandable that PLRs for voice and video flows under the situation reach the values described before. *In summary, the example indoor ESS mesh network is able to support 2 × 1-hop voice, 4 × 2-hop voice, 5 × 3-hop voice and 16 × 1-hop video flows in parallel.*

As shown in Figure 5-33b, when 2-hop video flows are used, both the voice and video packet delays increase relatively quickly with the number of video flows: When the number is 7, the mean voice and video packet delays are 18 and 23 ms, respectively, 8 and 13 ms higher than the respective value when the number is 1. Under a given number of 2-hop video flows, the mean video packet delay is higher than the mean voice packet delay since the video packet delay is now 2 hop end-to-end delay. The voice PLR increase more rapidly with 2-hop video flows compared to 1-hop video flows: When the number of 2-hop video flows is 7, the voice PLR is 2.3%, 8 times higher than with 1-hop video flows. Similarly, the video PLR starts to be larger than 0.01% when the number of 2-hop video flows is 5, and exceeds the tolerable value 0.1% when the number is 8. Since video traffic is highly bursty, when a video flow works on its peak rate, 2-hop leads to the twice the network traffic volume. Obviously, the probability of 1 video flow to be on the peak rate is much higher than the chance of 2 one-hop video flows to be on

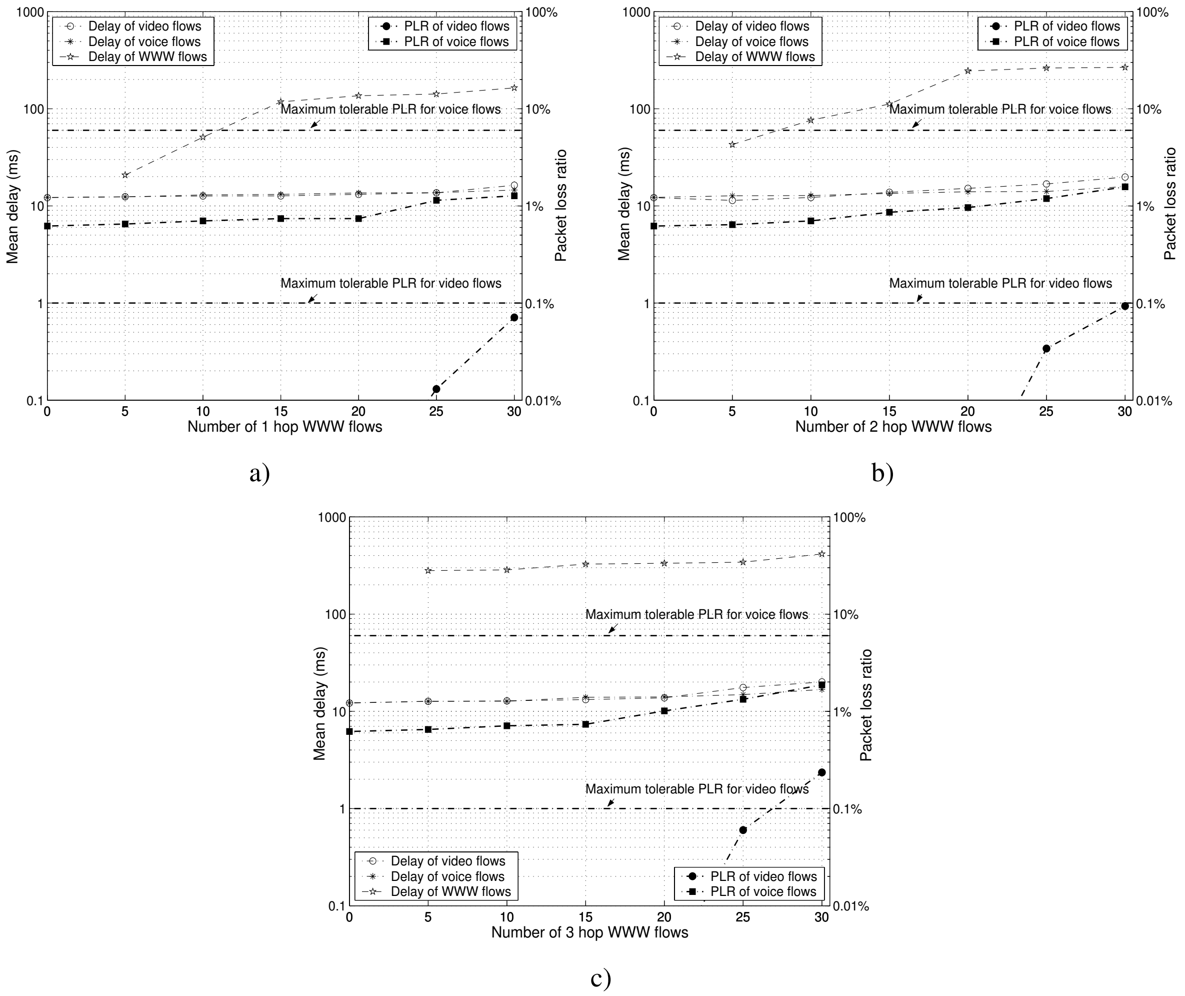

Figure 5-34. Impact of the number of given-hop WWW flows when 2 × 1-hop, 4 × 2-hop, 5 × 3-hop voice, 3 × 1-hop video, 3 × 2-hop video flows exist: a) 1 hop WWW flows; b) 2 hop WWW flows; c) 3 hop WWW flows.

the peak rate at the same time. Accordingly, 1 × 2-hop video flow is prone to generate a higher traffic load than 2 × 1-hop video flows. As a result, the supported number of concurrent 2-hop video flows is less than half the number when using 1-hop video flows. *In summary, the example indoor ESS mesh network is able to support 2 × 1-hop voice, 4 × 2-hop voice, 5 × 3-hop voice and 7 × 2-hop video flows in parallel.*

As analyzed in the last paragraph, the more hops video flows span, the smaller is the number of concurrent video flows that can be supported in mesh. This is proven for 3-hop video flows as shown in Figure 5-33c: *given that 2 × 1-hop voice, 4 × 2-hop voice, 5 × 3-hop voice flows exist, only 3 × 3-hop video flows can be supported in the indoor ESS mesh network.* Apparently, it is unreasonable to have multi-hop relayed video traffic in a mesh network, since the network is overwhelmed by video traffic then, even when the number of such video flows is small.

5.4.2.2 Impact of the Number of WWW Flows Concurrent to Voice and Video Traffic

- Evaluation scenario of Figure 5-3 – 2 × 1-hop voice, 4 × 2-hop voice and 5 × 3-hop voice, 3 × 1-hop video and 3 × 2-hop video conference flows, and a number of WWW flows spanning a given number of hops are launched together. Note all flows (or streams) are assumed long-lived.

The results when using 1-hop, 2-hop and 3-hop WWW flows are shown in Figure 5-34a, b and c, respectively. It can be seen that the delay and PLR performance of both voice flows and video flows, are almost the same when using 1-hop, 2-hop and 3-hop WWW flows. In contrast to this, the main difference between the graphs is the mean WWW packet delay: The more hop WWW traffic spans, the higher the WWW packet delay is.

In each figure, the mean voice and video packet delay is almost the same and increases very slightly with the number of WWW flows. The same trend applies to the voice and video PLR. When the number of WWW flows is 30, the voice and video packet delay is around 20 ms, and the voice PLR is about 1.5%, well under the QoS requirement. However, if the number of WWW flows is 30, the video PLRs are 0.07%, 0.09% and 0.23%, respectively, when 1-hop, 2-hop and 3-hop WWW flows are used. The last PLR exceeds the tolerable PLR value for video streaming. Apparently, the impact of the number of WWW flows on the delay and PLR performances of real-time traffic is very small.

The reasons for these results are as follows: As background traffic, WWW traffic is allowed to transmit only when the number of free TCHs in TDMA frame is sufficiently high. Since the real-time traffic is served with priority, when a network is highly loaded, only real-time traffic will be transmitted (see Section 3.3.4.4). Accordingly, the impact of the load of WWW traffic on the performance of real-time traffic is small.

5.4.2.3 Delay Performance under a Highly Loaded Mesh

- Evaluation scenario of Figure 5-3 – 2 × 1-hop voice, 4 × 2-hop voice and 5 × 3-hop voice, 3 × 1-hop video, 3 × 2-hop video flows, 10 × 1-hop WWW, 10 × 2-hop WWW and 10 × 3-hop WWW flows are initiated in parallel. Note all flows (streams) are assumed long-lived.

This study serves to reveal the delay performance for a highly loaded network. The traffic flows are assumed in 8 groups. Flows generated from a given traffic type spanning a given number of hops constitute a group. The Complementary CDF of end-to-end delay for each group is presented in Figure 5-35. As indicated in the figure, for a given type of traffic flows, the less the number of hops that flows spanning, the smaller the packet delay is. For a given number of hops, the packet delay of voice flows is smaller than that of video flows, which is in turn smaller than that of WWW flows. More than 99.999% voice and video packets, after spanning 3-hop experience a delay below 60 ms, well under the QoS delay requirement. It is worth noting that the 1-hop WWW packet

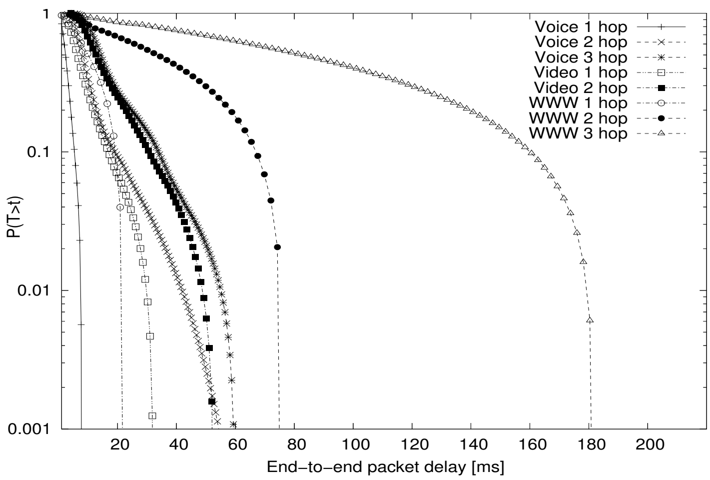

Figure 5-35. Complementary CDF of end-to-end delay for concurrent traffic groups in the indoor ESS mesh network. Two 1-hop voice, four 2-hop voice, five 3-hop voice, three 1-hop video, three 2-hop video, ten 1-hop WWW, ten 2-hop WWW and ten 3-hop WWW services are running in parallel.

delay in the indoor ESS mesh network is smaller than the 2-hop video packet delay, which is smaller than the 3-hop voice packet delay. This is totally different from the results achieved in the open space ESS mesh network, Figure 5-32, where the 1-hop WWW packet delay is larger than the 2-hop video packet delay, and the 2-hop voice packet delay is smaller than the 1-hop video packet delay. The reason for this is: In the indoor ESS mesh network the few links connecting to MP 3 permanently exist, to which different types of traffic flows are multiplexed (see Section 3.2.7), reducing access day for WWW packets. On the contrary, in the open space scenario network the links to MP 24 are much lower loaded each, since they are larger in number and therefore are more frequently being released, leading to larger access delay for low priority traffic.

It can be concluded that the indoor ESS mesh network is able to serve 57 mixed end-to-end traffic flows in parallel, meeting the particular QoS requirements. Moreover the delay performance in the indoor ESS mesh network for a given traffic spanning a given number of hops is better than that in the open space ESS mesh network. Besides the reason pointed out before, high spatial reuse is achieved in the indoor scenario owing to the existence of walls, which is not the case in the open space scenario.

CHAPTER 6

Conclusions and Outlook

WMNs are experiencing rapid development and are expected to become a key technology for the next generation wireless networks. Design of the MAC protocol able to operate efficiently and support QoS in the mesh environment is a real challenge. Based on study results for W-CHAMB networks from previous work, this thesis proposes MDCF, a MAC protocol that can be used to construct efficient WMNs with QoS guarantee in a fully distributed manner.

MDCF is based on TDMA/TDD technology, to operate under distributed control. A distributed synchronization algorithm, MTSF, is proposed and proven able to synchronize mesh points for TDMA operation in the mesh environment. MDCF is able to run on a single frequency channel independent of the radio modem. For instance, the PHY for MDCF can be the IEEE 802.11 a /b /g. MDCF is well designed to properly handle high load situations, hidden and exposed stations, and capture in mesh. For QoS support, besides a prioritized and fair channel access mechanism, a distributed RRC protocol is used to evaluate and allocate a fair portion of bandwidth to a specific traffic flow. The assigned portion of bandwidth for a flow adapts with the traffic load. As a result, MDCF is capable of efficiently exploiting channel capacity, fairly allocating bandwidth and supporting multi-hop relaying of a large number of concurrent real-time services in a mesh network.

The performance of MDCF is extensively evaluated by using both mathematical and simulation approaches. The elimination performance of the channel access protocol is investigated analytically. An analytical model based on the theory of queueing networks is used to study the traffic performance of MDCF in specific mesh scenarios. The accuracy of the model is verified by simulations. Based on the established analytical models, key parameters like the frame length can be well quantified, meeting the requirement of supporting QoS in the mesh environment while exploiting the channel capacity. Simulation is applied for performance evaluation on the more complicated realistic scenarios, assuming the IEEE 802.11a PHY. Simulation studies give evidence to how well MDCF can support multi-hop operation and QoS under fully distributed control. Simulation also reveals that the QoS capability of MDCF in two example ESS mesh networks does perfectly meet the requirements. Simulation results also show the outstanding performance of MDCF working in mesh that significantly outperforms the

802.11 DCF/EDCA.

Currently, major industrial organizations like IEEE 802.11 (WLAN), IEEE 802.16 (WMAN) and IEEE 802.15 (WPAN) are actively working on introducing the multi-hop mesh element to their next generation standards. The MDCF concept proposed in this thesis already considers the requirements of the IEEE 802.11s - Mesh WLAN (see the protocol stack of MDCF in Figure 3-1). The simulation results also prove that an IEEE 802.11 ESS mesh network based on MDCF is able to support multi-hop delivery of a large number of concurrent various traffic flows meeting their QoS requirements. MDCF has been submitted as a MAC proposal for the IEEE 802.11 TGs on July, 2005. It is still a candidate MAC solution for the IEEE 802.11s. It appears promising to adapt the MDCF concept to WMAN and WPAN mesh applications. Besides, wireless sensor networks, aiming at extreme low power consumption and low implementation cost, is another field where MDCF may find mass applications.

TABLE OF SYMBOLS

Symbol	Meaning	Chapter	Page
P_R	Received signal strength at receiver	2	5
P_T	Transmission power	2	5
g_T	Transmission antenna gain	2	5
g_R	Receiving antenna gain	2	5
d	Distance between sender and receiver	2	5
λ	Wavelength	2	5
γ	Attenuation coefficient	2	5
$SINR$	Signal-to-Interference-and-Noise-Ratio	2	6-9
S	Signal power	2	6-9
N	Noise power	2	6-9
I	Interference power	2	6-9
R_t	Transmission range	2	6-9
R_d	Carrier sensing range	2	6-9
R_i	Interference range	2	6-9
$Max(R_t)$	Maximum value of R_t	2	7-9
$Max(R_d)$	Maximum value of R_d	2	7-9
$Max(R_i)$	Maximum value of R_i	2	7-9
D_{th}	Decoding threshold	2	7-9
CS_{th}	Carrier sense threshold	2	7-9
K	$= g_T g_R (\lambda / 4\pi)^2$	2	7
P_T^T	Transmission power at transmission station	2	7-9
P_T^I	Transmission power at interference station	2	7-9
P_r^T	Received signal strength from transission station	2	7-9
P_r^I	Received signal strength from interference station	2	7-9
$SINR_B$	$SINR$ at station B	2	7
d_t	Distance between sending and receiving stations	2	7-9
d_i	Distance between interferencing and receiving stations	2	7-9
F_J	Fairness index	2	11
m	Total number of flows	2	11

Symbol	Meaning	Chapter	Page
γ_i	Proportion of received packets of flow *i* during run	2	11
$TH^{O}{}_{TMT}$	Normalized one-hop theoretical maximum throughput	3	22
N_{TCH}	Number of TCHs in a TDMA frame	3	22, 27
N_{ECH}	Number of ECHs in a TDMA frame	3	22
P_{TDMA}	Time period of a TDMA frame (unit: µs)	3	22-37
P_{Con}	Duration of a contention slot in the ACH	3	22
P_{TP}	Duration of the TP	3	22
P_{ECH}	Duration of an ECH slot	3	22
P_{TCH}	Duration of a TCH slot	3	22
O_{TCH}	Amount of overheads in a TCH slot	3	22
m	Contention slots in the PP of the ACH	3	21-26
n	Contention slots in the FEP of the ACH	3	21-26
K	Number of equal size non-overlapping CNGs	3	25-26
t^i	Variable counting the number of contention lost for the flow *i*	3	25
T^k	CNG Selection threshold	3	25
N	Number of MPs contend at the same time with the same PPCL	3	25-26
$p(N)$	Probability of only one winner in the contention	3	25-26
N'	Number of MPs generating the FEPCL numbers from a same CNG	3	26
$E(D_{acc})$	Mean access delay	3	26
$I_T{}^A$	Interarrval time of APDUs	3	37-38
Len_{APDU}	Length of APDUs in bits	3	37-38
SR_{APDU}	Stream generation rate at the application layer	3	37-38
P_H	Hang-on time in the units of the number of TDMA frames	3	37-38
$I_T{}^M$	Expected interarrival time of MPDUs on a TCH	3	37-38
$Int[\ \bullet\ ]$	Integer of a value	3	38
P_{TDMA}	Period of a TDMA frame	3	45-54
T_{guard}	Guard time in an energy signal and also in a TCH	3	45-54
BT_S	Minimal integer used for calculating a beacon generation period	3	45-54

Symbol	Meaning	Chapter	Page
BT_W	Window size used for calculating a beacon generation period	3	45-54
ST_{Li}^{n}	Start instant of the n[th] TDMA frame at MP i	3	45-54
ST_{Ri}^{n}	Derived start instant of the n[th] TDMA frame of the beacon sending MP, which is derived at the MP i on reception of a beacon without considering the propagation delay and the time skew between the beacon sending and receiving MPs.	3	45-54
ΔST_{RLi}^{n}	Time difference between ST_{Ri}^{n} and ST_{Li}^{n} (i.e. $\Delta ST_{RLi}^{n} = ST_{Ri}^{n} - ST_{Li}^{n}$) calculated at MP i.	3	45-54
T_i^n	Local time when receiving the last bit of a beacon frame at the n[th] TDMA frame at MP i.	3	45-54
D_{pro}	Amount of process delays on the way from sending a beacon to the completion of analyzing a beacon.	3	45-54
ΔX_{ij}	Time skew between the sending MP i and the receiving MP j in a beacon interval.	3	45-54
t_{ij}	Propagation delay between the MP i and j	3	45-54
d_i	Variable used to compensate the physical drift rate of MP I (unit: ppm)	3	45-54
T_{adj}	Time instant until when an MP is allowed to adjust d_i since it is synchronized.	3	45-54
T_{slow}	Time instant from when an MP is only allowed to slowly adjust d_i	3	45-54
T_{SYN}	Time instant since when an MP is synchronized	3	45-54
P_{ACH}	Duration of an ACH including PP, FEP and TP.	3	45-54
P_{PP}	Duration of the PP in an ACH	3	45-54
P_{FEP}	Duration of the FEP in an ACH	3	45-54
P_{TCH}	Duration of a TCH	3	45-54
S_B	Length of the beacon frame in bits	3	45-54
PHY_B	PHY data rate used to transmit beacons	3	45-54
TCH_i	An integer representing the i^{th} TCH slot where an MP receives a beacon.	3	45-54
$max(x)$	Symbol denoting the maximum value of a uncertain value x	3	45-54
$x(t)$	Time error of the oscillator relative to some standard	3	51-54
a	Initial time offset	3	51-54
b	Frequency offset	3	51-54
D	Frequency drift	3	51-54

Symbol	Meaning	Chapter	Page
$\varepsilon(t)$	Effect of random error	3	51-54
PLR	Packet loss ratio	3	56
PER	Packet error ratio	3	56
N_{hop}	Number of hops	3	56
WIN_t	Transmission window size	3	62-75
WIN_r	Receiving window size	3	62-75
L_{RPDU}	Length of RPDUs in bytes	3	63-75
$TH^o{}_{AM}$	One-hop SR-ARQ throughput	3	63-75
P_T	Threshold of the number of sent RPDUs that triggers to send a poll	3	63-75
T_P	Period of the polling timer	3	63-75
n_{TCH}	Number of TCHs used for transmission.	3	63-75
N_{TDD}	Number TDMA frames needed to complete a process of sending a status RPDU on a TCH and returning the right of transmitting on the TCH to the partner MP when using on-demand-TDD turnaround.	3	63-75
T_{Ack}	Acknowledgement period	3	63-75
$p(n)$	Probability that a data RPDU is successfully transmitted at the n^{th} retransmitting time	3	63-75
R_{Max}	Maximal retransmission time	3	63-75
$D^O{}_{AM}$	Mean one-hop packet delay under the AM	3	63-75
$B(RL)$	Burstiness of a traffic flow (ratio of RL_P to RL_M)	3	68-75
$min(a, b)$	Minimal value of a and b	3	68-75
$Num(RL_P)$	Nmber of TCHs in a TDMA frame needed to transmit a traffic flow without causing much queue delay when the flow operates at peak rate	3	68-75
$Num(RL_M)$	Nmber of TCHs in a TDMA frame needed to transmit a traffic flow without causing much queue delay when the flow operates at mean rate	3	68-75
$Num(RQ_{TCH})$	Requested number of TCHs in a TDMA frame by requesting MP	3	68-75
$Num(G)$	Granted number of TCHs in a TDMA frame by requested MP	3	68-75
TCH_A	Common free TCHs in a TDMA frame of the requesting and requested MPs	3	68-75
TCH_R	Free TCHs in a TDMA frame observed by the requested MP	3	68-75

Symbol	Meaning	Chapter	Page
TCH_S	Free TCHs in a TDMA frame observed by the requesting MP	3	68-75
$Num(TCH_A)$	Number of TCH_A	3	68-75
$Num(TCH_S)$	Number of TCH_S	3	68-75
$NUM(TCH)$	Number of TCHs in a TDMA frame	3	68-75
$Num(Need_{TCH})$	Number of TCHs in a TDMA frame needed by a requesting MP for transmission with an intended MP.	3	68-75
$Num(Sum(AL_M))$	Sum of the number of TCHs in a TDMA frame needed to transmit all real-time traffic flows which are generated or relayed at all the one-hop adjacent MPs of the requesting MP, when each of the flows operates at its mean rate	3	68-75
$Num(Sum(ML_M))$	Sum of the number of TCHs in TDMA frame needed to transmit all real-time traffic flows which are generated or relayed at the requesting MP, when each of the flows operates at its mean rate	3	68-75
$TH^o{}_{UM}$	One-hop UM throughput	3	73
U_T	TCH utilization factor	3	73
$Num(RL_M{}^{n\text{-}hop})$	Average number of TCHs in a TDMA frame needed for a n-hop real-time transmission	3	73
m	spatial reuse distance in hops	3	73
$N_{RPDU}{}^r$	Number of pending real-time RPDUs destined to my partner	3	73
$N_{RPDU}{}^T$	Number of pending total RPDUs destined to my partner	3	73
$N_{RPDU}{}^P$	Number of pending RPDUs of my partner	3	73
$N_{TCH}{}^P$	Number of TCHs in a TDMA frame used by my partner for transmitting with me	3	73
$N_{TCH}{}^M$	Number of TCHs in a TDMA frame used by me to transmit with my partner	3	73
$N_{TCH}{}^F$	Number of free TCHs in a TDMA frame observed by me	3	73
Thr_i $(1 \leq i \leq 6)$	Threshold values, implementation dependent	3	73
$N_{RPDU}{}^r(i)$	Number of pending real-time RPDUs destined to my adjacent MP i	3	74
$N_{RPDU}{}^T(i)$	Number of pending RPDUs destined to my my adjacent MP i	3	74

Symbol	Meaning	Chapter	Page
$N_{TCH}^{M}(i)$	Number of TCHs used by me for transmitting with my adjacent MP *i*	3	74
$Sum(N_{TCH}^{M})$	Sum of number of TCHs used by me for transmitting	3	74
Thr_1	A threshold, implementation dependent	3	74
N	Number of MPs contending at the same time with the same PPCL	4	78-81
$p(N, n)$	Probability of only one winner in the contention given the number of contention slots in the FEP is *n*	4	78-81
l	a FEPCL level	4	78-81
$p(L=l)$	Probability that the FEPCL is equal to *l*	4	78-81
$p(L<l)$	Probability that the FEPCL is smaller than *l*	4	78-81
N'	Number of MPs generating their FEPCLs from the same CNG	4	78-81
$p'(N', n, K)$	Probability of only one winner in the contention given 1) the number of contention slots in the FEP is *n* and 2) the number of CNGs is *K*.	4	78-81
g	Number of MPDUs in packet train	4	81-102
λ_{PT}	Mean packet train generation rate	4	81-102
N	The number of TCHs in a TDMA frame	4	83-102
$D_M^{j\text{-}hop}$	*j*-hop mean end-to-end MPDU delay, $j \in \{1, 2, 3\}$	4	83-102
D^i	End-to-end delay of the ith MPDU in a packet train, $i \in [1, m]$	4	83-102
$Q_{Acc}^{j\text{-}hop}$	Access delay of a packet train at the jth hop. It is the sum of the service time and waiting time in the ACH queue	4	83-96
X_{ACH}	Service time of the ACH queue	4	83-96
ρ_{ACH}	Utilization factor of the ACH server	4	83-96
W_{TCH}^{i}	Waiting time of the i^{th} MPDU in a packet train at a TCH, $i \in [1, g]$	4	83-96
P_{TDMA}	Length of a TDMA frame in ms	4	83-102
h	Hang-on time of a TCH (units: TDMA frames)	4	83-102

Symbol	Meaning	Chapter	Page
$Th_{PT}^{j\text{-}hop}$	*j*-hop packet train throughput, j ∈ {*1*, 2, 3}	4	84-96
$Th_{MPDU}^{j\text{-}hop}$	*j*-hop MPDU throughput, j ∈ {*1*, 2, 3}	4	84-96
$N(Th_{MPDU}^{j\text{-}hop})$	*j*-hop normalized MPDU throughput, j ∈ {*1*, 2, 3}	4	84-96
T_{Tran}	Transmission delay of an MPDU on a TCH	4	84-96
Λ	Time difference between the start of the ACH and start time of a TCH in a TDMA frame	4	84-96
T_{ACH}	Duration of an ACH slot	4	84-96
T_{TCH}	Duration of a TCH slot	4	84-96
T_{ECH}	Duration of an ECH slot	4	84-96
$max(x)$	Upper bound of an uncertain value x	4	84-96
p	Probability of 1 MPDUs in a packet train	4	97-102
$P(X= k)$	Probability of k MPDUs in a packet train, $k \in \{1, 2, 3, \ldots\}$	4	97-102
W_{PT}	Mean one-hop waiting time of packet trains at an Erlang-C network	4	97-102
μ	Mean service rate per server	4	97-102
ρ	Utilization factor of the Erlang-C queue	4	97-102

LIST OF ABBREVIATIONS

AC	*Access Categories*
ACH	*Access Channel*
AES	*Access-E-Signal*
AGC	*Automatic Gain Control*
AM	*Acknowledged Mode*
AP	*Access Point*
APDU	*Application protocol Data Unit*
ARQ	*Automatic Request*
ATSP	*Adaptive Timing Synchronization Procedure*
BB	*Black-burst*
BES	*Busy-E-Signal*
BS	*Base Station*
BSS	*Basic Service Set*
CA	*Collision Avoidance*
CAC	*Call Admission Control*
CBR	*Constant Bit Rate*
CCF	*Common Control Frame*
CDF	*Complementary Distribution Function*
CDMA	*Code Division Multiple Access*
CFP	*Contention Free Period*
CNG	*Contention Number Group*
CP	*Contention Free Period*
CRC	*Cyclic Redundancy Check*
CTS	*Clear to Send*
CW	*Contention Window*
DBTMA	*Dual Busy Tone Multiple Access*
DCA	*Dynamic Channel Assignment*
DCCA	*Distributed Controlled Channel Access*
DCF	*Distributed Coordination Function*
Des_ID	*Destination Identifier*
DRRP	*Distributed Reservation Request Protocol*

DSR	*Dynamic Source Routing*
DVB	*Double Value Busy-E- Signal*
EC	*Error Control*
ECH	*Echo Channel*
EDCA	*Enhanced Distributed Channel Access*
EIFS	*Extended Interframe Space*
ESS	*Extended Service Set*
FA	*Fair Access*
FEC	*Forward Error Correction*
FEP	*Fair Elimination Phase*
FEPCL	*FEP Contention Level*
FIFO	*First In and First Out*
FTP	*File Transfer Protocol*
GBN	*Go-Back-N*
GPS	*Global Position System*
GTE	*Global Time Error*
HCCA	*HCF Controlled Channel Access*
HCF	*Hybrid Coordination Function*
IETF	*Internet Engineering Task Force*
IP	*Internet Protocol*
LLC	*Logical Link Control*
LM	*Link Management*
MAC	*Media Access Control*
MACP	*Media Access Control Protocol*
MANET	*Mobile Ad Hoc Networks*
MAP	*Mesh AP*
MBOA	*Multi-band OFDM Alliance*
MCF	*Mesh Coordination Function*
MDCF	*Mesh Distributed Coordination Function*
MMR	*Mobile Multi-hop Relay*
MP	*Mesh Point*
MPDU	*MACP Protocol Data Unit*
MPME	*MACP Management Entities*
MSDU	*MAC Service Data Unit*
MT	*Maximum Throughput*
MTSF	*MDCF Time Synchronization Function*

MTSF *Multi-hop Timing Synchronization Function*

MTXOP *Mesh Transmission Opportunity*

NTP *Network Time Protocol*

OFDM *Orthogonal Frequency Division Multiplexing*

PCF *Point Coordinated Function*

PCM *Pulse Code Modulation*

PDU *Protocol Data Unit*

PER *Packet Error Ratio*

PHY *Physical Layer*

PLR *Packet Loss Ratio*

PLC *Packet Loss Concealment*

PNC *Piconet Coordinators*

PQ *Priority Queueing*

PQWRR *Priority Queueing Weighted Round Robin*

PMP *Point-to-Multipoint*

PP *Prioritization Phase*

PPCL *PP Contention Level*

PPM *Parts Per Million*

PTP *Point-to-Point*

QoS *Quality of Service*

QTS *QoS-related Traffic Specification*

RBS *Reference Broadcast Synchronization*

RLCP *Radio Link Control*

RLCP *Radio Link Control Protocol*

RPDU *RLCP Protocol Data Unit*

RRC *Radio Resource Control*

RS_PDU *Routing Security Protocol Data Unit*

RTP *Real-time Transport Protocol*

RTS *Ready to Send*

SAP *Service Access Point*

SDL *Specification and Description Language*

S-link_ID *Service Link Identifier*

SPEETCL *SDL Performance Evaluation Tool Class Library*

SR-ARQ *Selective Repeat Automatic Request*

SSCH	*Slotted Seeded Channel Hopping*
SVB	*Single Value Busy-E-Signal*
SW	*Stop-and-Wait*
TCH	*Traffic Channel*
TCP	*Transport Control Protocol*
TDD	*Time Division Duplex*
TDMA	*Time Division Multiplex Access*
TP	*Transmission Phase*
TSF	*Timing Synchronization Function*
TXOP	*Transmission Opportunity*
UDP	*User Datagram Protocol*
UM	*Unacknowledged Mode*
UTC	*Coordinated Universal Time*
UWB	*Ultra Wide Band*
WCD	*Wireless Collision Detection*
WLAN	*Wireless Local Area Network*
WMAN	*Wireless Metropolitan Area Network*
WMN	*Wireless Mesh Network*
WPAN	*Wireless Personal Area Network*
WRR	*Weighted Round Robin*
WSN	*Wireless Sensor Network*
WWW	*World Wide Web*

REFERENCES

[1] IEEE Std. 802.11. *Wireless LAN Media Access Control (MAC) and Physical Layer (PHY) Specification*. New York, 1999.

[2] IEEE 802.11e/D13.0. *Medium Access Control (MAC) Quality of Service (QoS) Enhancements*. New York, Jan. 2005.

[3] IEEE 802.11a. *Wireless LAN Medium Access Control (MAC) and Physical Layer (PHY) Specifications: High-speed Physical Layer in the 5 GHZ Band*. New York, Sep.1999.

[4] IEEE P802.15.1/D1.0.1. *Wireless Medium Access Control (MAC) and Physical Layer (PHY) specifications for Wireless Personal Area Networks (WPANs)*. New York, 2001.

[5] IEEE P802.15.3/D17. *Wireless Medium Access Control (MAC) and Physical Layer (PHY) Specifications for High Rate Wireless Personal Area Networks (WPAN)*. New York, 2003.

[6] IEEE P802.15 Working Group for Wireless Personal Area Networks (WPANs). *Multi-band OFDM Physical Layer Proposal for IEEE 802.15 Task Group 3a*. New York, 10. Nov. 2003.

[7] IEEE P802.15.4/D15. *Wireless Medium Access Control (MAC) and Physical Layer (PHY) specifications for Low Rate Wireless Personal Area Networks (LR-WPANs).* New York, Jun. 2002.

[8] IEEE P802.11 Wireless LANs. *Draft PAR for IEEE 802.11 ESS Mesh*. IEEE 802.11-04/054r2, Nov. 2003. Available from: http://www.802wirelessworld.com.

[9] IEEE 802.11 Task Group "s" on ESS Mesh Networking. *IEEE P802.11 Wireless LANs Usage Models.* IEEE 802.11-03/802r23, May 2004. Available from: http://www.802wirelessworld.com.

[10] IEEE 802.11 Task Group "s" on ESS Mesh Networking. Issues for mesh media access coordination component in 11s. IEEE P802.11-04/968r13, Jan. 2004. Available from: http://www.802wirelessworld.com.

[11] IEEE 802.11 Task Group "s" on ESS Mesh Networking. *802.11 TGs Simple Efficient Extensible Mesh (SEE-Mesh) Proposal*. IEEE 802.11-05/0562r2, Jul. 2005. Available from: http://www. 802wirelessworld.com.

[12] IEEE 802.11 Task Group "s" on ESS Mesh Networking. *802.11 TGs MAC Enhancement Proposal*. IEEE 802.11-05/0575r4, Jul. 2005. Available from: http://www.802wirelessworld.com.

[13] IEEE Std. 802.16. *Air Interface for Fixed Broadband Wireless Access Systems*. New York, Dec. 2001.

[14] IEEE P802.16a/D7-2002. *Air Interface for Fixed Broadband Wireless Access Systems -Medium Access Control Modifications and Additional Physical Layer Specifications for 2-11 GHz*. New York, Nov. 2002.

[15] IEEE 802.16 Standard Group Web Site. Available at: http://www.ieee802.org/16/ relay/index.html.

[16] ISO/IEC 7498-1. *Information technology—Open Systems Interconnection—Basic Reference Model: The Basic Model*. New York, 1994.

[17] IEEE Std. 802. *Overview and Architecture*. New York, May 1990.

[18] IEEE Std. 802.11g. *Wireless LAN Medium Access Control (MAC) and Physical Layer (PHY) specifications. Amendment 4: Further Higher Data Rate Extension in the 2.4 GHz Band*. New York, Jun. 2003.

[19] IEEE 802.11 Task Group "n". *Project Authorization Request for IEEE 802.11n*. IEEE 802.11-02/798r7, 2002. Available from: http://www.802wirelessworld.com.

[20] IEEE Std. 802.11i. *Wireless LAN Medium Access Control (MAC) and Physical Layer (PHY) specifications Amendment 6: Medium Access Control (MAC) Security Enhancements*. New York, Jul. 2004.

[21] Walke and V. Kumar. Spectrum issues and new air interfaces. In *Computer Communications*, Vol. 26, pp. 53-63, Jan. 2003.

[22] R. Pabst, B. Walke, D. Schultz, et al.. Relay-based deployment concepts for wireless and mobile broadband radio. *IEEE Communications Magazine*, pp. 80-89, New York, USA, Sep. 2004.

[23] I. F. Akyildiz, W. Su, et al.. A survey on sensor networks. *IEEE Communications Magazine*, pp. 102-114, New York, USA, Aug. 2002.

[24] I. F. Akyildiz, X. Wang. A survey on wireless mesh networks. *IEEE Communications Magazine*. Vol. 43, pp. 23 – 30, New York, USA, Sep. 2005.

[25] R. Jain, D. M. Chiu and W. R. Hawe. A quantitative measure of fairness and discrimination for resource allocation shared computer systems. *Digital Equipment Corporation technical report TR-301*, 1984.

[26] Z. J. Haas and J. Deng. Dual busy tone multiple access (DBTMA) - a multiple access control scheme for ad hoc networks. *IEEE Transactions on Communication*, pp. 975-985, Jun. 2002.

[27] A. C. V. Gummalla and J. O. Limb. Design of an Access Mechanism for a High Speed Distributed Wireless LAN. *IEEE Journal on Selected Areas in Communications*, Vol. 18, pp. 1740-1750, Sep. 2000.

[28] S. Xu and T. Saadawi. Does the IEEE 802.11 MAC protocol work well in multi-hop wireless ad hoc networks? *IEEE Communication Magazine*, pp. 130-137, Jun. 2001.

[29] N. H. Vaidya, P. Bahl, and S. Gupta. Distributed fair scheduling in a wireless LAN. In *Proc.*

ACM MobiCom 2002, Boston, USA, pp.167-178, Aug. 2000.

[30] X. L. Huang and B. Bensaou. On max-min fairness and scheduling in wireless ad-hoc networks: analytical framework and implementation. In *Proc. ACM MobiHoc 2001*, Long Beach, CA, USA, pp. 221-231, 2001.

[31] J. Chen, S.-H. Chan, et al.. Power adaptation for starvation avoidance (PASA): a distributed algorithm to improve short-term fairness for multimedia traffic in mobile ad hoc networks. *IEEE Journal on Selected Areas in Communications*, Dec. 2003.

[32] J. So and N. Vaidya. Multi-channel MAC for ad hoc networks: handling multi-channel hidden terminals using a single transceiver. In *Proc. ACM MobiHoc 2004*, Tokyo, Japan, May 2004.

[33] C. Ware, J. Judge, et al.. Unfairness and capture behavior in 802.11 ad hoc networks. In *Proc. IEEE ICC 2000*, No. 1, pp. 159-163, New Orleans, USA, Jun. 2000.

[34] P. Bahl, R. Chandra et al.. SSCH: slotted: seeded channel hopping for capacity improvement in IEEE 802.11 ad-hoc wireless networks. In *Proc. ACM MobiCom 2004*, Pennsylvania, PA, USA, Sep. 2004.

[35] S.-L. Wu, C.-Y. Lin, et al.. A new multi-channel MAC protocol with on-demand channel assignment for multi-Hop mobile ad hoc networks. In *Int'l Symp. on I-SPAN*, 2000.

[36] ETSI. *Broadband Radio Access Networks (BRAN); High Performance Radio Local Area Network (HIPERLAN) Type 1; Functional specification*. ETSI Draft Standard, Jul. 1995.

[37] ETSI. *Broadband Radio Access Networks (BRAN); HIPERLAN Type 2; Physical (PHY) layer.* ETSI Draft Standard, Apr. 2000.

[38] J. L. Sobrinho, et al.. Quality-of-service in ad hoc carrier sense multiple access wireless networks. *IEEE Journal on Selected Areas in Communications*, Vol.17, no.8, 1999.

[39] T. Korakis, G. Jakllari and L. Tassiulas. A MAC protocol for full exploitation of directional antennas in ad-hoc wireless networks. In *Proc. ACM MobiHoc 2003*, Boston, USA, Jun. 2003.

[40] A. Muqattash and M. Krunz. CDMA-based MAC protocol for wireless ad hoc networks. In *Proc. ACM MobiHoc 2003*, Boston, USA, Jun. 2003.

[41] MultiBand OFDM Alliance. Available from: http://www.wimedia.org.

[42] *MBOA - Wireless Medium Access Control (MAC) Specification for High Rate Wireless Personal Area networks (WPANs)*, MBOA MAC Specification Draft 0.72. Oct. 20, 2004.

[43] G. Orfanos, B. Walke and W. Butsch. An Adaptive MAC Protocol for MC-CDMA adhoc Wireless LAN, In *Proc. IEEE PIMRC 2005*, Berlin, Germany, Sep. 2005.

[44] G. Hiertz, J. Habetha, P. May, E. Weiss, R. Bagul and S. Mangold. A decentralized reservation scheme for IEEE 802.11 ad hoc networks. In *Proc. IEEE PIMRC 2003*, Beijing, China, Sep. 2003.

[45] J. Weinmiller, M. Schlaeger, A. Festag, and A. Wolisz. Performance study of access control in wireless LANs - IEEE 802.11 DFWMAC and ETSI RES10 HIPERLAN. *Mobile Networks and Applications (Special Issue on Channel Access)*, Vol. 2, pp. 55-76, Jun. 1997.

[46] S. Hara and P. Prasad. Overview of multi-carrier CDMA. *IEEE Communication Magazine*, Vol.35, no. 12, pp. 126-133, Dec. 1997.

[47] W. Rhee and J. M. Cioffi. Increase in capacity of multi-user OFDM system using dynamic subchannel allocation. In *Proc. IEEE VTC Spring 2000*, Vol. 2, pp. 1085 -1089, Tokyo, Japan, May 2000.

[48] L. Kleinrock and F. A. Tobagi. Packet switching in radio channel: Part I - carrier sense multiple-access modes and their throughput-delay characteristics. *IEEE Transactions on Communication*, vol. COM-23, pp. 1400-1416, Dec. 1975.

[49] F. A. Tobagi and L. Kleinrock. Packet switching in radio channels: part II - the hidden terminal problem in carrier sense multiple-access and the busy-tone solution. *IEEE Transactions on Communication*, Vol. COM-23, pp. 1417–1433, Dec. 1975.

[50] G. Bianchi. Performance analysis of the IEEE 802.11 distributed coordination function. *IEEE Journal on Selected Areas in Communications*, vol. 18, pp. 535-547, Mar. 2000.

[51] G. Pierobon, A. Zanella and A. Salloum. Contention-TDMA protocol: performance evaluation. *IEEE Transactions on Vehicular Technology*, vol.51, no.4, pp.781-788, Jul. 2002.

[52] Chaskar HM, Madhow U. Fair scheduling with tunable latency: A round-robin approach. *IEEE/ACM Transactions on Networking*, Vol. 11, pp, 592-610, Aug. 2003.

[53] B. Williams and T. Camp. Comparison of broadcasting techniques for mobile ad hoc network. In *Proc. ACM MobiHoc 2002*, pp.194–205, Lausanne, Switzerland, Jun. 2002.

[54] B. Maglaris, D. Anastasiou, P. Sen, G. Kalsson and J. D. Robbins. Performance models of statistical multiplexing in packet video communication. *IEEE Transactions on Communication*, Vol. 36, pp. 834-843, 1988.

[55] ETSI UMTS 30.03. *Selection Procedures for the Choice of Radio Transmission Technologies of the UMTS*. Apr. 1998.

[56] L. E Schrage and LW Miller. The queue M/G/1 with the shortest processing remaining time discipline. In *Operations Research*, Vol. 14, pp. 670-684, 1966.

[57] J. Mao, W. M. Moh, and B. Wei. PQWRR scheduling algorithm in supporting of DiffServ. In *Proc. IEEE ICC 2001*, vol. 3, pp. 679-684, Amsterdam, Netherlands, Jun. 2001.

[58] Chunck Semeria. *Supporting Differentiated Service Classes: Queue Scheduling Disciplines*. White paper of Juniper Networks, Inc. 2001. Available from: https://www.juniper.net.

[59] P. T. Brady. A Model for Generating On-Off Speech Patterns in Two-way Conservation. *Bell System Technology Journal*, vol. 48, pp. 2445-72, Sep. 1969.

[60] Intel Cooperation. *Designing and Troubleshooting the Data Network for Voice*. White paper

of Intel, Co., 2004. Available from: http://www.intel.com.

[61] D. Mills. Internet time synchronization: the network time protocol. *IEEE Transactions on Communication*, COM 39, No. 10, pp. 1482-1493, Oct. 1991.

[62] J. Elson, L. Girod and D. Estrin. Fine-grained network time synchronization using reference broadcasts. In *Proc. 5th symposium on Operating Systems Design and Implementation (OSDI)*, Dec. 2002.

[63] L. Huang, T. Lai. On the scalability of IEEE 802.11 ad hoc networks. In *Proc. ACM MobiHoc 2002*, Lausanne, Switzerland, Jun. 2002.

[64] J. So and N. Vaidya. *MTSF: A Timing Synchronization Protocol to Support Synchronous Operations in Multi-Hop Wireless Networks*. Technical Report, Oct. 2004. Available from: http://www.crhc.uiuc.edu/wireless/groupPubs.html.

[65] V. Claesson, H. Lonn and N. Suri. An efficient TDMA start-up and restart synchronization approach for distributed embedded systems. *IEEE Transactions on Parallel and Distributed Systems*, Vol. 15, pp.725 – 739, Aug. 2004.

[66] W. Zhu. TDMA frame synchronization of mobile stations using a radio clock signal for short range communications. In *Proc. IEEE VTC 1994*, Stockholm, Jun. 1994.

[67] H. Kopetz and W. Schwabl. *Global Time in Distributed Real-time Systems*. Technical Report 15/89, Technische Universität Wien, 1989.

[68] ED Kaplan. *Understanding GPS: Principles and Applications*. Artech House, 1996.

[69] D. W. Allan. Time and frequency (time-domain) characterization, estimation, and prediction of precision clocks and oscillators. In *IEEE Transactions on ultrasonic, ferroelectrics, and frequency control*, Vol. UEFC-34, No.6, Nov. 1987.

[70] A. J. Barnes. The measurement of linear frequency drift in oscillators. In *Proc. 15th Annual PTTI meeting*, 1983.

[71] D. L. Lu and J. F. Chang. Performance of ARQ protocols in nonindependent channel errors. *IEEE Transactions on Communication*, Vol. 41, pp. 721-730, May 1993.

[72] B. Walke. *Mobile Radio Networks Networking and Protocols (2nd Edition)*. John Wiley & Sons, 2002.

[73] Mobile Ad-Hoc Networks (MANET) Charter IETF. Available from: http://www.ietf.org/html.charters/manet-charter.html.

[74] C. E. Perkins and P. Bhagwat. Highly dynamic Destination-Sequenced Distance-Vector routing (DSDV) for mobile computers. In *Proc. ACM SIGCOMM 1994*, pp. 234–244, London, England, Aug. 1994.

[75] C. Perkins, E. Belding-Royer and S. Das. *Ad Hoc On-Demand Distance Vector (AODV) routing*. IETF RFC 3561, Jul., 2003. Available from: http://www.ietf.org/.

[76] D.B. Johnson, D.A. Maltz, Y.-C. Hu. *The Dynamic Source Routing Protocol for Mobile Ad Hoc Networks (DSR)*. IETF Internet-Draft: work in progress, Jul. 2004. Available from: http://www.ietf.org/.

[77] V. D. Park and M. S. Corson. *Temporally-Ordered Routing Algorithm (TORA) Version 4: Functional Specification*. Internet-Draft, Work in progress, Jul. 2001. Available from: http://www.ietf.org/.

[78] Z. J. Haas, M.R. Pearlman and P. Samar. *The Zone Routing Protocol (ZRP) for Ad Hoc Networks*. IETF Internet Draft, Jul. 2002. Available from: http://www.ietf.org/.

[79] L. Kleinrock. *Queueing Systems*, *Vol. I, Theory*. New York, John Wiley & Sons, 1975.

[80] L. Kleinrock. *Queueing Systems*, *Vol. II, Computer Applications.* New York, John Wiley & Sons, 1976.

[81] J. Walrand. *An Introduction to Queueing Networks*. New Jersey, Prentice Hall, Englewood Cliffs, 1988.

[82] C. G. Cassandras. *Discrete Event Systems: Modeling and Performance Analysis*. Homewood, Illinois, Irwin and Aksen Associates, 1993.

[83] M. Steppler. Performance analysis of communication systems formally specified in SDL. In *Proc. 1st International Workshop on Software and Performance 1998*, Oct. 1998.

[84] M. Lott, I. Forkel I. A multi-wall-and-floor model for indoor radio propagation. In *Proc. IEEE VTC Spring 2001*, Rhodes, Greek, May 2001.

[85] A. Kamerman and L. Monteban, WaveLAN-II: A high-performance wireless LAN for the unilicensed band. *Bell Labs Technical Journal*, Vol. 2, 1997.

[86] VINT Group. *UCB/LBNL/VINT Network Simulator ns (Version 2)*. Available from: http://www.isi.edu/nsnam/ns/.

[87] J. KunJush, P. Schramm, U. Wachsmann and F. Wenger. Structure and performance of the HIPERLAN/2 physical layer. In *Proc. IEEE VTC Fall 1999*, Amsterdam, Nederland, Sep. 1999.

[88] D. B. Johnson and D. A. Maltz. Dynamic source routing in ad hoc wireless networks. *Mobile Computing*, pp. 153–181. Kluwer Academic Publishers, 1996.

[89] V. Paxson and S. Floyd. Wide-area traffic: the failure of Poisson modeling. In *Proc. ACM SIGCOMM 1994*, pp. 257-268, London, United Kingdom, Aug. 1994,.

[90] D. D. Vleeschauwer and J. Janssen. *Voice Performance over Packet-Based Networks*. Alcatel white paper, 2002. Available from: http://www.alcatel.com.

[91] J. Jun, P. Peddabachagari, and M. Sichitiu, Theoretical maximum throughput of IEEE 802.11 and its applications. In *Proc. 2nd IEEE International Symposium on Network Computing and Applications (NCA'03)*, 2003, USA.

[92] R. Stevens. *TCP/IP Illustrated, Band I.* Addison-Wesley, Massachusetts, Oct. 1996.

[93] M. Lott and B. Walke. Performance analysis of a wireless ad hoc network with QoS support. *Telecommunication Systems*, Vol. 16, pp. 115-134, Jan. 2001.

[94] M. Lott. Random access for wireless ad hoc broadband networks. In *Proc. European Wireless 1999*, Munich, Germany, Oct. 1999.

[95] M. Lott. *Entwurf Eines Drahtlosen Multihop Ad-hoc-Funknetzes mit Dienstgüteunterstützung*. Ph. D. Dissertation, RWTH Aachen University, ABMT 24, p. 229, 2001.

[96] B. Xu and B. Walke. A new air interface concept for wireless multimedia communications beyond the 3rd generation. *Wireless Personal Communications,* Vol.23 No.1, pp. 121-135, Oct. 2002.

[97] B. Xu and B. Walke. Design issues of self-organizing broadband wireless networks. *Computer Networks*, Vol. 37, pp. 73-81, Sep. 2001.

[98] B. Xu. *Self-organizing Wireless Broadband Multi-hop Networks with Qos Guarantee*. Ph. D. Dissertation, RWTH Aachen University, ABMT 32, p. 200, 2002.

[99] K. Subramanian. *Development and Performance Evaluation of Raido Link Control (RLC) Functions for the W-CHAMB System*. Master Thesis, ComNets, RWTH Aachen University, Jul. 2004.

[100] S. Ramar. *Development and Performance Evaluation of Routing Protocols for the W-CHAMB System.* Master Thesis, ComNets, RWTH Aachen University, Jan. 2005.

[101] R. Zhao, B. Walke and G. R. Hiertz. An efficient IEEE 802.11 ESS mesh network supporting quality of service. *IEEE Journal on Selected Areas in Communications*, Vol. 24, pp. 2005-2017, Nov. 2006.

[102] R. Zhao and B. Walke. Modeling and performance analysis of mesh distributed coordination function. Submitted for review.

[103] R. Zhao, M. Einhaus, D. Schultz and B. Walke. Analysis of Performance of a TDMA-based Distributed MAC Protocol in Single-hop Wireless Networks. In *Proc. ChinaCom 2006*, p. 6, Beijing, China, Nov. 2006.

[104] R. Zhao and B. Walke. Decentrally controlled wireless multi-hop mesh networks for high quality multi-media communications. In *Proc. ACM MSWiM 2005*, pp. 200-208, Montréal, Canada, Oct. 2005.

[105] R. Zhao, B. Walke and M. Einhaus. Constructing efficient multi-hop mesh networks. In *Proc. IEEE LCN 2005*, pp. 166-173, Sydney, Australia, Nov. 2005.

[106] R. Zhao, B. Walke, M. Einhaus and G. Orfanos. A primary adaptation of the W-CHAMB protocol for gigabit WPANs. In *Proc. IEEE PIMRC 2005*, p. 6, Berlin, Germany, Sep. 2005.

[107] R. Zhao and B. Walke. Traffic performance of the wireless channel-oriented ad-hoc

multi-hop broadband system. In *Proc. IEEE VTC 2004*, Vol. 4, pp. 2779- 2783, Sep. 2004, Los Angels, USA.

[108] R. Zhao and B. Walke. A synchronization scheme for the Wireless Channel-oriented Ad-hoc Multi-hop Broadband (W-CHAMB) system. In *Proc. Wireless World Research Forum*, Zurich, Switzerland, Jul. 2003.

[109] R. Zhao, B. Walke and M. Einhaus. A MAC partial proposal for IEEE 802.11s, P802.11-05/595r1. In *IEEE 802.11 WLAN Working Group Session*, p. 54, San Francisco, CA, USA. Jul. 2005. Available from: http://www.802wirelessworld.com.

[110] R. Zhao, B. Walke and G. R. Hiertz. A new MAC for better support of mesh networks with QoS. P802.11-04/0991r0. In *IEEE 802.11 WLAN Working Group Session*, p. 10. Berlin, Germany. Sep. 2004. Available from: http://www.802wirelessworld.com.

ACKNOWLEDGMENT

This thesis is a result of my 5-year research activity at the Chair of Communication Networks (ComNets), RWTH Aachen University, Germany. My most sincere thanks go to my supervisor, Prof. Dr.-Ing Bernhard Walke, for his inspiration, invaluable advices, full range of support, and for bringing me into a highly competent environment and giving me a high level of freedom in research.

I would like to express my great appreciation to Prof. Dr. Petri Mähönen, the chair of Mobile Networks (Mobnets), RWTH Aachen University, Germany, for his support, inspired discussion and evaluatin of my thesis.

Further, I thank my colleagues Dipl.-Ing Michael Einhaus, Dipl.-Ing. Guido R. Hiertz, MS.c. Yunpeng Zang, Dipl.-Ing. Ralf Jennen, Dr.-Ing Lars Berlenmann, Dipl.-Ing. Jelena Mirkovic, Dipl.-Ing. Daniel Schultz, Dipl.-Ing. Ralf Pabst, Dipl.-Inform. Sebastian Max, Dipl.-Ing. Christian Hoymann, Dipl.-Ing. Tim Irnich, Dipl.-Ing. Stephan Goebbels, Dipl.-Ing. Benedikt Wolz, Dipl.-Inform. Zheng Xie, Dipl.-Ing. Ole Klein and Dipl.-Ing. Lothar Stibor for the fruitful discussion and their highly valuable comments to my thesis.

Special thanks go to my friends and ex-colleagues Dr.-Ing Bangnan Xu, Dr.-Ing Stefan Mangold, Dr.-Ing Lars Berlenmann, Dr.-Ing Georgios Orfanos, Dr.-Ing Christan Becker and Dr.-Ing Harianto Wijaya for their inspiration and valuable helps.

Many thanks go to my students MS.c Kumaran Subramanian, MS.c Sridharan Ramar, Mr. Mu Qiang, Mr. Xuejun Wang, Mr. Hashim Raza Khan, Mr. Tran Anh Tu and Mr. Arne Peter, for their valuable contributions to my research.

Sincere thanks go to my colleagues Ms. Karin von Czapiewsky, Ms. Cornelia hanf, Ms. Anne Schroeder, Ms. Gabi Reimann, Ms. Rosalia Söhnen, Ms. Doro Pawelzick, Mr. Norbert Konkol, Mr. Heinz Rochhausen and Mr. Felix Okon for their support and helps.

Special appreciation goes to my friends Dr. Enxu Zhou, Dr. Weipin Hu, MS.c Yuqi Zhang, Dr. Xiangping Yang, Dr. Jian Kan, Dr. Jianhua Wu and Dr. Hongqi Lue.

I would like to send my special thanks to my parents, for their endless love, support, inspiration and encouragement.

Finally, I would like to thank you, Dongjing, my beloved wife and Youzhen, my son, for your love, continuous support and always being with me.

Aachen, April 2007 Rui Zhao

CURRICULUM VITAE

Name	Zhao, Rui
Date of Birth:	29. March 1970
Place of Birth:	Sichuan, P. R. China
Nationality:	P. R. China
Marital Status:	Married

Sep. 1977 - Jul. 1983	Primary School *Sichuan, P. R. China*
Sep. 1983 - Jul. 1989	High School *Sichuan, P. R. China*
Sep. 1989 - Jul. 1993	Undergraduate study in South-West Institute of Technology *Sichuan, P. R. China*
Jul. 1993 - Mar. 1998	Principal Engineer at the Department of Automatic control in Sichuan Institute of Building Material *Sichuan, P. R. China*
Sept. 1998 - Mar. 2001	Postgraduate study in Beijing University of Aeronautic and Astronautic (BUAA) *Beijing, P. R. China*
Apr. 2001 - Mar. 2002	Member of Technical Staff in Bell-Labs China, Lucent technologies *Beijing, P. R. China*
Apr. 2002 - Apr. 2007	Research assistant at the Chair of Communication Networks, RWTH Aachen University *Aachen, Germany*